Alma Mater Studiorum – Università di Bologna

DOTTORATO DI RICERCA IN

Ingegneria Strutturale e Idraulica

Ciclo XXIV

Settore Concorsuale di afferenza: 08/B2

Settore Scientifico disciplinare: ICAR 08

TITOLO TESI

Static analysis of functionally graded cylindrical and conical shells or panels using the generalized unconstrained third order theory coupled with the stress recovery

Presentata da: **Luigi Rossetti**

Coordinatore Dottorato **Relatore**

Chiarissimo Prof. E. Viola **Chiarissimo Prof. E. Viola**

Esame finale anno 2013

Index

Abstract

A 2D Unconstrained Third Order Shear Deformation Theory (UTSDT) is presented for the evaluation of tangential and normal stresses in moderately thick functionally graded conical and cylindrical shells subjected to mechanical loadings. Several types of graded materials are investigated. The functionally graded material consists of ceramic and metallic constituents. A four parameter power law function is used. The UTSDT allows the presence of a finite transverse shear stress at the top and bottom surfaces of the graded shell. In addition, the initial curvature effect included in the formulation leads to the generalization of the present theory (GUTSDT). The Generalized Differential Quadrature (GDQ) method is used to discretize the derivatives in the governing equations, the external boundary conditions and the compatibility conditions. Transverse and normal stresses are also calculated by integrating the three dimensional equations of equilibrium in the thickness direction. In this way, the six components of the stress tensor at a point of the conical or cylindrical shell or panel can be given. The initial curvature effect and the role of the power law functions are shown for a wide range of functionally conical and cylindrical shells under various loading and boundary conditions. Finally, numerical examples of the available literature are worked out.

Chapter 1

Third order Shear Deformation Theory

Sommario

Dopo aver analizzato lo stato dell'arte, si è fatta strada l'idea di sviluppare una teoria generale di deformazione a taglio del terzo ordine di tipo svincolato per gusci/pannelli di rivoluzione a doppia curvatura, costituiti da uno strato singolo di materiale a stratificazione graduale. Si è operata la scrittura del modello cinematico a sette parametri indipendenti, delle relazioni tra deformazioni e spostamenti arricchite dell'effetto della curvatura, delle equazioni costitutive per una lamina singola in materiale a stratificazione graduale e delle caratteristiche di sollecitazione in funzione degli spostamenti. Definiti i carichi esterni uniformi di natura trasversale, assiale e circonferenziale, è stato applicato il principio degli spostamenti virtuali per ricavare le equazioni indefinite di equilibrio e le condizioni al contorno. Pertanto si è proceduti alla scrittura della equazioni fondamentali con la sostituzione delle relazioni delle azioni interne espresse in funzione degli spostamenti, nelle equazioni indefinite di equilibrio. Compiuta la scrittura del sistema fondamentale si è pervenuti alla soluzione di esso in termini delle sette variabili di spostamento indipendenti, applicando la tecnica di quadratura differenziale di tipo generalizzato in tutti i punti della superficie di riferimento del panello/guscio. Dunque è stato possibile determinare le tensioni membranali in un punto arbitrario appartenente alla superficie di riferimento del panello/guscio ed elaborare poi la distribuzione di esse lungo lo spessore dell'elemento strutturale. Successivamente con il fine di pervenire alla determinazione completa del tensore delle tensioni, ovvero delle tensioni trasversali normale e tagliante, si è operata l'integrazione delle equazioni indefinite di equilibrio sfruttando la conoscenza delle tensioni membranali, determinate indirettamente dal sistema fondamentale, sempre utilizzando il metodo generalizzato di quadratura differenziale. Pertanto si è pervenuti alla determinazione dei profili di tensione trasversale normale e tagliante lungo lo spessore del panello/guscio. In ambito letterario, il percorso proposto ha degli attributi di autenticità in quanto consente di calcolare profili di tensione trasversale che soddisfano al pieno le condizioni al contorno, anche in presenza di carichi taglianti alle superfici di estremità. In tal modo viene superato uno dei limiti propri della teoria di Reddy che diversamente ritiene nulli a priori i carichi taglianti alle estremità del panello/guscio.

1.1 General literature trends

Two significant classes of two dimensional shell theories can be found in literature: the first based on the assumed form of the displacement field and the second based on the assumed form of the stress field. In both cases, the displacement or stress fields are expanded in increasing powers of the thickness coordinate. Nevertheless, displacement – based theories are more recurrent because they do not require the strain/stress compatibility condition in addition to the kinematic and equilibrium equations. It is proved that a third order expansion of the displacement field is optimal because it gives quadratic variation of transverse strains and stresses, and require no "shear correction factors" compared to the first order theory, where the transverse strains and stresses are constant through the shell thickness. A brief overview of research done in third order shell theories is also included in here.

The simplest and oldest plate theory is the classical Kirchhoff plate theory [1]. The so called Kirchhoff hypothesis includes the following assumptions: straight lines remain perpendicular to the reference surface and inextensible after deformation. In this manner both transverse shear and normal strains [2,3] are neglected. These assumptions in the model simplify the three dimensional problem to a two dimensional one and the governing equations are expressed in terms of three displacements of a point on the midsurface. Moreover the theory does not qualify to be called first order because the first order terms or rotations are not independent of the transverse displacement component. The theory is very useful in a wide range of problems when thickness is very small (two orders of magnitude less than the smallest in plane dimension). Transverse shear strains are also negligible.

The simplest first order shear deformation shell theory (FSDT) often referred to as the Mindlin plate theory [4-6], is based on the displacement expansion till to the first order, where the first order terms are the rotations of a transverse normal line and are independent of the transverse displacement component. The first idea of such expansion can be found in earlier works by Basset [7], Hencky [8] and Hildebrand et al. [9]. The normality is not invoked and in this way the rotation are independent of membrane and transverse displacement components and the transverse shear strains are non zero but independent of out of plane coordinate. This leads to the introduction of shear correction factors in the evaluation of the transverse shear forces.

Second order and higher order theories relax the Kirchhoff hypothesis further by allowing the straight lines normal to the midsurface before deformation to become curves. Second order shell theories are not so diffused because they also require shear correction factors.

The third order theories provide a slight increase in accuracy relative to the FSDT solution, at the expense of an increase in computational effort and do no require shear correction factors.

Several third order plate theories have been developed by different researchers [10-24] but as pointed by Reddy [21] some of them are claimed to be new whereas they are not new, but only different in the form of the displacement expansions adopted.

Reddy [19,20] is the first one to develop the equilibrium equations of a third order shell theory with vanishing tractions for composite structures, using the principle of virtual displacements. By means of these assumptions, Reddy's theory reduces the independent displacement components from seven to five. The theory leads to the accurate reconstruction of the effective transverse shear components but it excludes the presence of transverse shear loads on the boundary surfaces of the shell.

1.2 The aim of the present work

In the present work, by moving from Leung's idea [25] a third order shear deformation theory has been developed by neglecting the Reddy's assumptions. The present third order model involves seven unknown independent parameters and it includes the possible presence of shear uniform loads in addition to the normal uniform one on the extreme surfaces of composite shell. As in the Reddy's theory no correction factor is introduced.

The third order shear deformation theory under discussion is formulated for a single lamina doubly curved shell of functionally graded material. The seven independent fundamental equations are achieved by applying the principle of virtual displacements and the fundamental system is solved by means of the GDQ method [26-62]. By using the GDQ solution in term of the generalized displacements of points on the reference surface, the membrane profiles of normal and shear stresses are determined throughout the thickness direction. Then, by considering the three dimensional equilibrium equations, by discretizing them via the GDQ method and by the knowledge of the membrane stress components, the transverse profiles of normal and shear stresses are determined with satisfaction of the boundary conditions at the extreme surfaces. The Reddy's model lead to accurate transverse stress profiles by supposing the null values of transverse shear stress component at the extreme surfaces, whereas the present one in conjunction with the stress recovery from the three dimensional equations leads to accurate transverse shear stress profiles even if shear uniform loadings are present on the boundary surfaces.

1.3 Problem formulation

In this study, a single lamina doubly curved shell of functionally graded material represents the basic configuration of the problem (Fig.1). φ, s are the coordinates along the meridian and circumferential directions of the reference surface, respectively. The third orthogonal coordinate to

the middle plane along the shell normal is ζ. ζ - coordinate defines the distance of each point from the shell mid surface $-h/2 \le \zeta \le h/2$ and h is the thickness of the shell. The angle between the extended normal **n** to the reference surface and the axis of rotation x_3, or the geometric axis x_3' of the meridian curve, is defined as the meridian angle φ. The angle formed by the parallel circle $R_0(\varphi)$ and the x_1 axis is designated as the circumferential angle ϑ. The meridian curves and the parallel circles are represented by the parametric coordinates (φ, s) upon the middle surface of the shell. The curvilinear abscissa $s(\varphi)$ of a generic parallel is related to the circumferential angle ϑ by the relation $s = \vartheta R_0$. The horizontal radius $R_0(\varphi)$ of a generic parallel of the shell represents the distance of each point from the axis of revolution x_3. R_b is the shift of the geometric axis of the curved meridian x_3' with reference to the axis of revolution x_3. The curvature radius R_ϑ for a shell of revolution is defined by the relation $R_\vartheta = R_0/\sin\varphi$. For a general shell of revolution, R_φ, R_ϑ, R_0 are all independent of the ϑ-angle. The well known equation of Gauss - Codazzi is also considered : $dR_0/d\varphi = R_\varphi \cos\varphi$.

The position of an arbitrary point within the shell material is defined by the coordinates φ $(\varphi_0 \le \varphi \le \varphi_1)$, s $(0 \le s \le s_0)$ upon the middle surface, and ζ directed along the outward normal and measured from the reference surface $(-h/2 \le \zeta \le h/2)$. In the present shell theory, the following assumptions are taken under consideration in the formulation: (1) the shell deflections are small and the strains are infinitesimal; (2) the transverse shear deformation is considered to influence the governing equations. In this manner the normal lines to the reference surface of the shell before deformation do not remain straight and normal after deformation; (3) the transverse normal strain is inextensible so that the normal strain is equal to zero; (4) the shell is moderately thick so that the transverse normal stress could be considered negligible; (5) the linear elastic behavior of composite materials is assumed; (5) the initial curvature effect is also taken into account.

1.3.1 Third order displacement expansion

Consistent with the assumptions of a moderately thick shell theory reported above, the displacement field considered in this study is that of the Third order Shear Deformation Theory and can be put in the following form :

$$\begin{aligned} U_\varphi(\varphi, s, \zeta) &= u_\varphi(\varphi, s) + \zeta\beta_\varphi(\varphi, s) + \zeta^3\eta_\varphi(\varphi, s) \\ U_s(\varphi, s, \zeta) &= u_s(\varphi, s) + \zeta\beta_s(\varphi, s) + \zeta^3\eta_s(\varphi, s) \\ W(\varphi, s, \zeta) &= w(\varphi, s) \end{aligned} \tag{1}$$

where u_φ, u_s, w are the displacement components of points lying on the reference surface ($\zeta = 0$) of the shell, along meridional, circumferential and normal directions, respectively. β_φ and β_s are normal to mid-surface rotations, respectively. η_φ and η_s are the higher order terms. The kinematic hypothesis expressed by Eq.(1) is enriched by the statement that the shell deflections are small and strains are infinitesimal, that is $w(\varphi, s) \ll h$.

1.3.2 Relations between strains and displacements

The relations of strains for a revolution shell are the followings [64]:

$$\varepsilon_\varphi = \frac{1}{R_\varphi\left(1+\frac{\zeta}{R_\varphi}\right)}\left(\frac{\partial U_\varphi}{\partial \varphi} + W\right) \tag{2}$$

$$\varepsilon_\vartheta = \frac{1}{R_0\left(1+\frac{\zeta \sin\varphi}{R_0}\right)}\left(\frac{\partial U_\vartheta}{\partial \vartheta} + U_\varphi \cos\varphi + W \sin\varphi\right) \tag{3}$$

By considering $\partial s = R_0 \partial \vartheta$, Eq.(3) can be written in the following form:

$$\varepsilon_s = \frac{1}{\left(1+\frac{\zeta}{R_\vartheta}\right)}\left(\frac{\partial U_s}{\partial s} + \frac{\cos\varphi}{R_0} U_\varphi + \frac{\sin\varphi}{R_0} W\right) \tag{3.1}$$

$$\varepsilon_n = \frac{\partial W}{\partial \zeta} \tag{4}$$

$$\gamma_{\varphi n} = \frac{1}{R_\varphi\left(1+\frac{\zeta}{R_\varphi}\right)}\frac{\partial W}{\partial \varphi} + R_\varphi\left(1+\frac{\zeta}{R_\varphi}\right)\frac{\partial}{\partial \zeta}\left(\frac{U_\varphi}{R_\varphi\left(1+\frac{\zeta}{R_\varphi}\right)}\right) \tag{5}$$

$$\gamma_{\vartheta n} = \frac{1}{R_0\left(1+\frac{\zeta}{R_\vartheta}\right)}\frac{\partial W}{\partial \vartheta} + R_0\left(1+\frac{\zeta}{R_\vartheta}\right)\frac{\partial}{\partial \zeta}\left(\frac{U_\vartheta}{R_0\left(1+\frac{\zeta}{R_\vartheta}\right)}\right) \tag{6}$$

By considering $\partial s = R_0 \partial \vartheta$, Eq.(6) can be written in the following form:

$$\gamma_{sn}=\frac{1}{\left(1+\frac{\zeta}{R_\vartheta}\right)}\frac{\partial W}{\partial s}+R_0\left(1+\frac{\zeta}{R_\vartheta}\right)\frac{\partial}{\partial\zeta}\left(\frac{U_s}{R_0\left(1+\frac{\zeta}{R_\vartheta}\right)}\right) \tag{6.1}$$

$$\gamma_{\varphi\vartheta}=\frac{1}{R_\varphi\left(1+\frac{\zeta}{R_\varphi}\right)}\frac{\partial U_\vartheta}{\partial\varphi}+\frac{1}{R_0\left(1+\frac{\zeta}{R_\vartheta}\right)}\left(\frac{\partial U_\varphi}{\partial\vartheta}-U_\vartheta\cos\varphi\right) \tag{7}$$

By considering $\partial s = R_0\partial\vartheta$, Eq.(7) can be written in the following form:

$$\gamma_{\varphi s}=\frac{1}{R_\varphi\left(1+\frac{\zeta}{R_\varphi}\right)}\frac{\partial U_s}{\partial\varphi}+\frac{1}{\left(1+\frac{\zeta}{R_\vartheta}\right)}\left(\frac{\partial U_\varphi}{\partial s}-\frac{\cos\varphi}{R_0}U_s\right) \tag{7.1}$$

By substituting Eq.(1) in Eqs.(2-7.1), relations between strains and displacements become:

$$\varepsilon_\varphi=\frac{1}{R_\varphi\left(1+\zeta/R_\varphi\right)}\left(\left(\frac{\partial u_\varphi}{\partial\varphi}+w\right)+\zeta\left(\frac{\partial\beta_\varphi}{\partial\varphi}\right)+\zeta^3\left(\frac{\partial\eta_\varphi}{\partial\varphi}\right)\right) \tag{8}$$

$$\varepsilon_\vartheta=\frac{1}{R_0\left(1+\zeta/R_\vartheta\right)}\left(\begin{array}{l}\left(\frac{\partial u_\vartheta}{\partial\vartheta}+u_\varphi\cos\varphi+w\sin\varphi\right)+\zeta\left(\frac{\partial\beta_\vartheta}{\partial\vartheta}+\beta_\varphi\cos\varphi\right)+\\+\zeta^3\left(\frac{\partial\eta_\vartheta}{\partial\vartheta}+\eta_\varphi\cos\varphi\right)\end{array}\right) \tag{9}$$

By considering $\partial s = R_0\partial\vartheta$, Eq.(9) can be written in the following form:

$$\varepsilon_s=\frac{1}{\left(1+\zeta/R_\vartheta\right)}\left(\begin{array}{l}\left(\frac{\partial u_s}{\partial s}+\frac{\cos\varphi}{R_0}u_\varphi+\frac{\sin\varphi}{R_0}w\right)+\zeta\left(\frac{\partial\beta_s}{\partial s}+\frac{\cos\varphi}{R_0}\beta_\varphi\right)+\\+\zeta^3\left(\frac{\partial\eta_s}{\partial s}+\frac{\cos\varphi}{R_0}\eta_\varphi\right)\end{array}\right) \tag{9.1}$$

$$\gamma_{\varphi n}=\frac{1}{\left(1+\zeta/R_\varphi\right)}\left(-\frac{1}{R_\varphi}u_\varphi+\frac{1}{R_\varphi}\frac{\partial w}{\partial\varphi}+\beta_\varphi+3\zeta^2\eta_\varphi+2\zeta^3\frac{\eta_\varphi}{R_\varphi}\right) \tag{10}$$

$$\gamma_{\vartheta n}=\frac{1}{\left(1+\zeta/R_{\vartheta}\right)}(-\frac{1}{R_{\vartheta}}u_{\vartheta}+\frac{1}{R_0}\frac{\partial w}{\partial \vartheta}+\beta_{\vartheta}+3\zeta^{2}\eta_{\vartheta}+2\zeta^{3}\frac{\eta_{\vartheta}}{R_{\vartheta}}) \tag{11}$$

By considering $\partial s = R_0 \partial \vartheta$, Eq.(11) can be written in the following form:

$$\gamma_{sn}=\frac{1}{\left(1+\zeta/R_{\vartheta}\right)}(-\frac{1}{R_{\vartheta}}u_{s}+\frac{\partial w}{\partial s}+\beta_{s}+3\zeta^{2}\eta_{s}+2\zeta^{3}\frac{\eta_{s}}{R_{\vartheta}}) \tag{11.1}$$

$$\begin{aligned}\gamma_{\varphi\vartheta}=&\frac{1}{R_{\varphi}\left(1+\zeta/R_{\varphi}\right)}\left(\frac{\partial u_{\vartheta}}{\partial \varphi}+\zeta\left(\frac{\partial \beta_{\vartheta}}{\partial \varphi}\right)+\zeta^{3}\left(\frac{\partial \eta_{\vartheta}}{\partial \varphi}\right)\right)+\\&+\frac{1}{R_0\left(1+\zeta/R_{\vartheta}\right)}\left(\frac{\partial u_{\varphi}}{\partial \vartheta}-u_{\vartheta}\cos\varphi+\zeta\left(\frac{\partial \beta_{\varphi}}{\partial \vartheta}-\beta_{\vartheta}\cos\varphi\right)+\zeta^{3}\left(\frac{\partial \eta_{\varphi}}{\partial \vartheta}-\eta_{\vartheta}\cos\varphi\right)\right)\end{aligned} \tag{12}$$

By considering $\partial s = R_0 \partial \vartheta$, Eq.(12) can be written in the following form:

$$\begin{aligned}\gamma_{\varphi s}=&\frac{1}{R_{\varphi}\left(1+\zeta/R_{\varphi}\right)}\left(\frac{\partial u_{s}}{\partial \varphi}+\zeta\left(\frac{\partial \beta_{s}}{\partial \varphi}\right)+\zeta^{3}\left(\frac{\partial \eta_{s}}{\partial \varphi}\right)\right)+\\&+\frac{1}{\left(1+\zeta/R_{\vartheta}\right)}\left(\frac{\partial u_{\varphi}}{\partial s}-\frac{\cos\varphi}{R_0}u_{s}+\zeta\left(\frac{\partial \beta_{\varphi}}{\partial s}-\frac{\cos\varphi}{R_0}\beta_{s}\right)+\zeta^{3}\left(\frac{\partial \eta_{\varphi}}{\partial s}-\frac{\cos\varphi}{R_0}\eta_{s}\right)\right)\end{aligned} \tag{12.1}$$

The transverse normal strain is $\varepsilon_n = 0$ as in the assumptions.

1.3.3 Relations between stresses and strains

Relations between stresses and strains for a single lamina functionally graded shell are as follows:

$$\begin{aligned}\sigma_{\varphi}&=\overline{Q}_{11}\varepsilon_{\varphi}+\overline{Q}_{12}\varepsilon_{s}\\\sigma_{s}&=\overline{Q}_{12}\varepsilon_{\varphi}+\overline{Q}_{22}\varepsilon_{s}\\\sigma_{n}&=0\\\tau_{\varphi s}&=\overline{Q}_{66}\gamma_{\varphi s}\\\tau_{\varphi n}&=\overline{Q}_{44}\gamma_{\varphi n}\\\tau_{sn}&=\overline{Q}_{55}\gamma_{sn}\end{aligned} \tag{13}$$

where [40,41]:

$$\overline{Q}_{11}=\overline{Q}_{22}=\frac{E(\zeta)}{1-\left(\nu(\zeta)\right)^2},\overline{Q}_{12}=\frac{\nu(\zeta)E(\zeta)}{1-\left(\nu(\zeta)\right)^2}$$
$$\overline{Q}_{66}=\overline{Q}_{44}=\overline{Q}_{55}=\frac{E(\zeta)}{2(1+\nu(\zeta))} \tag{14}$$

The material properties of the functionally graded lamina vary continuously and smoothly in the thickness direction ζ and are functions of volume fractions of constituent materials. Young's modulus $E(\zeta)$, Poisson's ratio $\nu(\zeta)$ and mass density $\rho(\zeta)$ of the functionally graded lamina can be expressed as a linear combination of the volume fraction:

$$\begin{aligned}\rho(\zeta)&=(\rho_C-\rho_M)V_C(\zeta)+\rho_M\\ E(\zeta)&=(E_C-E_M)V_C(\zeta)+E_M\\ \nu(\zeta)&=(\nu_C-\nu_M)V_C(\zeta)+\nu_M\end{aligned} \tag{15}$$

where $V_C(\zeta)$ is the volume fraction of the ceramic constituent material, while ρ_C, E_C, ν_C and ρ_M, E_M, ν_M represent mass density, Young's modulus, Poisson's ratio of the ceramic and metal constituent materials, respectively.

In this work, the ceramic volume fraction $V_C(\zeta)$ follows two simple four parameter power law distributions[40,41]:

$$FGM_{1,2(a,b,c,p)}:V_C(\zeta)=\left(1-a\left(\frac{1}{2}\pm\frac{\zeta}{h}\right)+b\left(\frac{1}{2}\pm\frac{\zeta}{h}\right)^c\right)^p \tag{16}$$

where the volume fraction index p ($0\le p\le\infty$) and the parameters a, b, c determine the material variation profile along the thickness direction. The elastic engineering constants are written as follows:

$$\left(A_{ij,}B_{ij,}D_{ij,}E_{ij,}F_{ij,}L_{ij,}H_{ij},M_{ij,}N_{ij},V_{ij}\right)=\int_{-\frac{h}{2}}^{+\frac{h}{2}}\overline{Q}_{ij}(1,\zeta,\zeta^2,\zeta^3,\zeta^4,\zeta^5,\zeta^6,\zeta^7,\zeta^8,\zeta^9)d\zeta \tag{17}$$

1.3.4 Internal forces and moment resultants

Normal forces, moments, and higher order moments, as well as the shear force and higher order shear force are all defined by the following expressions:

$$\left(N_{\varphi}, M_{\varphi}, P_{\varphi}\right) = \int_{-\frac{h}{2}}^{+\frac{h}{2}} \sigma_{\varphi}(1, \zeta, \zeta^3)\left(1+\frac{\zeta}{R_{\vartheta}}\right) d\zeta \tag{18}$$

$$\left(N_{s}, M_{s}, P_{s}\right) = \int_{-\frac{h}{2}}^{+\frac{h}{2}} \sigma_{s}(1, \zeta, \zeta^3)\left(1+\frac{\zeta}{R_{\varphi}}\right) d\zeta \tag{19}$$

$$\left(N_{\varphi s}, M_{\varphi s}, P_{\varphi s}\right) = \int_{-\frac{h}{2}}^{+\frac{h}{2}} \tau_{\varphi s}(1, \zeta, \zeta^3)\left(1+\frac{\zeta}{R_{\vartheta}}\right) d\zeta \tag{20}$$

$$\left(N_{s\varphi}, M_{s\varphi}, P_{s\varphi}\right) = \int_{-\frac{h}{2}}^{+\frac{h}{2}} \tau_{s\varphi}(1, \zeta, \zeta^3)\left(1+\frac{\zeta}{R_{\varphi}}\right) d\zeta \tag{21}$$

$$\left(T_{\varphi}, Q_{\varphi}, S_{\varphi}\right) = \int_{-\frac{h}{2}}^{+\frac{h}{2}} \tau_{\varphi n}(1, \zeta^2, \zeta^3)\left(1+\frac{\zeta}{R_{\vartheta}}\right) d\zeta \tag{22}$$

$$\left(T_{s}, Q_{s}, S_{s}\right) = \int_{-\frac{h}{2}}^{+\frac{h}{2}} \tau_{sn}(1, \zeta^2, \zeta^3)\left(1+\frac{\zeta}{R_{\varphi}}\right) d\zeta \tag{23}$$

By considering the effect of the initial curvature in the formulation, the stress resultants $N_{\varphi s}, M_{\varphi s}, P_{\varphi s}$ are not equal to the stress resultants $N_{s\varphi}, M_{s\varphi}, P_{s\varphi}$, respectively. This assumption derives from the consideration that the ratios ζ / R_{φ}, ζ / R_{ϑ} are not neglected with respect to unity. The effect of initial curvature is characterized by the following coefficients as firstly done by Toorani Lakis [63] and then improved by Tornabene [55]:

$$a_1=\frac{\sin\varphi}{R_0}-\frac{1}{R_\varphi},a_2=-\frac{1}{R_\varphi}\left(\frac{\sin\varphi}{R_0}-\frac{1}{R_\varphi}\right),a_3=\frac{1}{R_\varphi^2}\left(\frac{\sin\varphi}{R_0}-\frac{1}{R_\varphi}\right)$$
$$b_1=\frac{1}{R_\varphi}-\frac{\sin\varphi}{R_0},b_2=\frac{\sin\varphi}{R_0}\left(\frac{\sin\varphi}{R_0}-\frac{1}{R_\varphi}\right),b_3=-\frac{\sin^2\varphi}{R_0^2}\left(\frac{\sin\varphi}{R_0}-\frac{1}{R_\varphi}\right) \tag{24}$$

1.3.5 Normal and shear forces

By substituting Eqs.(13) in Eqs.(18-21), the following expressions are obtained:

$$\begin{aligned}N_\varphi=&\left(A_{11}+a_1B_{11}+a_2D_{11}+a_3E_{11}\right)\frac{1}{R_\varphi}\frac{\partial u_\varphi}{\partial\varphi}+A_{12}\frac{\cos\varphi}{R_0}u_\varphi+A_{12}\frac{\partial u_s}{\partial s}+\\&+A_{12}\frac{\sin\varphi}{R_0}w+\frac{1}{R_\varphi}\left(A_{11}+a_1B_{11}+a_2D_{11}+a_3E_{11}\right)w+\\&+\left(B_{11}+a_1D_{11}+a_2E_{11}+a_3F_{11}\right)\frac{1}{R_\varphi}\frac{\partial\beta_\varphi}{\partial\varphi}+B_{12}\frac{\cos\varphi}{R_0}\beta_\varphi+\\&+B_{12}\frac{\partial\beta_s}{\partial s}+\left(E_{11}+a_1F_{11}+a_2L_{11}+a_3H_{11}\right)\frac{1}{R_\varphi}\frac{\partial\eta_\varphi}{\partial\varphi}+E_{12}\frac{\cos\varphi}{R_0}\eta_\varphi+\\&+E_{12}\frac{\partial\eta_s}{\partial s}\end{aligned} \tag{25}$$

$$\begin{aligned}N_s=&A_{12}\frac{1}{R_\varphi}\frac{\partial u_\varphi}{\partial\varphi}+\frac{\cos\varphi}{R_0}\left(A_{22}+b_1B_{22}+b_2D_{22}+b_3E_{22}\right)u_\varphi+\\&+\left(A_{22}+b_1B_{22}+b_2D_{22}+b_3E_{22}\right)\frac{\partial u_s}{\partial s}+\\&+\frac{\sin\varphi}{R_0}\left(A_{22}+b_1B_{22}+b_2D_{22}+b_3E_{22}\right)w+\frac{1}{R_\varphi}A_{12}w+\\&+B_{12}\frac{1}{R_\varphi}\frac{\partial\beta_\varphi}{\partial\varphi}+\frac{\cos\varphi}{R_0}\left(B_{22}+b_1D_{22}+b_2E_{22}+b_3F_{22}\right)\beta_\varphi+\\&+\left(B_{22}+b_1D_{22}+b_2E_{22}+b_3F_{22}\right)\frac{\partial\beta_s}{\partial s}+\\&+E_{12}\frac{1}{R_\varphi}\frac{\partial\eta_\varphi}{\partial\varphi}+\frac{\cos\varphi}{R_0}\left(E_{22}+b_1F_{22}+b_2L_{22}+b_3H_{22}\right)\eta_\varphi+\\&+\left(E_{22}+b_1F_{22}+b_2L_{22}+b_3H_{22}\right)\frac{\partial\eta_s}{\partial s}\end{aligned} \tag{26}$$

$$N_{\varphi s} = A_{66}\frac{\partial u_\varphi}{\partial s} + \frac{1}{R_\varphi}\left(A_{66} + a_1 B_{66} + a_2 D_{66} + a_3 E_{66}\right)\frac{\partial u_s}{\partial \varphi} + A_{66}\left(-\frac{\cos\varphi}{R_0}\right)u_s +$$
$$+B_{66}\frac{\partial \beta_\varphi}{\partial s} + \frac{1}{R_\varphi}\left(B_{66} + a_1 D_{66} + a_2 E_{66} + a_3 F_{66}\right)\frac{\partial \beta_s}{\partial \varphi} + B_{66}\left(-\frac{\cos\varphi}{R_0}\right)\beta_s +$$
$$+E_{66}\frac{\partial \eta_\varphi}{\partial s} + \frac{1}{R_\varphi}\left(E_{66} + a_1 F_{66} + a_2 L_{66} + a_3 H_{66}\right)\frac{\partial \eta_s}{\partial \varphi} + E_{66}\left(-\frac{\cos\varphi}{R_0}\right)\eta_s \tag{27}$$

$$N_{s\varphi} = \left(A_{66} + b_1 B_{66} + b_2 D_{66} + b_3 E_{66}\right)\frac{\partial u_\varphi}{\partial s} + A_{66}\frac{1}{R_\varphi}\frac{\partial u_s}{\partial \varphi} +$$
$$+\left(-\frac{\cos\varphi}{R_0}\right)\left(A_{66} + b_1 B_{66} + b_2 D_{66} + b_3 E_{66}\right)u_s + \left(B_{66} + b_1 D_{66} + b_2 E_{66} + b_3 F_{66}\right)\frac{\partial \beta_\varphi}{\partial s} +$$
$$+B_{66}\frac{1}{R_\varphi}\frac{\partial \beta_s}{\partial \varphi} + \left(-\frac{\cos\varphi}{R_0}\right)\left(B_{66} + b_1 D_{66} + b_2 E_{66} + b_3 F_{66}\right)\beta_s +$$
$$+\left(E_{66} + b_1 F_{66} + b_2 L_{66} + b_3 H_{66}\right)\frac{\partial \eta_\varphi}{\partial s} + E_{66}\frac{1}{R_\varphi}\frac{\partial \eta_s}{\partial \varphi} + \left(-\frac{\cos\varphi}{R_0}\right)\left(E_{66} + b_1 F_{66} + b_2 L_{66} + b_3 H_{66}\right)\eta_s \tag{28}$$

1.3.6 Moments

By substituting Eqs.(13) in Eqs.(18-21), the following expressions are obtained:

$$M_\varphi = \left(B_{11} + a_1 D_{11} + a_2 E_{11} + a_3 F_{11}\right)\frac{1}{R_\varphi}\frac{\partial u_\varphi}{\partial \varphi} + B_{12}\frac{\cos\varphi}{R_0}u_\varphi + B_{12}\frac{\partial u_s}{\partial s} +$$
$$+B_{12}\frac{\sin\varphi}{R_0}w + \frac{1}{R_\varphi}\left(B_{11} + a_1 D_{11} + a_2 E_{11} + a_3 F_{11}\right)w +$$
$$+\left(D_{11} + a_1 E_{11} + a_2 F_{11} + a_3 L_{11}\right)\frac{1}{R_\varphi}\frac{\partial \beta_\varphi}{\partial \varphi} + D_{12}\frac{\cos\varphi}{R_0}\beta_\varphi +$$
$$+D_{12}\frac{\partial \beta_s}{\partial s} + \left(F_{11} + a_1 L_{11} + a_2 H_{11} + a_3 M_{11}\right)\frac{1}{R_\varphi}\frac{\partial \eta_\varphi}{\partial \varphi} + F_{12}\frac{\cos\varphi}{R_0}\eta_\varphi +$$
$$+F_{12}\frac{\partial \eta_s}{\partial s} \tag{29}$$

$$M_s = B_{12}\frac{1}{R_\varphi}\frac{\partial u_\varphi}{\partial \varphi} + \frac{\cos\varphi}{R_0}\left(B_{22} + b_1 D_{22} + b_2 E_{22} + b_3 F_{22}\right)u_\varphi +$$
$$+\left(B_{22} + b_1 D_{22} + b_2 E_{22} + b_3 F_{22}\right)\frac{\partial u_s}{\partial s} +$$
$$+\frac{\sin\varphi}{R_0}\left(B_{22} + b_1 D_{22} + b_2 E_{22} + b_3 F_{22}\right)w + \frac{1}{R_\varphi}B_{12}w +$$
$$+D_{12}\frac{1}{R_\varphi}\frac{\partial \beta_\varphi}{\partial \varphi} + \frac{\cos\varphi}{R_0}\left(D_{22} + b_1 E_{22} + b_2 F_{22} + b_3 L_{22}\right)\beta_\varphi +$$
$$+\left(D_{22} + b_1 E_{22} + b_2 F_{22} + b_3 L_{22}\right)\frac{\partial \beta_s}{\partial s} +$$
$$+F_{12}\frac{1}{R_\varphi}\frac{\partial \eta_\varphi}{\partial \varphi} + \frac{\cos\varphi}{R_0}\left(F_{22} + b_1 L_{22} + b_2 H_{22} + b_3 M_{22}\right)\eta_\varphi +$$
$$+\left(F_{22} + b_1 L_{22} + b_2 H_{22} + b_3 M_{22}\right)\frac{\partial \eta_s}{\partial s} \tag{30}$$

$$M_{\varphi s} = B_{66}\frac{\partial u_\varphi}{\partial s} + \frac{1}{R_\varphi}\left(B_{66} + a_1 D_{66} + a_2 E_{66} + a_3 F_{66}\right)\frac{\partial u_s}{\partial \varphi} + B_{66}\left(-\frac{\cos\varphi}{R_0}\right)u_s +$$
$$+D_{66}\frac{\partial \beta_\varphi}{\partial s} + \frac{1}{R_\varphi}\left(D_{66} + a_1 E_{66} + a_2 F_{66} + a_3 L_{66}\right)\frac{\partial \beta_s}{\partial \varphi} + D_{66}\left(-\frac{\cos\varphi}{R_0}\right)\beta_s +$$
$$+F_{66}\frac{\partial \eta_\varphi}{\partial s} + \frac{1}{R_\varphi}\left(F_{66} + a_1 L_{66} + a_2 H_{66} + a_3 M_{66}\right)\frac{\partial \eta_s}{\partial \varphi} + F_{66}\left(-\frac{\cos\varphi}{R_0}\right)\eta_s \tag{31}$$

$$M_{s\varphi} = \left(B_{66} + b_1 D_{66} + b_2 E_{66} + b_3 F_{66}\right)\frac{\partial u_\varphi}{\partial s} +$$
$$+B_{66}\frac{1}{R_\varphi}\frac{\partial u_s}{\partial \varphi} + \left(-\frac{\cos\varphi}{R_0}\right)\left(B_{66} + b_1 D_{66} + b_2 E_{66} + b_3 F_{66}\right)u_s +$$
$$+\left(D_{66} + b_1 E_{66} + b_2 F_{66} + b_3 L_{66}\right)\frac{\partial \beta_\varphi}{\partial s} +$$
$$+D_{66}\frac{1}{R_\varphi}\frac{\partial \beta_s}{\partial \varphi} + \left(-\frac{\cos\varphi}{R_0}\right)\left(D_{66} + b_1 E_{66} + b_2 F_{66} + b_3 L_{66}\right)\beta_s +$$
$$+\left(F_{66} + b_1 L_{66} + b_2 H_{66} + b_3 M_{66}\right)\frac{\partial \eta_\varphi}{\partial s} +$$
$$+F_{66}\frac{1}{R_\varphi}\frac{\partial \eta_s}{\partial \varphi} + \left(-\frac{\cos\varphi}{R_0}\right)\left(F_{66} + b_1 L_{66} + b_2 H_{66} + b_3 M_{66}\right)\eta_s \tag{32}$$

1.3.7 Higher order moments

By substituting Eqs.(13) in Eqs.(18-21), the following expressions are obtained:

$$
\begin{aligned}
P_{\varphi} &= \left(E_{11}+a_1F_{11}+a_2L_{11}+a_3H_{11}\right)\frac{1}{R_{\varphi}}\frac{\partial u_{\varphi}}{\partial\varphi}+E_{12}\frac{\cos\varphi}{R_0}u_{\varphi}\\
&+E_{12}\frac{\partial u_s}{\partial s}+E_{12}\frac{\sin\varphi}{R_0}w+\frac{1}{R_{\varphi}}\left(E_{11}+a_1F_{11}+a_2L_{11}+a_3H_{11}\right)w+\\
&+\left(F_{11}+a_1L_{11}+a_2H_{11}+a_3M_{11}\right)\frac{1}{R_{\varphi}}\frac{\partial\beta_{\varphi}}{\partial\varphi}+F_{12}\frac{\cos\varphi}{R_0}\beta_{\varphi}+\\
&+F_{12}\frac{\partial\beta_s}{\partial s}+\left(H_{11}+a_1M_{11}+a_2N_{11}+a_3V_{11}\right)\frac{1}{R_{\varphi}}\frac{\partial\eta_{\varphi}}{\partial\varphi}+H_{12}\frac{\cos\varphi}{R_0}\eta_{\varphi}+\\
&+H_{12}\frac{\partial\eta_s}{\partial s}
\end{aligned}
\tag{33}
$$

$$
\begin{aligned}
P_s &= E_{12}\frac{1}{R_{\varphi}}\frac{\partial u_{\varphi}}{\partial\varphi}+\frac{\cos\varphi}{R_0}\left(E_{22}+b_1F_{22}+b_2L_{22}+b_3H_{22}\right)u_{\varphi}+\\
&+\left(E_{22}+b_1F_{22}+b_2L_{22}+b_3H_{22}\right)\frac{\partial u_s}{\partial s}+\\
&+\frac{\sin\varphi}{R_0}\left(E_{22}+b_1F_{22}+b_2L_{22}+b_3H_{22}\right)w+\frac{1}{R_{\varphi}}E_{12}w+\\
&+F_{12}\frac{1}{R_{\varphi}}\frac{\partial\beta_{\varphi}}{\partial\varphi}+\frac{\cos\varphi}{R_0}\left(F_{22}+b_1L_{22}+b_2H_{22}+b_3M_{22}\right)\beta_{\varphi}+\\
&+\left(F_{22}+b_1L_{22}+b_2H_{22}+b_3M_{22}\right)\frac{\partial\beta_s}{\partial s}+\\
&+H_{12}\frac{1}{R_{\varphi}}\frac{\partial\eta_{\varphi}}{\partial\varphi}+\frac{\cos\varphi}{R_0}\left(H_{22}+b_1M_{22}+b_2N_{22}+b_3V_{22}\right)\eta_{\varphi}+\\
&+\left(H_{22}+b_1M_{22}+b_2N_{22}+b_3V_{22}\right)\frac{\partial\eta_s}{\partial s}
\end{aligned}
\tag{34}
$$

$$
\begin{aligned}
P_{\varphi s} &= E_{66}\frac{\partial u_{\varphi}}{\partial s}+\frac{1}{R_{\varphi}}\left(E_{66}+a_1F_{66}+a_2L_{66}+a_3H_{66}\right)\frac{\partial u_s}{\partial\varphi}+E_{66}\left(-\frac{\cos\varphi}{R_0}\right)u_s+\\
&+F_{66}\frac{\partial\beta_{\varphi}}{\partial s}+\frac{1}{R_{\varphi}}\left(F_{66}+a_1L_{66}+a_2M_{66}+a_3N_{66}\right)\frac{\partial\beta_s}{\partial\varphi}+F_{66}\left(-\frac{\cos\varphi}{R_0}\right)\beta_s+\\
&+H_{66}\frac{\partial\eta_{\varphi}}{\partial s}+\frac{1}{R_{\varphi}}\left(H_{66}+a_1M_{66}+a_2N_{66}+a_3V_{66}\right)\frac{\partial\eta_s}{\partial\varphi}+H_{66}\left(-\frac{\cos\varphi}{R_0}\right)\eta_s
\end{aligned}
\tag{35}
$$

$$P_{s\varphi} = \left(E_{66} + b_1 F_{66} + b_2 L_{66} + b_3 H_{66}\right)\frac{\partial u_\varphi}{\partial s} + E_{66}\frac{1}{R_\varphi}\frac{\partial u_s}{\partial \varphi} +$$
$$+\left(-\frac{\cos\varphi}{R_0}\right)\left(E_{66} + b_1 F_{66} + b_2 L_{66} + b_3 H_{66}\right)u_s +$$
$$+\left(F_{66} + b_1 L_{66} + b_2 H_{66} + b_3 M_{66}\right)\frac{\partial \beta_\varphi}{\partial s} + F_{66}\frac{1}{R_\varphi}\frac{\partial \beta_s}{\partial \varphi} +$$
$$+\left(-\frac{\cos\varphi}{R_0}\right)\left(F_{66} + b_1 L_{66} + b_2 H_{66} + b_3 M_{66}\right)\beta_s +$$
$$+\left(H_{66} + b_1 M_{66} + b_2 N_{66} + b_3 V_{66}\right)\frac{\partial \eta_\varphi}{\partial s} + H_{66}\frac{1}{R_\varphi}\frac{\partial \eta_s}{\partial \varphi} +$$
$$+\left(-\frac{\cos\varphi}{R_0}\right)\left(H_{66} + b_1 M_{66} + b_2 N_{66} + b_3 V_{66}\right)\eta_s \tag{36}$$

1.3.8 Shear forces

By substituting Eqs.(13) in Eqs.(22,23), the following expressions are obtained:

$$T_\varphi = -\frac{1}{R_\varphi}\left(A_{44} + a_1 B_{44} + a_2 D_{44} + a_3 E_{44}\right)u_\varphi +$$
$$+\left(\frac{1}{R_\varphi}\right)\left(A_{44} + a_1 B_{44} + a_2 D_{44} + a_3 E_{44}\right)\frac{\partial w}{\partial \varphi} +$$
$$+\left(A_{44} + a_1 B_{44} + a_2 D_{44} + a_3 E_{44}\right)\beta_\varphi +$$
$$+3\left(D_{44} + a_1 E_{44} + a_2 F_{44} + a_3 L_{44}\right)\eta_\varphi + \frac{2}{R_\varphi}\left(E_{44} + a_1 F_{44} + a_2 L_{44} + a_3 H_{44}\right)\eta_\varphi \tag{37}$$

$$T_s = -\frac{\sin\varphi}{R_0}\left(A_{55} + b_1 B_{55} + b_2 D_{55} + b_3 E_{55}\right)u_s$$
$$+\left(A_{55} + b_1 B_{55} + b_2 D_{55} + b_3 E_{55}\right)\frac{\partial w}{\partial s} + \left(A_{55} + b_1 B_{55} + b_2 D_{55} + b_3 E_{55}\right)\beta_s +$$
$$+3\left(D_{55} + b_1 E_{55} + b_2 F_{55} + b_3 L_{55}\right)\eta_s + \frac{2\sin\varphi}{R_0}\left(E_{55} + b_1 F_{55} + b_2 L_{55} + b_3 H_{55}\right)\eta_s \tag{38}$$

$$Q_\varphi = -\frac{1}{R_\varphi}\left(D_{44} + a_1E_{44} + a_2F_{44} + a_3L_{44}\right)u_\varphi + \left(\frac{1}{R_\varphi}\right)\left(D_{44} + a_1E_{44} + a_2F_{44} + a_3L_{44}\right)\frac{\partial w}{\partial \varphi} +$$
$$+\left(D_{44} + a_1E_{44} + a_2F_{44} + a_3L_{44}\right)\beta_\varphi +$$
$$+3\left(F_{44} + a_1L_{44} + a_2H_{44} + a_3M_{44}\right)\eta_\varphi + \frac{2}{R_\varphi}\left(L_{44} + a_1H_{44} + a_2M_{44} + a_3N_{44}\right)\eta_\varphi \tag{39}$$

$$Q_s = -\frac{\sin\varphi}{R_0}\left(D_{55} + b_1E_{55} + b_2F_{55} + b_3L_{55}\right)u_s + \left(D_{55} + b_1E_{55} + b_2F_{55} + b_3L_{55}\right)\frac{\partial w}{\partial s} +$$
$$+\left(D_{55} + b_1E_{55} + b_2F_{55} + b_3L_{55}\right)\beta_s + 3\left(F_{55} + b_1L_{55} + b_2H_{55} + b_3M_{55}\right)\eta_s +$$
$$+\frac{2\sin\varphi}{R_0}\left(F_{55} + b_1L_{55} + b_2H_{55} + b_3M_{55}\right)\eta_s \tag{40}$$

$$S_\varphi = -\frac{1}{R_\varphi}\left(E_{44} + a_1F_{44} + a_2L_{44} + a_3H_{44}\right)u_\varphi +$$
$$+\left(\frac{1}{R_\varphi}\right)\left(E_{44} + a_1F_{44} + a_2L_{44} + a_3H_{44}\right)\frac{\partial w}{\partial \varphi} +$$
$$+\left(E_{44} + a_1F_{44} + a_2L_{44} + a_3H_{44}\right)\beta_\varphi +$$
$$3\left(L_{44} + a_1H_{44} + a_2M_{44} + a_3N_{44}\right)\eta_\varphi + \frac{2}{R_\varphi}\left(H_{44} + a_1M_{44} + a_2N_{44} + a_3V_{44}\right)\eta_\varphi \tag{41}$$

$$S_s = -\frac{\sin\varphi}{R_0}\left(E_{55} + b_1F_{55} + b_2L_{55} + b_3H_{55}\right)u_s + \left(E_{55} + b_1F_{55} + b_2L_{55} + b_3H_{55}\right)\frac{\partial w}{\partial s} +$$
$$+\left(E_{55} + b_1F_{55} + b_2L_{55} + b_3H_{55}\right)\beta_s + 3\left(L_{55} + b_1H_{55} + b_2M_{55} + b_3N_{55}\right)\eta_s +$$
$$+\frac{2\sin\varphi}{R_0}\left(H_{55} + b_1M_{55} + b_2N_{55} + b_3V_{55}\right)\eta_s \tag{42}$$

1.3.9 Equilibrium equations

Here we use the principle of virtual displacements to derive the equilibrium equations consistent with the displacement field equations (1). The principle of virtual displacements can be stated in analytical form as:

$$\int_{-\frac{h}{2}}^{+\frac{h}{2}}\int_{\Omega}(\sigma_\varphi\delta\varepsilon_\varphi+\sigma_s\delta\varepsilon_s+\tau_{\varphi s}\delta\gamma_{\varphi s}+\tau_{\varphi n}\delta\gamma_{\varphi n}+\tau_{sn}\delta\gamma_{sn})d\zeta\,d\Omega-\int_{\Omega}p_\varphi\delta u_\varphi R_\varphi d\varphi ds-\int_{\Omega}p_s\delta u_s R_\varphi d\varphi ds+$$
$$-\int_{\Omega}p_n\delta w R_\varphi d\varphi ds-\int_{\Omega}m_\varphi\delta\beta_\varphi R_\varphi d\varphi ds-\int_{\Omega}m_s\delta\beta_s R_\varphi d\varphi ds-\int_{\Omega}r_\varphi\delta\eta_\varphi R_\varphi d\varphi ds-\int_{\Omega}r_s\delta\eta_s R_\varphi d\varphi ds=0 \tag{43}$$

where:

$$d\Omega=R_\varphi\left(1+\frac{\zeta}{R_\varphi}\right)d\varphi R_0\left(1+\frac{\zeta}{R_\vartheta}\right)d\vartheta \tag{43.1}$$

and $p_\varphi, p_s, p_n, m_\varphi, m_s, r_\varphi, r_s$ are the external uniform loadings applied on the reference surface.

By introducing Eqs.(8-12.1;13) into Eq.(43) and considering Eqs.(18-23), the following terms of the integral can be separated as follows:

$$\int_{-\frac{h}{2}}^{+\frac{h}{2}}\int_{\Omega}\sigma_\varphi\delta\varepsilon_\varphi d\Omega=$$
$$\int_{\Omega}N_\varphi\left(\frac{\partial\delta u_\varphi}{\partial\varphi}\right)R_0 d\varphi d\vartheta+\int_{\Omega}N_\varphi(\delta w)R_0 d\varphi d\vartheta+\int_{\Omega}M_\varphi\left(\frac{\partial\delta\beta_\varphi}{\partial\varphi}\right)R_0 d\varphi d\vartheta+\int_{\Omega}P_\varphi\left(\frac{\partial\delta\eta_\varphi}{\partial\varphi}\right)R_0 d\varphi d\vartheta \tag{43.2}$$

$$\int_{-\frac{h}{2}}^{+\frac{h}{2}}\int_{\Omega}\sigma_\vartheta\delta\varepsilon_\vartheta d\Omega=\int_{\Omega}N_\vartheta\left(\frac{\partial\delta u_\vartheta}{\partial\vartheta}\right)R_\varphi d\varphi d\vartheta+\int_{\Omega}N_\vartheta\cos\varphi(\delta u_\varphi)R_\varphi d\varphi d\vartheta+\int_{\Omega}N_\vartheta\sin\varphi(\delta w)R_\varphi d\varphi d\vartheta$$
$$+\int_{\Omega}M_\vartheta\left(\frac{\partial\delta\beta_\vartheta}{\partial\vartheta}\right)R_\varphi d\varphi d\vartheta+\int_{\Omega}M_\vartheta\cos\varphi(\delta\beta_\varphi)R_\varphi d\varphi d\vartheta+ \tag{43.3}$$
$$+\int_{\Omega}P_\vartheta\left(\frac{\partial\delta\eta_\vartheta}{\partial\vartheta}\right)R_\varphi d\varphi d\vartheta+\int_{\Omega}P_\vartheta\cos\varphi(\delta\eta_\varphi)R_\varphi d\varphi d\vartheta$$

$$\int_{-\frac{h}{2}}^{+\frac{h}{2}}\int_{\Omega}\tau_{\varphi\vartheta}\delta\gamma_{\varphi\vartheta}d\Omega=\int_{\Omega}N_{\varphi\vartheta}R_0\left(\frac{\partial\delta u_{\vartheta}}{\partial\varphi}\right)d\varphi d\vartheta+\int_{\Omega}M_{\varphi\vartheta}\left(\frac{\partial\delta\beta_{\vartheta}}{\partial\varphi}\right)R_0 d\varphi d\vartheta+\int_{\Omega}P_{\varphi\vartheta}\left(\frac{\partial\delta\eta_{\vartheta}}{\partial\varphi}\right)R_0 d\varphi d\vartheta+$$
$$+\int_{\Omega}N_{\vartheta\varphi}\left(\frac{\partial\delta u_{\varphi}}{\partial\vartheta}\right)R_{\varphi}d\varphi d\vartheta+\int_{\Omega}N_{\vartheta\varphi}\left(-\cos\varphi\right)(\delta u_{\vartheta})R_{\varphi}d\varphi d\vartheta+\int_{\Omega}M_{\vartheta\varphi}\left(\frac{\partial\delta\beta_{\varphi}}{\partial\vartheta}\right)R_{\varphi}d\varphi d\vartheta+ \quad (43.4)$$
$$+\int_{\Omega}M_{\vartheta\varphi}(-\cos\varphi)\delta\beta_{\vartheta}R_{\varphi}d\varphi d\vartheta+\int_{\Omega}P_{\vartheta\varphi}\left(\frac{\partial\delta\eta_{\varphi}}{\partial\vartheta}\right)R_{\varphi}d\varphi d\vartheta+\int_{\Omega}P_{\vartheta\varphi}(-\cos\varphi)R_{\varphi}\delta\eta_{\vartheta}d\varphi d\vartheta$$

$$\int_{-\frac{h}{2}}^{+\frac{h}{2}}\int_{\Omega}\tau_{\varphi n}\delta\gamma_{\varphi n}d\Omega=\int_{\Omega}(-T_{\varphi})\left(\delta u_{\varphi}\right)R_0 d\varphi d\vartheta+\int_{\Omega}T_{\varphi}\left(\frac{\partial\delta w}{\partial\varphi}\right)R_0 d\varphi d\vartheta+\int_{\Omega}T_{\varphi}\left(\delta\beta_{\varphi}\right)R_0 R_{\varphi}d\varphi d\vartheta+ \quad (43.5)$$
$$+\int_{\Omega}3Q_{\varphi}\left(\delta\eta_{\varphi}\right)R_0 R_{\varphi}d\varphi d\vartheta+\int_{\Omega}S_{\varphi}2\left(\delta\eta_{\varphi}\right)R_0 d\varphi d\vartheta$$

$$\int_{-\frac{h}{2}}^{+\frac{h}{2}}\int_{\Omega}\tau_{\vartheta n}\delta\gamma_{\vartheta n}d\Omega=\int_{\Omega}T_{\vartheta}\left(-\sin\varphi\right)\left(\delta u_{\vartheta}\right)R_{\varphi}d\varphi d\vartheta+\int_{\Omega}T_{\vartheta}\left(\frac{\partial\delta w}{\partial\vartheta}\right)R_{\varphi}d\varphi d\vartheta+\int_{\Omega}T_{\vartheta}\left(\delta\beta_{\vartheta}\right)R_{\varphi}R_0 d\varphi d\vartheta+$$
$$+\int_{\Omega}3Q_{\vartheta}\left(\delta\eta_{\vartheta}\right)R_{\varphi}R_0 d\varphi d\vartheta+\int_{\Omega}2S_{\vartheta}\left(\delta\eta_{\vartheta}\right)(\sin\varphi)R_{\varphi}d\varphi d\vartheta \quad (43.6)$$

By solving the integrals by parts in Eqs.(43.2-43.6), the resulting expressions are obtained:

$$\int_{\Omega}N_{\varphi}\left(\frac{\partial\delta u_{\varphi}}{\partial\varphi}\right)R_0 d\varphi d\vartheta=N_{\varphi}R_0\delta u_{\varphi}\Big|_{\partial\Omega}-\int_{\Omega}\left(\frac{\partial\left(N_{\varphi}R_0\right)}{\partial\varphi}\right)\delta u_{\varphi}d\varphi d\vartheta \quad (43.7)$$

$$\int_{\Omega}M_{\varphi}\left(\frac{\partial\delta\beta_{\varphi}}{\partial\varphi}\right)R_0 d\varphi d\vartheta=M_{\varphi}R_0\delta\beta_{\varphi}\Big|_{\partial\Omega}-\int_{\Omega}\left(\frac{\partial\left(M_{\varphi}R_0\right)}{\partial\varphi}\right)\delta\beta_{\varphi}d\varphi d\vartheta \quad (43.8)$$

$$\int_{\Omega}P_{\varphi}\left(\frac{\partial\delta\eta_{\varphi}}{\partial\varphi}\right)R_0 d\varphi d\vartheta=P_{\varphi}R_0\delta\eta_{\varphi}\Big|_{\partial\Omega}-\int_{\Omega}\left(\frac{\partial\left(P_{\varphi}R_0\right)}{\partial\varphi}\right)\delta\eta_{\varphi}d\varphi d\vartheta \quad (43.9)$$

$$\int_{\Omega} N_{\vartheta}\left(\frac{\partial \delta u_{\vartheta}}{\partial \vartheta}\right) R_{\varphi} d\varphi d\vartheta = N_{\vartheta} R_{\varphi} \delta u_{\vartheta}\Big|_{\partial\Omega} - \int_{\Omega}\left(\frac{\partial\left(N_{\vartheta} R_{\varphi}\right)}{\partial \vartheta}\right) \delta u_{\vartheta} d\varphi d\vartheta \tag{43.10}$$

$$\int_{\Omega} M_{\vartheta}\left(\frac{\partial \delta \beta_{\vartheta}}{\partial \vartheta}\right) R_{\varphi} d\varphi d\vartheta = M_{\vartheta} R_{\varphi} \delta \beta_{\vartheta}\Big|_{\partial\Omega} - \int_{\Omega}\left(\frac{\partial\left(M_{\vartheta} R_{\varphi}\right)}{\partial \vartheta}\right) \delta \beta_{\vartheta} d\varphi d\vartheta \tag{43.11}$$

$$\int_{\Omega} P_{\vartheta}\left(\frac{\partial \delta \eta_{\vartheta}}{\partial \vartheta}\right) R_{\varphi} d\varphi d\vartheta = P_{\vartheta} R_{\varphi} \delta \eta_{\vartheta}\Big|_{\partial\Omega} - \int_{\Omega}\left(\frac{\partial\left(P_{\vartheta} R_{\varphi}\right)}{\partial \vartheta}\right) \delta \eta_{\vartheta} d\varphi d\vartheta \tag{43.12}$$

$$\int_{\Omega} N_{\varphi\vartheta}\left(\frac{\partial \delta u_{\vartheta}}{\partial \varphi}\right) R_{0} d\varphi d\vartheta = N_{\varphi\vartheta} R_{0} \delta u_{\vartheta}\Big|_{\partial\Omega} - \int_{\Omega}\left(\frac{\partial\left(N_{\varphi\vartheta} R_{0}\right)}{\partial \varphi}\right) \delta u_{\vartheta} d\varphi d\vartheta \tag{43.13}$$

$$\int_{\Omega} M_{\varphi\vartheta}\left(\frac{\partial \delta \beta_{\vartheta}}{\partial \varphi}\right) R_{0} d\varphi d\vartheta = M_{\varphi\vartheta} R_{0} \delta \beta_{\vartheta}\Big|_{\partial\Omega} - \int_{\Omega}\left(\frac{\partial\left(M_{\varphi\vartheta} R_{0}\right)}{\partial \varphi}\right) \delta \beta_{\vartheta} d\varphi d\vartheta \tag{43.14}$$

$$\int_{\Omega} P_{\varphi\vartheta}\left(\frac{\partial \delta \eta_{\vartheta}}{\partial \varphi}\right) R_{0} d\varphi d\vartheta = P_{\varphi\vartheta} R_{0} \delta \eta_{\vartheta}\Big|_{\partial\Omega} - \int_{\Omega}\left(\frac{\partial\left(P_{\varphi\vartheta} R_{0}\right)}{\partial \varphi}\right) \delta \eta_{\vartheta} d\varphi d\vartheta \tag{43.15}$$

$$\int_{\Omega} N_{\vartheta\varphi}\left(\frac{\partial \delta u_{\varphi}}{\partial \vartheta}\right) R_{\varphi} d\varphi d\vartheta = N_{\vartheta\varphi} R_{\varphi} \delta u_{\varphi}\Big|_{\partial\Omega} - \int_{\Omega}\left(\frac{\partial\left(N_{\vartheta\varphi} R_{\varphi}\right)}{\partial \vartheta}\right) \delta u_{\varphi} d\varphi d\vartheta \tag{43.16}$$

$$\int_{\Omega} M_{\vartheta\varphi}\left(\frac{\partial \delta \beta_{\varphi}}{\partial \vartheta}\right) R_{\varphi} d\varphi d\vartheta = M_{\vartheta\varphi} R_{\varphi} \delta \beta_{\varphi}\Big|_{\partial\Omega} - \int_{\Omega}\left(\frac{\partial\left(M_{\vartheta\varphi} R_{\varphi}\right)}{\partial \vartheta}\right) \delta \beta_{\varphi} d\varphi d\vartheta \tag{43.17}$$

$$\int_{\Omega} P_{\vartheta\varphi}\left(\frac{\partial \delta \eta_{\varphi}}{\partial \vartheta}\right) R_{\varphi} d\varphi d\vartheta = P_{\vartheta\varphi} R_{\varphi} \delta \eta_{\varphi}\Big|_{\partial\Omega} - \int_{\Omega}\left(\frac{\partial\left(P_{\vartheta\varphi} R_{\varphi}\right)}{\partial \vartheta}\right) \delta \eta_{\varphi} d\varphi d\vartheta \tag{43.18}$$

$$\int_{\Omega} T_{\varphi}\left(\frac{\partial \delta w}{\partial \varphi}\right) R_0 d\varphi d\vartheta = T_{\varphi} R_0 \delta w\big|_{\partial\Omega} - \int_{\Omega}\left(\frac{\partial\left(T_{\varphi} R_0\right)}{\partial \varphi}\right)\delta w d\varphi d\vartheta \tag{43.19}$$

$$\int_{\Omega} T_{\vartheta}\left(\frac{\partial \delta w}{\partial \vartheta}\right) R_{\varphi} d\varphi d\vartheta = T_{\vartheta} R_{\varphi} \delta w\big|_{\partial\Omega} - \int_{\Omega}\left(\frac{\partial\left(T_{\vartheta} R_{\varphi}\right)}{\partial \vartheta}\right)\delta w d\varphi d\vartheta \tag{43.20}$$

By setting the coefficients of $\delta u_{\varphi}, \delta u_s, \delta w, \delta\beta_{\varphi}, \delta\beta_s, \delta\eta_{\varphi}, \delta\eta_s$ to zero separately, the equilibrium equations are obtained:

$$\delta u_{\varphi}: \ \frac{1}{R_{\varphi}}\frac{\partial N_{\varphi}}{\partial \varphi} + \frac{\partial N_{s\varphi}}{\partial s} + \frac{N_{\varphi} - N_s}{R_0}\cos\varphi + \frac{T_{\varphi}}{R_{\varphi}} + p_{\varphi} = 0 \tag{44}$$

$$\delta u_s: \ \frac{\partial N_s}{\partial s} + \frac{1}{R_{\varphi}}\frac{\partial N_{\varphi s}}{\partial \varphi} + \frac{N_{\varphi s} + N_{s\varphi}}{R_0}\cos\varphi + \frac{T_s}{R_0}\sin\varphi + p_s = 0 \tag{45}$$

$$\delta w: \ \frac{1}{R_{\varphi}}\frac{\partial T_{\varphi}}{\partial \varphi} + \frac{\partial T_s}{\partial s} + T_{\varphi}\frac{\cos\varphi}{R_0} - N_s\frac{\sin\varphi}{R_0} - \frac{N_{\varphi}}{R_{\varphi}} + p_n = 0 \tag{46}$$

$$\delta\beta_{\varphi}: \ \frac{1}{R_{\varphi}}\frac{\partial M_{\varphi}}{\partial \varphi} + \frac{\partial M_{s\varphi}}{\partial s} + \frac{\left(M_{\varphi} - M_s\right)}{R_0}\cos\varphi - T_{\varphi} + m_{\varphi} = 0 \tag{47}$$

$$\delta\beta_s: \ \frac{1}{R_{\varphi}}\frac{\partial M_{\varphi s}}{\partial \varphi} + \frac{\partial M_s}{\partial s} + \frac{M_{\varphi s} + M_{s\varphi}}{R_0}\cos\varphi - T_s + m_s = 0 \tag{48}$$

$$\delta\eta_{\varphi}: \ \frac{1}{R_{\varphi}}\frac{\partial P_{\varphi}}{\partial \varphi} + \frac{\partial P_{s\varphi}}{\partial s} + \frac{P_{\varphi} - P_s}{R_0}\cos\varphi - 3Q_{\varphi} - 2\frac{S_{\varphi}}{R_{\varphi}} + r_{\varphi} = 0 \tag{49}$$

$$\delta\eta_s: \ \frac{1}{R_{\varphi}}\frac{\partial P_{\varphi s}}{\partial \varphi} + \frac{\partial P_s}{\partial s} + \frac{P_{\varphi s} + P_{s\varphi}}{R_0}\cos\varphi - 3Q_s - 2S_s\frac{\sin\varphi}{R_0} + r_s = 0 \tag{50}$$

It is worth noting that Eqs.(44-50) are derived by taking into account the definitions (18-23) of forces and moment resultants. The first three Eqs.(44,45,46) express the translational equilibrium along the meridional φ, circumferential s, and normal ζ direction, respectively. The last four Eqs.(47,48,49,50) are rotational equilibrium equations about the s and φ directions, respectively. In particular, the first two are the effective rotational equilibrium equations, whereas the second two represent fictitious equations, which are derived by the computation of the additional terms of displacement.

Then, substituting the expressions (25-42) for the in-plane meridional, circumferential, and shearing force resultants $N_\varphi, N_s, N_{\varphi s}, N_{s\varphi}$, the analogous couples $M_\varphi, M_s, M_{\varphi s}, M_{s\varphi}, P_\varphi, P_s, P_{\varphi s}, P_{s\varphi}$ and the transverse shear force resultants $T_\varphi, T_s, Q_\varphi, Q_s, S_\varphi, S_s$, Eqs.(44-50) yield the fundamental system of equations.

It should be noted that the loadings on the middle surface can be expressed in terms of the loadings on the upper ($p_\varphi^t, p_s^t, p_n^t$) and lower ($p_\varphi^b, p_s^b, p_n^b$) boundary surfaces of the shell by using the static equivalence principle, as follows:

$$
\begin{aligned}
p_\varphi &= p_\varphi^t\left(1+\frac{h}{2R_\varphi}\right)\left(1+\frac{h\sin\varphi}{2R_0}\right)+p_\varphi^b\left(1-\frac{h}{2R_\varphi}\right)\left(1-\frac{h\sin\varphi}{2R_0}\right)\\
p_s &= p_s^t\left(1+\frac{h}{2R_\varphi}\right)\left(1+\frac{h\sin\varphi}{2R_0}\right)+p_s^b\left(1-\frac{h}{2R_\varphi}\right)\left(1-\frac{h\sin\varphi}{2R_0}\right)\\
p_n &= p_n^t\left(1+\frac{h}{2R_\varphi}\right)\left(1+\frac{h\sin\varphi}{2R_0}\right)+p_n^b\left(1-\frac{h}{2R_\varphi}\right)\left(1-\frac{h\sin\varphi}{2R_0}\right)\\
m_\varphi &= p_\varphi^t\frac{h}{2}\left(1+\frac{h}{2R_\varphi}\right)\left(1+\frac{h\sin\varphi}{2R_0}\right)-p_\varphi^b\frac{h}{2}\left(1-\frac{h}{2R_\varphi}\right)\left(1-\frac{h\sin\varphi}{2R_0}\right)\\
m_s &= p_s^t\frac{h}{2}\left(1+\frac{h}{2R_\varphi}\right)\left(1+\frac{h\sin\varphi}{2R_0}\right)-p_s^b\frac{h}{2}\left(1-\frac{h}{2R_\varphi}\right)\left(1-\frac{h\sin\varphi}{2R_0}\right)\\
r_\varphi &= p_\varphi^t\frac{h^3}{8}\left(1+\frac{h}{2R_\varphi}\right)\left(1+\frac{h\sin\varphi}{2R_0}\right)-p_\varphi^b\frac{h^3}{8}\left(1-\frac{h}{2R_\varphi}\right)\left(1-\frac{h\sin\varphi}{2R_0}\right)\\
r_s &= p_s^t\frac{h^3}{8}\left(1+\frac{h}{2R_\varphi}\right)\left(1+\frac{h\sin\varphi}{2R_0}\right)-p_s^b\frac{h^3}{8}\left(1-\frac{h}{2R_\varphi}\right)\left(1-\frac{h\sin\varphi}{2R_0}\right)
\end{aligned}
\qquad (51)
$$

where p_φ^t, p_s^t, p_n^t are the meridional, circumferential and normal forces applied to the upper surface, and p_φ^b, p_s^b , p_n^t are the meridional, circumferential and normal forces applied to the lower surface.

The boundary conditions considered in this study are the fully clamped edge boundary condition (C), the simply supported edge boundary condition (S) and the free edge boundary condition (F). They assume the following form:

Clamped edge boundary condition (C):

$$u_\varphi = u_s = w = \beta_\varphi = \beta_s = \eta_\varphi = \eta_s = 0 \text{ at } \varphi = \varphi_0 \text{ or } \varphi = \varphi_1 \quad 0 \le s \le s_0, \qquad (52)$$

$$u_\varphi = u_s = w = \beta_\varphi = \beta_s = \eta_\varphi = \eta_s = 0 \text{ at } s = 0 \text{ or } s = s_0 \quad \varphi_0 \le \varphi \le \varphi_1 \qquad (53)$$

Simply supported boundary condition (S):

$$u_\varphi = w = \beta_\varphi = \eta_\varphi = 0 \quad N_\varphi = M_\varphi = P_\varphi = 0 \text{ at } \varphi = \varphi_0 \text{ or } \varphi = \varphi_1 \;\; 0 \le s \le s_0, \tag{54}$$

$$u_s = w = \beta_s = \eta_s = 0 \;\; N_s = M_s = P_s = 0 \text{ at } s = 0 \text{ or } s = s_0 \;\; \varphi_0 \le \varphi \le \varphi_1 \tag{55}$$

Free edge boundary condition (F):

$$N_\varphi = N_{\varphi s} = T_\varphi = M_\varphi = M_{\varphi s} = P_\varphi = P_{\varphi s} = 0$$
$$\text{at } \varphi = \varphi_0 \text{ or } \varphi = \varphi_1, \;\; 0 \le s \le s_0 \tag{56}$$

$$N_s = N_{s\varphi} = T_s = M_s = M_{s\varphi} = P_s = P_{s\varphi} = 0$$
$$\text{at } s = 0 \text{ or } s = s_{0,} \;\; \varphi_0 \le \varphi \le \varphi_1 \tag{57}$$

In the above Eqs.(52-57) boundary conditions, it has been assumed $s_0 = 2\pi R_0$. In order to analyze the whole shell of revolution, and not a panel, the kinematic and physical compatibility must be added to the previous external boundary conditions. They represent the condition of continuity related to displacements and internal stress resultants. Their analytical forms are proposed as follows:

Kinematic compatibility conditions along the closing meridian $(s = 0, 2\pi R_0)$:

$$\begin{aligned} &u_\varphi(\varphi,0) = u_\varphi(\varphi,s_0), \;\; u_s(\varphi,0) = u_s(\varphi,s_0), \\ &w(\varphi,0) = w(\varphi,s_0), \;\; \beta_\varphi(\varphi,0) = \beta_\varphi(\varphi,s_0), \\ &\beta_s(\varphi,0) = \beta_s(\varphi,s_0), \;\; \eta_\varphi(\varphi,0) = \eta_\varphi(\varphi,s_0), \\ &\eta_s(\varphi,0) = \eta_s(\varphi,s_0) \;\; \varphi_0 \le \varphi \le \varphi_1 \end{aligned} \tag{58}$$

Physical compatibility conditions along the closing meridian $(s = 0, 2\pi R_0)$:

$$\begin{aligned} &N_s(\varphi,0) = N_s(\varphi,s_0), \;\; N_{s\varphi}(\varphi,0) = N_{s\varphi}(\varphi,s_0), \\ &T_s(\varphi,0) = T_s(\varphi,s_0), \;\; M_s(\varphi,0) = M_s(\varphi,s_0), \\ &M_{s\varphi}(\varphi,0) = M_{s\varphi}(\varphi,s_0) \;\; , P_s(\varphi,0) = P_s(\varphi,s_0), \\ &P_{s\varphi}(\varphi,0) = P_{s\varphi}(\varphi,s_0), \;\; \varphi_0 \le \varphi \le \varphi_1 \end{aligned} \tag{59}$$

1.3.9.1 The first fundamental equilibrium equation

By substituting Eqs.(25-42) in Eq.(44) the first fundamental equation is written as follows:

$$
\begin{aligned}
&\frac{1}{R_\varphi^2}\left(A_{11}+a_1B_{11}+a_2D_{11}+a_3E_{11}\right)\frac{\partial^2 u_\varphi}{\partial\varphi^2}+\left(A_{66}+b_1B_{66}+b_2D_{66}+b_3E_{66}\right)\frac{\partial^2 u_\varphi}{\partial s^2}+\\
&+\left(-\frac{1}{R_\varphi^3}\frac{\partial R_\varphi}{\partial\varphi}\right)\left(A_{11}+a_1B_{11}+a_2D_{11}+a_3E_{11}\right)\frac{\partial u_\varphi}{\partial\varphi}+\frac{1}{R_\varphi^2}\left(B_{11}\frac{\partial a_1}{\partial\varphi}+D_{11}\frac{\partial a_2}{\partial\varphi}+E_{11}\frac{\partial a_3}{\partial\varphi}\right)\frac{\partial u_\varphi}{\partial\varphi}+\\
&+\frac{\cos\varphi}{R_0R_\varphi}\left(A_{11}+a_1B_{11}+a_2D_{11}+a_3E_{11}\right)\frac{\partial u_\varphi}{\partial\varphi}+\\
&+A_{12}\left(-\frac{\sin\varphi}{R_0R_\varphi}\right)u_\varphi-\left(\frac{\cos\varphi}{R_0}\right)^2\left(A_{22}+b_1B_{22}+b_2D_{22}+b_3E_{22}\right)u_\varphi+\\
&-\frac{1}{R_\varphi^2}\left(A_{44}+a_1B_{44}+a_2D_{44}+a_3E_{44}\right)u_\varphi+\\
&+A_{12}\frac{1}{R_\varphi}\frac{\partial^2 u_s}{\partial\varphi\partial s}+A_{66}\frac{1}{R_\varphi}\frac{\partial^2 u_s}{\partial s\partial\varphi}+\\
&+\left(-\frac{\cos\varphi}{R_0}\right)\left(A_{66}+b_1B_{66}+b_2D_{66}+b_3E_{66}\right)\frac{\partial u_s}{\partial s}+\\
&-\frac{\cos\varphi}{R_0}\left(A_{22}+b_1B_{22}+b_2D_{22}+b_3E_{22}\right)\frac{\partial u_s}{\partial s}+
\end{aligned}
\tag{60}
$$

$$
\begin{aligned}
&+A_{12}\frac{\sin\varphi}{R_0R_\varphi}\frac{\partial w}{\partial\varphi}+\frac{1}{R_\varphi^2}\left(A_{11}+a_1B_{11}+a_2D_{11}+a_3E_{11}\right)\frac{\partial w}{\partial\varphi}+\frac{1}{R_\varphi^2}\left(A_{44}+a_1B_{44}+a_2D_{44}+a_3E_{44}\right)\frac{\partial w}{\partial\varphi}+\\
&+\left(-\frac{1}{R_\varphi^3}\frac{\partial R_\varphi}{\partial\varphi}\right)\left(A_{11}+a_1B_{11}+a_2D_{11}+a_3E_{11}\right)w+\frac{1}{R_\varphi^2}\left(B_{11}\frac{\partial a_1}{\partial\varphi}+D_{11}\frac{\partial a_2}{\partial\varphi}+E_{11}\frac{\partial a_3}{\partial\varphi}\right)w+\\
&+\frac{\cos\varphi}{R_0R_\varphi}\left(A_{11}+a_1B_{11}+a_2D_{11}+a_3E_{11}\right)w-\frac{\cos\varphi\sin\varphi}{R_0^2}\left(A_{22}+b_1B_{22}+b_2D_{22}+b_3E_{22}\right)w+\\
&+\frac{1}{R_\varphi^2}\left(B_{11}+a_1D_{11}+a_2E_{11}+a_3F_{11}\right)\left(\frac{\partial^2\beta_\varphi}{\partial\varphi^2}\right)+\left(B_{66}+b_1D_{66}+b_2E_{66}+b_3F_{66}\right)\frac{\partial^2\beta_\varphi}{\partial s^2}+\\
&-\frac{1}{R_\varphi^3}\frac{\partial R_\varphi}{\partial\varphi}\left(B_{11}+a_1D_{11}+a_2E_{11}+a_3F_{11}\right)\frac{\partial\beta_\varphi}{\partial\varphi}+\\
&+\frac{1}{R_\varphi^2}\left(D_{11}\frac{\partial a_1}{\partial\varphi}+E_{11}\frac{\partial a_2}{\partial\varphi}+F_{11}\frac{\partial a_3}{\partial\varphi}\right)\frac{\partial\beta_\varphi}{\partial\varphi}+\\
&+\frac{\cos\varphi}{R_0R_\varphi}\left(B_{11}+a_1D_{11}+a_2E_{11}+a_3F_{11}\right)\frac{\partial\beta_\varphi}{\partial\varphi}+\\
&-B_{12}\frac{\sin\varphi}{R_0R_\varphi}\beta_\varphi-\left(\frac{\cos\varphi}{R_0}\right)^2\left(B_{22}+b_1D_{22}+b_2E_{22}+b_3F_{22}\right)\beta_\varphi+\\
&+\frac{1}{R_\varphi}\left(A_{44}+a_1B_{44}+a_2D_{44}+a_3E_{44}\right)\beta_\varphi+\\
&+B_{12}\frac{1}{R_\varphi}\frac{\partial^2\beta_s}{\partial\varphi\partial s}+\frac{1}{R_\varphi}B_{66}\frac{\partial^2\beta_s}{\partial s\partial\varphi}+
\end{aligned}
\tag{60}
$$

$$
\begin{aligned}
&+\left(-\frac{\cos\varphi}{R_0}\right)\left(B_{66}+b_1D_{66}+b_2E_{66}+b_3F_{66}\right)\frac{\partial\beta_s}{\partial s}+\\
&-\frac{\cos\varphi}{R_0}\left(B_{22}+b_1D_{22}+b_2E_{22}+b_3F_{22}\right)\frac{\partial\beta_s}{\partial s}+\\
&+\frac{1}{R_\varphi^2}\left(E_{11}+a_1F_{11}+a_2L_{11}+a_3H_{11}\right)\left(\frac{\partial^2\eta_\varphi}{\partial\varphi^2}\right)+\\
&+\left(E_{66}+b_1F_{66}+b_2L_{66}+b_3H_{66}\right)\frac{\partial^2\eta_\varphi}{\partial s^2}+\\
&-\frac{1}{R_\varphi^3}\frac{\partial R_\varphi}{\partial\varphi}\left(E_{11}+a_1F_{11}+a_2L_{11}+a_3H_{11}\right)\frac{\partial\eta_\varphi}{\partial\varphi}+\frac{1}{R_\varphi^2}\left(F_{11}\frac{\partial a_1}{\partial\varphi}+L_{11}\frac{\partial a_2}{\partial\varphi}+H_{11}\frac{\partial a_3}{\partial\varphi}\right)\frac{\partial\eta_\varphi}{\partial\varphi}+\\
&+\frac{\cos\varphi}{R_0R_\varphi}\left(E_{11}+a_1F_{11}+a_2L_{11}+a_3H_{11}\right)\frac{\partial\eta_\varphi}{\partial\varphi}+
\end{aligned}
\tag{60}
$$

$$
\begin{aligned}
&-E_{12}\frac{\sin\varphi}{R_0R_\varphi}\eta_\varphi-\left(\frac{\cos\varphi}{R_0}\right)^2\left(E_{22}+b_1F_{22}+b_2L_{22}+b_3H_{22}\right)\eta_\varphi+\\
&+\frac{3}{R_\varphi}\left(D_{44}+a_1E_{44}+a_2F_{44}+a_3L_{44}\right)\eta_\varphi+\frac{2}{R_\varphi^2}\left(E_{44}+a_1F_{44}+a_2L_{44}+a_3H_{44}\right)\eta_\varphi+\\
&+\frac{1}{R_\varphi}E_{12}\frac{\partial^2\eta_s}{\partial\varphi\partial s}+\frac{1}{R_\varphi}E_{66}\frac{\partial^2\eta_s}{\partial s\partial\varphi}-\frac{\cos\varphi}{R_0}\left(E_{66}+b_1F_{66}+b_2L_{66}+b_3H_{66}\right)\frac{\partial\eta_s}{\partial s}+\\
&-\frac{\cos\varphi}{R_0}\left(E_{22}+b_1F_{22}+b_2L_{22}+b_3H_{22}\right)\frac{\partial\eta_s}{\partial s}+p_\varphi=0
\end{aligned}
\tag{60}
$$

1.3.9.2 The second fundamental equilibrium equation

By substituting Eqs.(25-42) in Eq.(45) the second fundamental equation is written as follows:

$$
\begin{aligned}
&\frac{1}{R_\varphi}A_{12}\frac{\partial^2u_\varphi}{\partial s\partial\varphi}+\frac{1}{R_\varphi}A_{66}\frac{\partial^2u_\varphi}{\partial\varphi\partial s}+\\
&+\frac{\cos\varphi}{R_0}\left(A_{22}+b_1B_{22}+b_2D_{22}+b_3E_{22}\right)\frac{\partial u_\varphi}{\partial s}+\\
&+\frac{\cos\varphi}{R_0}\left(A_{66}+b_1B_{66}+b_2D_{66}+b_3E_{66}\right)\frac{\partial u_\varphi}{\partial s}+\\
&+\left(A_{22}+b_1B_{22}+b_2D_{22}+b_3E_{22}\right)\frac{\partial^2u_s}{\partial s^2}+\\
&+\frac{1}{R_\varphi^2}\left(A_{66}+a_1B_{66}+a_2D_{66}+a_3E_{66}\right)\left(\frac{\partial^2u_s}{\partial\varphi^2}\right)+\\
&-\frac{1}{R_\varphi^3}\frac{\partial R_\varphi}{\partial\varphi}\left(A_{66}+a_1B_{66}+a_2D_{66}+a_3E_{66}\right)\frac{\partial u_s}{\partial\varphi}+\\
&+\frac{1}{R_\varphi^2}\left(B_{66}\frac{\partial a_1}{\partial\varphi}+D_{66}\frac{\partial a_2}{\partial\varphi}+E_{66}\frac{\partial a_3}{\partial\varphi}\right)\frac{\partial u_s}{\partial\varphi}+\\
&+\frac{\cos\varphi}{R_0R_\varphi}\left(A_{66}+a_1B_{66}+a_2D_{66}+a_3E_{66}\right)\frac{\partial u_s}{\partial\varphi}+\\
&+A_{66}\frac{\sin\varphi}{R_0R_\varphi}u_s-\left(\frac{\cos\varphi}{R_0}\right)^2\left(A_{66}+b_1B_{66}+b_2D_{66}+b_3E_{66}\right)u_s+\\
&-\left(\frac{\sin\varphi}{R_0}\right)^2\left(A_{55}+b_1B_{55}+b_2D_{55}+b_3E_{55}\right)u_s+
\end{aligned}
\tag{61}
$$

$$
\begin{aligned}
&+\frac{\sin\varphi}{R_0}\left(A_{22}+b_1B_{22}+b_2D_{22}+b_3E_{22}\right)\frac{\partial w}{\partial s}+A_{12}\frac{1}{R_\varphi}\frac{\partial w}{\partial s}+\\
&+\frac{\sin\varphi}{R_0}\left(A_{55}+b_1B_{55}+b_2D_{55}+b_3E_{55}\right)\frac{\partial w}{\partial s}+\\
&+B_{12}\frac{1}{R_\varphi}\frac{\partial^2\beta_\varphi}{\partial s\partial\varphi}+B_{66}\frac{1}{R_\varphi}\frac{\partial^2\beta_\varphi}{\partial\varphi\partial s}+\\
&+\frac{\cos\varphi}{R_0}\left(B_{22}+b_1D_{22}+b_2E_{22}+b_3F_{22}\right)\frac{\partial\beta_\varphi}{\partial s}+\\
&+\frac{\cos\varphi}{R_0}\left(B_{66}+b_1D_{66}+b_2E_{66}+b_3F_{66}\right)\frac{\partial\beta_\varphi}{\partial s}+\\
&+\left(B_{22}+b_1D_{22}+b_2E_{22}+b_3F_{22}\right)\frac{\partial^2\beta_s}{\partial s^2}+\\
&+\frac{1}{R_\varphi^2}\left(B_{66}+a_1D_{66}+a_2E_{66}+a_3F_{66}\right)\frac{\partial^2\beta_s}{\partial\varphi^2}+\\
&-\frac{1}{R_\varphi^3}\frac{\partial R_\varphi}{\partial\varphi}\left(B_{66}+a_1D_{66}+a_2E_{66}+a_3F_{66}\right)\frac{\partial\beta_s}{\partial\varphi}+\\
&+\frac{1}{R_\varphi^2}\left(D_{66}\frac{\partial a_1}{\partial\varphi}+E_{66}\frac{\partial a_2}{\partial\varphi}+F_{66}\frac{\partial a_3}{\partial\varphi}\right)\frac{\partial\beta_s}{\partial\varphi}+\\
&+\frac{\cos\varphi}{R_0R_\varphi}\left(B_{66}+a_1D_{66}+a_2E_{66}+a_3F_{66}\right)\frac{\partial\beta_s}{\partial\varphi}+\\
&+B_{66}\frac{\sin\varphi}{R_0R_\varphi}\beta_s-\left(\frac{\cos\varphi}{R_0}\right)^2\left(B_{66}+b_1D_{66}+b_2E_{66}+b_3F_{66}\right)\beta_s+\\
&+\frac{\sin\varphi}{R_0}\left(A_{55}+b_1B_{55}+b_2D_{55}+b_3E_{55}\right)\beta_s+
\end{aligned}
\tag{61}
$$

$$
\begin{aligned}
&+\frac{1}{R_\varphi}E_{12}\frac{\partial^2\eta_\varphi}{\partial s\partial\varphi}+E_{66}\frac{1}{R_\varphi}\frac{\partial^2\eta_\varphi}{\partial\varphi\partial s}+\\
&+\frac{\cos\varphi}{R_0}\left(E_{22}+b_1F_{22}+b_2L_{22}+b_3H_{22}\right)\frac{\partial\eta_\varphi}{\partial s}+\\
&+\frac{\cos\varphi}{R_0}\left(E_{66}+b_1F_{66}+b_2L_{66}+b_3H_{66}\right)\frac{\partial\eta_\varphi}{\partial s}+\\
&+\left(E_{22}+b_1F_{22}+b_2L_{22}+b_3H_{22}\right)\frac{\partial^2\eta_s}{\partial s^2}+\\
&+\frac{1}{R_\varphi^2}\left(E_{66}+a_1F_{66}+a_2L_{66}+a_3H_{66}\right)\frac{\partial^2\eta_s}{\partial\varphi^2}+\\
&-\frac{1}{R_\varphi^3}\frac{\partial R_\varphi}{\partial\varphi}\left(E_{66}+a_1F_{66}+a_2L_{66}+a_3H_{66}\right)\frac{\partial\eta_s}{\partial\varphi}+\\
&+\frac{1}{R_\varphi^2}\left(F_{66}\frac{\partial a_1}{\partial\varphi}+L_{66}\frac{\partial a_2}{\partial\varphi}+H_{66}\frac{\partial a_3}{\partial\varphi}\right)\frac{\partial\eta_s}{\partial\varphi}+\\
&+\frac{\cos\varphi}{R_0R_\varphi}\left(E_{66}+a_1F_{66}+a_2L_{66}+a_3H_{66}\right)\frac{\partial\eta_s}{\partial\varphi}+\\
&+E_{66}\frac{\sin\varphi}{R_0R_\varphi}\eta_s-\left(\frac{\cos\varphi}{R_0}\right)^2\left(E_{66}+b_1F_{66}+b_2L_{66}+b_3H_{66}\right)\eta_s+\\
&+3\frac{\sin\varphi}{R_0}\left(D_{55}+b_1E_{55}+b_2F_{55}+b_3L_{55}\right)\eta_s+\\
&+2\left(\frac{\sin\varphi}{R_0}\right)^2\left(E_{55}+b_1F_{55}+b_2L_{55}+b_3H_{55}\right)\eta_s+p_s=0
\end{aligned}
\tag{61}
$$

1.3.9.3 The third fundamental equilibrium equation

By substituting Eqs.(25-42) in Eq.(46) the third fundamental equation is written as follows:

$$
\begin{aligned}
&-\frac{1}{R_\varphi^2}\left(A_{44}+a_1B_{44}+a_2D_{44}+a_3E_{44}\right)\frac{\partial u_\varphi}{\partial\varphi}+\\
&-\frac{1}{R_\varphi^2}\left(A_{11}+a_1B_{11}+a_2D_{11}+a_3E_{11}\right)\frac{\partial u_\varphi}{\partial\varphi}+\\
&-A_{12}\frac{\sin\varphi}{R_0R_\varphi}\frac{\partial u_\varphi}{\partial\varphi}+\\
&+\frac{1}{R_\varphi^3}\frac{\partial R_\varphi}{\partial\varphi}\left(A_{44}+a_1B_{44}+a_2D_{44}+a_3E_{44}\right)u_\varphi-\frac{1}{R_\varphi^2}\left(B_{44}\frac{\partial a_1}{\partial\varphi}+D_{44}\frac{\partial a_2}{\partial\varphi}+E_{44}\frac{\partial a_3}{\partial\varphi}\right)u_\varphi+\\
&-\frac{\sin\varphi\cos\varphi}{R_0^2}\left(A_{22}+b_1B_{22}+b_2D_{22}+b_3E_{22}\right)u_\varphi-A_{12}\frac{\cos\varphi}{R_0R_\varphi}u_\varphi+\\
&-\frac{\cos\varphi}{R_0R_\varphi}\left(A_{44}+a_1B_{44}+a_2D_{44}+a_3E_{44}\right)u_\varphi+
\end{aligned}
\tag{62}
$$

$$
\begin{aligned}
&-\frac{\sin\varphi}{R_0}\left(A_{55}+b_1B_{55}+b_2D_{55}+b_3E_{55}\right)\frac{\partial u_s}{\partial s}+\\
&-A_{12}\frac{1}{R_\varphi}\frac{\partial u_s}{\partial s}-\frac{\sin\varphi}{R_0}\left(A_{22}+b_1B_{22}+b_2D_{22}+b_3E_{22}\right)\frac{\partial u_s}{\partial s}+\\
&+\frac{1}{R_\varphi^2}\left(A_{44}+a_1B_{44}+a_2D_{44}+a_3E_{44}\right)\left(\frac{\partial^2 w}{\partial\varphi^2}\right)+\\
&+\left(A_{55}+b_1B_{55}+b_2D_{55}+b_3E_{55}\right)\frac{\partial^2 w}{\partial s^2}+\\
&-\frac{1}{R_\varphi^3}\frac{\partial R_\varphi}{\partial\varphi}\left(A_{44}+a_1B_{44}+a_2D_{44}+a_3E_{44}\right)\frac{\partial w}{\partial\varphi}+\\
&+\frac{1}{R_\varphi^2}\left(B_{44}\frac{\partial a_1}{\partial\varphi}+D_{44}\frac{\partial a_2}{\partial\varphi}+E_{44}\frac{\partial a_3}{\partial\varphi}\right)\left(\frac{\partial w}{\partial\varphi}\right)+\\
&+\frac{\cos\varphi}{R_0R_\varphi}\left(A_{44}+a_1B_{44}+a_2D_{44}+a_3E_{44}\right)\frac{\partial w}{\partial\varphi}+\\
&-2A_{12}\frac{\sin\varphi}{R_0R_\varphi}w-\frac{1}{R_\varphi^2}\left(A_{11}+a_1B_{11}+a_2D_{11}+a_3E_{11}\right)w+\\
&-\left(\frac{\sin\varphi}{R_0}\right)^2\left(A_{22}+b_1B_{22}+b_2D_{22}+b_3E_{22}\right)w+\\
&+\frac{1}{R_\varphi}\left(A_{44}+a_1B_{44}+a_2D_{44}+a_3E_{44}\right)\frac{\partial\beta_\varphi}{\partial\varphi}+\\
&-\frac{1}{R_\varphi^2}\left(B_{11}+a_1D_{11}+a_2E_{11}+a_3F_{11}\right)\frac{\partial\beta_\varphi}{\partial\varphi}+
\end{aligned}
\tag{62}
$$

$$
\begin{aligned}
&-B_{12}\frac{\sin\varphi}{R_0R_\varphi}\frac{\partial\beta_\varphi}{\partial\varphi}+\\
&+\frac{1}{R_\varphi}\left(B_{44}\frac{\partial a_1}{\partial\varphi}+D_{44}\frac{\partial a_2}{\partial\varphi}+E_{44}\frac{\partial a_3}{\partial\varphi}\right)\beta_\varphi+\frac{\cos\varphi}{R_0}\left(A_{44}+a_1B_{44}+a_2D_{44}+a_3E_{44}\right)\beta_\varphi+\\
&-B_{12}\frac{\cos\varphi}{R_0R_\varphi}\beta_\varphi-\frac{\sin\varphi\cos\varphi}{R_0^2}\left(B_{22}+b_1D_{22}+b_2E_{22}+b_3F_{22}\right)\beta_\varphi+\\
&+\left(A_{55}+b_1B_{55}+b_2D_{55}+b_3E_{55}\right)\frac{\partial\beta_s}{\partial s}+\\
&-\frac{1}{R_\varphi}B_{12}\frac{\partial\beta_s}{\partial s}-\frac{\sin\varphi}{R_0}\left(B_{22}+b_1D_{22}+b_2E_{22}+b_3F_{22}\right)\frac{\partial\beta_s}{\partial s}+\\
&+\frac{3}{R_\varphi}\left(D_{44}+a_1E_{44}+a_2F_{44}+a_3L_{44}\right)\frac{\partial\eta_\varphi}{\partial\varphi}+\frac{2}{R_\varphi^2}\left(E_{44}+a_1F_{44}+a_2L_{44}+a_3H_{44}\right)\frac{\partial\eta_\varphi}{\partial\varphi}+\\
&-\frac{1}{R_\varphi^2}\left(E_{11}+a_1F_{11}+a_2L_{11}+a_3H_{11}\right)\frac{\partial\eta_\varphi}{\partial\varphi}-E_{12}\frac{\sin\varphi}{R_0R_\varphi}\frac{\partial\eta_\varphi}{\partial\varphi}+\\
&+\frac{3}{R_\varphi}\left(E_{44}\frac{\partial a_1}{\partial\varphi}+F_{44}\frac{\partial a_2}{\partial\varphi}+L_{44}\frac{\partial a_3}{\partial\varphi}\right)\eta_\varphi-\frac{2}{R_\varphi^3}\frac{\partial R_\varphi}{\partial\varphi}\left(E_{44}+a_1F_{44}+a_2L_{44}+a_3H_{44}\right)\eta_\varphi+\\
&+\frac{2}{R_\varphi^2}\left(F_{44}\frac{\partial a_1}{\partial\varphi}+L_{44}\frac{\partial a_2}{\partial\varphi}+H_{44}\frac{\partial a_3}{\partial\varphi}\right)\eta_\varphi+\\
&+\frac{3\cos\varphi}{R_0}\left(D_{44}+a_1E_{44}+a_2F_{44}+a_3L_{44}\right)\eta_\varphi+\frac{2\cos\varphi}{R_0R_\varphi}\left(E_{44}+a_1F_{44}+a_2L_{44}+a_3H_{44}\right)\eta_\varphi+\\
&-E_{12}\frac{\cos\varphi}{R_0R_\varphi}\eta_\varphi-\frac{\sin\varphi\cos\varphi}{R_0^2}\left(E_{22}+b_1F_{22}+b_2L_{22}+b_3H_{22}\right)\eta_\varphi+\\
&+3\left(D_{55}+b_1E_{55}+b_2F_{55}+b_3L_{55}\right)\frac{\partial\eta_s}{\partial s}+\\
&+\frac{2\sin\varphi}{R_0}\left(E_{55}+b_1F_{55}+b_2L_{55}+b_3H_{55}\right)\frac{\partial\eta_s}{\partial s}-E_{12}\frac{1}{R_\varphi}\frac{\partial\eta_s}{\partial s}+\\
&-\frac{\sin\varphi}{R_0}\left(E_{22}+b_1F_{22}+b_2L_{22}+b_3H_{22}\right)\frac{\partial\eta_s}{\partial s}+p_n=0
\end{aligned}
\tag{62}
$$

1.3.9.4 The fourth fundamental equilibrium equation

By substituting Eqs.(25-42) in Eq.(47) the fourth fundamental equation is written as follows:

$$
\begin{aligned}
&\frac{1}{R_\varphi^2}\left(B_{11}+a_1D_{11}+a_2E_{11}+a_3F_{11}\right)\frac{\partial^2 u_\varphi}{\partial\varphi^2}+\\
&+\left(B_{66}+b_1D_{66}+b_2E_{66}+b_3F_{66}\right)\frac{\partial^2 u_\varphi}{\partial s^2}+\\
&-\frac{1}{R_\varphi^3}\frac{\partial R_\varphi}{\partial\varphi}\left(B_{11}+a_1D_{11}+a_2E_{11}+a_3F_{11}\right)\frac{\partial u_\varphi}{\partial\varphi}+\\
&+\frac{1}{R_\varphi^2}\left(D_{11}\frac{\partial a_1}{\partial\varphi}+E_{11}\frac{\partial a_2}{\partial\varphi}+F_{11}\frac{\partial a_3}{\partial\varphi}\right)\frac{\partial u_\varphi}{\partial\varphi}+\\
&+\frac{\cos\varphi}{R_0R_\varphi}\left(B_{11}+a_1D_{11}+a_2E_{11}+a_3F_{11}\right)\frac{\partial u_\varphi}{\partial\varphi}+\\
&-B_{12}\frac{\sin\varphi}{R_0R_\varphi}u_\varphi-\left(\frac{\cos\varphi}{R_0}\right)^2\left(B_{22}+b_1D_{22}+b_2E_{22}+b_3F_{22}\right)u_\varphi+\\
&+\frac{1}{R_\varphi}\left(A_{44}+a_1B_{44}+a_2D_{44}+a_3E_{44}\right)u_\varphi+\\
&+B_{12}\frac{1}{R_\varphi}\frac{\partial^2 u_s}{\partial\varphi\partial s}+\frac{1}{R_\varphi}B_{66}\frac{\partial^2 u_s}{\partial s\partial\varphi}-\frac{\cos\varphi}{R_0}\left(B_{66}+b_1D_{66}+b_2E_{66}+b_3F_{66}\right)\frac{\partial u_s}{\partial s}+\\
&-\frac{\cos\varphi}{R_0}\left(B_{22}+b_1D_{22}+b_2E_{22}+b_3F_{22}\right)\frac{\partial u_s}{\partial s}+
\end{aligned}
\tag{63}
$$

$$+\frac{\sin\varphi}{R_0 R_\varphi}B_{12}\frac{\partial w}{\partial\varphi}+\frac{1}{R_\varphi^2}\left(B_{11}+a_1D_{11}+a_2E_{11}+a_3F_{11}\right)\frac{\partial w}{\partial\varphi}+$$
$$-\left(\frac{1}{R_\varphi}\right)\left(A_{44}+a_1B_{44}+a_2D_{44}+a_3E_{44}\right)\frac{\partial w}{\partial\varphi}+$$
$$-\frac{1}{R_\varphi^3}\frac{\partial R_\varphi}{\partial\varphi}\left(B_{11}+a_1D_{11}+a_2E_{11}+a_3F_{11}\right)w+$$
$$+\frac{1}{R_\varphi^2}\left(D_{11}\frac{\partial a_1}{\partial\varphi}+B_{11}\frac{\partial a_2}{\partial\varphi}+F_{11}\frac{\partial a_3}{\partial\varphi}\right)w+$$
$$+\frac{\cos\varphi}{R_0 R_\varphi}\left(B_{11}+a_1D_{11}+a_2E_{11}+a_3F_{11}\right)w+$$
$$-\frac{\cos\varphi\sin\varphi}{R_0^2}\left(B_{22}+b_1D_{22}+b_2E_{22}+b_3F_{22}\right)w+$$
$$+\frac{1}{R_\varphi^2}\left(D_{11}+a_1E_{11}+a_2F_{11}+a_3L_{11}\right)\frac{\partial^2\beta_\varphi}{\partial\varphi^2}+$$
$$+\left(D_{66}+b_1E_{66}+b_2F_{66}+b_3L_{66}\right)\frac{\partial^2\beta_\varphi}{\partial s^2}+$$
$$-\frac{1}{R_\varphi^3}\frac{\partial R_\varphi}{\partial\varphi}\left(D_{11}+a_1E_{11}+a_2F_{11}+a_3L_{11}\right)\frac{\partial\beta_\varphi}{\partial\varphi}+\frac{1}{R_\varphi^2}\left(E_{11}\frac{\partial a_1}{\partial\varphi}+F_{11}\frac{\partial a_2}{\partial\varphi}+L_{11}\frac{\partial a_3}{\partial\varphi}\right)\frac{\partial\beta_\varphi}{\partial\varphi}+$$
$$+\frac{\cos\varphi}{R_0 R_\varphi}\left(D_{11}+a_1E_{11}+a_2F_{11}+a_3L_{11}\right)\frac{\partial\beta_\varphi}{\partial\varphi}+$$

(63)

$$
\begin{aligned}
&-D_{12}\frac{\sin\varphi}{R_0R_\varphi}\beta_\varphi-\left(\frac{\cos\varphi}{R_0}\right)^2\left(D_{22}+b_1E_{22}+b_2F_{22}+b_3L_{22}\right)\beta_\varphi+\\
&-\left(A_{44}+a_1B_{44}+a_2D_{44}+a_3E_{44}\right)\beta_\varphi+\\
&+D_{12}\frac{1}{R_\varphi}\frac{\partial^2\beta_s}{\partial\varphi\partial s}+\frac{1}{R_\varphi}D_{66}\frac{\partial^2\beta_s}{\partial s\partial\varphi}\\
&-\frac{\cos\varphi}{R_0}\left(D_{66}+b_1E_{66}+b_2F_{66}+b_3L_{66}\right)\frac{\partial\beta_s}{\partial s}+\\
&-\frac{\cos\varphi}{R_0}\left(D_{22}+b_1E_{22}+b_2F_{22}+b_3L_{22}\right)\frac{\partial\beta_s}{\partial s}+\\
&+\frac{1}{R_\varphi^2}\left(F_{11}+a_1L_{11}+a_2H_{11}+a_3M_{11}\right)\frac{\partial^2\eta_\varphi}{\partial\varphi^2}+\\
&+\left(F_{66}+b_1L_{66}+b_2H_{66}+b_3M_{66}\right)\frac{\partial^2\eta_\varphi}{\partial s^2}+\\
&-\frac{1}{R_\varphi^3}\frac{\partial R_\varphi}{\partial\varphi}\left(F_{11}+a_1L_{11}+a_2H_{11}+a_3M_{11}\right)\frac{\partial\eta_\varphi}{\partial\varphi}+\\
&+\frac{1}{R_\varphi^2}\left(L_{11}\frac{\partial a_1}{\partial\varphi}+H_{11}\frac{\partial a_2}{\partial\varphi}+M_{11}\frac{\partial a_3}{\partial\varphi}\right)\frac{\partial\eta_\varphi}{\partial\varphi}+\\
&+\frac{\cos\varphi}{R_0R_\varphi}\left(F_{11}+a_1L_{11}+a_2H_{11}+a_3M_{11}\right)\frac{\partial\eta_\varphi}{\partial\varphi}+\\
&-F_{12}\frac{\sin\varphi}{R_0R_\varphi}\eta_\varphi-\left(\frac{\cos\varphi}{R_0}\right)^2\left(F_{22}+b_1L_{22}+b_2H_{22}+b_3M_{22}\right)\eta_\varphi+\\
&-3\left(D_{44}+a_1E_{44}+a_2F_{44}+a_3L_{44}\right)\eta_\varphi-\frac{2}{R_\varphi}\left(E_{44}+a_1F_{44}+a_2L_{44}+a_3H_{44}\right)\eta_\varphi+\\
&+\frac{1}{R_\varphi}F_{12}\frac{\partial^2\eta_s}{\partial\varphi\partial s}+\frac{1}{R_\varphi}F_{66}\frac{\partial^2\eta_s}{\partial s\partial\varphi}+\\
&-\frac{\cos\varphi}{R_0}\left(F_{66}+b_1L_{66}+b_2H_{66}+b_3M_{66}\right)\frac{\partial\eta_s}{\partial s}-\frac{\cos\varphi}{R_0}\left(F_{22}+b_1L_{22}+b_2H_{22}+b_3M_{22}\right)\frac{\partial\eta_s}{\partial s}+m_\varphi=0
\end{aligned}
\tag{63}
$$

1.3.9.5 The fifth fundamental equilibrium equation

By substituting Eqs.(25-42) in Eq.(48) the fifth fundamental equation is written as follows:

$$
\begin{aligned}
&B_{66}\frac{1}{R_\varphi}\frac{\partial^2 u_\varphi}{\partial\varphi\partial s}+\frac{1}{R_\varphi}B_{12}\frac{\partial^2 u_\varphi}{\partial s\partial\varphi}+\\
&+\frac{\cos\varphi}{R_0}\left(B_{22}+b_1D_{22}+b_2E_{22}+b_3F_{22}\right)\frac{\partial u_\varphi}{\partial s}+\\
&+\frac{\cos\varphi}{R_0}\left(B_{66}+b_1D_{66}+b_2E_{66}+b_3F_{66}\right)\frac{\partial u_\varphi}{\partial s}+\\
&+\frac{1}{R_\varphi^2}\left(B_{66}+a_1D_{66}+a_2E_{66}+a_3F_{66}\right)\frac{\partial^2 u_s}{\partial\varphi^2}+\\
&+\left(B_{22}+b_1D_{22}+b_2E_{22}+b_3F_{22}\right)\frac{\partial^2 u_s}{\partial s^2}+\\
&-\frac{1}{R_\varphi^3}\frac{\partial R_\varphi}{\partial\varphi}\left(B_{66}+a_1D_{66}+a_2E_{66}+a_3F_{66}\right)\frac{\partial u_s}{\partial\varphi}+\\
&+\frac{1}{R_\varphi^2}\left(D_{66}\frac{\partial a_1}{\partial\varphi}+E_{66}\frac{\partial a_2}{\partial\varphi}+F_{66}\frac{\partial a_3}{\partial\varphi}\right)\frac{\partial u_s}{\partial\varphi}+\\
&+\frac{\cos\varphi}{R_0R_\varphi}\left(B_{66}+a_1D_{66}+a_2E_{66}+a_3F_{66}\right)\frac{\partial u_s}{\partial\varphi}+\\
&+B_{66}\frac{\sin\varphi}{R_0R_\varphi}u_s-\left(\frac{\cos\varphi}{R_0}\right)^2\left(B_{66}+b_1D_{66}+b_2E_{66}+b_3F_{66}\right)u_s\\
&+\frac{\sin\varphi}{R_0}\left(A_{55}+b_1B_{55}+b_2D_{55}+b_3E_{55}\right)u_s+\\
&+\frac{\sin\varphi}{R_0}\left(B_{22}+b_1D_{22}+b_2E_{22}+b_3F_{22}\right)\frac{\partial w}{\partial s}+B_{12}\frac{1}{R_\varphi}\frac{\partial w}{\partial s}+\\
&-\left(A_{55}+b_1B_{55}+b_2D_{55}+b_3E_{55}\right)\frac{\partial w}{\partial s}+\\
&+\frac{1}{R_\varphi}D_{66}\frac{\partial^2\beta_\varphi}{\partial\varphi\partial s}+D_{12}\frac{1}{R_\varphi}\frac{\partial^2\beta_\varphi}{\partial s\partial\varphi}+\\
&+\frac{\cos\varphi}{R_0}\left(D_{22}+b_1E_{22}+b_2F_{22}+b_3L_{22}\right)\frac{\partial\beta_\varphi}{\partial s}+\\
&+\frac{\cos\varphi}{R_0}\left(D_{66}+b_1E_{66}+b_2F_{66}+b_3L_{66}\right)\frac{\partial\beta_\varphi}{\partial s}+
\end{aligned}
\tag{64}
$$

$$
\begin{aligned}
&+\frac{1}{R_\varphi^2}\left(D_{66}+a_1E_{66}+a_2F_{66}+a_3L_{66}\right)\frac{\partial^2\beta_s}{\partial\varphi^2}+\\
&+\left(D_{22}+b_1E_{22}+b_2F_{22}+b_3L_{22}\right)\frac{\partial^2\beta_s}{\partial s^2}+\\
&-\frac{1}{R_\varphi^3}\frac{\partial R_\varphi}{\partial\varphi}\left(D_{66}+a_1E_{66}+a_2F_{66}+a_3L_{66}\right)\frac{\partial\beta_s}{\partial\varphi}+\frac{1}{R_\varphi^2}\left(E_{66}\frac{\partial a_1}{\partial\varphi}+F_{66}\frac{\partial a_2}{\partial\varphi}+L_{66}\frac{\partial a_3}{\partial\varphi}\right)\frac{\partial\beta_s}{\partial\varphi}+\\
&+\frac{\cos\varphi}{R_0R_\varphi}\left(D_{66}+a_1E_{66}+a_2F_{66}+a_3L_{66}\right)\frac{\partial\beta_s}{\partial\varphi}+D_{66}\frac{\sin\varphi}{R_0R_\varphi}\beta_s+\\
&-\left(\frac{\cos\varphi}{R_0}\right)^2\left(D_{66}+b_1E_{66}+b_2F_{66}+b_3L_{66}\right)\beta_s-\left(A_{55}+b_1B_{55}+b_2D_{55}+b_3E_{55}\right)\beta_s+\\
&+\frac{1}{R_\varphi}F_{66}\frac{\partial^2\eta_\varphi}{\partial\varphi\partial s}+\frac{1}{R_\varphi}F_{12}\frac{\partial^2\eta_\varphi}{\partial s\partial\varphi}+\\
&+\frac{\cos\varphi}{R_0}\left(F_{22}+b_1L_{22}+b_2H_{22}+b_3M_{22}\right)\frac{\partial\eta_\varphi}{\partial s}+\\
&+\frac{\cos\varphi}{R_0}\left(F_{66}+b_1L_{66}+b_2H_{66}+b_3M_{66}\right)\frac{\partial\eta_\varphi}{\partial s}+\\
&+\frac{1}{R_\varphi^2}\left(F_{66}+a_1L_{66}+a_2H_{66}+a_3M_{66}\right)\frac{\partial^2\eta_s}{\partial\varphi^2}+\\
&+\left(F_{22}+b_1L_{22}+b_2H_{22}+b_3M_{22}\right)\frac{\partial^2\eta_s}{\partial s^2}+\\
&-\frac{1}{R_\varphi^3}\frac{\partial R_\varphi}{\partial\varphi}\left(F_{66}+a_1L_{66}+a_2H_{66}+a_3M_{66}\right)\frac{\partial\eta_s}{\partial\varphi}+\\
&+\frac{1}{R_\varphi^2}\left(L_{66}\frac{\partial a_1}{\partial\varphi}+H_{66}\frac{\partial a_2}{\partial\varphi}+M_{66}\frac{\partial a_3}{\partial\varphi}\right)\frac{\partial\eta_s}{\partial\varphi}+\\
&+\frac{\cos\varphi}{R_0R_\varphi}\left(F_{66}+a_1L_{66}+a_2H_{66}+a_3M_{66}\right)\frac{\partial\eta_s}{\partial\varphi}+\\
&+F_{66}\frac{\sin\varphi}{R_0R_\varphi}\eta_s-\left(\frac{\cos\varphi}{R_0}\right)^2\left(F_{66}+b_1L_{66}+b_2H_{66}+b_3M_{66}\right)\eta_s+\\
&-3\left(D_{55}+b_1E_{55}+b_2F_{55}+b_3L_{55}\right)\eta_s-\frac{2\sin\varphi}{R_0}\left(E_{55}+b_1F_{55}+b_2L_{55}+b_3H_{55}\right)\eta_s+m_s=0
\end{aligned}
\tag{64}
$$

1.3.9.6 The sixth fundamental equilibrium equation

By substituting Eqs.(25-42) in Eq.(49) the sixth fundamental equation is written as follows:

$$\frac{1}{R_\varphi^2}\left(E_{11}+a_1F_{11}+a_2L_{11}+a_3H_{11}\right)\frac{\partial^2 u_\varphi}{\partial\varphi^2}+\left(E_{66}+b_1F_{66}+b_2L_{66}+b_3H_{66}\right)\frac{\partial^2 u_\varphi}{\partial s^2}+$$
$$-\frac{1}{R_\varphi^3}\frac{\partial R_\varphi}{\partial\varphi}\left(E_{11}+a_1F_{11}+a_2L_{11}+a_3H_{11}\right)\frac{\partial u_\varphi}{\partial\varphi}+\frac{1}{R_\varphi^2}\left(F_{11}\frac{\partial a_1}{\partial\varphi}+L_{11}\frac{\partial a_2}{\partial\varphi}+H_{11}\frac{\partial a_3}{\partial\varphi}\right)\frac{\partial u_\varphi}{\partial\varphi}+$$
$$+\frac{\cos\varphi}{R_0R_\varphi}\left(E_{11}+a_1F_{11}+a_2L_{11}+a_3H_{11}\right)\frac{\partial u_\varphi}{\partial\varphi}+$$
$$-E_{12}\frac{\sin\varphi}{R_0R_\varphi}u_\varphi-\left(\frac{\cos\varphi}{R_0}\right)^2\left(E_{22}+b_1F_{22}+b_2L_{22}+b_3H_{22}\right)u_\varphi+$$
$$+\frac{3}{R_\varphi}\left(D_{44}+a_1E_{44}+a_2F_{44}+a_3L_{44}\right)u_\varphi+\frac{2}{R_\varphi^2}\left(E_{44}+a_1F_{44}+a_2L_{44}+a_3H_{44}\right)u_\varphi+$$
$$+E_{12}\frac{1}{R_\varphi}\frac{\partial^2 u_s}{\partial\varphi\partial s}+\frac{1}{R_\varphi}E_{66}\frac{\partial^2 u_s}{\partial s\partial\varphi}+\left(-\frac{\cos\varphi}{R_0}\right)\left(E_{66}+b_1F_{66}+b_2L_{66}+b_3H_{66}\right)\frac{\partial u_s}{\partial s}+$$

(65)

$$
\begin{aligned}
&-\frac{\cos\varphi}{R_0}\left(E_{22}+b_1F_{22}+b_2L_{22}+b_3H_{22}\right)\frac{\partial u_s}{\partial s}+\\
&+\frac{\sin\varphi}{R_0R_\varphi}E_{12}\frac{\partial w}{\partial\varphi}+\frac{1}{R_\varphi^2}\left(E_{11}+a_1F_{11}+a_2L_{11}+a_3H_{11}\right)\frac{\partial w}{\partial\varphi}+\\
&-\left(\frac{3}{R_\varphi}\right)\left(D_{44}+a_1E_{44}+a_2F_{44}+a_3L_{44}\right)\frac{\partial w}{\partial\varphi}+\\
&-\left(\frac{2}{R_\varphi^2}\right)\left(E_{44}+a_1F_{44}+a_2L_{44}+a_3H_{44}\right)\frac{\partial w}{\partial\varphi}+\\
&-\frac{1}{R_\varphi^3}\frac{\partial R_\varphi}{\partial\varphi}\left(E_{11}+a_1F_{11}+a_2L_{11}+a_3H_{11}\right)w+\\
&+\frac{1}{R_\varphi^2}\left(F_{11}\frac{\partial a_1}{\partial\varphi}+L_{11}\frac{\partial a_2}{\partial\varphi}+H_{11}\frac{\partial a_3}{\partial\varphi}\right)w+\\
&+\frac{\cos\varphi}{R_0R_\varphi}\left(E_{11}+a_1F_{11}+a_2L_{11}+a_3H_{11}\right)w+\\
&-\frac{\sin\varphi\cos\varphi}{R_0^2}\left(E_{22}+b_1F_{22}+b_2L_{22}+b_3H_{22}\right)w+\\
&+\frac{1}{R_\varphi^2}\left(F_{11}+a_1L_{11}+a_2H_{11}+a_3M_{11}\right)\frac{\partial^2\beta_\varphi}{\partial\varphi^2}+\\
&+\left(F_{66}+b_1L_{66}+b_2H_{66}+b_3M_{66}\right)\frac{\partial^2\beta_\varphi}{\partial s^2}+\\
&-\frac{1}{R_\varphi^3}\frac{\partial R_\varphi}{\partial\varphi}\left(F_{11}+a_1L_{11}+a_2H_{11}+a_3M_{11}\right)\frac{\partial\beta_\varphi}{\partial\varphi}+
\end{aligned}
\qquad (65)
$$

$$
\begin{aligned}
&+\frac{1}{R_\varphi^2}\left(L_{11}\frac{\partial a_1}{\partial\varphi}+H_{11}\frac{\partial a_2}{\partial\varphi}+M_{11}\frac{\partial a_3}{\partial\varphi}\right)\frac{\partial\beta_\varphi}{\partial\varphi}+\\
&+\frac{\cos\varphi}{R_0R_\varphi}\left(F_{11}+a_1L_{11}+a_2H_{11}+a_3M_{11}\right)\frac{\partial\beta_\varphi}{\partial\varphi}-F_{12}\frac{\sin\varphi}{R_0R_\varphi}\beta_\varphi\\
&-\left(\frac{\cos\varphi}{R_0}\right)^2\left(F_{22}+b_1L_{22}+b_2H_{22}+b_3M_{22}\right)\beta_\varphi-3\left(D_{44}+a_1E_{44}+a_2F_{44}+a_3L_{44}\right)\beta_\varphi+\\
&-\frac{2}{R_\varphi}\left(E_{44}+a_1F_{44}+a_2L_{44}+a_3H_{44}\right)\beta_\varphi+\\
&+F_{12}\frac{1}{R_\varphi}\frac{\partial^2\beta_s}{\partial\varphi\partial s}+\frac{1}{R_\varphi}F_{66}\frac{\partial^2\beta_s}{\partial s\partial\varphi}+\\
&-\frac{\cos\varphi}{R_0}\left(F_{66}+b_1L_{66}+b_2H_{66}+b_3M_{66}\right)\frac{\partial\beta_s}{\partial s}+\\
&-\frac{\cos\varphi}{R_0}\left(F_{22}+b_1L_{22}+b_2H_{22}+b_3M_{22}\right)\frac{\partial\beta_s}{\partial s}+\\
&+\frac{1}{R_\varphi^2}\left(H_{11}+a_1M_{11}+a_2N_{11}+a_3V_{11}\right)\frac{\partial^2\eta_\varphi}{\partial\varphi^2}+\\
&+\left(H_{66}+b_1M_{66}+b_2N_{66}+b_3V_{66}\right)\frac{\partial^2\eta_\varphi}{\partial s^2}+\\
&-\frac{1}{R_\varphi^3}\frac{\partial R_\varphi}{\partial\varphi}\left(H_{11}+a_1M_{11}+a_2N_{11}+a_3V_{11}\right)\frac{\partial\eta_\varphi}{\partial\varphi}+\\
&+\frac{1}{R_\varphi^2}\left(M_{11}\frac{\partial a_1}{\partial\varphi}+N_{11}\frac{\partial a_2}{\partial\varphi}+V_{11}\frac{\partial a_3}{\partial\varphi}\right)\frac{\partial\eta_\varphi}{\partial\varphi}+\\
&+\frac{\cos\varphi}{R_0R_\varphi}\left(H_{11}+a_1M_{11}+a_2N_{11}+a_3V_{11}\right)\frac{\partial\eta_\varphi}{\partial\varphi}+\\
&-H_{12}\frac{\sin\varphi}{R_0R_\varphi}\eta_\varphi-\left(\frac{\cos\varphi}{R_0}\right)^2\left(H_{22}+b_1M_{22}+b_2N_{22}+b_3V_{22}\right)\eta_\varphi+\\
&-9\left(F_{44}+a_1L_{44}+a_2H_{44}+a_3M_{44}\right)\eta_\varphi-\frac{6}{R_\varphi}\left(L_{44}+a_1H_{44}+a_2M_{44}+a_3N_{44}\right)\eta_\varphi+\\
&-\frac{6}{R_\varphi}\left(L_{44}+a_1H_{44}+a_2M_{44}+a_3N_{44}\right)\eta_\varphi-\frac{4}{R_\varphi^2}\left(H_{44}+a_1M_{44}+a_2N_{44}+a_3V_{44}\right)\eta_\varphi+\\
&+H_{12}\frac{1}{R_\varphi}\frac{\partial^2\eta_s}{\partial\varphi\partial s}+\frac{1}{R_\varphi}H_{66}\frac{\partial^2\eta_s}{\partial s\partial\varphi}+\\
&-\frac{\cos\varphi}{R_0}\left(H_{66}+b_1M_{66}+b_2N_{66}+b_3V_{66}\right)\frac{\partial\eta_s}{\partial s}+\\
&-\frac{\cos\varphi}{R_0}\left(H_{22}+b_1M_{22}+b_2N_{22}+b_3V_{22}\right)\frac{\partial\eta_s}{\partial s}+r_\varphi=0
\end{aligned}
\tag{65}
$$

1.3.9.7 The seventh fundamental equilibrium equation

By substituting Eqs.(25-42) in Eq.(50) the seventh fundamental equation is written as follows:

$$
\begin{aligned}
&\frac{1}{R_\varphi}E_{66}\frac{\partial^2 u_\varphi}{\partial\varphi\partial s}+\frac{1}{R_\varphi}E_{12}\frac{\partial^2 u_\varphi}{\partial s\partial\varphi}+\frac{\cos\varphi}{R_0}\left(E_{22}+b_1F_{22}+b_2L_{22}+b_3H_{22}\right)\frac{\partial u_\varphi}{\partial s}+\\
&+\frac{\cos\varphi}{R_0}\left(E_{66}+b_1F_{66}+b_2L_{66}+b_3H_{66}\right)\frac{\partial u_\varphi}{\partial s}+\\
&+\frac{1}{R_\varphi^2}\left(E_{66}+a_1F_{66}+a_2L_{66}+a_3H_{66}\right)\frac{\partial^2 u_s}{\partial\varphi^2}+\\
&+\left(E_{22}+b_1F_{22}+b_2L_{22}+b_3H_{22}\right)\frac{\partial^2 u_s}{\partial s^2}+\\
&-\frac{1}{R_\varphi^3}\frac{\partial R_\varphi}{\partial\varphi}\left(E_{66}+a_1F_{66}+a_2L_{66}+a_3H_{66}\right)\frac{\partial u_s}{\partial\varphi}+\\
&+\frac{1}{R_\varphi^2}\left(F_{66}\frac{\partial a_1}{\partial\varphi}+L_{66}\frac{\partial a_2}{\partial\varphi}+H_{66}\frac{\partial a_3}{\partial\varphi}\right)\frac{\partial u_s}{\partial\varphi}+\\
&+\frac{\cos\varphi}{R_0R_\varphi}\left(E_{66}+a_1F_{66}+a_2L_{66}+a_3H_{66}\right)\frac{\partial u_s}{\partial\varphi}+\\
&+E_{66}\frac{\sin\varphi}{R_0R_\varphi}u_s-\left(\frac{\cos\varphi}{R_0}\right)^2\left(E_{66}+b_1F_{66}+b_2L_{66}+b_3H_{66}\right)u_s+\\
&+3\frac{\sin\varphi}{R_0}\left(D_{55}+b_1E_{55}+b_2F_{55}+b_3L_{55}\right)u_s+\\
&+2\left(\frac{\sin\varphi}{R_0}\right)^2\left(E_{55}+b_1F_{55}+b_2L_{55}+b_3H_{55}\right)u_s+\\
&+\frac{\sin\varphi}{R_0}\left(E_{22}+b_1F_{22}+b_2L_{22}+b_3H_{22}\right)\frac{\partial w}{\partial s}+E_{12}\frac{1}{R_\varphi}\frac{\partial w}{\partial s}+\\
&-3\left(D_{55}+b_1E_{55}+b_2F_{55}+b_3L_{55}\right)\frac{\partial w}{\partial s}-\frac{2\sin\varphi}{R_\varphi}\left(E_{55}+b_1F_{55}+b_2L_{55}+b_3H_{55}\right)\frac{\partial w}{\partial s}+\\
&+F_{66}\frac{1}{R_\varphi}\frac{\partial^2\beta_\varphi}{\partial\varphi\partial s}+F_{12}\frac{1}{R_\varphi}\frac{\partial^2\beta_\varphi}{\partial s\partial\varphi}\\
&+\frac{\cos\varphi}{R_0}\left(F_{22}+b_1L_{22}+b_2H_{22}+b_3M_{22}\right)\frac{\partial\beta_\varphi}{\partial s}+
\end{aligned}
\tag{66}
$$

$$+\frac{\cos\varphi}{R_0}\left(F_{66}+b_1L_{66}+b_2H_{66}+b_3M_{66}\right)\frac{\partial\beta_\varphi}{\partial s}+$$

$$+\frac{1}{R_\varphi^2}\left(F_{66}+a_1L_{66}+a_2H_{66}+a_3M_{66}\right)\frac{\partial^2\beta_s}{\partial\varphi^2}+$$

$$+\left(F_{22}+b_1L_{22}+b_2H_{22}+b_3M_{22}\right)\frac{\partial^2\beta_s}{\partial s^2}-\frac{1}{R_\varphi^3}\frac{\partial R_\varphi}{\partial\varphi}\left(F_{66}+a_1L_{66}+a_2H_{66}+a_3M_{66}\right)\frac{\partial\beta_s}{\partial\varphi}+$$

$$+\frac{1}{R_\varphi^2}\left(L_{66}\frac{\partial a_1}{\partial\varphi}+H_{66}\frac{\partial a_2}{\partial\varphi}+M_{66}\frac{\partial a_3}{\partial\varphi}\right)\frac{\partial\beta_s}{\partial\varphi}+\frac{\cos\varphi}{R_0R_\varphi}\left(F_{66}+a_1L_{66}+a_2M_{66}+a_3N_{66}\right)\frac{\partial\beta_s}{\partial\varphi}+$$

$$+F_{66}\frac{\sin\varphi}{R_0R_\varphi}\beta_s-\left(\frac{\cos\varphi}{R_0}\right)^2\left(F_{66}+b_1L_{66}+b_2H_{66}+b_3M_{66}\right)\beta_s+$$

$$-3\left(D_{55}+b_1E_{55}+b_2F_{55}+b_3L_{55}\right)\beta_s+$$

$$-\frac{2\sin\varphi}{R_0}\left(E_{55}+b_1F_{55}+b_2L_{55}+b_3H_{55}\right)\beta_s+\frac{1}{R_\varphi}H_{66}\frac{\partial^2\eta_\varphi}{\partial\varphi\partial s}+\frac{1}{R_\varphi}H_{12}\frac{\partial^2\eta_\varphi}{\partial s\partial\varphi}+$$

$$+\frac{\cos\varphi}{R_0}\left(H_{22}+b_1M_{22}+b_2N_{22}+b_3V_{22}\right)\frac{\partial\eta_\varphi}{\partial s}+\frac{\cos\varphi}{R_0}\left(H_{66}+b_1M_{66}+b_2N_{66}+b_3V_{66}\right)\frac{\partial\eta_\varphi}{\partial s}+$$

$$+\frac{1}{R_\varphi^2}\left(H_{66}+a_1M_{66}+a_2N_{66}+a_3V_{66}\right)\frac{\partial^2\eta_s}{\partial\varphi^2}+\left(H_{22}+b_1M_{22}+b_2N_{22}+b_3V_{22}\right)\frac{\partial^2\eta_s}{\partial s^2}+$$

$$-\frac{1}{R_\varphi^3}\frac{\partial R_\varphi}{\partial\varphi}\left(H_{66}+a_1M_{66}+a_2N_{66}+a_3V_{66}\right)\frac{\partial\eta_s}{\partial\varphi}+\frac{1}{R_\varphi^2}\left(M_{66}\frac{\partial a_1}{\partial\varphi}+N_{66}\frac{\partial a_2}{\partial\varphi}+V_{66}\frac{\partial a_3}{\partial\varphi}\right)\frac{\partial\eta_s}{\partial\varphi}+$$

$$+\frac{\cos\varphi}{R_0R_\varphi}\left(H_{66}+a_1M_{66}+a_2N_{66}+a_3V_{66}\right)\frac{\partial\eta_s}{\partial\varphi}+H_{66}\frac{\sin\varphi}{R_0R_\varphi}\eta_s+$$

$$-\left(\frac{\cos\varphi}{R_0}\right)^2\left(H_{66}+b_1M_{66}+b_2N_{66}+b_3V_{66}\right)\eta_s-9\left(F_{55}+b_1L_{55}+b_2H_{55}+b_3M_{55}\right)\eta_s+$$

$$-\frac{6\sin\varphi}{R_0}\left(F_{55}+b_1L_{55}+b_2H_{55}+b_3M_{55}\right)\eta_s-6\frac{\sin\varphi}{R_0}\left(L_{55}+b_1H_{55}+b_2M_{55}+b_3N_{55}\right)\eta_s+$$

$$-4\left(\frac{\sin\varphi}{R_0}\right)^2\left(H_{55}+b_1M_{55}+b_2N_{55}+b_3V_{55}\right)\eta_s+r_s=0 \qquad (66)$$

1.4 Equilibrium equations for doubly curved shells

The elastic potential energy for a revolution shell can be expressed as follows:

$$\Phi = \int_{\varphi}\int_{\vartheta}\int_{\zeta} \frac{1}{2}\left(\sigma_{\varphi}\varepsilon_{\varphi} + \sigma_{\vartheta}\varepsilon_{\vartheta} + \sigma_{n}\varepsilon_{n} + \tau_{\varphi\vartheta}\gamma_{\varphi\vartheta} + \tau_{\varphi n}\gamma_{\varphi n} + \tau_{\vartheta n}\gamma_{\vartheta n}\right) R_{\varphi}R_{0}\left(1+\frac{\zeta}{R_{\varphi}}\right)\left(1+\frac{\zeta}{R_{\vartheta}}\right) d\zeta\, d\vartheta\, d\varphi \tag{67}$$

By assuming the work of external forces equal to zero, the total potential energy becomes equal to the deformation energy:

$$\Pi = \Phi + H = \Phi - W_{e} = \Phi \tag{67.1}$$

The principle of virtual displacement has been applied in order to write the 3D equilibrium equations.

$$\delta\Pi = \delta\Phi = 0 \;\; \forall \delta U \tag{67.2}$$

By considering Eq.(67.2) in Eq.(67), the following relation is obtained:

$$\begin{aligned} &\delta\Phi = \int_{\varphi}\int_{\vartheta}\int_{\zeta} \left(\sigma_{\varphi}\delta\varepsilon_{\varphi} + \sigma_{\vartheta}\delta\varepsilon_{\vartheta} + \sigma_{n}\delta\varepsilon_{n} + \tau_{\varphi\vartheta}\delta\gamma_{\varphi\vartheta} + \tau_{\varphi n}\delta\gamma_{\varphi n} + \tau_{\vartheta n}\delta\gamma_{\vartheta n}\right) \\ &\left(\zeta + R_{\varphi}\right)\left(\zeta\sin\varphi + R_{0}\right) d\zeta\, d\vartheta\, d\varphi = 0 \;\; \forall \delta U \end{aligned} \tag{67.3}$$

By considering Eqs.(2-7.1) in Eq.(67.3), the total functional can be divided into six terms as follows:

$$\delta\Phi_{1} = \int_{V} \sigma_{\varphi}\delta\varepsilon_{\varphi}\left(\zeta + R_{\varphi}\right)\left(\zeta\sin\varphi + R_{0}\right) dV = 0 \;\; \forall \delta U \tag{67.4}$$

$$\delta\Phi_{1} = \int_{V} \sigma_{\varphi}\left(\frac{\partial \delta U_{\varphi}}{\partial\varphi} + \delta W\right)\left(\zeta\sin\varphi + R_{0}\right) dV = 0 \;\; \forall \delta U \tag{67.4.1}$$

By integrating by parts, the first part of the functional can be expressed as follows:

$$\delta\Phi_{1} = \int_{V} -\frac{\partial}{\partial\varphi}\left(\sigma_{\varphi}(\zeta\sin\varphi + R_{0})\delta U_{\varphi} + \left(\sigma_{\varphi}\left(\zeta\sin\varphi + R_{0}\right)\right)\delta W dV = 0 \;\; \forall \delta U \tag{67.5}$$

The second term of the functional is expressed as follows:

$$\delta\Phi_2 = \int_V \sigma_\vartheta \delta\varepsilon_\vartheta \left(\zeta + R_\varphi\right)\left(\zeta \sin\varphi + R_0\right) dV = 0 \;\; \forall \delta U \tag{67.6}$$

By considering Eqs.(2-7.1) in Eq.(67.6), the second term becomes:

$$\delta\Phi_2 = \int_V \sigma_\vartheta \left(\frac{\partial \delta U_\vartheta}{\partial \vartheta} + \delta U_\varphi \cos\varphi + \delta W \sin\varphi \right)\left(\zeta + R_\varphi\right) dV = 0 \;\; \forall \delta U \tag{67.6.1}$$

By integrating by parts, the second part of the functional becomes:

$$\delta\Phi_2 = \int_V -\frac{\partial}{\partial \vartheta}\left(\sigma_\vartheta \left(\zeta + R_\varphi\right)\right)\delta U_\vartheta + \sigma_\vartheta \left(\zeta + R_\varphi\right)\left(\delta U_\varphi \cos\varphi + \delta W \sin\varphi\right) dV = 0 \;\; \forall \delta U \tag{67.7}$$

The third term of the functional is the following:

$$\delta\Phi_3 = \int_V \sigma_n \delta\varepsilon_n \left(\zeta + R_\varphi\right)\left(\zeta \sin\varphi + R_0\right) dV = 0 \;\; \forall \delta U \tag{67.8}$$

By considering Eqs.(2-7.1) in Eq.(67.8), the third term becomes:

$$\delta\Phi_3 = \int_V \sigma_n \left(\zeta + R_\varphi\right)\left(\zeta \sin\varphi + R_0\right) \frac{\partial \delta W}{\partial \zeta} dV = 0 \;\; \forall \delta U \tag{67.8.1}$$

By means of integration by parts, the third part becomes:

$$\delta\Phi_3 = \int_V -\frac{\partial}{\partial \zeta}\left(\sigma_n \left(\zeta + R_\varphi\right)\left(\zeta \sin\varphi + R_0\right)\right)\delta W dV = 0 \;\; \forall \delta U \tag{67.9}$$

The fourth part of the functional is written as follows:

$$\delta\Phi_4 = \int_V \tau_{\varphi\vartheta}\left(\frac{1}{\zeta + R_\varphi}\frac{\partial \delta U_\vartheta}{\partial \varphi} + \frac{1}{\zeta \sin\varphi + R_0}\left(\frac{\partial \delta U_\varphi}{\partial \vartheta} - \delta U_\vartheta \cos\varphi \right)\right) \left(\zeta + R_\varphi\right)\left(\zeta \sin\varphi + R_0\right) dV = 0 \;\; \forall \delta U \tag{67.10}$$

By integrating by pars, the fourth part is written as follows:

$$\delta\Phi_4 = \int_V -\frac{\partial}{\partial \varphi}\left(\tau_{\varphi\vartheta}\left(\zeta \sin\varphi + R_0\right)\right)\delta U_\vartheta - \frac{\partial}{\partial \vartheta}\left(\tau_{\varphi\vartheta}\left(\zeta + R_\varphi\right)\right)\delta U_\varphi + -\tau_{\varphi\vartheta}\left(\zeta + R_\varphi\right)\delta U_\vartheta \cos\varphi dV = 0 \;\; \forall \delta U \tag{67.11}$$

The fifth term of the functional is the following:

$$\delta\Phi_5 = \int_V \tau_{\varphi n}\delta\gamma_{\varphi n}\left(\zeta + R_\varphi\right)\left(\zeta\sin\varphi + R_0\right)dV = 0 \;\; \forall\delta U \tag{67.12}$$

By considering Eqs.(2-7.1) in Eq.(67.12), the fifth term becomes:

$$\delta\Phi_5 = \int_V \tau_{\varphi n}\left(\frac{1}{\zeta + R_\varphi}\frac{\partial\delta W}{\partial\varphi} + \left(\zeta + R_\varphi\right)\frac{\partial}{\partial\zeta}\left(\frac{\delta U_\varphi}{\zeta + R_\varphi}\right)\right)\left(\zeta + R_\varphi\right)\left(\zeta\sin\varphi + R_0\right)dV = 0 \;\; \forall\delta U \tag{67.12.1}$$

By integrating by parts it becomes:

$$\begin{aligned}\delta\Phi_5 = \int_V &-\frac{\partial}{\partial\varphi}\left(\tau_{\varphi n}\left(\zeta\sin\varphi + R_0\right)\right)\delta W - \frac{\partial}{\partial\zeta}\left(\tau_{\varphi n}\left(\zeta + R_\varphi\right)\left(\zeta\sin\varphi + R_0\right)\right)\delta U_\varphi + \\ &-\tau_{\varphi n}\left(\zeta\sin\varphi + R_0\right)\delta U_\varphi dV = 0 \;\; \forall\delta U\end{aligned} \tag{67.13}$$

The sixth term is written as follows:

$$\begin{aligned}\delta\Phi_6 = \int_V &\tau_{\vartheta n}\left(\frac{1}{\zeta\sin\varphi + R_0}\frac{\partial\delta W}{\partial\vartheta} + \left(\zeta\sin\varphi + R_0\right)\frac{\partial}{\partial\zeta}\left(\frac{\delta U_\vartheta}{\zeta\sin\varphi + R_0}\right)\right) \\ &\left(\zeta + R_\varphi\right)\left(\zeta\sin\varphi + R_0\right)dV = 0 \;\; \forall\delta U\end{aligned} \tag{67.14}$$

By integrating by parts, the sixth term becomes:

$$\delta\Phi_6 = \int_V -\left(\begin{aligned}&\left(\zeta + R_\varphi\right)\frac{\partial\tau_{\vartheta n}}{\partial\vartheta}\delta W + \frac{\partial}{\partial\zeta}\left(\tau_{\vartheta n}\left(\zeta\sin\varphi + R_0\right)\left(\zeta + R_\varphi\right)\right)\delta U_\vartheta + \\ &+\sin\varphi\left(\zeta + R_\varphi\right)\delta U_\vartheta\end{aligned}\right)dV = 0 \;\; \forall\delta U \tag{67.15}$$

By adding the six terms of the potential elastic energy, the total potential energy is expressed as a function of the virtual displacements and the equilibrium equations can be derived as follows:

The first equilibrium equation is written as follows:

$$\begin{aligned}&\frac{1}{\zeta + R_\varphi}\frac{\partial\sigma_\varphi}{\partial\varphi} + \frac{\cos\varphi}{\zeta\sin\varphi + R_0}\left(\sigma_\varphi - \sigma_s\right) + \frac{R_0}{\zeta\sin\varphi + R_0}\frac{\partial\tau_{\varphi s}}{\partial s} + \frac{\partial\tau_{\varphi n}}{\partial\zeta} + \\ &+\tau_{\varphi n}\left(\frac{2}{\zeta + R_\varphi} + \frac{\sin\varphi}{\zeta\sin\varphi + R_0}\right) = 0\end{aligned} \tag{68}$$

The second equilibrium equation is written as follows:

$$\frac{1}{\zeta+R_\varphi}\frac{\partial\tau_{\varphi s}}{\partial\varphi}+\frac{2\cos\varphi}{\zeta\sin\varphi+R_0}\tau_{\varphi s}+\frac{R_0}{\zeta\sin\varphi+R_0}\frac{\partial\sigma_s}{\partial s}+\frac{\partial\tau_{sn}}{\partial\zeta}+$$
$$+\tau_{sn}\left(\frac{1}{\zeta+R_\varphi}+\frac{2\sin\varphi}{\zeta\sin\varphi+R_0}\right)=0 \tag{69}$$

The third equilibrium equation is written as follows:

$$\frac{1}{\zeta+R_\varphi}\frac{\partial\tau_{\varphi n}}{\partial\varphi}+\frac{\cos\varphi}{\zeta\sin\varphi+R_0}\tau_{\varphi n}-\frac{1}{\zeta+R_\varphi}\sigma_\varphi-\frac{\sin\varphi}{\zeta\sin\varphi+R_0}\sigma_s+$$
$$+\frac{R_0}{\zeta\sin\varphi+R_0}\frac{\partial\tau_{sn}}{\partial s}+\frac{\partial\sigma_n}{\partial\zeta}+\sigma_n\left(\frac{1}{\zeta+R_\varphi}+\frac{\sin\varphi}{\zeta\sin\varphi+R_0}\right)=0 \tag{70}$$

1.4.1 Stress recovery via GDQ

After solving the 2D problem, the solution of the 3D differential equilibrium equations can be reached. By means of the GQD solution of the fundamental system (Eqs.(60-66)), the membrane stresses are correctly estimated using the constitutive equations (Eqs.(13)). Then, by discretizing the 3D equilibrium equations (Eqs.(68-70)) and by the knowledge of membrane stresses and their derivatives via the GDQ method, the transverse shear and normal stresses can be determined.

Figures.

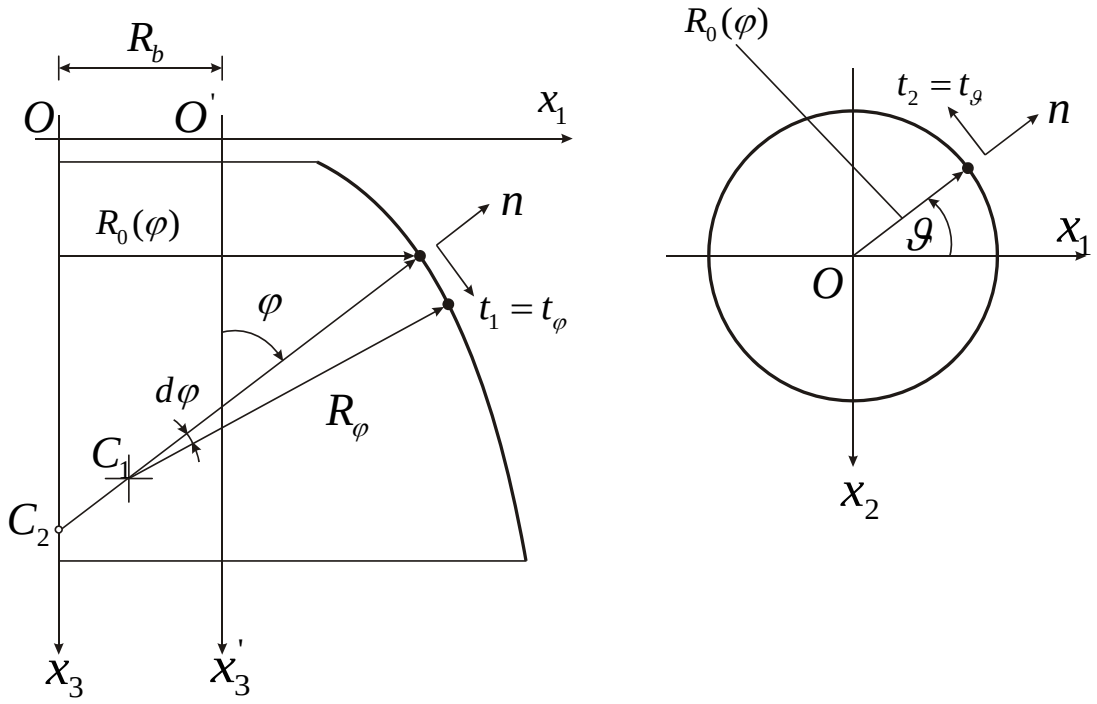

Fig.1 Shell geometry: meridional section and circumferential section

References.

[1] Kirchhoff G. **Uber das Gleichgwich und die Bewegung einer elastischen Scheibe**. J Angew Math 1850; 40: 51-88.

[2] Reddy JN. **Mechanics of laminated composite plates and shells: theory and analysis**. 2nd ed. Boca Raton, Florida: CRC Press; 2004.

[3] Reddy JN. **Theory and analysis elastic plates and shells**. 2nd ed. Boca Raton, Florida: CRC Press; 2007.

[4] Reissner E. **The effect of transverse shear deformation on the bending of elastic plates**. J Appl Mech 1945; 12: A69-77.

[5] Reissner E. **Small bending and stretching of sandwich type shells**. NACA-TN 1832, 1949.

[6] Mindlin RD. **Influence of rotary inertia and shear on flexural motion of isotropic elastic plates**. ASME J Appl Mech 1951; 18: 31-8.

[7] Basset AB. **On the extension and flexure of cylindrical and spherical thin elastic shells**. Phil Trans Roy Soc Lond Ser A 1890; 81:433-80.

[8] Hencky H. **Uber die Beriicksichtigung der Schubverzerrung in ebenen Platten**. Ing Arch 1947; 16: 72-6.

[9] Hildbrand FB., Reissner E., Thomas B. **Notes on the foundations of the theory of small displacements of orthotropic shells**. NACA TN-1833, Washington, DC; 1949.

[10]Vlasov BF. **Ob uravnieniakh izgiba plastinok (On equations of bending of plates)**. Doklo Ak Nauk Azerbeijanskoi SSR 1957;3:955-9. In Russian.

[11] Jemielita G. **Techniczna Teoria Plyt Sredniej Grubbosci (Technical theory of plates with moderate thickness).** Rozpruwy nzynierskie (Eng Trans) Polska Akademia Nauk 1975; 23:483-99.

[12] Schmidt R. **A refined nonlinear theory of plates with transverse shear deformation**. J Math Soc 1977; 27:23-38.

[13] Krishna Murty AV. **Higher order theory for vibration of thick plates**. AIAA J 1977;I8: 1823-4.

[14] Lo KH., Christensen RM., Wu EM. **A higher order theory of plate deformation-part 1: homogeneous plates**. J Appl Mech, Trans ASME 1977;44(4):663-8.

[15] Lo KH., Christensen RM., Wu EM. **A higher order theory of plate deformation-part 2: laminated plates**. J Appl Mech, Trans ASME 1977;44(4):669-76.

[16] Levinson M. **An accurate simple theory of the statics and dynamics of elastic plates**. Mech Res Commun 1980;7:343-50.

[17] Murthy MVV. **An improved transverse shear deformation theory for laminated anisotropic plates**. NASA Technical Paper 1903; 1981-p.1-37.

[18] Kant T. **Numerical analysis of thick plates**. Comput Methods Appl Mech Eng 1982; 31: 1-18.

[19] Reddy JN. **A simple higher order theory for laminated composite plates**. J Appl Mech 1984; 51:745-52.

[20] Reddy JN. **A refined nonlinear theory of plates with transverse shear deformation**. Int J Solids Struct 1984; 20:881-96.

[21] Reddy JN. **A general non linear third order theory of plates with moderate thickness**. Int J Non Linear Mech 1990;25(6):677-86.

[22] Bhimaraddi A., Stevens LK. **A higher order theory for free vibration of orthotropic, homogeneous, and laminated rectangular plates**. J Appl Mech 1984; 51:195-8.

[23] Bose P., Reddy JN. **Analysis of composite plates using various plate theories, part. 2: finite element model and numerical results**. Struct Eng Mech 1998;6(7):727-46.

[24] Von Karman Th. Festigkeistprobleme in Mascinenbau. Encyklopadie der Mathematischen Wissenschaften 1910;4(4):311-385.

[25] Leung AYT. **An Unconstrained third order plate theory**. Computers & Structures 1991; 40(4): 871-875.

[26] Shu C. **Differential quadrature and its application in engineering**. Springer 2000.

[27] Bert C., Malik M. **Differential quadrature method in computational mechanics**. Appl Mech Rev 1996; 49:1-27.

[28] Liew KM., Han JB., Xiao ZM. **Differential quadrature method for thick symmetric cross ply laminates with first order shear flexibility**. Int J Solids Struct 1996; 33: 2647-58.

[29] Shu C., Du H. **Free vibration analysis of composites cylindrical shells by DQM**. Compos Part B – Eng 1997; 28B:267-74.

[30] Liew KM, Teo TM. **Modeling via differential quadrature method: three dimensional solutions for rectangular plates**. Comput Methods Appl Mech Eng 1998; 159: 369-81.

[31] Liu F-L., Liew KM. **Differential quadrature element method: a new approach for free vibration of polar Mindlin plates having discontinuities**. Comput Methods Appl Mech Eng 1999; 179: 407-23.

[32] Viola E., Tornabene F. **Vibration analysis of damaged circular arches with varying cross-section**. Struct Integr Durab (SID-SDHM) 2005; 1: 155-69.

[33] Viola E., Tornabene F. **Vibration analysis of conical shell shell structures using GDQ method**. Far East J Appl Math 2006; 25: 23-39.

[34] Tornabene F. **Modellazione e Soluzione di Strutture a Guscio in Materiale Anisotropo**. PhD thesis, University of Bologna, DISTART Department; 2007.

[35] Tornabene F., Viola E. **Vibration analysis of spherical structural elements using the GDQ method**. Comput Math Appl 2007; 53: 1538-60.

[36] Viola E., Dilena M., Tornabene F. **Analytical and numerical results for vibration analysis of multi – stepped and multi – damaged circular arches**. J Sound Vib 2007; 299: 143-63.

[37] Marzani A., Tornabene F., Viola E. **Nonconservative stability problems via generalized differential quadrature method**. J Sound Vib 2008; 315: 176-96.

[38] Tornabene F., Viola E. **2-D solution for free vibrations of parabolic shells using generalized differential quadrature method**. Eur J Mech A – Solid 2008; 27: 1001-25

[39] Alibeigloo A., Modoliat R. **Static analysis of cross ply laminated plates with integrated surface piezoelectric layers using differential quadrature**. Compos Struct 2009; 88: 342-53.

[40] Tornabene F. **Vibration analysis of functionally graded conical, cylindrical and annular shell structures with a four parameter power law distribution**. Comput Methods Appl Mech Eng 2009; 198: 2911-35.

[41] Tornabene F., Viola E. **Free vibrations of four parameter functionally graded parabolic panels and shell of revolution**. Eur J Mech A – Solid 2009; 28: 991-1013.

[42] Tornabene F., Viola E. **Free vibration analysis of functionally graded panels and shells of revolution**. Meccanica 2009; 44: 255-81.

[43] Tornabene F., Viola E., Inman DJ. **2-D differential quadrature solution for vibration analysis of functionally graded conical, cylindrical and annular shell structures**. J Sound Vib 2009; 328: 259-90.

[44] Viola E., Tornabene F. **Free vibrations of three parameter functionally graded parabolic panels of revolution**. Mech Res Commun 2009; 36: 587-94.

[45] Yang L., Zhifei S. **Free vibration of a functionally graded piezoelectric beam via state space based differential quadrature**. Compos Struct 2009; 87: 257-64.

[46] Alibeigloo A., Nouri V., **Static analysis of functionally graded cylindrical shell with piezoelectric layers using differential quadrature method**. Compos Struct 2010; 92: 1775-85.

[47] Andakhshideh A., Maleki S., Aghdam MM. **Non linear bending analysis of laminated sector plates using generalized differential quadrature**. Compos Struct 2010; 92: 2258-64.

[48] Hosseini Hashemi Sh., Fadaee M., Es'haghi M. **A novel approach for in plane / out of plane frequency analysis of functionally graded circular /annular plates**. Int J Mech Sci 2010; 52:1025-35.

[49] Malekzadeh P., Alibeygi Beni A. **Free vibration of functionally graded arbitrary straight – sided quadrilateral plates in thermal environment**. Compos Struct 2010; 92: 2758-67.

[50] Sepahi O., Forouzan MR, Malekzadeh P. **Large deflection analysis of thermo mechanical loaded annular FGM plates on nonlinear elastic foundation via DQM**. Compos Struct 2010; 92: 2369-78.

[51] Tornabene F., Marzani A., Viola E., Elishakoff I. **Critical flow speeds of pipes conveying fluid by the generalized differential quadrature method**. Adv Theor Appl Mech 2010; 3:121-38.

[52] Yas MH, Sobhani Aragh B. **Three dimensional analysis for thermoelastic response of functionally graded fiber reinforced cylindrical panel**. Compos Struct 2010; 92: 2391-9.

[53] Tornabene F. **Free vibrations of laminated composite doubly – curved shells and panels of revolution via the GDQ method**. Comput Methods Appl Mech Eng 2011; 200: 931-52.

[54] Tornabene F. **2-D GDQ solution for free vibration of anisotropic doubly curved shells and panels of revolution**. Compos Struct 2011; 93: 1854-76.

[55] Tornabene F., Liverani A., Caligiana G. **FGM and laminated doubly curved shells and panels of revolution with a free form meridian: a 2-D GDQ solution for free vibrations**. Int J Mech Sci 2011; 53: 446-70.

[56] Zhao X., Liew KM. **Free vibration analysis of functionally graded conical shell panels by a meshless method**. Compos Struct 2011; 93: 649-64.

[57] Tornabene F. **Free vibrations of anisotropic doubly curved shells and panels of revolution with a free form meridian resting on Winkler Pasternak elastic foundations**. Compos Struct 2011; 94: 186-206.

[58] Yaghoubshahi M., Asadi E., Fariborz SJ. **A higher order shell model applied to shells with mixed boundary conditions**. Proc I Mech E Part C 2011; 225: 292-303.

[59] Tornabene F., Liverani A., Caligiana G. **Laminated composite rectangular and annular plates: a GDQ solution for static analysis with a posteriori shear and normal stress recovery**. Compos Part B – Eng 2012; 43: 1847-72.

[60] Tornabene F., Liverani A., Caligiana G. **Static analysis of laminated composite curved shells and panels of revolution with a posteriori shear and normal stress recovery using generalized differential quadrature method**. Int J Mech 2012; 61: 71-87.

[61] Tornabene F., Liverani A., Caligiana G. **General anisotropic doubly curved shell theory: a differential quadrature solution for free vibrations of shells and panels of revolution with a free form meridian**. J Sound Vib 2012; 331: 4848-69

[62] Viola E., Rossetti L., Fantuzzi N. **Numerical investigation of functionally graded cylindrical shells and panels using the generalized unconstrained third order theory coupled with the stress recovery**. Compos Struct 2012; 94: 3736-58.

[63] Toorani MH, Lakis AA. **General equations of anisotropic plates and shells including transverse shear deformations, rotary inertia, and initial curvature effects.** J Sound Vib 2000; 237(4): 561-615.

[64] Sokolnikoff IS, **Mathematical theory of Elasticity**, McGraw-Hill 1956, New York.

Chapter 2

Static analysis of functionally graded cylindrical shells and panels using the generalized unconstrained third order theory coupled with the stress recovery

Sommario

Dopo l'analisi dello stato dell'arte, si è proceduti con la scrittura di una teoria generale di deformazione a taglio del terzo ordine di tipo svincolato per gusci/pannelli cilindrici. Si è operata la scrittura del modello cinematico a sette parametri indipendenti, delle relazioni tra deformazioni e spostamenti arricchite dell'effetto della curvatura, delle equazioni costitutive per una lamina singola in materiale a stratificazione graduale e delle caratteristiche di sollecitazione in funzione degli spostamenti. Definiti i carichi esterni uniformi di natura trasversale, assiale e circonferenziale, è stato applicato il principio degli spostamenti virtuali per ricavare le equazioni indefinite di equilibrio e le condizioni al contorno. Pertanto si è proceduti alla scrittura della equazioni fondamentali con la sostituzione delle relazioni delle azioni interne espresse in funzione degli spostamenti, nelle equazioni indefinite di equilibrio. Risolto il sistema fondamentale con il metodo generalizzato di quadratura differenziale, si è pervenuti alla conoscenza dei sette parametri indipendenti di spostamento, in tutti i punti della superficie di riferimento del panello/guscio cilindrico. Utilizzando le equazioni costitutive e la soluzione del sistema fondamentale, si è giunti alla determinazione delle tensioni membranali in un punto arbitrario della superficie di riferimento del panello/guscio, per poi elaborare la distribuzione di esse lungo lo spessore dell'elemento strutturale. Per determinare le tensioni trasversali normale e tagliante, si è proceduti con la scrittura delle equazioni di equilibrio dell'elasticità tridimensionale. Compiuta la discretizzazione di esse con il metodo di quadratura differenziale di tipo generalizzato, sfruttando la conoscenza delle tensioni membranali determinate indirettamente dal sistema fondamentale, sono stati calcolati i profili di tensione trasversale normale e tagliante lungo lo spessore del panello/guscio cilindrico. I profili di tensione trasversale ottenuti in questo modo soddisfano al pieno le condizioni al contorno anche in presenza di carichi taglianti alle superfici estreme. In questo modo è stato superato il limite della teoria di Reddy che assumeva nulli a priori i carichi taglianti alle superfici di estremità. Sono stati anche discussi l'influenza della curvatura iniziale e del materiale nei profili ottenuti.

2.1 Introduction

Composite circular cylindrical shells are extensively used in many engineering applications. As far as the behaviour of cylindrical shells is concerned, by acting on material type, fiber orientation and thickness, a designer can tailor different properties of a laminate to suit a particular application. However, serious shortcomings due to stress concentrations between layers could lead to delamination failures. In order to overcome the variation of the material properties, the functionally graded material (FGM) was proposed by Koizumi and Yamanouchi [1,2], characterized by a smooth and continuous variation from the core to the external surfaces. The possibility to graduate the material properties through the thickness avoids abrupt changes in the stress and displacement distributions.

Many researchers have furnished several results in the study of the FGM cylindrical shell [3-32].

Basset [3] presented an overview on the extension and flexure of cylindrical and spherical thin shells. Bhimaraddi [4] developed a higher order theory for free vibration analysis of circular cylindrical shells. Obata and Noda [5] studied circular hollow cylinders structured from FGM material to analyze steady thermal stress at high temperature. Loy et al. [6] reached frequency spectra of FGM cylindrical shells for simply supported boundary conditions. Hua and Lam [7] calculated the frequency characteristics of a thin rotating cylindrical shell using the generalized differential quadrature method. Horgan and Chan [8] analyzed the deformations of a FG cylinder composed of a compressible isotropic linear elastic material, where the elastic modulus was a power law function of the radius and the Poisson's ratio was constant. Pradhan et al. [9] investigated the vibration characteristics of a FGM shell made up of stainless steel and zirconia, for various boundary conditions. Liew et al. [10] gave a three dimensional elasticity solution to the free vibration problem of thick cylindrical shell panels of rectangular platform. Wu et al. [11] formulated a high order theory to examine the electromechanical behavior of piezoelectric generic shells with graded material properties in the thickness direction. Zhu et al. [12] discussed the dynamic stability of functionally graded piezoelectric circular cylindrical shells. Shen and Noda [13] characterized post buckling phenomena of FGM under combined axial and radial mechanical loads in high-temperature state. Patel et al. [14] carried out the vibration analysis of a functionally graded shell using a higher order theory. Najafizadeh and Isvandzibaei [15] used a higher order shear deformation plate theory to study the vibration of simply supported FG cylindrical shells with ring supports. Wu and Syu [16] found exact solutions of functionally graded piezoelectric shells under cylindrical bending. Haddadpour et al. [17] conducted the free vibration analysis of functionally graded cylindrical shells including thermal effects. Arshad et al. [18] reported the frequency analysis of functionally graded material cylindrical shells with various volume fraction

laws. Iqbal et al. [19] examined the vibration characteristics of FGM circular cylindrical shells filled with fluid using wave propagation approach. Matsunaga [20] treated a higher order shear deformation theory in order to assess the natural frequencies and buckling stresses of functionally graded circular cylindrical shells. Tornabene and Viola [21] and Tornabene [22] dealt with the dynamic behavior of moderately thick FG cylindrical shells, by using the four parameter power law distribution. Zhao et al. [23] calculated the static response and free vibration of FGM cylindrical shells subjected to mechanical or thermomechanical loading using the element-free k_p-Ritz Method. Sobhany Aragh and Yas [24,25] considered the three dimensional analysis of thermal stresses, static and free vibration analysis of continuously graded fiber reinforced cylindrical shells by using the generalized power law distribution. In the studies under consideration, the influence of the power-law exponent and the power-law distribution were investigated. Several symmetric, asymmetric, and classic profiles were considered. A recent work by Arshad et al. [26] furnished a detailed analysis of the effects of the exponential volume fraction law on the natural frequencies of FGM cylindrical shells under various boundary conditions. Alibeigloo [27] estimated the thermoelastic solution to static deformations of functionally graded cylindrical shell bonded to thin piezoelectric layers. Sepiani et al. [28] focused on the vibration and buckling analysis of two layered functionally graded cylindrical shell, considering the effects of transverse shear and rotary inertia. Nie and Batra [29] evaluated exact solutions and material tailoring for functionally graded hollow circular cylinders. Alibeigloo and Nouri [30] developed the static analysis of functionally graded cylindrical shells with piezoelectric layers using differential quadrature method.

Sofiyev [31] presented an analytical study on the dynamic behavior of the infinitely long FGM cylindrical shell subjected to the combined action of axial tension, internal compressive load and ring shaped compressive pressure with constant velocity. Sobhani Aragh and Yas [32] studied the dynamic behavior of four parameter continuous grading fiber reinforced cylindrical panels resting on Pasternak foundation.

In the last decades, numerous studies have been also conducted on FGM cylindrical shells and plates, dealing with a variety of subjects such as thermal elasticity [33-35], static bending [36], free vibration and dynamic response [37,38], buckling and post buckling [39], among others.

Literature review shows that there are quite a few numerical works presenting static analysis of FGM cylindrical shells. Moreover, the models proposed by different authors in literature are based on the classical theory, the first order shear deformation theory [33,40-44] and the third order shear deformation theory by Reddy [45,46].

To the best knowledge of the authors, the literature background on the static analysis of FGM cylindrical shells by using the unconstrained shear deformation theory of Leung [47] is quite poor.

It should be noticed that in Leung's theory the additional constraint typical of Reddy's third order shear deformation theory vanishes [45,46]. In addition, the use of four parameter power law distributions seems to be absent in the investigation of cylindrical shells, when the initial curvature effect is included in the model and a GDQ solution [21,22,48,49,50] to the problem is given.

This paper is motivated by this lack of studies and presents a static analysis of thick FGM cylindrical shells by using an unconstrained third order shear deformation theory. The initial curvature effect is involved in the analytical formulation as it was included in the first order shear deformation theory (FSDT) by Toorani and Lakis in the past decade [51] and recently improved by Tornabene et al. [52]. Furthermore, the stress recovery is worked out.

Firstly, a basic scheme is followed to write the fundamental equilibrium equations. It starts with the definition of the displacement field which includes higher order terms, the strain components, the FGM material by means of a four parameter power law distribution, and the elastic engineering stiffnesses , the stress - strain relations, as well as the relations between the internal actions and the generalized components of displacement and the definition of external applied loads.

Secondly, seven indefinite equilibrium equations are determined by applying the principle of virtual displacements. The fundamental equations are obtained by substituting in them the constitutive equations expressed in terms of generalized components of displacement.

Thirdly, the fundamental equations are discretized via GDQ [53-58] and the differential equilibrium equations appear in the form of algebraic equations. The boundary conditions also take the analogous algebraic form. The solution is given in terms of generalized components of displacement of nodal points on the middle surface domain.

Fourthly, the through-thickness distribution of in plane stress ($\bar{\sigma}_x, \bar{\sigma}_s, \bar{\tau}_{xs}$) are given.

Fifthly, the in plane stress components calculated from the constitutive relations by using the third order unconstrained theory are compared with those determined via the first order shear deformation theory, for several types of functionally graded cylindrical shells. Both the transverse shear stress components (τ_{xn}, τ_{sn}) along the thickness direction are determined from the constitutive equations using the unconstrained first and third order theories, respectively. In order to satisfy the zero shear conditions on the lateral surfaces which is not imposed a priori in the unconstrained theory, the transverse shear stress components (τ'_{xn}, τ'_{sn}) are calculated by integrating the 3D differential equilibrium equations in the thickness direction [20], using the in plane stress components ($\sigma_x, \sigma_s, \tau_{xs}$) determined via the constitutive relations. The effects of the material power law function and the initial curvature are discussed and graphically shown in all the numerical results.

Sixthly, the transverse normal stress component (σ_n') is carried out by using the recovery technique, as for the transverse shear stress (τ_{xn}', τ_{sn}') components. All the recovered transverse stress components are improved as reported in [59].

Finally, in order to prove the validity of the present formulation, the numerical examples proposed by Aghdam et al. [60], Zhao et al. [61], Fereidoon et al. [62] and Ferreira et al. [63,64] are also considered. The center deflections of isotropic and functionally graded cylindrical panels were obtained in the present study and compared with the ones reported in [60] and [61]. The vertical displacements and membrane normal stresses in the central node of functionally graded rectangular plates were carried out and compared with those reported in [62] and [63,64]. The transverse displacement component, the membrane normal and transverse shear stresses calculated at an arbitrary point of functionally graded rectangular plates were compared with the ones derived from Zenkour [65].

Further publications are reported in [66-73].

2.2. Functionally graded composite cylindrical shell and fundamental system

2.2.1 Fundamental hypotheses

In this paper, a graded composite circular cylindrical shell is considered. L_0, R_0, h denote the length, the mean radius and the total thickness of the shell, respectively. The position of an arbitrary point P within the shell is located by the coordinates x $(0 \le x \le L_0)$, s $(0 \le s \le s_0 = \vartheta R_0)$ upon the middle surface, and ζ directed along the outward normal **n**, and measured from the reference surface $(-h/2 \le \zeta \le h/2)$, as shown in Fig.1.

When the general case of shell of revolution changes into the case under study, the radii of curvature in the meridional R_φ and circumferential directions R_ϑ assume the following values:

$$R_\varphi = R_x = \infty, \quad R_\vartheta = R_0 \tag{1}$$

The fundamental hypotheses which characterize the present formulation are the following :

1. the normal strain is inextensible, so the corresponding deformation does not exist;
2. the transverse shear deformation is taken into account in the governing equations, and the normal lines to the reference surface do not remain straight and normal after deformation;
3. the shell deflections are small and the strains are infinitesimal;
4. the shell is moderately thick, and consequently the normal stress could be negligible;

5. the shear correction factor vanishes and the presence of a finite shear transverse strain on the top and bottom of the cylindrical circular shell is accepted. Thus, the model releases the additional constrain imposed by the TSDT of Reddy [45,46];
6. the anisotropic material is assumed to be linearly elastic;
7. the initial curvature effect is taken into account.

2.2.2 Displacement field and constitutive equations

The unconstrained third-order shear deformation theory is based on the following representation of the displacement field across the thickness of the cylindrical shell [47]:

$$\begin{aligned} U_x(x,s,\zeta) &= u_x(x,s) + \zeta\beta_x(x,s) + \zeta^3\eta_x(x,s) \\ U_s(x,s,\zeta) &= u_s(x,s) + \zeta\beta_s(x,s) + \zeta^3\eta_s(x,s) \\ W(x,s,\zeta) &= w(x,s) \end{aligned} \tag{2}$$

where U_x, U_s, W are the displacements along the meridional, circumferential and normal directions, respectively; u_x, u_s are the in-plane displacements, w is the transverse displacement of a point (x,s) on the middle surface. The functions β_x, β_s are rotations of the normal to the middle plane about s and x axes, respectively. The parameters η_x, η_s are the higher order terms in Taylor's series expansion and represent the higher order transverse cross-sectional deformation modes.

By substitution of the displacement relations (2) into the strain-displacement equations of the classical theory of elasticity, the following relations are obtained [72]:

$$\varepsilon_x = \left(\frac{\partial u_x}{\partial x}\right) + \zeta\left(\frac{\partial \beta_x}{\partial x}\right) + \zeta^3\left(\frac{\partial \eta_x}{\partial x}\right) \tag{3}$$

$$\varepsilon_s = \frac{1}{\left(1+\zeta/R_0\right)}\left(\left(\frac{\partial u_s}{\partial s} + \frac{w}{R_0}\right) + \zeta\left(\frac{\partial \beta_s}{\partial s}\right) + \zeta^3\left(\frac{\partial \eta_s}{\partial s}\right)\right) \tag{4}$$

$$\gamma_{xn} = \frac{\partial w}{\partial x} + \beta_x + 3\zeta^2\eta_x \tag{5}$$

$$\gamma_{sn} = \frac{1}{\left(1+\zeta/R_0\right)}\left(-\frac{u_s}{R_0} + \frac{\partial w}{\partial s} + \beta_s + 3\zeta^2\eta_s + 2\zeta^3\frac{\eta_s}{R_0}\right) \tag{6}$$

$$\gamma_{xs}=\left(\frac{\partial u_s}{\partial x}+\zeta\left(\frac{\partial \beta_s}{\partial x}\right)+\zeta^3\left(\frac{\partial \eta_s}{\partial x}\right)\right)+\frac{1}{\left(1+\zeta/R_0\right)}\left(\frac{\partial u_x}{\partial s}+\zeta\left(\frac{\partial \beta_x}{\partial s}\right)+\zeta^3\left(\frac{\partial \eta_x}{\partial s}\right)\right) \tag{7}$$

Eqs. (3-7) take the initial curvature $1/R_0$ effect into account.

The shell material assumed in the following is a functionally graded composite linear elastic one. The elastic engineering stiffness $A_{ij,}B_{ij,}D_{ij,}E_{ij,}F_{ij,}L_{ij,}H_{ij},M_{ij,}N_{ij},V_{ij}$ are defined as [21,22]:

$$\left(A_{ij,}B_{ij,}D_{ij,}E_{ij,}F_{ij,}L_{ij,}H_{ij},M_{ij,}N_{ij},V_{ij}\right)=\int_{-\frac{h}{2}}^{+\frac{h}{2}}Q_{ij}(1,\zeta,\zeta^2,\zeta^3,\zeta^4,\zeta^5,\zeta^6,\zeta^7,\zeta^8,\zeta^9)d\zeta \tag{8}$$

where the elastic constants $Q_{ij}=Q_{ij}(\zeta)$ depend on the thickness coordinate ζ and assume the expressions suggested below:

$$\begin{aligned}
&Q_{11}=\frac{E(\zeta)}{1-\nu^2(\zeta)}\\
&Q_{12}=\nu(\zeta)Q_{11}\\
&Q_{44}=Q_{55}=Q_{66}=\frac{E(\zeta)}{2(1+\nu(\zeta))}\\
&Q_{16}=Q_{26}=Q_{45}=0
\end{aligned} \tag{9}$$

In (9) $E\left(\zeta\right)$, $\nu\left(\zeta\right)$ are the elastic parameters of the composite material which are also functions of the thickness coordinate ζ.

The FGM shell under investigation consists of a mixture of two basic components : the ceramic (C) and the metal (M) constituents. Their properties follow a continuous and a smoothly change in the thickness direction ζ, and they are function of volume fractions of the constituent materials. The three characteristics parameters, the Young's modulus $E(\zeta)$, the Poisson's ratio $\nu(\zeta)$, the density $\rho(\zeta)$, which identify the FGM material, are presented in the form of a linear combination, as follows [21,22]:

$$\begin{aligned}
&\rho(\zeta)=(\rho_C-\rho_M)V_C+\rho_M\\
&E\left(\zeta\right)=(E_C-E_M)V_C+E_M\\
&\nu(\zeta)=(\nu_C-\nu_M)V_C+\nu_M
\end{aligned} \tag{10}$$

where ρ_C, E_C, ν_C, V_C, and ρ_M, E_M, ν_M, V_M are the volumic mass, the elastic modulus, the Poisson's coefficient, the volume fraction of the ceramic (C), and the metal (M) constituents, respectively.
The power law distributions for the volume fraction of the ceramic component are proposed, where four parameters are involved. As mentioned above, the material is inhomogeneous and the material properties varying through the thickness are described by the following four parameter power law distribution [21,22] :

$$FGM_{1(\mathrm{a/b/c/p})} : V_C = \left(1 - \mathrm{a}\left(\frac{1}{2} + \frac{\zeta}{h}\right) + \mathrm{b}\left(\frac{1}{2} + \frac{\zeta}{h}\right)^{\mathrm{c}}\right)^{\mathrm{p}} \tag{11}$$

or

$$FGM_{2(\mathrm{a/b/c/p})} : V_C = \left(1 - \mathrm{a}\left(\frac{1}{2} - \frac{\zeta}{h}\right) + \mathrm{b}\left(\frac{1}{2} - \frac{\zeta}{h}\right)^{\mathrm{c}}\right)^{\mathrm{p}} \tag{12}$$

In Eqs. (11-12) the four characteristic parameters are the volume fraction index p ($0 \le \mathrm{p} \le \infty$), and the coefficients a,b,c. By varying them, the mode of variation of the ceramic volume fraction changes through the thickness. It is assumed that the sum of the volume fractions of the two basic components (ceramic and metal component) is equal to unity. Therefore, it can be noticed that when the exponent p is set to zero or equal to infinity, the FGM material becomes the homogeneous isotropic material, as stated below:

$$\begin{aligned} &\mathrm{p} = 0 \rightarrow V_C = 1,\ V_M = 0 \rightarrow \rho(\zeta) = \rho_C,\ E(\zeta) = E_C,\ \nu(\zeta) = \nu_C \\ &\mathrm{p} = \infty \rightarrow V_C = 0,\ V_M = 1 \rightarrow \rho(\zeta) = \rho_M,\ E(\zeta) = E_M,\ \nu(\zeta) = \nu_M \end{aligned} \tag{13}$$

For the FGM shell the constitutive equations can be written as follows:

$$\begin{aligned} &\sigma_x = Q_{11}\varepsilon_x + Q_{12}\varepsilon_s \\ &\sigma_s = Q_{12}\varepsilon_x + Q_{22}\varepsilon_s \\ &\sigma_n = 0 \\ &\tau_{xs} = Q_{66}\gamma_{xs} \\ &\tau_{xn} = Q_{66}\gamma_{xn} \\ &\tau_{sn} = Q_{66}\gamma_{sn} \end{aligned} \tag{14}$$

2.2.3 Forces and moments resultants

Normal forces, moments, and higher order moments, as well as shear forces and higher order shear forces are all defined by the following expressions:

$$\left(N_x, M_x, P_x\right) = \int_{-\frac{h}{2}}^{+\frac{h}{2}} \sigma_x(1, \zeta, \zeta^3)\left(1+\frac{\zeta}{R_0}\right)d\zeta \tag{15}$$

$$\left(N_s, M_s, P_s\right) = \int_{-\frac{h}{2}}^{+\frac{h}{2}} \sigma_s(1, \zeta, \zeta^3)d\zeta \tag{16}$$

$$\left(N_{xs}, M_{xs}, P_{xs}\right) = \int_{-\frac{h}{2}}^{+\frac{h}{2}} \tau_{xs}(1, \zeta, \zeta^3)\left(1+\frac{\zeta}{R_0}\right)d\zeta \tag{17}$$

$$\left(N_{sx}, M_{sx}, P_{sx}\right) = \int_{-\frac{h}{2}}^{+\frac{h}{2}} \tau_{xs}(1, \zeta, \zeta^3)d\zeta \tag{18}$$

$$\left(T_x, Q_x, S_x\right) = \int_{-\frac{h}{2}}^{+\frac{h}{2}} \tau_{xn}(1, \zeta^2, \zeta^3)\left(1+\frac{\zeta}{R_0}\right)d\zeta \tag{19}$$

$$(T_s, Q_s, S_s) = \int_{-\frac{h}{2}}^{+\frac{h}{2}} \tau_{sn}(1, \zeta^2, \zeta^3)d\zeta \tag{20}$$

By considering the effect of initial curvature in the formulation, the stress resultants N_{xs}, M_{xs}, P_{xs} are not equal to the stress resultants N_{sx}, M_{sx}, P_{sx}, respectively. This assumption derives from the consideration that the ratio ζ / R_0 is not neglected with respect to unity. The effect of initial curvature is emphasized by the following coefficients:

$$a_1 = \frac{1}{R_0};\ b_1 = -\frac{1}{R_0};\ b_2 = \frac{1}{R_0^2};\ b_3 = -\frac{1}{R_0^3} \tag{21}$$

Using Eqs. (3-7), (14-21), the relations which characterize the internal stresses as functions of the displacement parameters can be obtained.

2.2.3.1 Normal and shear forces

$$N_x = \left(A_{11} + a_1 B_{11}\right)\frac{\partial u_x}{\partial x} + A_{12}\left(\frac{\partial u_s}{\partial s} + \frac{w}{R_0}\right) + \\ + \left(B_{11} + a_1 D_{11}\right)\frac{\partial \beta_x}{\partial x} + B_{12}\frac{\partial \beta_s}{\partial s} + \left(E_{11} + a_1 F_{11}\right)\frac{\partial \eta_x}{\partial x} + E_{12}\frac{\partial \eta_s}{\partial s} \tag{22}$$

$$N_s = A_{12}\frac{\partial u_x}{\partial x} + \left(A_{11} + b_1 B_{11} + b_2 D_{11} + b_3 E_{11}\right)\left(\frac{\partial u_s}{\partial s} + \frac{w}{R_0}\right) + \\ + B_{12}\frac{\partial \beta_x}{\partial x} + \left(B_{11} + b_1 D_{11} + b_2 E_{11} + b_3 F_{11}\right)\frac{\partial \beta_s}{\partial s} + E_{12}\frac{\partial \eta_x}{\partial x} \\ + \left(E_{11} + b_1 F_{11} + b_2 L_{11} + b_3 H_{11}\right)\frac{\partial \eta_s}{\partial s} \tag{23}$$

$$N_{xs} = A_{66}\frac{\partial u_x}{\partial s} + \left(A_{66} + a_1 B_{66}\right)\frac{\partial u_s}{\partial x} + \\ + B_{66}\frac{\partial \beta_x}{\partial s} + \left(B_{66} + a_1 D_{66}\right)\frac{\partial \beta_s}{\partial x} + E_{66}\frac{\partial \eta_x}{\partial s} + \left(E_{66} + a_1 F_{66}\right)\frac{\partial \eta_s}{\partial x} \tag{24}$$

$$N_{sx} = \left(A_{66} + b_1 B_{66} + b_2 D_{66} + b_3 E_{66}\right)\frac{\partial u_x}{\partial s} + A_{66}\frac{\partial u_s}{\partial x} + \\ + \left(B_{66} + b_1 D_{66} + b_2 E_{66} + b_3 F_{66}\right)\frac{\partial \beta_x}{\partial s} + B_{66}\frac{\partial \beta_s}{\partial x} + \\ + \left(E_{66} + b_1 F_{66} + b_2 L_{66} + b_3 H_{66}\right)\frac{\partial \eta_x}{\partial s} + E_{66}\frac{\partial \eta_s}{\partial x} \tag{25}$$

2.2.3.2 Moments

$$M_x = \left(B_{11} + a_1 D_{11}\right)\frac{\partial u_x}{\partial x} + B_{12}\left(\frac{\partial u_s}{\partial s} + \frac{w}{R_0}\right) + \\ + \left(D_{11} + a_1 E_{11}\right)\frac{\partial \beta_x}{\partial x} + D_{12}\frac{\partial \beta_s}{\partial s} + \left(F_{11} + a_1 L_{11}\right)\frac{\partial \eta_x}{\partial x} + F_{12}\frac{\partial \eta_s}{\partial s} \tag{26}$$

$$M_s = B_{12}\frac{\partial u_x}{\partial x} + \left(B_{11} + b_1 D_{11} + b_2 E_{11} + b_3 F_{11}\right)\left(\frac{\partial u_s}{\partial s} + \frac{w}{R_0}\right) +$$
$$+ D_{12}\frac{\partial \beta_x}{\partial x} + \left(D_{11} + b_1 E_{11} + b_2 F_{11} + b_3 L_{11}\right)\frac{\partial \beta_s}{\partial s} + F_{12}\frac{\partial \eta_x}{\partial x} + \quad (27)$$
$$+ \left(F_{11} + b_1 L_{11} + b_2 H_{11} + b_3 M_{11}\right)\frac{\partial \eta_s}{\partial s}$$

$$M_{xs} = B_{66}\frac{\partial u_x}{\partial s} + \left(B_{66} + a_1 D_{66}\right)\frac{\partial u_s}{\partial x} +$$
$$+ D_{66}\frac{\partial \beta_x}{\partial s} + \left(D_{66} + a_1 E_{66}\right)\frac{\partial \beta_s}{\partial x} + F_{66}\frac{\partial \eta_x}{\partial s} + \left(F_{66} + a_1 L_{66}\right)\frac{\partial \eta_s}{\partial x} \quad (28)$$

$$M_{sx} = \left(B_{66} + b_1 D_{66} + b_2 E_{66} + b_3 F_{66}\right)\frac{\partial u_x}{\partial s} + B_{66}\frac{\partial u_s}{\partial x} +$$
$$+ \left(D_{66} + b_1 E_{66} + b_2 F_{66} + b_3 L_{66}\right)\frac{\partial \beta_x}{\partial s} + D_{66}\frac{\partial \beta_s}{\partial x} + \quad (29)$$
$$+ \left(F_{66} + b_1 L_{66} + b_2 H_{66} + b_3 M_{66}\right)\frac{\partial \eta_x}{\partial s} + F_{66}\frac{\partial \eta_s}{\partial x}$$

2.2.3.3 Higher order moments

$$P_x = \left(E_{11} + a_1 F_{11}\right)\frac{\partial u_x}{\partial x} + E_{12}\left(\frac{\partial u_s}{\partial s} + \frac{w}{R_0}\right) +$$
$$+ \left(F_{11} + a_1 L_{11}\right)\frac{\partial \beta_x}{\partial x} + F_{12}\frac{\partial \beta_s}{\partial s} + \left(H_{11} + a_1 M_{11}\right)\frac{\partial \eta_x}{\partial x} + H_{12}\frac{\partial \eta_s}{\partial s} \quad (30)$$

$$P_s = E_{12}\frac{\partial u_x}{\partial x} + \left(E_{11} + b_1 F_{11} + b_2 L_{11} + b_3 H_{11}\right)\left(\frac{\partial u_s}{\partial s} + \frac{w}{R_0}\right) +$$
$$+ F_{12}\frac{\partial \beta_x}{\partial x} + \left(F_{11} + b_1 L_{11} + b_2 H_{11} + b_3 M_{11}\right)\frac{\partial \beta_s}{\partial s} + H_{12}\frac{\partial \eta_x}{\partial x} + \quad (31)$$
$$+ \left(H_{11} + b_1 M_{11} + b_2 N_{11} + b_3 V_{11}\right)\frac{\partial \eta_s}{\partial s}$$

$$P_{xs} = E_{66}\frac{\partial u_x}{\partial s} + \left(E_{66} + a_1 F_{66}\right)\frac{\partial u_s}{\partial x} +$$
$$+ F_{66}\frac{\partial \beta_x}{\partial s} + \left(F_{66} + a_1 L_{66}\right)\frac{\partial \beta_s}{\partial x} + H_{66}\frac{\partial \eta_x}{\partial s} + \left(H_{66} + a_1 M_{66}\right)\frac{\partial \eta_s}{\partial x} \quad (32)$$

$$P_{sx} = \left(E_{66} + b_1 F_{66} + b_2 L_{66} + b_3 H_{66}\right)\frac{\partial u_x}{\partial s} + E_{66}\frac{\partial u_s}{\partial x} +$$
$$+\left(F_{66} + b_1 L_{66} + b_2 H_{66} + b_3 M_{66}\right)\frac{\partial \beta_x}{\partial s} + F_{66}\frac{\partial \beta_s}{\partial x} + \tag{33}$$
$$+\left(H_{66} + b_1 M_{66} + b_2 N_{66} + b_3 V_{66}\right)\frac{\partial \eta_x}{\partial s} + H_{66}\frac{\partial \eta_s}{\partial x}$$

2.2.3.4 Shear Forces

$$T_x = \left(A_{66} + a_1 B_{66}\right)\frac{\partial w}{\partial x} + \left(A_{66} + a_1 B_{66}\right)\beta_x + 3\left(D_{66} + a_1 E_{66}\right)\eta_x \tag{34}$$

$$T_s = \left(A_{66} + b_1 B_{66} + b_2 D_{66} + b_3 E_{66}\right)\left(-\frac{u_s}{R_0} + \frac{\partial w}{\partial s}\right) +$$
$$+\left(A_{66} + b_1 B_{66} + b_2 D_{66} + b_3 E_{66}\right)\beta_s + \tag{35}$$
$$+\left(3\left(D_{66} + b_1 E_{66} + b_2 F_{66} + b_3 L_{66}\right) + \frac{2}{R_0}\left(E_{66} + b_1 F_{66} + b_2 L_{66} + b_3 H_{66}\right)\right)\eta_s$$

2.2.3.5 Higher order shear resultants

$$Q_x = \left(D_{66} + a_1 E_{66}\right)\left(\frac{\partial w}{\partial x} + \beta_x\right) + 3\left(F_{66} + a_1 L_{66}\right)\eta_x \tag{36}$$

$$Q_s = \left(D_{66} + b_1 E_{66} + b_2 F_{66} + b_3 L_{66}\right)\left(-\frac{u_s}{R_0} + \frac{\partial w}{\partial s}\right) +$$
$$+\left(D_{66} + b_1 E_{66} + b_2 F_{66} + b_3 L_{66}\right)\beta_s + \left(3 + \frac{2}{R_0}\right)\left(F_{66} + b_1 L_{66} + b_2 H_{66} + b_3 M_{66}\right)\eta_s \tag{37}$$

$$S_x = \left(E_{66} + a_1 F_{66}\right)\left(\frac{\partial w}{\partial x} + \beta_x\right) + 3\left(L_{66} + a_1 H_{66}\right)\eta_x \tag{38}$$

$$S_s = \left(E_{66} + b_1 F_{66} + b_2 L_{66} + b_3 H_{66}\right)\left(-\frac{u_s}{R_0} + \frac{\partial w}{\partial s} + \beta_s\right) +$$
$$+\left(3\left(L_{66} + b_1 H_{66} + b_2 M_{66} + b_3 N_{66}\right) + \frac{2}{R_0}\left(H_{66} + b_1 M_{66} + b_2 N_{66} + b_3 V_{66}\right)\right)\eta_s \tag{39}$$

2.2.4 Equilibrium equations

Here we use the principle of virtual displacements to derive the equilibrium equations consistent with the displacement field equations (2). The principle of virtual displacements can be stated in analytical form as:

$$\int_{-\frac{h}{2}}^{+\frac{h}{2}}\int_{\Omega}(\sigma_x\delta\varepsilon_x+\sigma_s\delta\varepsilon_s+\tau_{xs}\delta\gamma_{xs}+\tau_{xn}\delta\gamma_{xn}+\tau_{sn}\delta\gamma_{sn})d\zeta\,d\Omega-\int_{\Omega}p_x\delta u_x dxds-\int_{\Omega}p_s\delta u_s dxds+$$
$$-\int_{\Omega}p_n\delta w dxds-\int_{\Omega}m_x\delta\beta_x dxds-\int_{\Omega}m_s\delta\beta_s dxds-\int_{\Omega}r_x\delta\eta_x dxds-\int_{\Omega}r_s\delta\eta_s dxds=0 \tag{40}$$

where:

$$d\Omega=\left(1+\frac{\zeta}{R_0}\right)R_0\,d\vartheta dx$$

and $p_x, p_s, p_n, m_x, m_s, r_x, r_s$ are the external loads applied on the reference surface. Introducing Eqs. (3-7) into Eq.(40), and integrating the resulting expressions by parts, and setting the coefficients of $\delta u_x, \delta u_s, \delta w, \delta\beta_x, \delta\beta_s, \delta\eta_x, \delta\eta_s$ to zero separately, the following equations of equilibrium are obtained:

$$\begin{aligned}
&\delta u_x:\ \frac{\partial N_x}{\partial x}+\frac{\partial N_{sx}}{\partial s}+p_x=0\\
&\delta u_s:\ \frac{\partial N_s}{\partial s}+\frac{\partial N_{xs}}{\partial x}+\frac{T_s}{R_0}+p_s=0\\
&\delta w:\ \frac{\partial T_x}{\partial x}+\frac{\partial T_s}{\partial s}-\frac{N_s}{R_0}+p_z=0\\
&\delta\beta_x:\ \frac{\partial M_x}{\partial x}+\frac{\partial M_{sx}}{\partial s}-T_x+m_x=0\\
&\delta\beta_s:\ \frac{\partial M_s}{\partial s}+\frac{\partial M_{xs}}{\partial x}-T_s+m_s=0\\
&\delta\eta_x:\ \frac{\partial P_x}{\partial x}+\frac{\partial P_{sx}}{\partial s}-3Q_x+r_x=0\\
&\delta\eta_s:\ \frac{\partial P_s}{\partial s}+\frac{\partial P_{xs}}{\partial x}-3Q_s-2\frac{S_s}{R_0}+r_s=0
\end{aligned} \tag{41}$$

It is worth noting that Eqs.(41) are derived by taking into account the definitions (15-20) of forces and moment resultants. The first three Eqs.(41) express the translational equilibrium along the meridional x, circumferential s, and normal ζ direction, respectively. The last four Eqs.(41) are rotational equilibrium equations about the s and x directions, respectively. In particular, the first

two are the effective rotational equilibrium equations, whereas the second two represent fictitious equations, which are derived by the computation of the additional terms of displacement.

Then, substituting the expressions (22-39) for the in-plane meridional, circumferential, and shearing force resultants N_x, N_s, N_{xs}, N_{sx}, the analogous couples $M_x, M_s, M_{xs}, M_{sx}, P_x, P_s, P_{xs}, P_{sx}$ and the transverse shear force resultants $T_x, T_s, Q_x, Q_s, S_x, S_s$, Eqs.(41) yield the fundamental system of equations:

$$\begin{bmatrix} R_{11} & R_{12} & R_{13} & R_{14} & R_{15} & R_{16} & R_{17} \\ R_{21} & R_{22} & R_{23} & R_{24} & R_{25} & R_{26} & R_{27} \\ R_{31} & R_{32} & R_{33} & R_{34} & R_{35} & R_{36} & R_{37} \\ R_{41} & R_{42} & R_{43} & R_{44} & R_{45} & R_{46} & R_{47} \\ R_{51} & R_{52} & R_{53} & R_{54} & R_{55} & R_{56} & R_{57} \\ R_{61} & R_{62} & R_{63} & R_{64} & R_{65} & R_{66} & R_{67} \\ R_{71} & R_{72} & R_{73} & R_{74} & R_{75} & R_{76} & R_{77} \end{bmatrix} \begin{bmatrix} u_x \\ u_s \\ w \\ \beta_x \\ \beta_s \\ \eta_x \\ \eta_s \end{bmatrix} = \begin{Bmatrix} p_x \\ p_s \\ p_n \\ m_x \\ m_s \\ r_x \\ r_s \end{Bmatrix} \tag{42}$$

where the explicit forms of the equilibrium operators $R_{ij}, i, j = 1,...,7$ are listed in Appendix A.

It can be noticed that the analytical expressions of most of the equilibrium operators in (42) are characterized by the presence of the coefficients a_1, b_1, b_2, b_3 (21), which incorporate the effect of the initial curvature, as declared above. By putting $a_1 = b_1 = b_2 = b_3 = 0$, the effect of initial curvature can be neglected.

It should be noted that the loadings on the middle surface can be expressed in terms of the loadings on the upper and lower surfaces of the shell as follows:

$$\begin{aligned} p_x &= p_x^t\left(1+\frac{h}{2R_0}\right)+p_x^b\left(1-\frac{h}{2R_0}\right) \\ p_s &= p_s^t\left(1+\frac{h}{2R_0}\right)+p_s^b\left(1-\frac{h}{2R_0}\right) \\ p_n &= p_n^t\left(1+\frac{h}{2R_0}\right)+p_n^b\left(1-\frac{h}{2R_0}\right) \\ m_x &= p_x^t\frac{h}{2}\left(1+\frac{h}{2R_0}\right)-p_x^b\frac{h}{2}\left(1-\frac{h}{2R_0}\right) \\ m_s &= p_s^t\frac{h}{2}\left(1+\frac{h}{2R_0}\right)-p_s^b\frac{h}{2}\left(1-\frac{h}{2R_0}\right) \end{aligned} \tag{43}$$

$$r_x = p_x^t \frac{h^3}{8}\left(1+\frac{h}{2R_0}\right) - p_x^b \frac{h^3}{8}\left(1-\frac{h}{2R_0}\right)$$

$$r_s = p_s^t \frac{h^3}{8}\left(1+\frac{h}{2R_0}\right) - p_s^b \frac{h^3}{8}\left(1-\frac{h}{2R_0}\right)$$

where p_x^t, p_s^t, p_n^t are the meridional, circumferential and normal forces applied to the upper surface, and p_x^b, p_s^b , p_n^t are the meridional, circumferential and normal forces applied to the lower surface.

The boundary conditions considered in this study are the fully clamped edge boundary condition (C), the simply supported edge boundary condition (S) and the free edge boundary condition (F). They assume the following form:

Clamped edge boundary condition (C):

$$u_x = u_s = w = \beta_x = \beta_s = \eta_x = \eta_s = 0 \text{ at } x = 0 \text{ or } x = L_0 \quad 0 \le s \le s_0, \tag{44}$$

$$u_x = u_s = w = \beta_x = \beta_s = \eta_x = \eta_s = 0 \text{ at } s = 0 \text{ or } s = s_0 \quad 0 \le x \le L_0 \tag{45}$$

Simply supported boundary condition (S):

$$u_x = w = \beta_x = \eta_x = 0 \quad N_x = M_x = P_x = 0 \text{ at } x = 0 \text{ or } x = L_0 \quad 0 \le s \le s_0, \tag{46}$$

$$u_s = w = \beta_s = \eta_s = 0 \quad N_s = M_s = P_s = 0 \text{ at } s = 0 \text{ or } s = s_0 \quad 0 \le x \le L_0 \tag{47}$$

Free edge boundary condition (F):

$$N_x = N_{xs} = T_x = M_x = M_{xs} = P_x = P_{xs} = 0$$
$$\text{at } x = 0 \text{ or } x = x_{0,} \quad 0 \le s \le s_0 \tag{48}$$

$$N_s = N_{sx} = T_s = M_s = M_{sx} = P_s = P_{sx} = 0$$
$$\text{at } s = 0 \text{ or } s = s_{0,} \quad 0 \le x \le L_0 \tag{49}$$

In the above (44)-(49) boundary conditions, it has been assumed $s_0 = 2\pi R_0$. In order to analyze the whole shell of revolution, and not a panel, the kinematic and physical compatibility must be added to the previous external boundary conditions. They represent the condition of continuity related to displacements and internal stress resultants. Their analytical forms are proposed as follows:

Kinematic compatibility conditions along the closing meridian $(s = 0, 2\pi R_0)$:

$$
\begin{aligned}
&u_x(x,0)=u_x(x,s_0),\ u_s(x,0)=u_s(x,s_0),\\
&w(x,0)=w(x,s_0),\ \beta_x(x,0)=\beta_x(x,s_0),\\
&\beta_s(x,0)=\beta_s(x,s_0),\ \eta_x(x,0)=\eta_x(x,s_0),\\
&\eta_s(x,0)=\eta_s(x,s_0)\ \ 0\le x\le L_0
\end{aligned}
\tag{50}
$$

Physical compatibility conditions along the closing meridian $(s=0,2\pi R_0)$:

$$
\begin{aligned}
&N_s(x,0)=N_s(x,s_0),\ N_{sx}(x,0)=N_{sx}(x,s_0),\\
&T_s(x,0)=T_s(x,s_0),\ M_s(x,0)=M_s(x,s_0),\\
&M_{sx}(x,0)=M_{sx}(x,s_0)\ ,P_s(x,0)=P_s(x,s_0),\\
&P_{sx}(x,0)=P_{sx}(x,s_0),\ \ 0\le x\le L_0
\end{aligned}
\tag{51}
$$

2.3 Discretized equations and stress recovery

The generalized differential quadrature method (GDQ) [53-58] is used to discretize the derivatives in the governing equations (42), as well as the external boundary conditions and the compatibility conditions. In this paper, the Chebyshev-Gauss-Lobatto grid distribution is adopted, where the coordinates of grid points along the reference surface are identified by the following relations:

$$
\begin{aligned}
&x_i=\left(1-\cos\left(\frac{i-1}{N-1}\pi\right)\right)\frac{(x_1-x_0)}{2}+x_0\\
&i=1,2,....,N,\ \ for\ \ x\in[0,L_0]\\
&s_j=\left(1-\cos\left(\frac{j-1}{M-1}\pi\right)\right)\frac{s_0}{2},\\
&j=1,2,....,M,\ \ for\ \ s\in[0,s_0]
\end{aligned}
\tag{52}
$$

where N, M are the total number of sampling points which discretize the domain in x and s directions, respectively. This particular choice of the C-G-L sampling points rule with respect to the others suggested in literature is justified by the tested efficiency of the GDQ technique.
By writing the fundamental equilibrium equations (42) by means of GDQ technique, the following matrix form is obtained:

$$
\begin{bmatrix}\boldsymbol{K}_{bb} & \boldsymbol{K}_{bd}\\ \boldsymbol{K}_{db} & \boldsymbol{K}_{dd}\end{bmatrix}\begin{bmatrix}\boldsymbol{\delta}_b\\ \boldsymbol{\delta}_d\end{bmatrix}=\begin{bmatrix}\boldsymbol{p}_b\\ \boldsymbol{p}_d\end{bmatrix}
\tag{53}
$$

In the present formulation the subscripts b and d stand for *boundary* and *domain*, respectively. The b-equations define the external boundary conditions and compatibility conditions written on the constrained edges of the cylindrical shell, and the d-equations represent the scripture of the fundamental equations at the points which belong to the domain. The solution procedure by means of the GDQ technique is implemented with the support of a MATLAB code.

According to the Reddy's constrained theory, the transverse shear stresses satisfy a priori the zero shear condition on the upper and lower surfaces of the graded cylindrical shell. As it is well known, and differently from the constrained theory by Reddy, the transverse shear stress determined from the 2D-Unconstrained Theory of first and third order does not satisfy the zero shear condition on the lateral surfaces of the cylindrical shell. A possible approach for solving this difficulty is to recovery the out of plane shear stress using 3D-equilibrium equations. In the case of plates, a general presentation of the stress recovery problem is reported in [59].

Using the stationary principle of total potential energy, the 3D elastic equilibrium equations for a functionally graded cylindrical shell are written as follows:

$$\frac{\partial \tau'_{xn}}{\partial \zeta} + \tau'_{xn}\left(\frac{1}{\zeta + R_0}\right) = -\frac{\partial \sigma_x}{\partial x} - \left(\frac{R_0}{\zeta + R_0}\right)\frac{\partial \tau_{xs}}{\partial s} \tag{54}$$

$$\frac{\partial \tau'_{sn}}{\partial \zeta} + \tau'_{sn}\left(\frac{2}{\zeta + R_0}\right) = -\frac{\partial \tau_{xs}}{\partial x} - \frac{R_0}{\zeta + R_0}\frac{\partial \sigma_s}{\partial s} \tag{55}$$

$$\frac{\partial \sigma'_n}{\partial \zeta} + \sigma'_n\left(\frac{1}{1 + R_0}\right) = -\frac{\partial \tau'_{xn}}{\partial x} + \frac{1}{\zeta + R_0}\sigma_s - \frac{R_0}{\zeta + R_0}\frac{\partial \tau'_{sn}}{\partial s} \tag{56}$$

By the knowledge of the membrane stresses ($\sigma_x, \sigma_s, \tau_{xs}$) and their derivatives in all the points of the 3D cylindrical shell, the present equations (54-56) of the first order can be solved via the GDQ along the thickness direction. The C-G-L grid distribution is selected for the grid points ζ_m along the thickness direction:

$$\zeta_m = \left(1 - \cos\left(\frac{m-1}{T-1}\pi\right)\right)\frac{h}{2} - \frac{h}{2},\ m = 1, 2.., T\ ,\ \zeta \in \left[-\frac{h}{2}, -\frac{h}{2}\right] \tag{57}$$

By imposing the boundary conditions at the bottom surface of the shell, equations (54) and (55) are written via the GDQ method in the algebraic form and solved in terms of τ'_{xn}, τ'_{sn}.

$$\begin{cases} \sum_{k=1}^{T} \zeta_{mk}^{\zeta(1)} \tau'_{xn(ijk)} + \dfrac{\tau'_{xn(ijm)}}{\zeta_m + R_0} = -\left.\dfrac{\partial \sigma_x}{\partial x}\right|_{(ijm)} - \dfrac{R_0}{\zeta_m + R_0}\left.\dfrac{\partial \tau_{xs}}{\partial s}\right|_{(ijm)} m = 2, 3.....T \\ \tau'_{xn(ij1)} = \bar{p}_{x(ij)} \end{cases} \tag{58}$$

$$\begin{cases} \sum_{k=1}^{T} \zeta_{mk}^{\zeta(1)} \tau'_{sn(ijk)} + \tau'_{sn(ijm)} \dfrac{2}{\zeta_m + R_0} = -\dfrac{\partial \tau_{xs}}{\partial x}\bigg|_{(ijm)} - \dfrac{R_0}{\zeta_m + R_0} \dfrac{\partial \sigma_s}{\partial s}\bigg|_{(ijm)} \; m = 2,3....T \\ \tau'_{sn(ij1)} = p^{-}_{s(ij)} \end{cases} \tag{59}$$

The shear stress distributions τ'_{xn}, τ'_{sn} carried out by the linear systems (58) and (59) do not satisfy the boundary condition at the top surface of shell structure. Consequently, the transverse shear stress representations are improved via the refinement suggested by Auricchio and Sacco [66] and Tornabene et al. [59], in the following manner:

$$\begin{aligned} \tau^{r}_{xn(ijm)} &= \tau'_{xn(ijm)} + \frac{p^{+}_{x(ij)} - \tau'_{xn(ijT)}}{h}\left(\zeta_m + \frac{h}{2}\right) \\ \tau^{r}_{sn(ijm)} &= \tau'_{sn(ijm)} + \frac{p^{+}_{s(ij)} - \tau'_{sn(ijT)}}{h}\left(\zeta_m + \frac{h}{2}\right) \quad m = 1,2.....T \end{aligned} \tag{60}$$

Finally, the transverse normal stress σ'_n profiles are derived by solving the equation (56) via the GDQ method:

$$\begin{cases} \sum_{k=1}^{T} \zeta_{mk}^{\zeta(1)} \sigma'_{n(ijk)} + \dfrac{\sigma'_{n(ijm)}}{\zeta_m + R_0} = -\dfrac{\partial \tau^{r}_{xn}}{\partial x}\bigg|_{(ijm)} - \dfrac{R_0}{\zeta_m + R_0} \dfrac{\partial \tau^{r}_{sn}}{\partial s}\bigg|_{(ijm)} + \dfrac{\sigma_{s(ijm)}}{\zeta_m + R_0} \quad m = 2,3....T \\ \sigma'_{n(ij1)} = p^{-}_{n(ij)} \end{cases} \tag{61}$$

In order to satisfy the boundary condition at the top surface, the σ'_n distributions are also corrected as follows:

$$\sigma^{r}_{n(ijm)} = \sigma'_{n(ijm)} + \frac{p^{+}_{n(ij)} - \sigma'_{n(ijT)}}{h}\left(\zeta_m + \frac{h}{2}\right) \quad m = 1,2....T \tag{62}$$

2.4 Numerical results

2.4.1 Classes of graded materials

In this numerical study, the static analysis of FGM cylindrical shells is conducted and the through the thickness stress distributions are furnished. The theoretical formulations are based on two shear deformation models: the generalized unconstrained third (GUTSDT) and first order (GFSDT) shear deformation theories. They are labeled as generalized because they are enriched by the initial curvature effect. The stress recovery is also proposed in order to define the correct profile of the

transverse shear and normal stress profiles, by the knowledge of the membrane stress components derived from the 2D shear deformation model. In this manner the shear effect is definitely improved. The numerical analysis is done by means of the GDQ numerical technique.

The basic constituents of FGM materials are taken to be zirconia (ceramic component) and aluminum (metal component). Young's modulus and Poisson's ratio for the zirconia are $E_C = 168\ GPa$, $\nu_C = 0.3$, and for the aluminum are $E_M = 70\ GPa$, $\nu_M = 0.3$, respectively. The ceramic volume fraction is varied by means of the four parameter power law distribution [21,22].

The main objectives of the numerical study reported in this section are the followings:

1. to study the role of the four parameters of the power law function for various classes of graded materials;
2. to compare the numerical results via the unconstrained third order model with those via the first order one;
3. to clarify the influence of the initial curvature effect in the numerical analysis, developed herein;
4. to emphasize the key role of the stress recovery technique in determining the transverse normal and tangential stress components.

In order to characterize the effect of the volume fraction gradation as a function of the material coefficients, eight types of graded materials are investigated. In Fig.2*a* the distributions of the ceramic volume fraction V_C across the thickness for a wide range of p-values are presented for the $\mathrm{FGM1}_{(1,0,0,\mathrm{p})}$ class. It should be noticed that the lower surface $(\zeta/h = -0.5)$ of the composite structure is fully ceramic, and the top surface $(\zeta/h = 0.5)$ is purely metallic. For $0.1 \le \mathrm{p} \le 2$ (Fig.2*a*), the material composition is continuously graded throughout the thickness. Differently, for $\mathrm{p} = 5$ the ceramic volume fraction gradually changes only for $-0.5 \le \zeta/h \le 0.25$, and for the remaining thickness it attains a null value. For $\mathrm{p} = 8$, the ceramic volume fraction is continuously graded from the bottom surface to the middle layer, and for the rest it has a null value. For $\mathrm{p} = 50{,}100$, the variation of the ceramic volume fraction is very restricted to the layers which are closer to the bottom one, and moving away the ceramic volume fraction becomes equal to zero. In Fig.2*b*, the distributions of the ceramic volume fraction are shown for the $\mathrm{FGM1}_{(1,1,4,\mathrm{p})}$ class for several p-values [22]. All the $\mathrm{FGM1}_{(1,1,4,\mathrm{p})}$ composite shells are fully ceramic at the top and bottom surfaces. For $\mathrm{p} \le 1$ the ceramic volume fraction remains higher than 50%, whereas for $\mathrm{p} = 2$ the ceramic

volume fraction V_C has the analogous trend but it reaches values lower than 50%. For $0 \le \zeta/h \le 0.5$ and $p \le 1$, the ceramic volume fraction rapidly increases and it remains higher than 50%. For $p = 0.05$, the distribution of the ceramic volume fraction is quasi ceramic. For $p = 20, 50$ the graded microstructure only belongs to the lower and upper layers of the $FGM1_{(1,1,4,p)}$ cylindrical shell, and reveals an homogeneous composition rich in the metal constituent inside the composite structure. In Fig.2*c*, the ceramic volume fraction of the $FGM1_{(1,0.5,2,p)}$ graded material is plotted versus the dimensionless shell thickness [22]. The bottom surface of the composite shell structure is fully ceramic for all the p- values. The top surface is made of a mixture of ceramic and metallic constituents for $p = 0.6, 2, 5$, with increasing metallic content with respect to the ceramic one, respectively. For $p = 10, 20, 50$ the ceramic volume fraction is continuously graded from the bottom surface till ζ/h variable, respectively, equal to 0.25, -0.25, -0.375. Consequently, the resulting composite material for $p = 50$ is prevalently metallic. In Fig.2*d*, the distributions of the ceramic volume fraction across thickness for several a-values are presented for the $FGM1_{(a,0.2,3,2)}$ class [24,32]. It appears that the bottom surface of the composite structure is purely ceramic, and the top surface changes its composition with the variation of the a-parameter. For $a = 0.2$ the top surface of the $FGM1_{(a,0.2,3,2)}$ cylindrical shell is also ceramic. By varying the a-parameter from 0.3 to 1, the top surface becomes a mixture of ceramic and metallic constituents. In particular, with the increase of a, the top surface becomes richer and richer of the metallic component. In Fig.3*a*, the distributions of the ceramic volume fraction across the thickness for several a-values are presented for the $FGM2_{(a,0.2,3,2)}$ class. In contrast with the previous case, it appears that the top surface of the composite structure is purely ceramic, and the bottom surface changes its composition with the variation of the a-parameter. For $a = 0.2$ the bottom surface of the $FGM2_{(a,0.2,3,2)}$ cylindrical shell is also ceramic. By varying the a-parameter from 0.3 to 1, the bottom surface is made from a mixture of ceramic and metallic constituents. In particular, with the increase of a, the bottom surface becomes richer and richer of the metallic component. For all the a-values, the ceramic volume fraction is continuously graded throughout the shell thickness. In Fig.3*b*, the distributions of the ceramic volume fraction across the thickness for several a-values are presented for the $FGM2_{(0,b,2,1)}$ class [24,32]. It appears that the top surface of the composite structure is purely ceramic, and the bottom surface changes its composition with the variation of the b-parameter. By varying the b-parameter from -0.2 to -0.9, the bottom surface is made from a mixture of ceramic and metallic constituents. In particular, with the decrease of b, the bottom surface becomes richer

and richer of the metallic component. For $b=-1$ the bottom surface is purely metallic. From Figs. 3a,b it appears that for all the a and b values, the ceramic volume fraction is continuously graded throughout the shell thickness. In Fig.3*c*, the ceramic volume fraction of the $FGM1_{(1,0.5,c,2)}$ curves versus the shell thickness is presented. It is noted that the top surface is compositionally made of the 25% in the ceramic constituent, and the 75% in the metallic one, for all the c-values. Differently, the bottom layer is fully ceramic. In Fig.3*d* the ceramic volume fraction profiles of the $FGM1_{(1,1,c,1)}$ are also proposed [24,32]. For all the c-values the ceramic volume fraction follows a parabolic pattern. The external surfaces are ceramic rich. With decreasing values of the c – parameter the ceramic volume fraction attains maximum values at layers nearer to the middle one.

2.4.2 Stress profiles of $FGM1_{(1,0,0,p)}$ cylindrical panels

2.4.2.1 Generalized and traditional unconstrained theories

Prevalently, the geometric and boundary conditions, as well as the external loading, are always taken as in the reference configuration, which is defined as follows: the shell thickness is assumed $h=0.1\ m$, the ϑ-angle is equal to 120°, the parallel radius R_0 and the cylinder height L_0 are both equal to 1m. The boundary condition of clamped edges is considered and the radial (p_n) constant compressive pressure, equal to 0.1MPa, is applied over the top layer. The normal and shear stresses are calculated at the point $(0.25L_0;0.25s_0)$ along the ζ - direction, being $s_0=2\pi R_0$. All the stress components are furnished by using the scaled form as follows:

$$\begin{aligned}\overline{g}&=\alpha g\left(0.25L_0,0.25s_0,\zeta\right)\\ g^*&=\alpha g\left(0.25L_0,0.25s_0,\zeta\right)\end{aligned}\qquad(63)$$

where $\overline{g}$ or g^* represent the scaled stress component, g is the stress component calculated at a fixed point and α the scale factor used for the representation and reported in caption.

In Figs.4*a,b,c,d,e,f* the shear $\tau_{xn}^*,\tau_{sn}^*,\overline{\tau}_{xs}$ and normal $\overline{\sigma}_x,\overline{\sigma}_s,\sigma_n^*$ stresses distributions are shown for the $FGM1_{(1,0,0,0.1)}$ and $FGM1_{(1,0,0,2)}$ cylindrical panels, by adopting in the calculation the standard geometrical data, loading distribution value and boundary condition. The tangential and normal stresses distributions are plotted across the dimensionless panel thickness for two p- values, via the GUTSDT, UTSDT and stress recovery technique with regard to the transverse stress components. In Fig.4*a* the transverse shear τ_{xn}^* stress curves are presented and the initial curvature effect does not appear relevant. Differently, by considering the transverse shear τ_{sn}^* stress profiles in Fig.4*b*, the differences between the stress curves are quite significant as well as the unconstrained third order formulation is enriched by the initial curvature effect. In Figs.4*c,d* the membrane shear $\overline{\tau}_{xs}$ and

normal $\bar{\sigma}_x$ stress distributions are proposed. At a fixed p - value the deviations between the $\bar{\tau}_{xs}$ stress curves gradually reduce from the inner to the outer layer, whereas the opposite trend characterizes the $\bar{\sigma}_x$ stress distributions with and without the improved initial curvature effect. In Fig.4*e* the membrane $\bar{\sigma}_s$ stress distributions are suggested by means of the GUTSDT and UTSDT. It appears that the stress curves from the GUTSDT and the UTSDT theories are significantly divergent for both p-values. In Fig.4*f* the transverse normal σ_n^* stress component is showed and the deviation between the stress curves with and without the initial curvature effect addition is negligible throughout the panel thickness.

2.4.3 Stress profiles of $\text{FGM1}_{(1,1,4,\text{p})}$ cylindrical shells

2.4.3.1 Generalized unconstrained third and first order theories

In Figs.5*a,b,c,d* the tangential τ_{xn}^* and normal $\bar{\sigma}_x, \bar{\sigma}_s, \sigma_n^*$ stress distributions along the thickness direction are presented for $\text{p} = 0, 0.5, 5$, via the GUTSDT and GFSDT coupled with the stress recovery, when the radial uniform compressive pressure p_n is only considered. The geometrical parameters and boundary conditions adopted in the numerical example are as in the standard case. With the elevation of the power exponent, the divergence between the stress profile via the GUTSDT and GFSDT results very restricted for the most part of the stress components. It appears that, by considering the τ_{xn}^* shear stress curves in Fig.5*a*, the deviation between the first and third order static response slightly appears around the τ_{xn}^* maximum shear stress values.

2.4.4 Stress profiles of $\text{FGM1}_{(1,0.5,2,\text{p})}$ cylindrical shells

2.4.4.1 Generalized and traditional unconstrained theories

In Figs.6*a,b,c,d* the tangential and normal stress distributions along the ζ direction are shown for the $\text{FGM1}_{(1,0.5,2,\text{p})}$ cylindrical shells by using the GUTSDT and UTSDT with the stress recovery. The geometric parameters are assumed as in the standard configuration. The edges of the cylindrical shell are clamped and supported, and the composite structure is subjected to the radial compressive pressure, equal to 0.1MPa. All the stress profiles are calculated for $p = 5, 10$. In Fig.6*a*, the shear stress profiles via the generalized unconstrained theory approach to a maximum value, which is lower that the one of the corresponding shear stress curves obtained by the unconstrained theory, where the initial curvature effect is neglected. In Fig.6*b* the normal $\bar{\sigma}_x$ stress curves exhibit no significant variations by considering or not the initial curvature effect. Differently, the influence of the initial curvature effect on the normal $\bar{\sigma}_s$ stress curves is more significant away from the

reference layer, as shown in Fig.6*c*. In Fig.6*d*, the transverse normal stress curves derived from the stress recovery are presented. It appears that the normal σ_n^* stress curves show little differences for both p-values, by considering or not the initial curvature effect.

2.4.5 Stress profiles of $\mathrm{FGM1}_{(a,0.2,3,2)}$ and $\mathrm{FGM2}_{(a,0.2,3,2)}$ cylindrical panels

2.4.5.1 The generalized unconstrained theory

In Figs.7*a,b,c,d,e,f* the tangential ($\tau_{xn}^*, \tau_{sn}^*, \bar{\tau}_{xs}$) shear and normal ($\bar{\sigma}_x, \bar{\sigma}_s, \sigma_n^*$) stress profiles of the $\mathrm{FGM1,2}_{(a,0.2,3,2)}$ cylindrical panels are presented for several a-values, by using the reference configuration. All the stress profiles refer to four values of the parameter $a = 0.2, 0.4, 0.8, 1$. The GUTSDT with the stress recovery is considered for the numerical analysis. It appears that by increasing the a-value, the deviation between the stress curves of the structure graded by means of the first form and the ones corresponding to the second form of the four parameter power exponent function, significantly increases.

2.4.6 Stress profiles of $\mathrm{FGM1}_{(1,0.5,c,2)}$ cylindrical panels

2.4.6.1 Generalized unconstrained first and third order theories

In Figs.8*a,b,c,d,e,f* the stress profiles of the $\mathrm{FGM1}_{(1,0.5,c,2)}$ cylindrical shells are determined by means of the unconstrained first and third order theories. All the geometric and boundary conditions are unvaried with respect to the reference configuration. The loading condition consider the radial and axial compressive pressures at the top surface, both equal to 0.1MPa. The GUTSDT with the stress recovery is used in the present numerical analysis. In Fig.8*a*, the transverse shear τ_{xn}^* stress curves are almost juxtaposed for both c-values and for both the shear deformation models. It is noticed how by considering the further action of the axial constant compressive pressure at the top layer, the transverse shear τ_{xn}^* stress profile releases the external load at the top layer and the null value at the inner one, by making the boundary condition satisfied. In Fig.8*b*, the transverse shear τ_{sn}^* stress profiles are plotted along the shell thickness and a little deviation is recognizable between the static response of the first and third order around the τ_{sn}^* maximum value. For the rest, the divergence between the two order is negligible for the membrane shear $\bar{\tau}_{xs}$ stress curves and for the transverse normal σ_n^* ones. Whereas it could be considered limited as far as the membrane normal ($\bar{\sigma}_x, \bar{\sigma}_s$) distributions are examined along the panel thickness, as shown in Fig.8*d*,8*e*.

2.4.7 The stress recovery approach for the generalized unconstrained first and third order theories

In Figs.9*a,b,c,d* and 10*a,b,c,d* the transverse shear stress $\bar{\tau}_{xn}, \tau^{*}_{xn}$ and $\bar{\tau}_{sn}, \tau^{*}_{sn}$ curves, respectively, are plotted along the panel thickness, by means of the first and third order unconstrained model for four different types of graded materials: $\mathrm{FGM1}_{(1,0,0,2)}$, $\mathrm{FGM1}_{(1,0.5,2,5)}$, $\mathrm{FGM2}_{(0,-0.5,2,1)}$, $\mathrm{FGM1}_{(1,1,5,1)}$. The geometric and boundary configuration are considered as in the reference configuration. For each couple of tangential stresses, the loading condition is inclusive of one (p_n), two (p_x, p_n) or (p_s, p_n), or all the three radial (p_n), axial (p_x) and circumferential (p_s) constant compressive pressures at the top surface of the graded structure. The distributed compressive pressure is fixed at 0.1 MPa in every direction. All the transverse shear stress curves are derived from the first and third order formulations and also reconstructed via the stress recovery technique.

It is quite evident how the static response urges the need of the stress recovery approach in order to achieve the correct pattern which satisfies the boundary conditions in all the loading cases suggested. In particular, the divergence between the first and third order static response in terms of both transverse shear stresses under investigation results quite relevant by comparing the recovered stress profiles with the unrecovered ones. Differently from the Constrained order theory by Reddy, the Unconstrained one coupled with the Stress recovery allows the computation of the external shear loading pressures on the boundary surfaces of the cylindrical structure under consideration. The relaxation of the Reddy's hypothesis on the boundary, which enforces the null value of shear pressure at the outer and inner layer, is the proper advantage in using the UTSDT and the Stress recovery.

2.5 Literature numerical examples worked out for comparison

In this section several numerical examples are considered in order to compare the present results with the existing ones in literature. Aghdam et al. [60] investigated the bending of moderately thick clamped functionally graded (FG) conical panels subjected to uniform and non uniform distributed loadings. They used the first order shear deformation theory by taking into account the initial curvature effect in the formulation. In the present work, the numerical results reported in [60] for a cylindrical isotropic panel are considered for comparison. The material properties are: $E_M = 3.1\,\mathrm{GPa}$, $\nu_M = 0.3$ and the geometry parameters are: $\vartheta = 11.46°$, $R_0 = 2.54\,\mathrm{m}$, $h/R_0 = 0.00125$, $L/R_0 = 0.2$. The cylindrical isotropic panel is clamped and subjected to the transverse distributed load 275.8 Pa. The maximum center deflection is reported in Table 1a, and the numerical value from the reference under consideration is compared with the ones calculated in

this paper by using the first and third order shear deformation theories. Zhao et al. [61] analyzed the static response of metal and ceramic functionally graded shells, by means of the first order shear deformation theory (FSDT). Here, the prediction reported in [61] for a cylindrical isotropic panel is suggested for comparison. Material properties and geometrical parameters are the same as above. The cylindrical isotropic panel is clamped and subjected to a transverse distributed load 257.9 Pa. Table 1b shows a comparison between the vertical displacements at the panel center obtained from the first and third order theories, respectively, and the one reported in [61]. In the same paper [61] the numerical results concerning the non dimensional center deflections of Al/Z_rO_2 cylindrical panels under a uniform transverse load, are also reported. The results refer to the following material properties: $E_{Al} = 70\,\text{GPa}$, $\nu_{Al} = 0.3$, $E_{ZrO_2} = 151\text{GPa}$, $\nu_{ZrO_2} = 0.3$, and geometrical parameters: $\vartheta = 11.46°$, $R_0 = 1\,\text{m}$, $h = 0.01\,\text{m}$, $L = 0.2\,\text{m}$. The functionally graded cylindrical panel is subjected to a uniform transverse load 1MPa and the external edges are variously constrained (i.e. all edges simply supported (SSSS), all edges clamped (CCCC), two opposite edges simply supported and two clamped (CSCS), two edges clamped and two opposite edges free (CFCF), and one edge clamped and the other three edges free (CFFF)). By varying the power exponent law, the non dimensional center deflection ($\overline{w} = w/h$) is calculated by means of several theories. The numerical values calculated according to these theories, are reported in Tables 2a,b and compared with those of Zhao et al. [61]. The effect of two distinct values of the radius to thickness ratio at the center deflection ($\overline{w} = w/h$) is also analyzed, as far as Al/Z_rO_2 cylindrical panels under a transverse uniform pressure are concerned. Several p values are considered and the following geometrical parameters $\vartheta = 11.46°$, $R_0 = 1\,\text{m}$, $L = 0.2\,\text{m}$, $h = 0.02\,\text{m}$ or $0.005\,\text{m}$, are assumed.

Tables 3a,b shows the results of central displacement for simply supported and clamped cylindrical panels via the present theories and the one from Zhao et al [61]. From Tables 2a,b and Tables 3a,b it appears that the present results agree well with those obtained by Aghdam et al. [60] and Zhao et al. [61].

The numerical results from the present theory are also verified by considering the existing results in literature about the rectangular plates. Fereidoon et al. [62] developed the bending analysis of thin rectangular plates using the GDQ method. They considered functionally graded square plates subjected to a distributed transverse load with all simply supported edges and the following material properties: $L_x = 1\,\text{m}$, $h = 0.02\,\text{m}$, $E_1 = 5\times10^{10}\,\text{N/m}^2$, $\nu = 0.3$, $q_0 = 1\times10^5\,\text{N/m}^2$. Table 4 presents the maximum dimensionless deflection $\overline{w} = \left(D_0/q_0\,L_x^4\right)w$, with $D_0 = E_1h^3\Big/\left(12\left(1-\nu^2\right)\right)$ for different values of the following parameters: the non homogeneity power (p), the non homogeneity ratio

(E_2/E_1), and the aspect ratio (L_x/L_y). It appears that our results agree quite closely with the ones reported in [62].

Ferreira et al. [63,64] conducted the analysis of composite plates using higher order shear deformation theory and a finite point formulation based on the multiquadric radial basis function method. A simply supported square isotropic plate under uniform load is considered. The length and thickness of the plate are denoted by L and h, respectively. The modulus of elasticity and the Poisson's ratio are $10920\,\text{Pa}$, and $v = 0.25$, respectively. In the central node of the plate the following normalized displacement and normal stress are considered $\overline{w} = Eh^3 10^2 w(a/2, a/2, 0)/qL^4$, $\overline{\sigma}_x = \sigma_x(L/2, L/2, -h/2)h^2/qL^2$. The numerical results achieved from the present theories are in good agreement with solutions by [63,64,69,70], as shown in Table 5. Zenkour[65] presented the static response for a simply supported functionally graded rectangular plate subjected to a transverse uniform load. He simplified the theory by enforcing traction free boundary condition at the plate faces. Here, the center deflection w and the distribution across the plate thickness of in - plane longitudinal stress σ_x and longitudinal tangential stress τ_{xy} are compared with the results of the classic solution [70], 3D solution by Werner [71] and Zenkour [65], as shown in Tables 6,7. Moreover, the effect of the volume fraction exponent on the dimensionless stresses and displacements of a FGM square plate ($L_x/h = 10$) is investigated. The various non dimensional parameters used are: $\overline{\sigma}_x = (h/a\,q_0)\sigma_x\left(L_x/2, L_y/2\right)$, $\overline{\tau}_{xn} = \left(h/L_x\,q_0\right)\tau_{xn}\left(L_x/2, 0, h/6\right)$, $\overline{w} = \left(10h^3 E_c/L_x^4\,q_0\right)w\left(L_x/2, L_y/2,\right)$, $\overline{\tau}_{yn} = \left(h/L_x\,q_0\right)\tau_{yn}\left(0, L_y/2, 0\right)$. Tables 8,9,10,11a,11b,12a,12b show comparisons between results for graded plates subjected to uniform distributed load as in Zenkour [65] and the theories developed in the present study. It is noted that the present results are in good agreement with the ones from literature, as far as the transverse displacement and membrane stresses are concerned.

2.6 Final remarks and conclusion

The cylindrical shell problem described in terms of seven differential equations (42) has been solved by using the GDQ method. Among the methods of approximation, the GDQ procedure starts directly from the strong statement of the problem under consideration. It should be noted that the GDQ technique of obtaining algebraic equations does not require the construction of any variational formulation of the problem. As it is well known, the GDQ method is based on the idea that the partial derivative of a field variable at the i-th discrete point in the computational domain is approximated by a weighted linear sum of values of the field variable, along the line that passes

through that point, which is parallel to the coordinate direction of the derivative [21,22]. The weighting coefficients, associated with the derivatives, may be obtained directly from an explicit recursive formula [53-58].

The suggested theoretical model which involves the initial curvature effect, solved by means of the GDQ procedure, was derived from a 2-D third order shear deformation theory. Such theory does not enforce any boundary condition and maintains the unconstrained nature proper of the pioneer shear deformation theory by Timoshenko [70]. The resultant 2D theory under discussion is more complicated than Reddy's one, due to the introduction of two additional generalized displacement parameters (the higher order terms in the displacement field) and, consequently, the addition of fictitious internal actions. In the proposed formulation, the initial hypotheses regarding the null entity of the transverse normal stress is removed with its calculation by means of the integration of the three dimensional equilibrium equations. The source data which are useful for the integration are the membrane stresses derived from the solution of the fundamental system via the GDQ method. In this manner, the transverse shear stress are re-calculated and make the boundary condition satisfied, just as in the Reddy's constrained model. The proper advantage deriving from the use of GUTSDT with respect to the constrained one by Reddy is due to the possibility to apply distributed loads of various nature over the extreme surfaces, which are sliding bounded in the constrained model by Reddy. In fact, by considering the shear deformation model by Reddy, the null value of transverse shear stresses is a priori enforced inside the formulation. Whereas the unconstrained theory suggested in this paper leads to the accurate determination of transverse stress profiles even if distributed meridional and circumferential pressures are applied at the top or bottom surfaces. As shown in the numerical results, the stress recovery becomes a powerful technique to reconstruct the correct distribution of transverse stress components under various loading combination at the extreme surfaces.

The main contribute given by the present study consists in determining accurate stress profiles in functionally graded cylindrical shells. A global higher order theory, that accounts for the unconstrained third order formulation and the transverse normal and shear stress recovery, has been set up from the 3D elastic equilibrium equations.

The initial curvature effect is discussed and the role of the four parameters in the power law function is clarified. The role of the power exponent law is presented for the $FGM1_{(1,0,0,p)}, FGM1_{(1,1,4,p)}, FGM1_{(1,0.5,2,p)}$ cylindrical shells. The effects of the a, b, c parameters on the stress responses are illustrated for the $FGM1,2_{(a,0.2,3,2)}, FGM2_{(0,b,2,1)}, FGM1_{(1,0.5,c,2)}, FGM1_{(1,1,c,1)}$ cylindrical shells and panels. Various theories have been examined and numerical examples have been worked out to see how theories are similar and how they are different.

It should be noted that the procedure introduced in this paper can be also extended to other types of graded shells [67].

References

[1] Koizumi M, Yamanouchi M. **Proceedings of the 1st International Symposium on Functionally Gradient Materials**. Tokyo 1990.

[2] Koizumi M. **The concept of FGM**. Ceramic Transactions 1993; 34: 3-10.

[3] Basset AB. **On the extension and flexure of cylindrical and spherical thin elastic shell**s. Philosophical Transactions of the Royal Society of London Part A 1990; 181: 433-480.

[4] Bhimaraddi A. **A Higher order theory for free vibration analysis of circular cylindrical shells**. International Journal of Solids and Structures 1984; 20(7): 623-630.

[5] Obata Y, Noda N. **Steady thermal stresses in a hollow circular cylinder and a hollow sphere of a functionally gradient material**. Journal of Thermal Stresses 1994; 17(3):471-487.

[6] Loy CT, Lam KY, Reddy JN. **Vibration of functionally graded cylindrical shells**. International Journal of Mechanical Sciences 1999; 41(3): 309-324.

[7] Hua L, Lam KY. **Frequency characteristics of a thin rotating cylindrical shell using the generalized differential quadrature method**. International Journal of Mechanical Sciences 1998; 40(5): 443-459.

[8] Horgan CO, Chan AM. **The pressurized hollow cylinder or disk problem for functionally graded isotropic linear elastic materials**. Journal of Elasticity 1999; 55(1): 43-59.

[9] Pradhan SC. Loy CT, Lam KY, Reddy JN. **Vibration characteristics of functionally graded cylindrical shells under various boundary conditions**. Applied Acoustics 2000; 61:111-129.

[10] Liew KM, Bergman LA, Ng TY, Lam KY. **Three dimensional vibration of cylindrical shells panels - solution by continuum and discrete approaches**. Computational Mechanics 2000; 26: 208-221.

[11] Wu XH, Chen C, Shen YP, Tian XG. **A high order theory for functionally graded piezoelectric shells**. International Journal of Solids and Structures 2002; 39(20): 5325-5344.

[12] Zhu J, Chen C, Shen Y, Wang S. **Dynamic stability of functionally graded piezoelectric circular cylindrical shells**. Materials Letters 2005; 59(4): 477-485.

[13] Shen HS, Noda N. **Postbuckling of FGM cylindrical shells under combined axial and radial mechanical loads in thermal environments**. International Journal of Solids and Structures 2005; 42(16-17): 4641-4662.

[14] Patel BP, Gupta SS, Loknath MS, Kadu CP. **Free vibration analysis of functionally graded elliptical cylindrical shells using higher order theory**. Composites Structures 2005; 69(3): 259-270.

[15] Najafizadeh MN, Isvandzibaei MR, **Vibration of functionally graded cylindrical shells based on higher order deformation plate theory with ring support**. Acta Mechanica 2007; 191: 75-91.

[16] Wu CP, Syu YS. **Exact solutions of functionally graded piezoelectric shells under cylindrical bending**. International Journal of Solids and Structures 2007; 44(20): 6450-6472.

[17] Haddadpour H, Mahmoudkhani S, Navazi HM. **Free vibration analysis of functionally graded cylindrical shells including thermal effects**. Thin Walled Structures 2007; 45(6), 591-599.

[18] Arshad SH, Naeem MN, Sultana N. **Frequency analysis of functionally graded material cylindrical shells with various volume fraction laws**. Journal of Mechanical Engineering Science Part C 2007; 221:1483-1495.

[19] Iqbal Z, Naeem MN, Sultana N, Arshad SH, Shah AG. **Vibration characteristics of FGM circular cylindrical shells filled with fluid using wave propagation approach**. Applied Mathematics and Mechanics (English Edition) 2009; 30(11):1393-1404.

[20] Matsunaga H. **Free vibration and stability of functionally graded circular cylindrical shells according to a 2D higher order deformation theory**. Composites Structures 2009; 88(4): 519-531.

[21] Tornabene F, Viola E. **Free vibrations of four – parameter functionally graded parabolic panels and shells of revolution**. European Journal of Mechanics A/Solids 2009; 28: 991-1013.

[22] Tornabene F. **Free vibration analysis of functionally graded conical, cylindrical shell and annular plate structures with a four parameter power law distribution**. Computer Methods in Applied Mechanics and Engineering 2009;198(37-40):2911-2935.

[23] Zhao X, Lee YY, Liew KM. **Thermoelastic and vibration analysis of functionally graded cylindrical shells**. International Journal of Mechanical Sciences 2009; 51(9-10):694-707.

[24] Sobhani Aragh B, Yas MH. **Static and free vibration analyses of continuously graded fiber reinforced cylindrical shells using generalized power law distribution**. Acta Mechanica 2010;. 215(1-4):155-173.

[25] Sobhani Aragh B., Yas MH., **Three dimensional analysis of thermal stresses in four parameter continuous grading fiber reinforced cylindrical panels**. International Journal of Mechanical Sciences 2010; 52(8): 1047-1063.

[26] Arshad S.H., Naeem M.N., Sultana N, Iqbal Z, Shah AG. **Effects of exponential volume fraction law on the natural frequencies of FGM cylindrical shells under various boundary conditions**. Archive of Applied Mechanics 2011; 81(8): 999-1016.

[27] Alibeigloo A. **Thermoelastic solution for static deformations of functionally graded cylindrical shell bonded to thin piezoelectric layers**. Composite Structures 2011; 93(2): 961-972.

[28] Sepiani HA, Rastgoo A, Ebrahimi F, Ghorbanpour Arani A. **Vibration and buckling analysis of two layered functionally graded cylindrical shell, considering the effects of transverse shear and rotary inertia**. Materials & Design 2010; 31(3):1063-1069.

[29] Nie GJ, Batra RC. **Exact solutions and material tailoring for functionally graded hollow circular cylinders**. Journal of Elasticity 2010; 99(2): 179-201.

[30] Alibeigloo A, Nouri V. **Static analysis of functionally graded cylindrical shell with piezoelectric layers using differential quadrature method**. Composite Structures 2010; 9(8): 1775-1785.

[31] Sofiyev AH. **Dynamic response of an FGM cylindrical shell under moving loads**. Composite Structures 2010; 93(1):58-66.

[32] Sobhani Aragh B, Yas MH. **Three dimensional free vibration analysis of four parameter continuous grading fiber reinforced cylindrical panels resting on Pasternak foundations**. Archive of Applied Mechanics 2011; 81:1759-1779.

[33] Liew KM, Kitipornchai S, Zhang XZ, Lim CW. **Analysis of the thermal stress behavior of functionally graded hollow circular cylinders**. International Journal of Solids and Structures 2003; 40(10): 2355-2380.

[34] Bodaghi M, Saidi AR. **Thermoelastic buckling behavior of thick functionally graded rectangular plates**. Archive of Applied Mechanics 2011; 81(11): 1555-1572.

[35] Alibeigloo A. **Exact solution for thermo-elastic response of functionally graded rectangular plates**. Composite Structures 2010; 92(1): 113-121.

[36] Fereidoon A, Seyedmahalle MA, Mohyeddin A. **Bending analysis of thin functionally graded plates using generalized differential quadrature method**. Archive of Applied Mechanics 2011; 81(1): 1523-1539.

[37] Bert CW, Kumar M. **Vibration of cylindrical shells of bimodulus composite materials**. Journal of Sound and Vibration 1982; 81(1): 107-121.

[38] Hua L, Lam KY. **Frequency characteristics of a thin rotating cylindrical shell using the generalized differential quadrature method**. International Journal of Mechanical Sciences 1998; 40(5): 443-459.

[39] Li ZM, Zhao YX, Chen XD, Wang WR. **Nonlinear buckling and postbuckling of a shear deformable anisotropic laminated cylindrical panel under axial compression**. Mechanics of Composite Materials 2010; 46(6): 599-626.

[40] Flugge W. **Stresses in Shells**. Berlin, Springer 1973.

[41] Sanders JR. **An improved first order approximation theory for thin shells**. NASA Technical Report 1959; R24.

[42] Soldatos KP. **A comparison of some shell theories used for the dynamic analysis of cross-ply laminated circular cylindrical panels**. Journal of Sound and Vibration 1984; 97(2), 305-319.

[43] Kumar P. **Assesment of shell theories for the static analysis of laminated circular cylindrical shells**. M.Sc. thesis 1993, Indian Institute of Science, India.

[44] Chandrashekhara K, Kumar P. **Assessment of shell theories for the static analysis of cross-ply laminated circular cylindrical shells**. Thin Walled Structures 1995; 22(4):291-318.

[45] Reddy JN. **Exact solutions of moderately thick laminated shells**. Journal of Engineering Mechanics 1984; 110(5): 794-809.

[46] Reddy JN, Liu CF. **A higher order shear deformation theory of laminated elastic shells**. International Journal of Engineering Science 1985; 23(3): 319-330.

[47] Leung AYT. **An unconstrained third order plate theory**. Computers & Structures 1991; 40(4): 871-875.

[48] Tornabene F. **2-D GDQ solution for free vibrations of anisotropic doubly-curved shells and panels of revolution**. Composite Structures 2011; 93(7): 1854-1876.

[49] Viola E, Tornabene F. **Free vibrations of three parameter functionally graded parabolic panels of revolution**. Mechanics Research Communications 2009; 36(5): 587-594.

[50] Tornabene F, Viola E, Inman DJ. **2-D differential quadrature solution for vibration analysis of functionally graded conical, cylindrical shell and annular plate structures**. Journal of Sound and Vibration 2009; 328(3): 259-290.

[51] Toorani MH, Lakis AA. **General equations of anisotropic plates and shells including transverse shear deformations, rotary inertia, and initial curvature effects.** Journal of Sound and Vibration 2000; 237(4): 561-615.

[52] Tornabene F, Liverani A, Caligiana G. **FGM and laminated doubly curved shells and panels of revolution with a free – form meridian: A 2-D GDQ solution for free vibrations**. International Journal of Mechanical Sciences 2011; 53: 446-470.

[53] Bellman R, Casti J. **Differntial quadrature and long term integration**. Journal of Mathematical Analysis and Application 1971; 34: 234-238.

[54] Bellman R, Kashef BG, Casti J. **Differential quadrature: a technique for the rapid solution of non linear partial differential equations**. Journal of Computational Physics 1972; 10(1): 40-52.

[55] Civan F., Sliepcevich CM. **Differential quadrature for multi – dimensional problems**. Journal of Mathematical Analysis and Applications 1984; 101(2): 423-443.

[56] Shu C. **Generalized differential – integral quadrature and application to the simulation of incompressible viscous flows including parallel computation**. University of Glasgow, Ph.D. Thesis, 1991.

[57] Shu C. **Differential and its application in engineering**. Berlin, Springer 2000.

[58] Bert CW, Malik M. **Differential quadrature method in computational mechanics: a review**. Applied Mechanics Reviews 1996; 49(1): 1-27.

[59] Tornabene F, Caligiana A, Liverani A. **Laminate composite rectangular and annular plates: A GDQ solution for static analysis with a posteriori shear and normal stress recovery**. Composites: Part B 2012; 43: 1847-1872.

[60] Aghdam MM, Shahmansouri N, Bigdeli K. **Bending analysis of moderately thick functionally graded conical panels**. Composite Structures 2011; 93: 1376-1384

[61] Zhao X, Lee YY, Liew KM. **Thermoelastic and vibration analysis of functionally graded cylindrical shells**. International Journal of Mechanical Sciences 2009; 51: 694-707

[62] Fereidoon A, Asghardokht Seyedmahalle M, Mohyeddin A. **Bending analysis of thin functionally graded plates using generalized differential quadrature method**. Archive of Applied Mechanics 2011; 81: 1523-1539.

[63] Ferreira AJM, Roque CMC, Martins PALS. **Analysis of composite plates using higher order shear deformation theory and a finite point formulation based on the multiquadric radial basis function method**. Composites: Part B 34 2003; 627-636.

[64] Ferreira AJM, Castro LMS, Bertoluzza S. **A high order collocation method for the static and vibration analysis of composite plates using a first order theory**. Composite Structures 2009; 89: 424-432.

[65] Zenkour AM. **Generalized shear deformation theory for bending analysis of functionally graded plates**. Applied Mathematical Modelling 2006; 30: 67-84.

[66] Auricchio F, Sacco E. **A mixed enhanced finite element for the analysis of laminated composite plates**. International Journal for Numerical Methods in Engineering 1999; 44:1481-504.

[67] Rossetti L, Fantuzzi N, Viola E. **Stress and displacement recovery for functionally graded conical shells**. International Conference on Mechanics of Nano, Micro and Macro Composite Structures, Torino, June 2012.

[68] Reddy JN. **Introduction to the finite element method**. New York: McGraw-Hill; 1993

[69] Reddy JN. **Energy and variational methods in applied mechanics**. New York: Wiley; 1984

[70] Timoshenko SP, Woinowsky Krieger S. **Theory of Plates and Shells**. McGraw – Hill, New York, 1959.

[71] Werner H. **A three dimensional solution for rectangular plate bending free of transversal normal stresses**. Communications in Numerical Methods in Engineering 1999; 15: 295-302.

[72] Sokolnikoff IS, **Mathematical theory of Elasticity**, McGraw-Hill 1956, New York.

[73] Akhras G, Cheung MS, Li W. **Finite strip analysis for anisotropic laminated composite plates using higher-order deformation theory**. Computers & Structures 1994; 52(3):471-7

Figures.

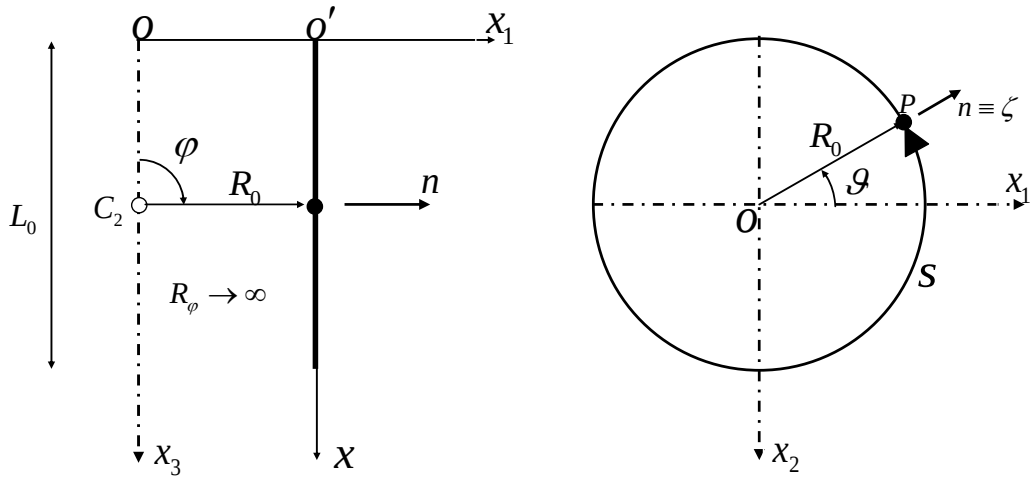

Fig.1 Geometric parameters of the cylindrical shell

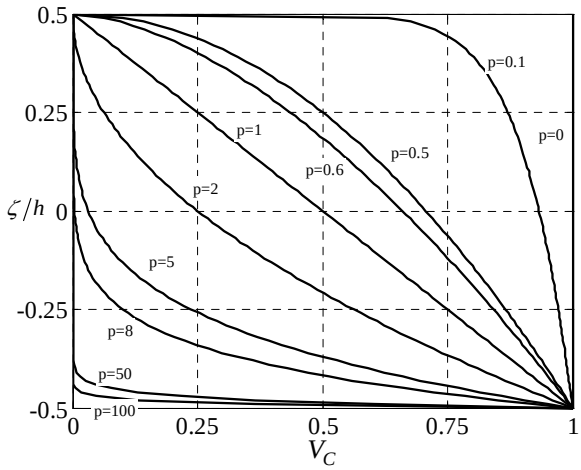

2*a*. FGM1$_{(1,0,0,p)}$

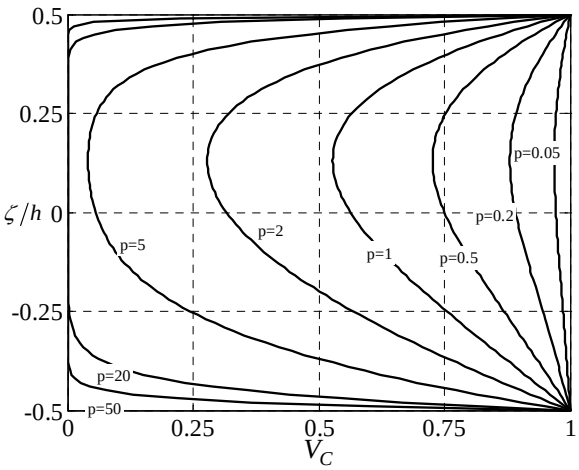

2*b*. FGM1$_{(1,1,4,p)}$

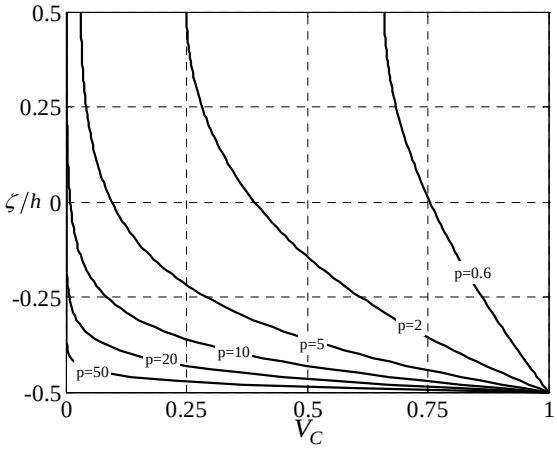

2*c*. FGM1$_{(1,0.5,2,p)}$

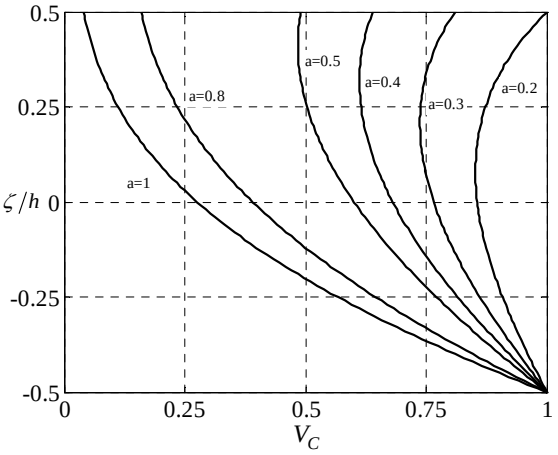

2*d*. FGM1$_{(a,0.2,3,2)}$

Figs.2*a*,*b*,*c*,*d*: Ceramic volume fraction V_c versus dimensionless thickness ζ/h for the FGM1 class.

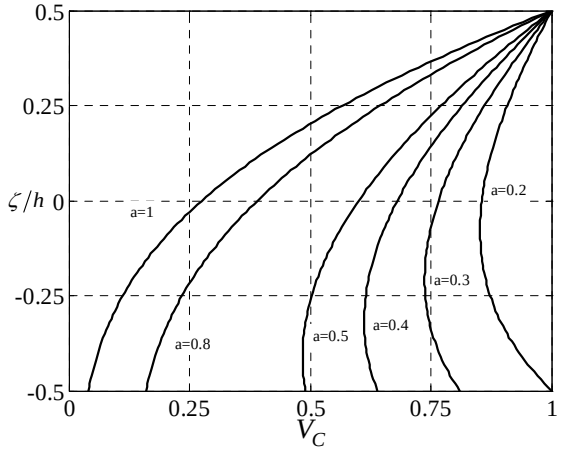

3*a*. FGM2$_{(a,0.2,3,2)}$

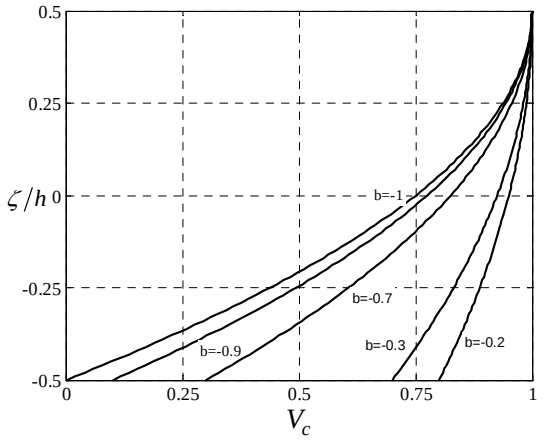

3*b*. FGM2$_{(0,b,2,1)}$

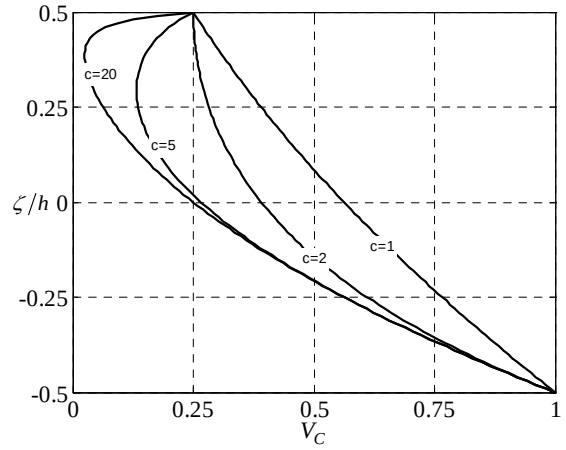

3*c*. FGM1$_{(1,0.5,c,2)}$

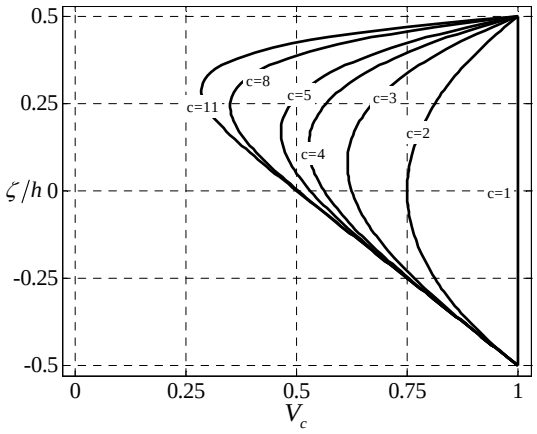

3*d*. FGM1$_{(1,1,c,1)}$

Figs.3*a*,*b*,*c*,*d*: Ceramic volume fraction V_c versus dimensionless thickness ζ/h for the FGM1 and FGM2 classes.

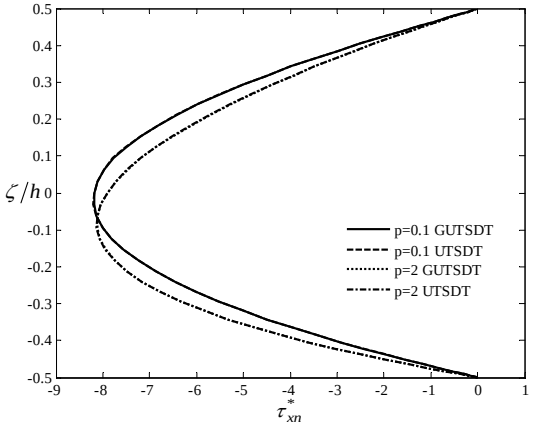

4*a*. transverse shear stress (τ^*_{xn})

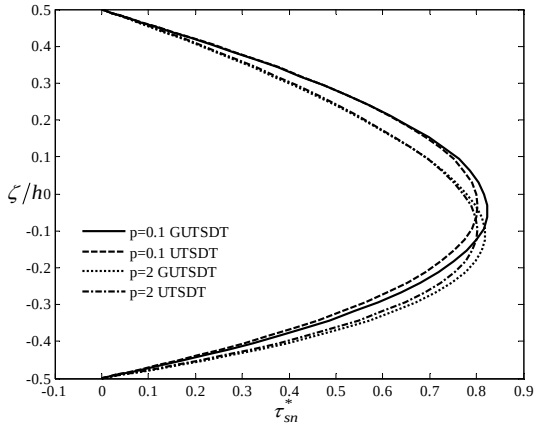

4*b*. transverse shear stress (τ^*_{sn})

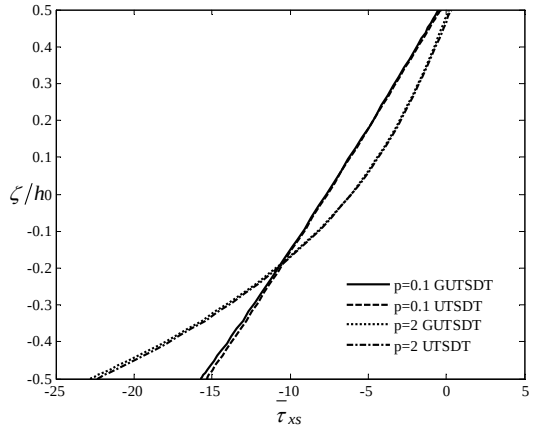

4*c*. membrane shear stress ($\bar{\tau}_{xs}$)

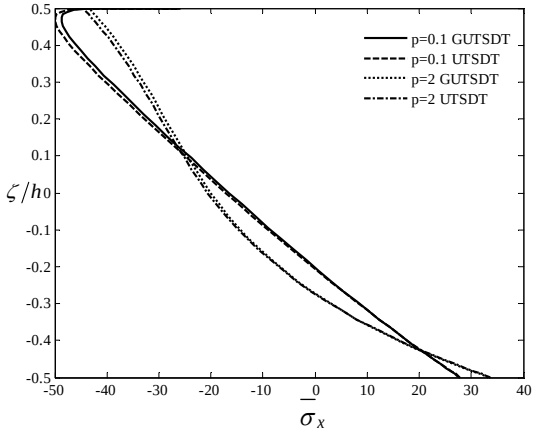

4*d*. meridional normal stress ($\bar{\sigma}_x$)

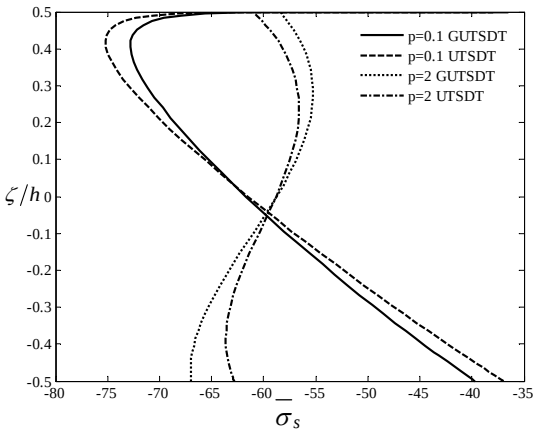

4*e*. circumferential normal stress ($\bar{\sigma}_s$)

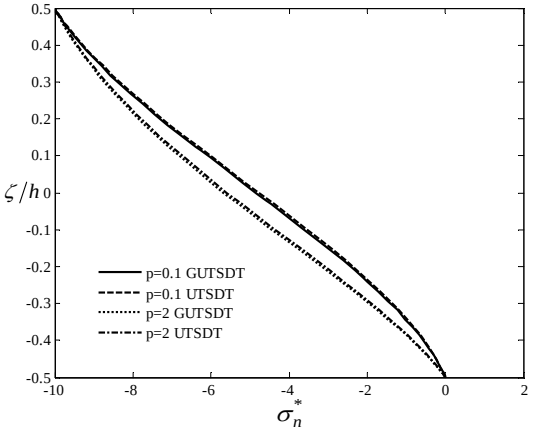

4f. transverse normal stress (σ^*_n)

Figs.4*a,b,c,d,e,f*: Comparisons between stress [Pa] profiles for the generalized (GUTSDT) and unconstrained (UTSDT) third order theories (scale factor: $\alpha = 10^{-4}$).

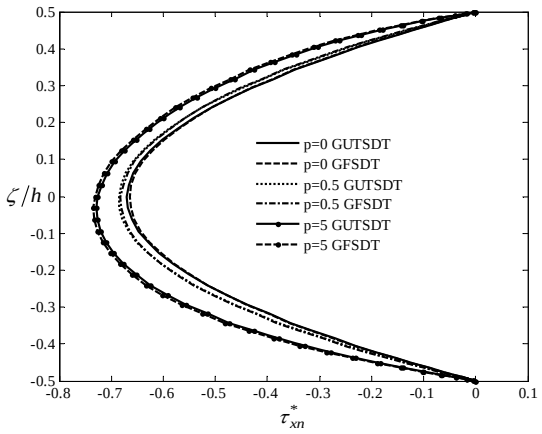

5*a*. tangential shear stress (τ^*_{xn})

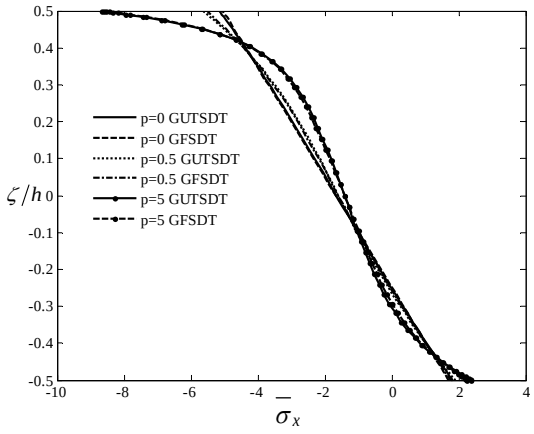

5*b*. meridional normal stress ($\overline{\sigma}_x$)

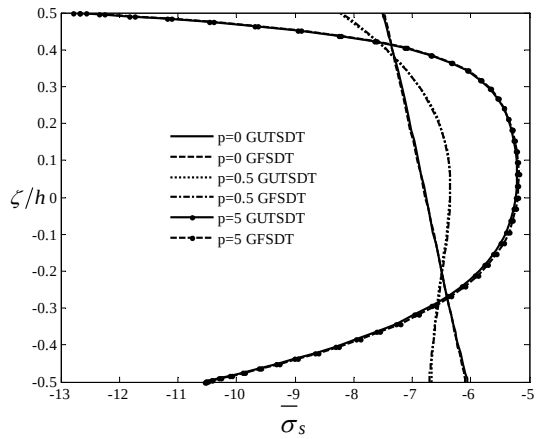

5*c*. circumferential normal stress ($\overline{\sigma}_s$)

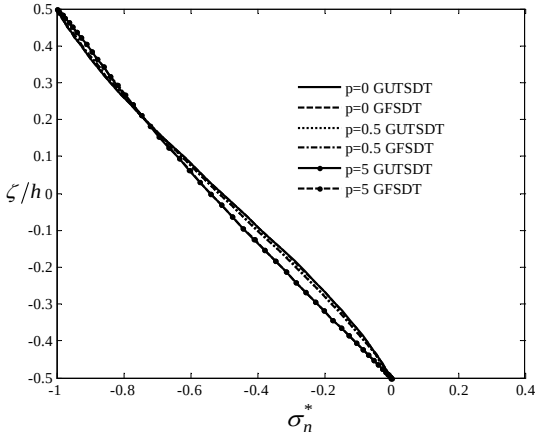

5*d*. transverse normal stress (σ^*_n)

Figs.5*a*,*b*,*c*,*d*: Stress profiles comparison between the GUTSDT and GFSDT for tangential and normal stresses [Pa] (scale factor: $\alpha = 10^{-5}$).

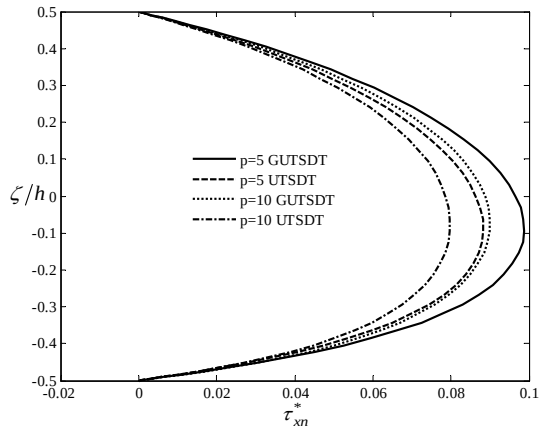

6*a*. tangential shear stress (τ^*_{xn})

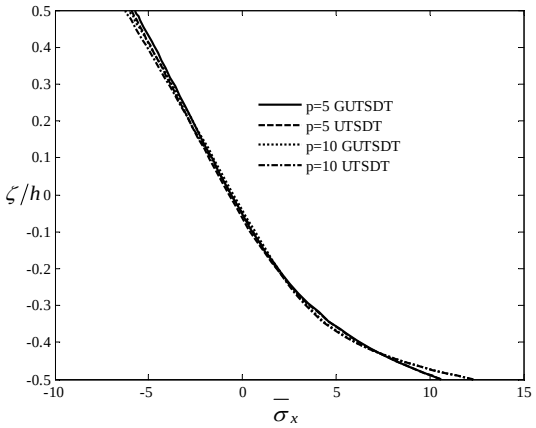

6*b*. meridional normal stress ($\overline{\sigma}_x$)

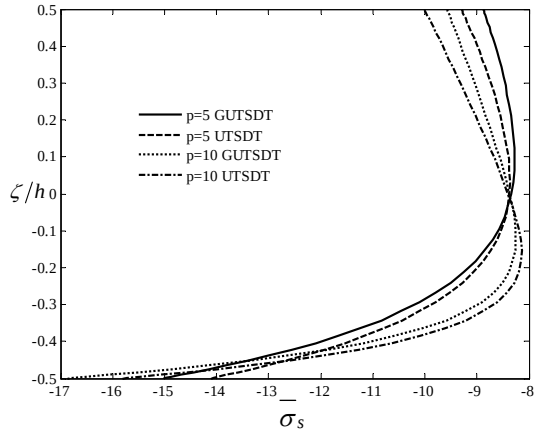

6*c*. circumferential normal stress ($\overline{\sigma}_s$)

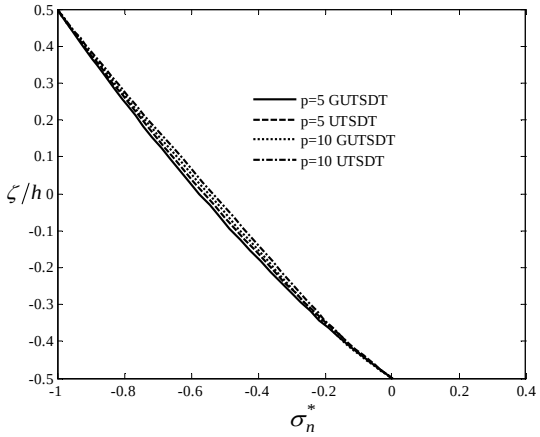

6*d*. transverse normal stress (σ^*_n)

Figs.6*a*,*b*,*c*,*d*: Stress profiles comparison between two theories for tangential and normal stresses [Pa] (scale factor: $\alpha = 10^{-5}$).

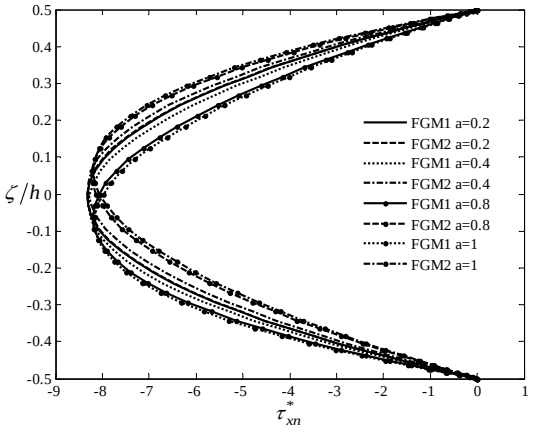

7*a*. transverse shear stress (τ^*_{xn})

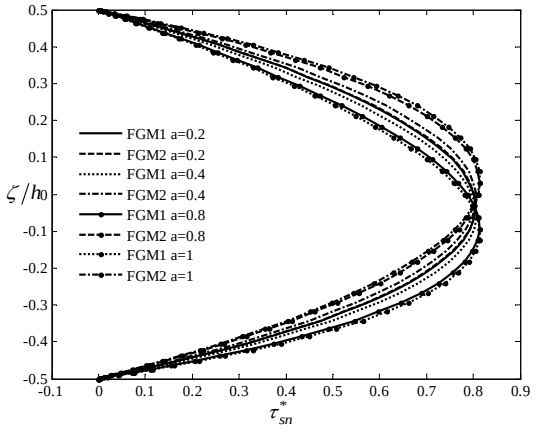

7*b*. transverse shear stress (τ^*_{sn})

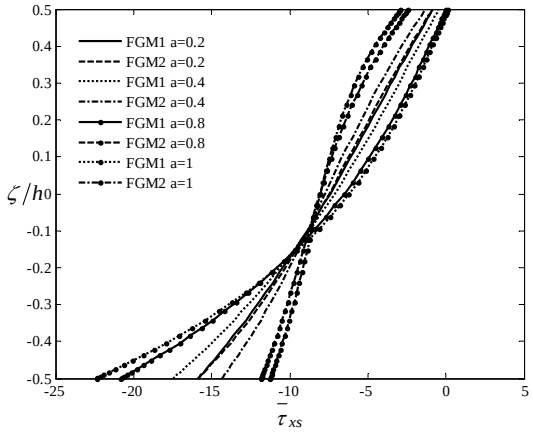

7*c*. membrane shear stress ($\bar{\tau}_{xs}$)

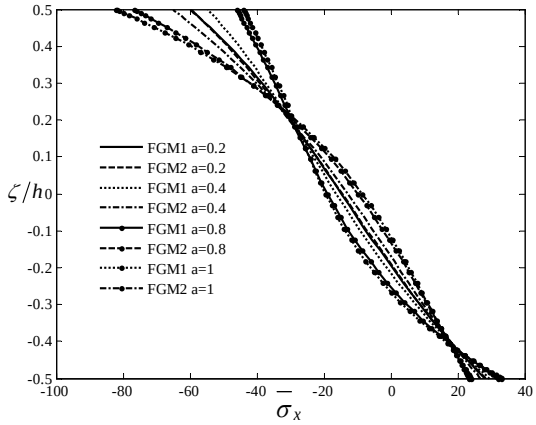

7***d*.** meridional normal stress (σ_x)

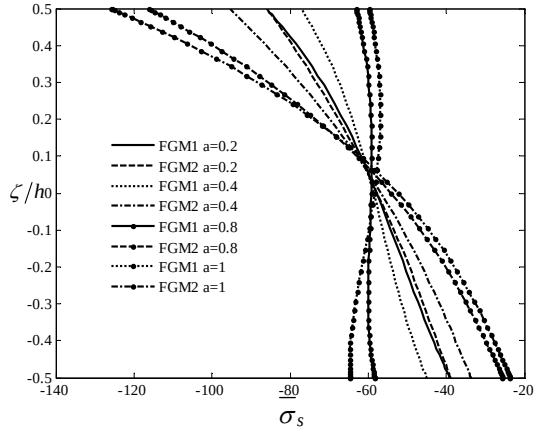

7*e*. circumferential normal stress ($\bar{\sigma}_s$)

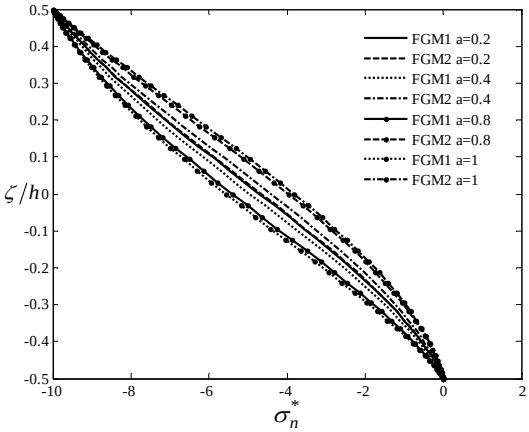

7*f*. transverse normal stress (σ^*_n)

Figs.7*a,b,c,d,e,f*: Stress profiles using the GUTSDT for tangential and normal stresses [Pa] (scale factor: $\alpha = 10^{-4}$).

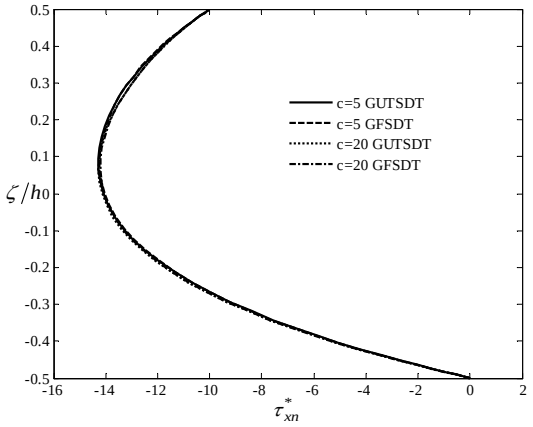

8*a*. transverse shear stress (τ^*_{xn})

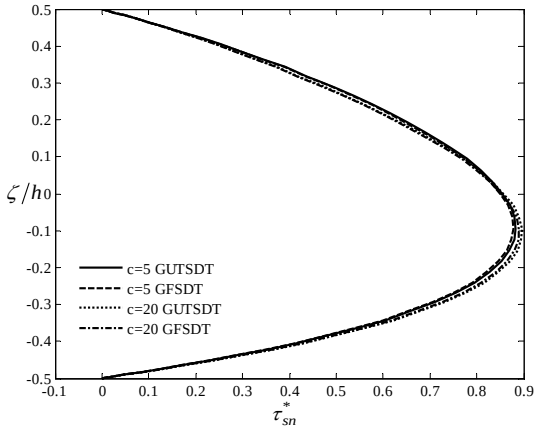

8*b*. transverse shear stress (τ^*_{sn})

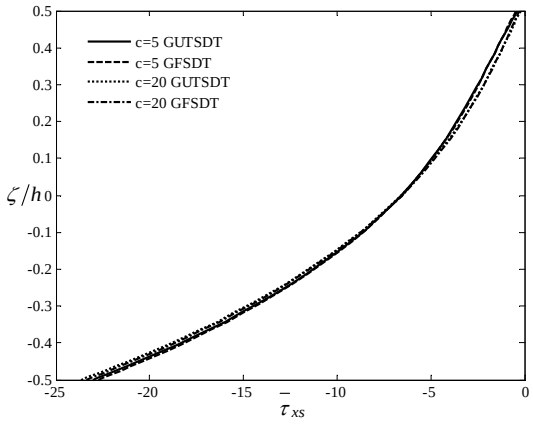

8*c*. membrane shear stress ($\bar{\tau}_{xs}$)

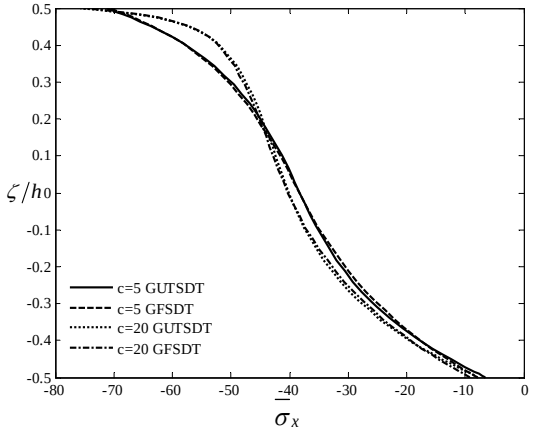

8*d*. meridional normal stress ($\bar{\sigma}_x$)

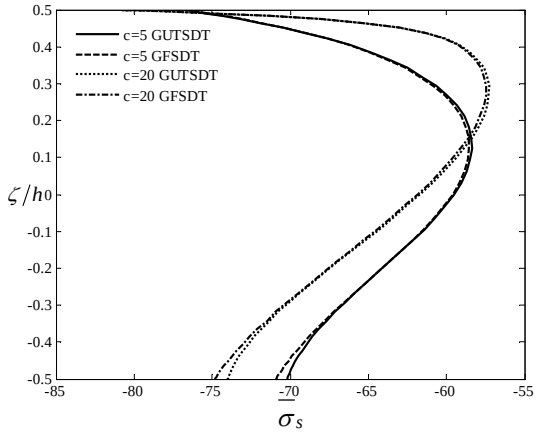

8*e*. circumferential normal stress ($\bar{\sigma}_s$)

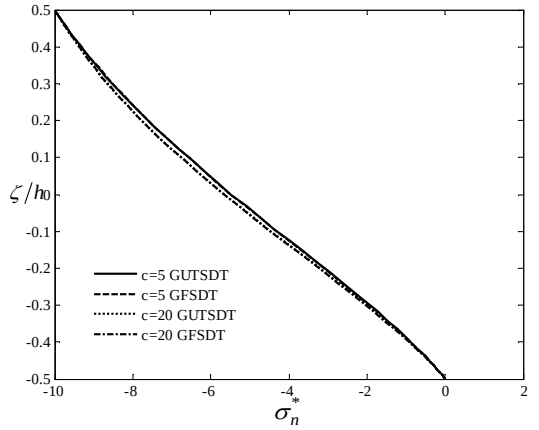

8*f*. transverse normal stress (σ^*_n)

Figs.8*a,b,c,d,e,f*: Stress profiles comparison between the GUTSDT and GFSDT for tangential and normal stresses [Pa] (scale factor: $\alpha = 10^{-4}$).

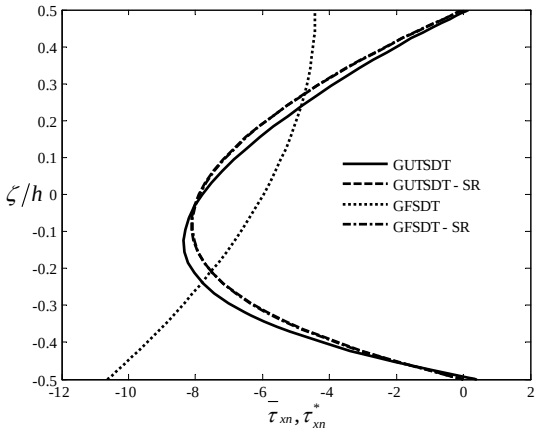

9*a*. FGM1$_{(1,0,0,2)}$ cylindrical panel under p_n

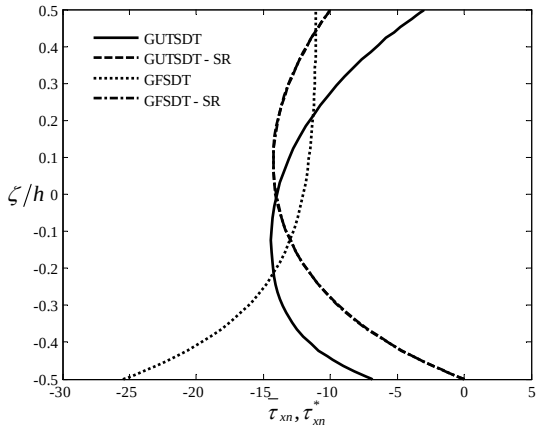

9*b*. FGM1$_{(1,0.5,2,5)}$ cylindrical panel under p_x , p_n

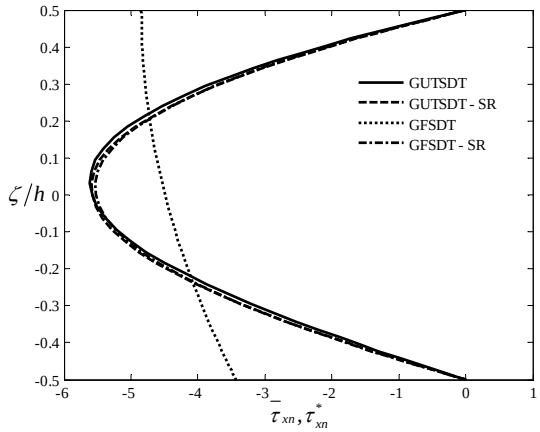

9*c*. FGM2$_{(0,-0.5,2,1)}$ cylindrical panel under p_s , p_n

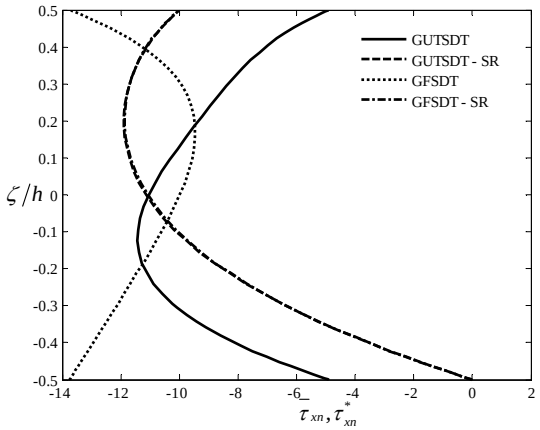

9***d*.** FGM1$_{(1,1,5,1)}$ cylindrical panel under p_x, p_s , p_n

Figs.9*a,b,c,d*: Stress profiles comparison among GUTSDT, GFSDT and the stress recovery (SR) technique for transverse shear stress $\bar{\tau}_{xn}, \tau^*_{xn}$ [Pa] (scale factor: $\alpha = 10^{-4}$).

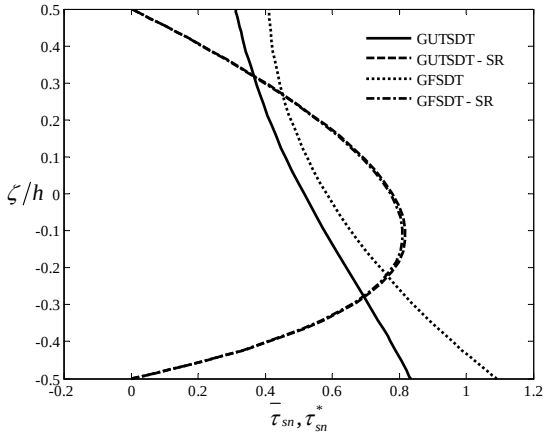

10*a*. FGM1$_{(1,0,0,2)}$ cylindrical panel under p_n

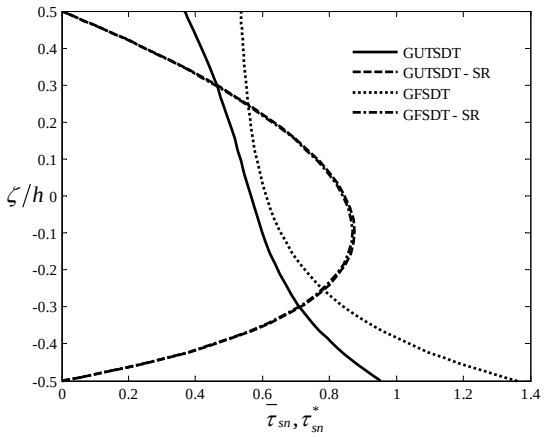

10b. FGM1$_{(1,0.5,2,5)}$ cylindrical panel under p_x , p_n

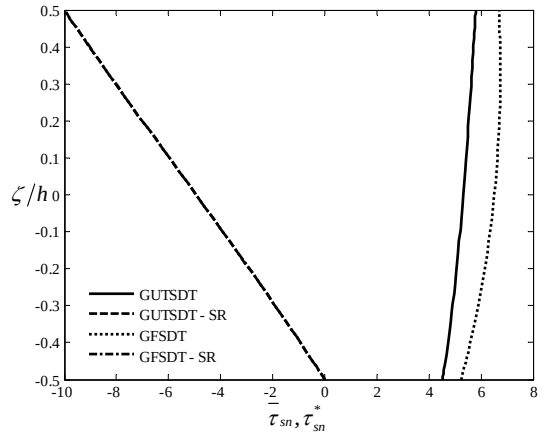

10*c*. FGM2$_{(0,-0.5,2,1)}$ cylindrical panel under p_s , p_n

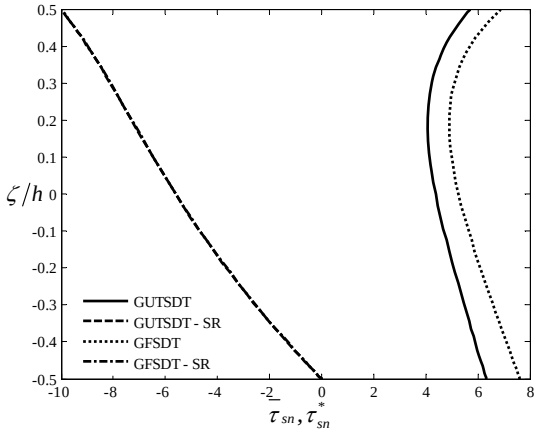

10*d*. FGM1$_{(1,1,5,1)}$ cylindrical panel under p_x, p_s , p_n

Figs.10*a,b,c,d*: Stress profiles comparison among GUTSDT, GFSDT and the stress recovery (SR) technique for transverse shear stress $\bar{\tau}_{sn}, \tau^*_{sn}$ [Pa] (scale factor: $\alpha = 10^{-4}$).

Tables.

Table 1*a*: Center transverse displacement of a clamped cylindrical shell under the uniform load 275.8 Pa

		$w[mm]$
Reference	[60]	0.2880
Present theories	FSDT	0.2869
	GFSDT	0.2887
	UTSDT	0.2869
	GUTSDT	0.2887

Table 1*b*: Center transverse displacement of a clamped cylindrical shell under the uniform load 257.9 Pa

		$w[mm]$
Reference	[61]	0.28128
Present theories	FSDT	0.26995
	GFSDT	0.26996
	UTSDT	0.26996
	GUTSDT	0.26996

Table 2*a*: Non dimensional center deflections of Al/Z_rO_2 cylindrical panels under uniform load with $R_0/h = 50$

		p	0	0.2	0.5	1	2	5
SSSS			$\overline{w}$	$\overline{w}$	$\overline{w}$	$\overline{w}$	$\overline{w}$	$\overline{w}$
	Reference	[61]	0.042760	0.048170	0.054370	0.060860	0.066720	0.072510
	Present theories	FSDT	0.042991	0.048413	0.054633	0.061137	0.067027	0.072850
		GFSDT	0.043019	0.048446	0.054671	0.06118	0.067076	0.072901
		UTSDT	0.042967	0.048384	0.054600	0.061104	0.067004	0.072842
		GUTSDT	0.042995	0.048416	0.054638	0.061147	0.067052	0.072894
CCCC								
	Reference	[61]	0.01341	0.015140	0.01702	0.019050	0.020910	0.022780
	Present theories	FSDT	0.013831	0.015563	0.017553	0.019644	0.021563	0.023488
		GFSDT	0.013834	0.015566	0.017556	0.019647	0.021566	0.023492
		UTSDT	0.013802	0.015529	0.017514	0.019605	0.021534	0.023477
		GUTSDT	0.013805	0.015532	0.017517	0.019608	0.021538	0.023481
CSCS								
	Reference	[61]	0.021220	0.023910	0.027000	0.030220	0.033100	0.035930
	Present theories	FSDT	0.021749	0.024508	0.027671	0.030966	0.033921	0.036819
		GFSDT	0.021757	0.024518	0.027682	0.030977	0.033932	0.036833
		UTSDT	0.021735	0.024487	0.027645	0.030945	0.033927	0.036869
		GUTSDT	0.021744	0.024496	0.027656	0.030956	0.033938	0.036882

Table 2*b*: Non dimensional center deflection of Al/Z_rO_2 cylindrical panels under a uniform load with $R_0/h = 200$

		p	0	0.2	0.5	1	2	5
CFCF			$\overline{w}$	$\overline{w}$	$\overline{w}$	$\overline{w}$	$\overline{w}$	$\overline{w}$
	Reference	[61]	0.027780	0.031300	0.03535	0.039560	0.043330	0.047030
	Present theories	FSDT	0.028823	0.032484	0.03668	0.041050	0.044968	0.048804
		GFSDT	0.028830	0.032456	0.03661	0.040936	0.044828	0.048690
		UTSDT	0.028818	0.032469	0.03666	0.041037	0.044992	0.048888
		GUTSDT	0.028825	0.032435	0.03657	0.040902	0.044828	0.048752
CFFF								
	Reference	[61]	0.44603	0.50162	0.56555	0.63307	0.69574	0.75900
	Present theories	FSDT	0.45155	0.50779	0.57259	0.64091	0.70428	0.76839
		GFSDT	0.45157	0.51119	0.57972	0.65174	0.71743	0.78013
		UTSDT	0.45084	0.50700	0.57162	0.63983	0.70319	0.76698
		GUTSDT	0.45088	0.51091	0.57983	0.65221	0.71802	0.78043

Tables 3*a,b*: Aspect ratio effect on the center deflections ($\overline{w}$) of Al/Z_rO_2 cylindrical panel under a uniform load

3*a*.

R/h		SSSS			CCCC		
50	p	0.5	1.0	2.0	0.5	1.0	2.0
Reference	[61]	0.00382400	0.00427900	0.0046830	0.001309000	0.00146500	0.0016110
Present theories	FSDT	0.00386875	0.00432800	0.0047361	0.001347535	0.00150780	0.0016573
	GFSDT	0.00387155	0.00433115	0.0047396	0.001347650	0.00150810	0.0016576
	UTSDT	0.00385875	0.00431800	0.0047290	0.001335200	0.00149545	0.0016477
	GUTSDT	0.00386150	0.00432110	0.0047324	0.001335450	0.00149570	0.0016479

3*b*.

R/h		SSSS			CCCC		
200	p	0.5	1.0	2.0	0.5	1.0	2.0
Reference	[61]	0.65030	0.72830	0.80570	0.20260	0.22690	0.25090
Present theories	FSDT	0.65140	0.72946	0.80710	0.20644	0.23118	0.25576
	GFSDT	0.65176	0.72990	0.80760	0.20646	0.23120	0.25578
	UTSDT	0.65132	0.72940	0.80706	0.20638	0.23112	0.25572
	GUTSDT	0.65170	0.72984	0.80756	0.20640	0.23114	0.25574

Table 4 : Maximum dimensionless deflection of FG plates calculated by means of a few theories

			Reference	Present theories	
			[62]	FSDT	UTSDT
p	L_x/L_y	E_2/E_1	$\overline{w}$	$\overline{w}$	$\overline{w}$
1	0.5	0.5	0.01536013000	0.0140417582	0.0140417582
		1	0.01109343000	0.0101417582	0.0101417582
		2	0.00768006000	0.0070287910	0.0070287910
2	1	0.5	0.00629457	0.00608700	0.00608750
		1	0.00444773	0.00407000	0.00407070
		2	0.00314728	0.00304300	0.00304370
5	2	0.5	0.00100004	0.00102000	0.00101930
		1	0.00069333	0.00063700	0.00063630
		2	0.00050002	0.00051000	0.00050970

Table 5: Square isotropic plate under uniform load

L/h			$\overline{w}$	$\overline{\sigma}_x$
10	Reference	Reddy [68]	4.770000	0.28990
		Exact [73]	4.791000	0.27620
		Ferriera et al. [64]	4.790600	0.27620
		Ferriera et al. [63]	4.701500	0.27390
	Present theories	UTSDT	4.789695	0.27785
		FSDT	4.790468	0.27627
20	Reference	Reddy [68]	4.570000	0.26830
		Exact [73]	4.625000	0.27620
		Ferriera et al. [64]	4.623600	0.27620
		Ferriera et al. [63]	4.559400	0.27370
	Present theories	UTSDT	4.625362	0.27666
		FSDT	4.625399	0.27627
50	Reference	Reddy [68]	4.496000	0.266700
		Exact [73]	4.579000	0.276200
		Ferriera et al. [64]	4.569200	0.275700
		Ferriera et al. [63]	4.634100	0.266700
	Present theories	UTSDT	4.578982	0.276331
		FSDT	4.578987	0.276268
100	Reference	Reddy [68]	4.482000	0.26640
		Exact [73]	4.572000	0.27620
		Ferriera et al. [64]	4.538300	0.27440
		Ferriera et al. [63]	4.752500	0.28440
	Present theories	UTSDT	4.572356	0.27629
		FSDT	4.572357	0.27627

Table 6: Center deflection of isotropic homogeneous plates

h[m]	$w\left[\mathrm{m}\right]$				
	Reference			Present theories	
	Classic [70]	3D [71]	Zenkour [65]	UTSDT	FSDT
0.01	44360.900	44384.700	44383.840	44383.864	44383.880
0.03	1643.0000	1650.9400	1650.6460	1650.6526	1650.6576
0.1	44.36090	46.74430	46.65481	46.65730	46.65940

Table 7: Normal and shear stress at the bottom surface of isotropic homogeneous plates

h[m]	$\sigma_x(0.5L_x, 0.5L_y, -h/2)$ [Pa]			
	Reference		Present theories	
	3D[71]	Zenkour[65]	UTSDT	FSDT
0.01	2873.3000	2873.3900	2873.3754	2873.2000
0.03	319.4000	319.4450	319.4173	319.2421
0.1	28.8900	29.9307	28.9087	28.7316

h[m]	$\tau_{xy}\left(0, 0, -h/2\right)$ [Pa]			
	Reference		Present theories	
	3D[71]	Zenkour[65]	UTSDT	FSDT
0.01	1949.600	1949.360	1945.864	1945.500
0.03	217.1100	217.1560	216.6606	216.2766
0.1	19.9200	20.0476	19.8866	19.4836

Table 8. Volume fraction exponent effect on the dimensionless transverse displacement $\overline{w}$ of a FGM square plate

p			$\overline{w}$
1	Reference	[65]	0.928700
	Present theories	UTSDT	0.928796
		FSDT	0.928796
2	Reference	[65]	1.1940
	Present theories	UTSDT	1.1940
		FSDT	1.1910
3	Reference	[65]	1.320000
	Present theories	UTSDT	1.319854
		FSDT	1.312330
4	Reference	[65]	1.389000
	Present theories	UTSDT	1.388748
		FSDT	1.376968
5	Reference	[65]	1.435600
	Present theories	UTSDT	1.435410
		FSDT	1.420478
6	Reference	[65]	1.472700
	Present theories	UTSDT	1.472462
		FSDT	1.455400
7	Reference	[65]	1.504900
	Present theories	UTSDT	1.504686
		FSDT	1.486750
8	Reference	[65]	1.534300
	Present theories	UTSDT	1.534060
		FSDT	1.515782
9	Reference	[65]	1.561700
	Present theories	UTSDT	1.561496
		FSDT	1.543332
10	Reference	[65]	1.587600
	Present theories	UTSDT	1.587412
		FSDT	1.569666

Table 9. Volume fraction exponent effect on the dimensionless membrane stress $\overline{\sigma}_x$ of a FGM square plate

p			$\overline{\sigma}_x$
1	Reference	[65]	4.4795
	Present theories	UTSDT	4.4706
		FSDT	4.4406
2	Reference	[65]	5.2296
	Present theories	UTSDT	5.2264
		FSDT	5.1852
3	Reference	[65]	5.6108
	Present theories	UTSDT	5.6094
		FSDT	5.5575
4	Reference	[65]	5.8915
	Present theories	UTSDT	5.8916
		FSDT	5.8314
5	Reference	[65]	6.1504
	Present theories	UTSDT	6.1511
		FSDT	6.0856
6	Reference	[65]	6.4053
	Present theories	UTSDT	6.4049
		FSDT	6.3363
7	Reference	[65]	6.6547
	Present theories	UTSDT	6.6547
		FSDT	6.5846
8	Reference	[65]	6.8999
	Present theories	UTSDT	6.8992
		FSDT	6.8285
9	Reference	[65]	7.1383
	Present theories	UTSDT	7.1368
		FSDT	7.0661
10	Reference	[65]	7.3689
	Present theories	UTSDT	7.3665
		FSDT	7.2962

Table10. Volume fraction exponent effect on the dimensionless membrane stress $\overline{\sigma}_y$ of a FGM square plate

p			$\overline{\sigma}_y$
1	Reference	[65]	2.1692
	Present theories	UTSDT	2.1680
		FSDT	2.1748
2	Reference	[65]	2.0338
	Present theories	UTSDT	2.0321
		FSDT	2.0417
3	Reference	[65]	1.8593
	Present theories	UTSDT	1.8571
		FSDT	1.8694
4	Reference	[65]	1.7197
	Present theories	UTSDT	1.7173
		FSDT	1.7313
5	Reference	[65]	1.6104
	Present theories	UTSDT	1.6080
		FSDT	1.6228
6	Reference	[65]	1.5214
	Present theories	UTSDT	1.5191
		FSDT	1.5340
7	Reference	[65]	1.4467
	Present theories	UTSDT	1.4445
		FSDT	1.4592
8	Reference	[65]	1.3829
	Present theories	UTSDT	1.3810
		FSDT	1.3951
9	Reference	[65]	1.3283
	Present theories	UTSDT	1.3267
		FSDT	1.3401
10	Reference	[65]	1.2820
	Present theories	UTSDT	1.2806
		FSDT	1.2933

Table11*a*. Volume fraction exponent effect on the dimensionless transverse shear stress $\bar{\tau}_{yn}$ of a FGM square plate

p			$\bar{\tau}_{yn}$
1	Reference	[65]	0.5446
	Present theories	UTSDT	0.5452
		UTSDT+SR	0.5300
		FSDT	0.4979
2	Reference	[65]	0.573400
	Present theories	UTSDT	0.573939
		UTSDT+SR	0.526141
		FSDT	0.485400
3	Reference	[65]	0.5629
	Present theories	UTSDT	0.5647
		UTSDT+SR	0.5097
		FSDT	0.4443
4	Reference	[65]	0.5346
	Present theories	UTSDT	0.5374
		UTSDT + SR	0.4974
		FSDT	0.4026
5	Reference	[65]	0.5031
	Present theories	UTSDT	0.5060
		UTSDT + SR	0.4894
		FSDT	0.3688
6	Reference	[65]	0.4755
	Present theories	UTSDT	0.4782
		UTSDT+SR	0.4840
		FSDT	0.3444

Table11*b*. Volume fraction exponent effect on dimensionless transverse shear stress $\bar{\tau}_{yn}$ of a FGM square plate

p			$\bar{\tau}_{yn}$
7	Reference	[65]	0.4543
	Present theories	UTSDT	0.4565
		UTSDT+SR	0.4800
		FSDT	0.3282
8	Reference	[65]	0.4392
	Present theories	UTSDT	0.4409
		UTSDT+SR	0.4769
		FSDT	0.3183
9	Reference	[65]	0.4291
	Present theories	UTSDT	0.4303
		UTSDT+SR	0.4744
		FSDT	0.3130
10	Reference	[65]	0.4227
	Present theories	UTSDT	0.4235
		UTSDT+SR	0.4722
		FSDT	0.3109

Table12*a*. Volume fraction exponent effect on the dimensionless transverse shear stress $\bar{\tau}_{xn}$ of a FGM square plate

p			$\bar{\tau}_{xn}$
1	Reference	[65]	0.5114
	Present theories	UTSDT	0.4964
		UTSDT+SR	0.5003
		FSDT	0.4050
2	Reference	[65]	0.470000
	Present theories	UTSDT	0.458503
		UTSDT+SR	0.472992
		FSDT	0.344600
3	Reference	[65]	0.4367
	Present theories	UTSDT	0.4292
		UTSDT+SR	0.4596
		FSDT	0.2986
4	Reference	[65]	0.4204
	Present theories	UTSDT	0.4151
		UTSDT + SR	0.4548
		FSDT	0.2742
5	Reference	[65]	0.4177
	Present theories	UTSDT	0.4130
		UTSDT + SR	0.4531
		FSDT	0.2653
6	Reference	[65]	0.4277
	Present theories	UTSDT	0.4178
		UTSDT+SR	0.4525
		FSDT	0.2652

Table12*b*. Volume fraction exponent effect on the dimensionless transverse shear stress $\bar{\tau}_{xn}$ of a FGM square plate

p				$\bar{\tau}_{xn}$
7	Reference	[65]		0.4310
	Present theories	UTSDT	4.25E+05	0.4253
		UTSDT+SR	4.52E+05	0.4522
		FSDT	2.70E+05	0.2697
8	Reference	[65]		0.4399
	Present theories	UTSDT	4.33E+05	0.4331
		UTSDT+SR	452133.50	0.4521
		FSDT	276151.95	0.2762
9	Reference	[65]		0.4481
	Present theories	UTSDT	4.40E+05	0.4403
		UTSDT+SR	452147.98	0.4521
		FSDT	283142.70	0.2831
10	Reference	[65]		0.4552
	Present theories	UTSDT	4.46E+05	0.4463
		UTSDT+SR	4.52E+05	0.4523
		FSDT	2.90E+05	0.2900

Appendix.

In the followings all the equilibrium operators are reported.

Equilibrium operators of the 1st fundamental equation R_{1j}, $j=1...7$

$$R_{11} = A_{11}\frac{\partial^2}{\partial x^2} + A_{66}\frac{\partial^2}{\partial s^2} + a_1 B_{11}\frac{\partial^2}{\partial x^2} + \left(b_1 B_{66} + b_2 D_{66} + b_3 E_{66}\right)\frac{\partial^2}{\partial s^2} \tag{A.1}$$

$$R_{12} = \left(A_{12} + A_{66}\right)\frac{\partial^2}{\partial x \partial s} \tag{A.2}$$

$$R_{13} = \frac{1}{R_0} A_{12}\frac{\partial}{\partial x} \tag{A.3}$$

$$R_{14} = B_{11}\frac{\partial^2}{\partial x^2} + B_{66}\frac{\partial^2}{\partial s^2} + a_1 D_{11}\frac{\partial^2}{\partial x^2} + \left(b_1 D_{66} + b_2 E_{66} + b_3 F_{66}\right)\frac{\partial^2}{\partial s^2} \tag{A.4}$$

$$R_{15} = \left(B_{12} + B_{66}\right)\frac{\partial^2}{\partial x \partial s} \tag{A.5}$$

$$R_{16} = E_{11}\frac{\partial^2}{\partial x^2} + E_{66}\frac{\partial^2}{\partial s^2} + a_1 F_{11}\frac{\partial^2}{\partial x^2} + \left(b_1 F_{66} + b_2 L_{66} + b_3 H_{66}\right)\frac{\partial^2}{\partial s^2} \tag{A.6}$$

$$R_{17} = \left(E_{12} + E_{66}\right)\frac{\partial^2}{\partial x \partial s} \tag{A.7}$$

Equilibrium operators of the 2nd fundamental equation R_{2j}, $j=1...7$

$$R_{21} = \left(A_{12} + A_{66}\right)\frac{\partial^2}{\partial s \partial x} \tag{A.8}$$

$$R_{22} = A_{66}\frac{\partial^2}{\partial x^2} + A_{11}\frac{\partial^2}{\partial s^2} - \frac{1}{R_0^2} A_{66} + a_1 B_{66}\frac{\partial^2}{\partial x^2} + \left(b_1 B_{11} + b_2 D_{11} + b_3 E_{11}\right)\frac{\partial^2}{\partial s^2} + - \frac{1}{R_0^2}\left(b_1 B_{66} + b_2 D_{66} + b_3 E_{66}\right) \tag{A.9}$$

$$R_{23} = \frac{\left(A_{11} + A_{66}\right)}{R_0}\frac{\partial}{\partial s} + \left(\frac{b_1\left(B_{11} + B_{66}\right)}{R_0} + \frac{b_2\left(D_{11} + D_{66}\right)}{R_0} + \frac{b_3\left(E_{11} + E_{66}\right)}{R_0}\right)\frac{\partial}{\partial s} \tag{A.10}$$

$$R_{24} = \left(B_{12} + B_{66}\right)\frac{\partial^2}{\partial s \partial x} \tag{A.11}$$

$$R_{25} = B_{66}\frac{\partial^2}{\partial x^2} + B_{11}\frac{\partial^2}{\partial s^2} + \frac{A_{66}}{R_0} + a_1 D_{66}\frac{\partial^2}{\partial x^2} + \left(b_1 D_{11} + b_2 E_{11} + b_3 F_{11}\right)\frac{\partial^2}{\partial s^2} + + \frac{\left(b_1 B_{66} + b_2 D_{66} + b_3 E_{66}\right)}{R_0} \tag{A.12}$$

$$R_{26} = \left(E_{12} + E_{66}\right)\frac{\partial^2}{\partial s \partial x} \tag{A.13}$$

$$R_{27} = E_{66}\frac{\partial^2}{\partial x^2} + E_{11}\frac{\partial^2}{\partial s^2} + \frac{1}{R_0}\left(3D_{66} + \frac{2}{R_0}E_{66}\right) + a_1 F_{66}\frac{\partial^2}{\partial x^2} + \left(b_1 F_{11} + b_2 L_{11} + b_3 H_{11}\right)\frac{\partial^2}{\partial s^2} + \\ + \frac{b_1}{R_0}\left(3E_{66} + \frac{2}{R_0}F_{66}\right) + \frac{b_2}{R_0}\left(3F_{66} + \frac{2}{R_0}L_{66}\right) + \frac{b_3}{R_0}\left(3L_{66} + \frac{2}{R_0}H_{66}\right) \tag{A.14}$$

Equilibrium operators of the 3rd fundamental equation R_{3j}, $j = 1...7$

$$R_{31} = -\frac{A_{12}}{R_0}\frac{\partial}{\partial x} \tag{A.15}$$

$$R_{32} = -\frac{\left(A_{66} + A_{11}\right)}{R_0}\frac{\partial}{\partial s} - \left(\frac{b_1\left(B_{66} + B_{11}\right)}{R_0} + \frac{b_2\left(D_{66} + D_{11}\right)}{R_0} + \frac{b_3\left(E_{66} + E_{11}\right)}{R_0}\right)\frac{\partial}{\partial s} \tag{A.16}$$

$$R_{33} = A_{66}\frac{\partial^2}{\partial x^2} + A_{66}\frac{\partial^2}{\partial s^2} - \frac{A_{11}}{R_0^2} + a_1 B_{66}\frac{\partial^2}{\partial x^2} + \left(b_1 B_{66} + b_2 D_{66} + b_3 E_{66}\right)\frac{\partial^2}{\partial s^2} \\ - \frac{\left(b_1 B_{11} + b_2 D_{11} + b_3 E_{11}\right)}{R_0^2} \tag{A.17}$$

$$R_{34} = \left(A_{66} - \frac{B_{12}}{R_0}\right)\frac{\partial}{\partial x} + a_1 B_{66}\frac{\partial}{\partial x} \tag{A.18}$$

$$R_{35} = \left(A_{66} - \frac{B_{11}}{R_0}\right)\frac{\partial}{\partial s} + \left(b_1\left(B_{66} - \frac{D_{11}}{R_0}\right) + b_2\left(D_{66} - \frac{E_{11}}{R_0}\right) + b_3\left(E_{66} - \frac{F_{11}}{R_0}\right)\right)\frac{\partial}{\partial s} \tag{A.19}$$

$$R_{36} = \left(3D_{66} - \frac{E_{12}}{R_0}\right)\frac{\partial}{\partial x} + 3a_1 E_{66}\frac{\partial}{\partial x} \tag{A.20}$$

$$R_{37} = \left(3D_{66} + \left(\frac{2E_{66} - E_{11}}{R_0}\right)\right)\frac{\partial}{\partial s} + \left(\begin{array}{l} b_1\left(3E_{66} + \dfrac{2F_{66} - F_{11}}{R_0}\right) + b_2\left(3F_{66} + \dfrac{2L_{66} - L_{11}}{R_0}\right) + \\ + b_3\left(3L_{66} + \dfrac{2H_{66} - H_{11}}{R_0}\right) \end{array}\right)\frac{\partial}{\partial s} \tag{A.21}$$

Equilibrium operators of the 4th fundamental equation R_{4j}, $j = 1...7$

$$R_{41} = B_{11}\frac{\partial^2}{\partial x^2} + B_{66}\frac{\partial^2}{\partial s^2} + a_1 D_{11}\frac{\partial^2}{\partial x^2} + \left(b_1 D_{66} + b_2 E_{66} + b_3 F_{66}\right)\frac{\partial^2}{\partial s^2} \tag{A.22}$$

$$R_{42} = \left(B_{12} + B_{66}\right)\frac{\partial^2}{\partial x \partial s} \tag{A.23}$$

$$R_{43} = \left(\frac{B_{12}}{R_0} - A_{66} \right) \frac{\partial}{\partial x} - a_1 B_{66} \frac{\partial}{\partial x} \tag{A.24}$$

$$R_{44} = D_{11} \frac{\partial^2}{\partial x^2} + D_{66} \frac{\partial^2}{\partial s^2} - A_{66} + a_1 E_{11} \frac{\partial^2}{\partial x^2} + \left(b_1 E_{66} + b_2 F_{66} + b_3 L_{66} \right) \frac{\partial^2}{\partial s^2} - a_1 B_{66} \tag{A.25}$$

$$R_{45} = \left(D_{12} + D_{66} \right) \frac{\partial^2}{\partial x \partial s} \tag{A.26}$$

$$R_{46} = F_{11} \frac{\partial^2}{\partial x^2} + F_{66} \frac{\partial^2}{\partial s^2} - 3D_{66} + a_1 L_{11} \frac{\partial^2}{\partial x^2} + \left(b_1 L_{66} + b_2 H_{66} + b_3 M_{66} \right) \frac{\partial^2}{\partial s^2} - 3a_1 E_{66} \tag{A.27}$$

$$R_{47} = \left(F_{12} + F_{66} \right) \frac{\partial^2}{\partial x \partial s} \tag{A.28}$$

Equilibrium operators of the 5th fundamental equation R_{5j}, $j = 1...7$

$$R_{51} = \left(B_{12} + B_{66} \right) \frac{\partial^2}{\partial x \partial s} \tag{A.29}$$

$$R_{52} = B_{66} \frac{\partial^2}{\partial x^2} + B_{11} \frac{\partial^2}{\partial s^2} + \frac{A_{66}}{R_0} + a_1 D_{66} \frac{\partial^2}{\partial x^2} + \left(b_1 D_{11} + b_2 E_{11} + b_3 F_{11} \right) \frac{\partial^2}{\partial s^2} + \frac{\left(b_1 B_{66} + b_2 D_{66} + b_3 E_{66} \right)}{R_0} \tag{A.30}$$

$$R_{53} = \left(\frac{B_{11}}{R_0} - A_{66} \right) \frac{\partial}{\partial s} + \left(b_1 \left(\frac{D_{11}}{R_0} - B_{66} \right) + b_2 \left(\frac{E_{11}}{R_0} - D_{66} \right) + b_3 \left(\frac{F_{11}}{R_0} - E_{66} \right) \right) \frac{\partial}{\partial s} \tag{A.31}$$

$$R_{54} = \left(D_{12} + D_{66} \right) \frac{\partial^2}{\partial x \partial s} \tag{A.32}$$

$$R_{55} = D_{66} \frac{\partial^2}{\partial x^2} + D_{11} \frac{\partial^2}{\partial s^2} - A_{66} + a_1 E_{66} \frac{\partial^2}{\partial x^2} + \left(b_1 E_{11} + b_2 F_{11} + b_3 L_{11} \right) \frac{\partial^2}{\partial s^2} + - \left(b_1 B_{66} + b_2 D_{66} + b_3 E_{66} \right) \tag{A.33}$$

$$R_{56} = \left(F_{12} + F_{66} \right) \frac{\partial^2}{\partial x \partial s} \tag{A.34}$$

$$R_{57} = F_{66}\frac{\partial^2}{\partial x^2} + a_1 L_{66}\frac{\partial^2}{\partial x^2} + F_{11}\frac{\partial^2}{\partial s^2} + \left(b_1 L_{11} + b_2 H_{11} + b_3 M_{11}\right)\frac{\partial^2}{\partial s^2} +$$
$$-\left(3D_{66} + \frac{2}{R_0}E_{66}\right) - b_1\left(3E_{66} + \frac{2}{R_0}F_{66}\right) - b_2\left(3F_{66} + \frac{2}{R_0}L_{66}\right) + \quad \text{(A.35)}$$
$$-b_3\left(3L_{66} + \frac{2}{R_0}H_{66}\right)$$

Equilibrium operators of the 6th fundamental equation R_{6j}, $j = 1...7$

$$R_{61} = E_{11}\frac{\partial^2}{\partial x^2} + E_{66}\frac{\partial^2}{\partial s^2} + a_1 F_{11}\frac{\partial^2}{\partial x^2} + \left(b_1 F_{66} + b_2 L_{66} + b_3 H_{66}\right)\frac{\partial^2}{\partial s^2} \quad \text{(A.36)}$$

$$R_{62} = \left(E_{12} + E_{66}\right)\frac{\partial^2}{\partial x \partial s} \quad \text{(A.37)}$$

$$R_{63} = \left(\frac{E_{12}}{R_0} - 3D_{66}\right)\frac{\partial}{\partial x} - 3a_1 E_{66}\frac{\partial}{\partial x} \quad \text{(A.38)}$$

$$R_{64} = F_{11}\frac{\partial^2}{\partial x^2} + F_{66}\frac{\partial^2}{\partial s^2} + a_1 L_{11}\frac{\partial^2}{\partial x^2} + \left(b_1 L_{66} + b_2 H_{66} + b_3 M_{66}\right)\frac{\partial^2}{\partial s^2} - 3\left(D_{66} + a_1 E_{66}\right) \quad \text{(A.39)}$$

$$R_{65} = \left(F_{12} + F_{66}\right)\frac{\partial^2}{\partial x \partial s} \quad \text{(A.40)}$$

$$R_{66} = H_{11}\frac{\partial^2}{\partial x^2} + H_{66}\frac{\partial^2}{\partial s^2} - 9F_{66} + a_1 M_{11}\frac{\partial^2}{\partial x^2} + \left(b_1 M_{66} + b_2 N_{66} + b_3 V_{66}\right)\frac{\partial^2}{\partial s^2} - 9a_1 L_{66} \quad \text{(A.41)}$$

$$R_{67} = \left(H_{12} + H_{66}\right)\frac{\partial^2}{\partial x \partial s} \quad \text{(A.42)}$$

Equilibrium operators of the 7th fundamental equation R_{7j}, $j = 1...7$

$$R_{71} = \left(E_{12} + E_{66}\right)\frac{\partial^2}{\partial x \partial s} \quad \text{(A.43)}$$

$$R_{72} = E_{66}\frac{\partial^2}{\partial x^2} + E_{11}\frac{\partial^2}{\partial s^2} + \frac{1}{R_0}\left(3D_{66} + \frac{2E_{66}}{R_0}\right) + a_1 F_{66}\frac{\partial^2}{\partial x^2} + \left(b_1 F_{11} + b_2 L_{11} + b_3 H_{11}\right)\frac{\partial^2}{\partial s^2} +$$
$$+\frac{b_1}{R_0}\left(3E_{66} + \frac{2F_{66}}{R_0}\right) + \frac{b_2}{R_0}\left(3F_{66} + \frac{2L_{66}}{R_0}\right) + \frac{b_3}{R_0}\left(3L_{66} + \frac{2H_{66}}{R_0}\right) \quad \text{(A.44)}$$

$$R_{73}=\left(\frac{E_{11}}{R_0}-3D_{66}\right)\frac{\partial}{\partial s}+\left(b_1\left(\frac{F_{11}}{R_0}-3E_{66}\right)+b_2\left(\frac{L_{11}}{R_0}-3F_{66}\right)+b_3\left(\frac{H_{11}}{R_0}-3L_{66}\right)\right)\frac{\partial}{\partial s} \tag{A.45}$$

$$R_{74}=\left(F_{12}+F_{66}\right)\frac{\partial^2}{\partial x\partial s} \tag{A.46}$$

$$R_{75}=F_{66}\frac{\partial^2}{\partial x^2}+F_{11}\frac{\partial^2}{\partial s^2}+a_1L_{66}\frac{\partial^2}{\partial x^2}+\left(b_1L_{11}+b_2H_{11}+b_3M_{11}\right)\frac{\partial^2}{\partial s^2}+$$
$$-\left(3D_{66}+\frac{2E_{66}}{R_0}\right)-b_1\left(3E_{66}+\frac{2F_{66}}{R_0}\right)-b_2\left(3F_{66}+\frac{2L_{66}}{R_0}\right)-b_3\left(3L_{66}+\frac{2H_{66}}{R_0}\right) \tag{A.47}$$

$$R_{76}=\left(H_{12}+H_{66}\right)\frac{\partial^2}{\partial x\partial s} \tag{A.48}$$

$$R_{77}=H_{66}\frac{\partial^2}{\partial x^2}+H_{11}\frac{\partial^2}{\partial s^2}+a_1M_{66}\frac{\partial^2}{\partial x^2}+\left(b_1M_{11}+b_2N_{11}+b_3V_{11}\right)\frac{\partial^2}{\partial s^2}$$
$$-3\left(3+\frac{2}{R_0}\right)\left(F_{66}+b_1L_{66}+b_2H_{66}+b_3M_{66}\right)-\frac{6}{R_0}\left(L_{66}+b_1H_{66}+b_2M_{66}+b_3N_{66}\right)+ \tag{A.49}$$
$$-\frac{4}{R_0^2}\left(H_{66}+b_1M_{66}+b_2N_{66}+b_3V_{66}\right)$$

Chapter 3

Static analysis of functionally graded conical shells and panels using the generalized unconstrained third order theory coupled with the stress recovery

Sommario

Dopo l'analisi dello stato dell'arte, si è proceduti con la scrittura di una teoria generale di deformazione a taglio del terzo ordine di tipo svincolato per gusci/pannelli conici. Si è operata la scrittura del modello cinematico a sette parametri indipendenti, delle relazioni tra deformazioni e spostamenti arricchite dell'effetto della curvatura, delle equazioni costitutive per una lamina singola in materiale a stratificazione graduale e delle caratteristiche di sollecitazione in funzione degli spostamenti. Definiti i carichi esterni uniformi di natura trasversale, assiale e circonferenziale, è stato applicato il principio degli spostamenti virtuali per ricavare le equazioni indefinite di equilibrio e le condizioni al contorno. Pertanto si è proceduti alla scrittura della equazioni fondamentali con la sostituzione delle relazioni delle azioni interne espresse in funzione degli spostamenti, nelle equazioni indefinite di equilibrio. Risolto il sistema fondamentale con il metodo generalizzato di quadratura differenziale, si è pervenuti alla conoscenza dei sette parametri indipendenti di spostamento, in tutti i punti della superficie di riferimento del panello/guscio conico. Utilizzando le equazioni costitutive e la soluzione del sistema fondamentale, si è giunti alla determinazione delle tensioni membranali in un punto arbitrario della superficie di riferimento del panello/guscio, per poi elaborare la distribuzione di esse lungo lo spessore dell'elemento strutturale. Per determinare le tensioni trasversali normale e tagliante, si è proceduti con la scrittura delle equazioni di equilibrio dell'elasticità tridimensionale. Compiuta la discretizzazione di esse con il metodo di quadratura differenziale di tipo generalizzato e sfruttando la conoscenza delle tensioni membranali, determinate indirettamente dal sistema fondamentale, sono stati determinati i profili di tensione trasversale normale e tagliante lungo lo spessore dell'elemento strutturale in esame. I profili di tensione trasversale ottenuti in questo modo soddisfano al pieno le condizioni al contorno anche in presenza di carichi taglianti alle superfici estreme. In questo modo è stato superato il limite della teoria di Reddy che assumeva nulli a priori i carichi taglianti alle superfici di estremità. Sono stati anche discussi l'influenza della curvatura iniziale, del materiale e dei parametri geometrici nei profili ottenuti.

3.1 Introduction

As it is well known, the classical bending and shear deformation theories have been developed for the analysis of composite structures. Structures with a ratio of thickness to representative dimensions equal to 1/20 or less are considered to be thin and the classical bending theory will be adopted, whereas structures with the ratio grater than 20 are studied by means of shear deformation theories. Reissner [1,2] proposed the first order shear deformation plate and shell theories based on kinematics analysis. Mindlin [3] suggested a first order shear deformation plate theory that included rotary inertia terms for the free vibrations of plates. Because the first order shear deformation theories based on Reissner - Mindlin kinematics violated the zero shear stress condition on the top and bottom surfaces of the shell or plate, a shear correction factor was required to compensate for the error due to a constant shear strain assumption through the thickness. The Reissner-Mindlin theory has been applied to the analysis of a variety of structures. Whitney [4,5] investigated the shear correction factors for orthotropic laminates under static loads and analysed the effects of shear deformation on the bending of laminated plates. Whitney and Pagano [6] considered the shear deformation of heterogeneous anisotropic plates and Reissner [7] developed a consistent treatment of transverse shear deformations in laminated anisotropic plates. However, in order to obtain a better prediction of shear deformation and transverse normal strains in laminated structures, higher order theories are required. Over the years, several higher order shear deformation theories have been developed by different authors [8-20], prevalently with reference to the plate structure and cubic expansion of displacement field. Lo et al. [9] wrote a theory of homogeneous plate deformation which accounts for the effects of transverse shear deformation, transverse normal strain, and a nonlinear distribution of the in plane displacements with respect to the thickness coordinate. A particular problem involving a plate acted upon by a sinusoidal surface pressure was considered. Later, they extended their third order formulation to laminated plates [10]. Murthy [11] presented an improved transverse shear deformation theories for laminated anisotropic plates under bending. The displacement field was chosen so that the transverse shear stress vanished on the plate surfaces with the aim to remove the use of shear correction factor in computing shear stresses. Levinson [12] presented a refined theory for the static and dynamic analyses of isotropic plates by using different displacement field expressions. Reddy [15] pointed out that the equilibrium equations derived by Murthy [11] and Levinson [12] resulted variationally inconsistent. He wrote a simple higher order theory for laminated composites plates with a consistent derivation of the displacement field and associated equilibrium equations. He considered the membrane displacement components as cubic function of the thickness coordinate and the transverse displacement as constant. Later, Reddy and Liew [16] extended the higher order shear deformation theory to shells.

Therefore, the aforementioned higher order shear deformation theories often fail to provide accurate three dimensional stresses and strains at the ply level near geometric and material discontinuities. So, several layerwise models were developed which contain full three dimensional kinematics and constitutive relations. Reddy [17] suggested a layer wise theory by giving an accurate description of the three dimensional displacement field which was expanded as a linear combination of thickness coordinate and unknown functions of position of each layer. Di Sciuva [18,19] formulated an improved shear deformation theory, the so called zig-zag theory. He considered a two dimensional theory by adopting a displacement field with piecewise linear variation of the membrane displacement and constant value of the transverse displacement through the thickness. The fulfilment of the static and geometric continuity conditions was obtained and the influence of the distortion of the deformed normal was included. Reddy [20] pointed out that all the higher order theories are substantially disguised in the form of the displacement expansions used. Moreover, even when the displacement used was the same, the equilibrium equations were carried out in two different ways. Some authors used the vector approach, the equations did not contain the effect of higher order terms in the form of higher order stress resultants. The higher order terms were included in the strains computed. The other approach was to use the principle of virtual displacements which gave many more additional terms in the form of higher stress resultants. In this manner, the resulting set of equations for all the theories higher than first order were different from those obtained using the vector approach. Bisegna and Sacco [21] derived a general procedure, based on the conjecture that plate theories can be carried out from the three dimensional elasticity, by imposing suitable constraints on the stress and strain fields. By following the framework of the constrained three dimensional elasticity, the imposed constraint was assumed to be frictionless. And by taking into account the reactive fields, the equilibrium, congruence and constitutive equations turned out to be exactly satisfied. They used the equilibrium equations to carry out the shear stress in the thickness of the plate. A layer wise laminate theory rationally deduced from the three dimensional elasticity was also presented [22]. Bischoff and Ramm [23] discussed on the physical significance of higher order kinematic and static variables in a three dimensional shell formulation. Auricchio and Sacco [24] presented new mixed variational formulations for a first order shear deformation laminate theory and considered the out of plane stresses as primary variables of the problem. They determined the shear stress profile either by independent piecewise quadratic functions in the thickness or by satisfying the three dimensional equilibrium equations written in terms of midplane strains and curvatures. Carrera [25,26] proved that the Reissner's mixed variational theorem offered a convenient way of analyzing multilayered structures, as well as interlaminar continuity of transverse stresses and the zig-zag form of displacements in the thickness

plate/shell direction are easily introduced. He traced a critical overview which showed the capability of the Reissner's mixed variational theorem (RMVT) to study multilayered plates and shells. He stated that the interface continuity of transverse shear stresses, as well as the zig-zag form of displacements in the thickness shell direction, were easily introduced by RMWT. Kulikov and Plotnikova [27] developed models for the analyses of multilayered Timoshenko-Mindlin-type shells for the analysis of composite shells where the effect of transverse shear and transverse normal strains were included. They calculated the axial displacement, the vertical displacement, and the moments resultant by varying the geometric shell parameters. Carrera and Brischetto [28] extended the thickness locking mechanism to shell geometries by considering thin shell theory, first order shear deformation theory, higher order theories, mixed theories and layer wise theories. Their investigation confirmed that the thickness locking can be identified as a shell theory problem and had no relation with the numerical methods. Moreover, they observed that in order to avoid the thickness locking the shell theories would require at least a parabolic distribution of transverse displacement component. Matsunaga [29] determined the natural frequency, the buckling stress and the stress distribution of functionally graded shallow shells. He used the method of power series expansion of displacements components and derived the fundamental set of governing equations through the Hamilton's principle. With the aim to calculate the transverse shear and normal stresses, he conducted the integration of the fundamental equilibrium equation with satisfying the surface boundary conditions of the shell structure. He proved that a 2D higher order deformation theory can predict accurately not only the natural frequencies and buckling stresses but also the through the thickness stress and displacement distributions. Cinefra et al. [30] proposed a variable kinematic shell model, based on Carrera's unified formulation, to dynamic and static shell cases. They compared classical shell theories with the refined ones based on the Reissner mixed variational theorem. They furnished a better exploitation of the response of various shell theories by considering the distribution of the vibration modes and stress components in the thickness shell directions. Carrera et al. [31] evaluated the effect of thickness stretching in functionally graded plate/shell structures in the thickness direction. They compared plate/shell theories with constant transverse displacement with the ones where the transverse displacement function is expanded till to the fourth order in the thickness direction. They considered various FGM plates and shells with different geometry and material properties as proposed by Zenkour [32] and Kashtalyan [33]. They confirmed the Koiter's recommendation [34] which states that an increase in the order of expansion for in plane displacements can result meaningless if the thickness stretching is discarded in the plate/shell theories (constant transverse displacement). Liew at al. [35] presented an overview on the development of element free or meshless methods in the analysis of composite structures.

Meshless methods can provide more accurate approximations for structures with complex geometries than FEM. Their distinctive feature is related to the shape functions which are constructed in terms of higher order continuous weight functions. Their applications involve static analysis, free vibration, buckling and post buckling, non linear analysis and transient dynamics. Recently, Asemi et al. [36] furnished an elastic solution of a two dimensional functionally graded thick truncated cone with finite length under hydrostatic combined loads, such as internal, external, and axial pressure. They applied finite element method (FEM) by using Rayleigh – Ritz energy formulation. They analyzed the influence of semi vertex angle of the cone and the power law exponents on different distributions of displacements and stresses. They proposed numerical solutions for all types of axisymmetric structures as thick hollow cylindrical and truncated conical shells with finite and infinite lengths, and various loading and boundary conditions. Aghdam et al. [37] conducted the bending analysis of moderately thick functionally graded conical panels, subjected to uniform and non uniform distributed loadings. They applied the first order shear deformation theory and solved the governing equations by the extended Kantorovich method. The influence of the volume fraction exponent on the distribution of the normalized deflection and moment was underlined.

A lot of works deals with the dynamic response of conical shells [38-63]. For the sake of brevity only a few will be quoted [38-47].

Khatri and Asnani [38] conducted the vibration and damping analysis of multilayered conical shells. They wrote the governing equation of motion for axisymmetric and antisymmetric vibrations of a general multilayered conical shell consisting of an arbitrary number of orthotropic material layers. They applied the Galerkin method for finding the approximate solutions of the shell with various edge conditions. Lam et al. [39] used the generalized differential quadrature method as numerical technique for the analysis of the free vibration of truncated conical panels. They considered clamped and simply supported isotropic truncated conical panels and studied the effect of the semi vertex angle on the frequency characteristics. Liew et al. [40] studied the free vibration of conical shells via the element free k_p Ritz method, by using the classical thin shell theory. They reached the frequency characteristics of the conical shell by varying the semi vertex angle and the boundary conditions. Li et al [41] calculated the natural frequencies and the forced vibration responses of conical shell, using the Rayleigh-Ritz method. Sofiyev [42] analysed the vibration and stability behaviour of freely supported truncated and complete FGM conical shells subjected to external pressure. The material properties were assumed to vary continuously through the thickness of the conical shells, by following a simple power law. According to the thin shell theory, the basic relations, the dynamic stability and compatibility equations of FGM truncated conical shells were

written. The buckling pressures, the fundamental cyclic frequencies and corresponding waves numbers of FGM conical shells were found by recurring to the Galerkin method. The overall effects of the conical shell geometrical characteristics and material composition profiles on the buckling pressure and fundamental frequencies were examined in the numerical results. The dynamic behaviour of functionally graded conical shells by means of the FSDT and the GDQ numerical technique was analysed in [43-44]. A double form of the simple power law distributions was considered and the effect of the power exponent on the natural frequencies of the graded conical shells was studied. The domain was discretized by making use of different types of non-uniform grid point distributions. The formulation was based on the FSDT and the GDQ technique. The role of the power exponent and the other material coefficients on the natural frequencies of the graded conical shells was clarified. Cinefra et al. [45] arrived to closed form solutions of free vibration problems of simply supported functionally graded shells. By considering the framework of the Carrera unified formulation, the variable kinematic shell model was carried out. The numerical results showed that the used theory appeared to be able to obtain accurate stress values throughout the thickness direction. Zhao and Liew [46] developed the free vibration analysis of functionally graded conical shell panels by a meshless method. The element free k_p Ritz method was adopted and the FSDT theory is used. The accuracy of the proposed method is verified by executing convergence studies in terms of the number of nodes. They monitored the effects of the volume fraction, boundary condition, semi-vertex angle, and length to thickness ratio on the frequency characteristics of the functionally graded conical shells. Recently, Tornabene et al. [47] recently studied the functionally graded and laminated doubly curved shells and panels of revolution with a free-form meridian. They furnished a 2D G.D.Q. solution for free vibration, by deriving the theoretical formulation with the use of the first order shear deformation theory (FSDT). They generalized the shell theory with the inclusion of the curvature effect in the formulation.

Among the numerical works which dealt with the bucking of conical shell, the following ones are considered. Seide [48] examined the axisymmetric buckling of circular cones under axial compressions. Mushtari and Sachenkov [49] focused on the stability of cylindrical and conical shells of circular cross section by considering the simultaneous action of axial compression and external normal pressure. Singer [50] analyzed the buckling of circular conical shells under axisymmetric external pressure. Seide [51] developed calculations for the stability of thin conical frustums subjected to external uniform hydrostatic pressure and axial load. Singer [52] furnished Donnel type equation for buckling of orthotropic conical shells. Serpico [53] studied the elastic stability of orthotropic conical and cylindrical shells subjected to axisymmetric loading conditions.

Lu and Chang [54] examined the non linear thermal buckling of conical shells. Baruch et al. [55] analyzed the influence of in plane boundary conditions on the stability of conical shells under hydrostatic pressure. Bushnell and Smith [56] studied the buckling of non uniformly heated cylindrical and conical shells. Wu and Chiu [57] focused on the thermally induced dynamic instability of composite conical shells. Dulmir et al. [58] studied the axisymmetric static and dynamic buckling of composite truncated conical cap. Bhangale et al. [59] characterized the linear thermoelastic buckling and free vibration behaviour of functionally graded truncated conical shells. Sofiyev [60] analyzed the stability of functionally graded truncated conical shells under aperiodic impulsive loading. Naj et al. [61] examined the thermal and mechanical instability of functionally graded conical shells. Sofiyev [62] analyzed the stability behaviour of freely supported FGM conical shells subjected to external pressure. Recently, Sofiyev [63] characterized the influence of the initial imperfection on the linear buckling response of FGM truncated conical shells.

The aim of the present study is to extend the previous formulation by the authors [64] to the determination of accurate stress profiles for functionally conical shells and panels. As far as the static analysis of functionally graded conical panels and shells is concerned, shear deformation theories of various degree have been applied. The kinematic model of the first order conceived by Reissner and Mindlin has been overcome by the higher order theories which lead to the accurate determination of the sliding strain. By fixing the Taylor's expansion of displacement field at the third order and taking constant the transverse displacement, two third order shear deformation theories are recurrent in the literature background: the third order theories of constrained and unconstrained nature. The first one was originally formulated by Reddy [16], whereas the second one was firstly proposed by Leung [65] and is considered as an evolution of the FSDT. The need to constrain the resulting kinematic model in the Reddy's formulation by enforcing the null value of sliding strains on the boundary surfaces, has the proper advantage to make the boundary conditions satisfied. Differently, the Leung's third order model does not introduce any constraint and it also allows to consider shearing loads even if it does not satisfy the boundary condition.

In this paper, the authors reconsider the unconstrained third order theory and write it for the functionally graded conical panels and shells. As in the previous work for the FGM cylindrical shells and panels [64], they combine the Leung's theory with the stress recovery technique in order to conduct the static analysis with the satisfaction of boundary conditions under shear and normal constant loads at the extreme surfaces of graded conical shell or panels.

Here, open conical shell and panels made up of a single functionally graded layer are considered. The ceramic volume fraction follows a four parameter power exponent law. They start from the definition of a seven parameter displacement field, use the strain - displacement relations enriched

by the initial curvature effect and the constitutive equations and the internal actions in terms of the displacement parameters. With the definition of the external transverse and shear uniform loads written in terms of the ones acting on the upper and lower surfaces, the principle of virtual displacement is applied and the indefinite equilibrium equations and the boundary conditions are derived. The substitution of the internal actions in terms of generalized displacements in the indefinite equilibrium equation system leads to seven fundamental equations. The generalized differential quadrature method (GDQ) [66-90] is applied in order to solve the fundamental system and obtain the solution in terms of the seven independent displacement parameters. Using the constitutive equations, the membrane meridional and circumferential stress response along the thickness direction for different class of functionally graded materials are determined. With the in plane stress components indirectly derived from the GDQ - solution [66-90] of the fundamental system, the integration of the three dimensional indefinite equilibrium equations is carried out. In order to satisfy the boundary condition at extreme surfaces, the determined transverse shear or normal stress was refined as shown in the previous paper by the authors [64]. In this manner, the throughout the thickness transverse and normal stress could be plotted by means of the GDQ solution of the 3D indefinite equilibrium equation along the thickness direction, for different types of functionally graded open conical panels and shells. The influence of the initial curvature effect, the semi vertex angle of the conical shell, the open angle of the conical panel, the thickness to radius ratio, the thickness to length ratio on the stress profiles are set forth. Moreover, the comparisons between the first and third order mechanical response, the effect of the material coefficients, the difference between the mechanical behaviour of cylindrical and open conical structures are studied and shown.

Further publications related with the present paper are reported in [91-94].

3.2 Functionally graded composite conical shells and fundamental systems

3.2.1 Fundamental hypotheses

In this paper a graded truncated conical shell is considered. L_0, R_0, h denote the height, the parallel radius and the total thickness of the shell, respectively. The position of an arbitrary point P within the shell is located by the coordinates $x\ (0 \le x \le x_0 = L_0/\cos\alpha)$, $s\ (0 \le s \le s_0 = \vartheta R_0)$ upon the middle surface, and ζ directed along the outward normal **n**, and measured from the reference surface $(-h/2 \le \zeta \le h/2)$, as shown in Fig.1. The α - parameter is the angle of the semi-vertex of the cone and the φ - parameter is the angle between the normal to the shell surface and the $x_3^{'}$ - axis. The R_b - radius represents the shift of the $x_3^{'}$ - axis with respect to the x_3 - axis of revolution. When the general case of shell of revolution changes into the case under study, the radii of curvature in the meridional R_φ and circumferential R_ϑ directions assume the following values:

$$R_\varphi = R_x = \infty,\ R_0(x) = R_b + x\sin\alpha = R_b + x\cos\varphi,\ R_\vartheta = R_0/\sin\varphi \tag{1}$$

It is noticed that the conical structure derives from the one under consideration for $\alpha = 0$, and the circular plate for $\alpha = \pi/2$.

The fundamental topics which characterize the present formulation are :

1. the normal strain is inextensible, so the corresponding deformation does not exist;
2. the transverse shear deformation is taken into account in the governing equations, and the normal lines to the reference surface do not remain straight and normal after deformation;
3. the shell deflections are small and the strains are infinitesimal;
4. the shell is moderately thick, and consequently the normal stress could be negligible;
5. the shear correction factor vanishes and the presence of a finite shear transverse strain on the top and bottom of the open conical shell is accepted. Thus, the model releases the additional constrain imposed by the TSDT of Reddy [16];
6. the anisotropic material is assumed to be linearly elastic;
7. the initial curvature effect is taken into account.

3.2.2 Displacement field and constitutive equations

The unconstrained third-order shear deformation theory is based on the following representation of the displacement field across the thickness of the open conical shell:

$$\begin{aligned} U_x(x,s,\zeta) &= u_x(x,s) + \zeta\beta_x(x,s) + \zeta^3\eta_x(x,s) \\ U_s(x,s,\zeta) &= u_s(x,s) + \zeta\beta_s(x,s) + \zeta^3\eta_s(x,s) \\ W(x,s,\zeta) &= w(x,s) \end{aligned} \tag{2}$$

where U_x, U_s, W are the displacements along the meridional, circumferential and normal directions, respectively; u_x, u_s are the in-plane displacements, w is the transverse displacement of a point (x,s) on the middle surface. The functions β_x, β_s are rotations of the normal to the middle plane about s and x axes, respectively. The parameters η_x, η_s are the higher order terms in Taylor's series expansion and represent the higher order transverse cross-sectional deformation modes.

By substitution of the displacement relations (2) into the strain-displacement equations of the classical theory of elasticity, the following relations are obtained:

$$\varepsilon_x = \left(\frac{\partial u_x}{\partial x}\right) + \zeta\left(\frac{\partial \beta_x}{\partial x}\right) + \zeta^3\left(\frac{\partial \eta_x}{\partial x}\right) \tag{3}$$

$$\varepsilon_s = \frac{1}{(1+\zeta/R_\vartheta)}\left(\begin{array}{l}\left(\frac{\partial u_s}{\partial s} + \frac{\cos\varphi}{R_0}u_x + \frac{\sin\varphi}{R_0}w\right) + \zeta\left(\frac{\partial \beta_s}{\partial s} + \frac{\cos\varphi}{R_0}\beta_x\right) + \\ +\zeta^3\left(\frac{\partial \eta_s}{\partial s} + \frac{\cos\varphi}{R_0}\eta_x\right)\end{array}\right) \tag{4}$$

$$\gamma_{xn} = \frac{\partial w}{\partial x} + \beta_x + 3\zeta^2\eta_x \tag{5}$$

$$\gamma_{sn} = \frac{1}{(1+\zeta/R_\vartheta)}\left(-\frac{\sin\varphi}{R_0}u_s + \frac{\partial w}{\partial s} + \beta_s + 3\zeta^2\eta_s + 2\zeta^3\frac{\sin\varphi}{R_0}\eta_s\right) \tag{6}$$

$$\begin{aligned}\gamma_{xs} &= \left(\frac{\partial u_s}{\partial x} + \zeta\left(\frac{\partial \beta_s}{\partial x}\right) + \zeta^3\left(\frac{\partial \eta_s}{\partial x}\right)\right) + \\ &+ \frac{1}{(1+\zeta/R_\vartheta)}\left(\frac{\partial u_x}{\partial s} - \frac{\cos\varphi}{R_0}u_s + \zeta\left(\frac{\partial \beta_x}{\partial s} - \frac{\cos\varphi}{R_0}\beta_s\right) + \zeta^3\left(\frac{\partial \eta_x}{\partial s} - \frac{\cos\varphi}{R_0}\eta_s\right)\right)\end{aligned} \tag{7}$$

Eqs.(3-7) take into account the initial curvature effect into account. The shell material assumed in the following is a functionally graded composite linear elastic one. The elastic engineering stiffness $A_{ij,}B_{ij,}D_{ij,}E_{ij,}F_{ij,}L_{ij,}H_{ij},M_{ij,}N_{ij},V_{ij}$ are defined as [64]:

$$\left(A_{ij,}B_{ij,}D_{ij,}E_{ij,}F_{ij,}L_{ij,}H_{ij},M_{ij,}N_{ij},V_{ij}\right)=\int_{-\frac{h}{2}}^{+\frac{h}{2}}Q_{ij}(1,\zeta,\zeta^2,\zeta^3,\zeta^4,\zeta^5,\zeta^6,\zeta^7,\zeta^8,\zeta^9)d\zeta \tag{8}$$

where the elastic constants $Q_{ij}=Q_{ij}(\zeta)$ depend on the thickness coordinate ζ and they assume the expressions suggested below:

$$\begin{aligned}
&Q_{11}=Q_{22}=\frac{E(\zeta)}{1-\nu^2(\zeta)}\\
&Q_{12}=\frac{\nu(\zeta)E(\zeta)}{1-\nu^2(\zeta)}\\
&Q_{44}=Q_{55}=Q_{66}=\frac{E(\zeta)}{2(1+\nu(\zeta))}\\
&Q_{16}=Q_{26}=Q_{45}=0
\end{aligned} \tag{9}$$

In (9) $E\left(\zeta\right)$, $\nu\left(\zeta\right)$ are the elastic parameters of the composite material which are also functions of the thickness coordinate ζ.

The FGM shell under investigation consists of a mixture of two basic components : the ceramic (C) and the metal (M) constituents. Their properties follow a continuous and a smoothly change in the thickness direction ζ, and they are function of volume fractions of the constituent materials. The three characteristics parameters, the Young's modulus $E(\zeta)$, the Poisson's ratio $\nu(\zeta)$, the density $\rho(\zeta)$, which identify the FGM material, are presented in the form of a linear combination, as follows [64]:

$$\begin{aligned}
&\rho(\zeta)=(\rho_C-\rho_M)V_C+\rho_M\\
&E\left(\zeta\right)=(E_C-E_M)V_C+E_M\\
&\nu(\zeta)=(\nu_C-\nu_M)V_C+\nu_M
\end{aligned} \tag{10}$$

where ρ_C,E_C,ν_C,V_C, and ρ_M,E_M,ν_M,V_M are the volumic mass, the elastic modulus, the Poisson's coefficient, the volume fraction of the ceramic (C), and the metal (M) constituents, respectively.

The power law distribution for the volume fraction of the ceramic component are suggested, where four parameters are involved. As mentioned above, the material is inhomogeneous and the material properties varying through the thickness are described by the following two four parameter power law distributions [64]:

$$FGM_{1(a/b/c/p)}:V_C=\left(1-a\left(\frac{1}{2}+\frac{\zeta}{h}\right)+b\left(\frac{1}{2}+\frac{\zeta}{h}\right)^c\right)^p \tag{11}$$

or

$$FGM_{2(a/b/c/p)}:V_C=\left(1-a\left(\frac{1}{2}-\frac{\zeta}{h}\right)+b\left(\frac{1}{2}-\frac{\zeta}{h}\right)^c\right)^p \tag{12}$$

In Eqs. (11-12) the four characteristic parameters are the volume fraction index p ($0\le p\le\infty$), and the coefficients a,b,c. By varying them, the mode of variation of the ceramic volume fraction changes through the shell thickness. It is assumed that the sum of the volume fractions of the two basic component (ceramic and metal component) is equal to unity. Therefore, it can be noticed that when the exponent *p* is set to zero or equal to infinity, the FGM material becomes the homogeneous isotropic material, as stated below:

$$\begin{aligned} &p=0\rightarrow V_C=1,V_M=0\rightarrow \rho(\zeta)=\rho_C,\ E(\zeta)=E_C,\ \nu(\zeta)=\nu_C\\ &p=\infty\rightarrow V_C=0,V_M=1\rightarrow \rho(\zeta)=\rho_M,\ E(\zeta)=E_M,\ \nu(\zeta)=\nu_M \end{aligned} \tag{13}$$

For the FGM shell the constitutive equations can be written as follows:

$$\begin{aligned} &\sigma_x=Q_{11}\varepsilon_x+Q_{12}\varepsilon_s\\ &\sigma_s=Q_{12}\varepsilon_x+Q_{22}\varepsilon_s\\ &\sigma_n=0\\ &\tau_{xs}=Q_{66}\gamma_{xs}\\ &\tau_{xn}=Q_{66}\gamma_{xn}\\ &\tau_{sn}=Q_{66}\gamma_{sn} \end{aligned} \tag{14}$$

3.2.3 Forces and moments resultants

Normal forces, moments, and higher order moments, as well as the shear force and higher order shear force are all defined by the following expressions:

$$\left(N_x, M_x, P_x\right) = \int_{-\frac{h}{2}}^{+\frac{h}{2}} \sigma_x(1, \zeta, \zeta^3)\left(1+\frac{\zeta}{R_\vartheta}\right)d\zeta \tag{15}$$

$$\left(N_s, M_s, P_s\right) = \int_{-\frac{h}{2}}^{+\frac{h}{2}} \sigma_s(1, \zeta, \zeta^3)d\zeta \tag{16}$$

$$\left(N_{xs}, M_{xs}, P_{xs}\right) = \int_{-\frac{h}{2}}^{+\frac{h}{2}} \tau_{xs}(1, \zeta, \zeta^3)\left(1+\frac{\zeta}{R_\vartheta}\right)d\zeta \tag{17}$$

$$\left(N_{sx}, M_{sx}, P_{sx}\right) = \int_{-\frac{h}{2}}^{+\frac{h}{2}} \tau_{sx}(1, \zeta, \zeta^3)d\zeta \tag{18}$$

$$\left(T_x, Q_x, S_x\right) = \int_{-\frac{h}{2}}^{+\frac{h}{2}} \tau_{xn}(1, \zeta^2, \zeta^3)\left(1+\frac{\zeta}{R_\vartheta}\right)d\zeta \tag{19}$$

$$\left(T_s, Q_s, S_s\right) = \int_{-\frac{h}{2}}^{+\frac{h}{2}} \tau_{sn}(1, \zeta^2, \zeta^3)d\zeta \tag{20}$$

By considering the effect of the initial curvature in the formulation, the stress resultants N_{xs}, M_{xs}, P_{xs} are not equal to the stress resultants N_{sx}, M_{sx}, P_{sx}, respectively. This assumption derives from the consideration that the ratio ζ / R_0 is not neglected with respect to unity. The effect of initial curvature is emphasized by the following coefficients:

$$a_1 = \frac{\sin\varphi}{R_0};\ b_1 = -\frac{\sin\varphi}{R_0};\ b_2 = \frac{\left(\sin\varphi\right)^2}{R_0^2}; b_3 = -\frac{\left(\sin\varphi\right)^3}{R_0^3} \tag{21}$$

Using Eqs. (3-7), (14-21) the relations which characterize the internal stresses as function of the displacement parameters can be obtained.

3.2.3.1 Normal and shear forces

$$N_x = \left(A_{11} + a_1 B_{11}\right)\frac{\partial u_x}{\partial x} + A_{12}\frac{\cos\varphi}{R_0}u_x + A_{12}\left(\frac{\partial u_s}{\partial s} + \frac{\sin\varphi}{R_0}w\right) +$$
$$+\left(B_{11} + a_1 D_{11}\right)\frac{\partial \beta_x}{\partial x} + B_{12}\frac{\cos\varphi}{R_0}\beta_x + B_{12}\frac{\partial \beta_s}{\partial s} + \tag{22}$$
$$+\left(E_{11} + a_1 F_{11}\right)\frac{\partial \eta_x}{\partial x} + E_{12}\frac{\cos\varphi}{R_0}\eta_x + E_{12}\frac{\partial \eta_s}{\partial s}$$

$$N_s = A_{12}\frac{\partial u_x}{\partial x} + \left(A_{11} + b_1 B_{11} + b_2 D_{11} + b_3 E_{11}\right)\left(\frac{\cos\varphi}{R_0}u_x + \frac{\partial u_s}{\partial s} + \frac{\sin\varphi}{R_0}w\right) +$$
$$+B_{12}\frac{\partial \beta_x}{\partial x} + \left(B_{11} + b_1 D_{11} + b_2 E_{11} + b_3 F_{11}\right)\left(\frac{\cos\varphi}{R_0}\beta_x + \frac{\partial \beta_s}{\partial s}\right) + \tag{23}$$
$$+E_{12}\frac{\partial \eta_x}{\partial x} + \left(E_{11} + b_1 F_{11} + b_2 L_{11} + b_3 H_{11}\right)\left(\frac{\cos\varphi}{R_0}\eta_x + \frac{\partial \eta_s}{\partial s}\right)$$

$$N_{xs} = A_{66}\frac{\partial u_x}{\partial s} + \left(A_{66} + a_1 B_{66}\right)\frac{\partial u_s}{\partial x} + A_{66}\left(-\frac{\cos\varphi}{R_0}\right)u_s + \tag{24}$$
$$+B_{66}\frac{\partial \beta_x}{\partial s} + \left(B_{66} + a_1 D_{66}\right)\frac{\partial \beta_s}{\partial x} + B_{66}\left(-\frac{\cos\varphi}{R_0}\right)\beta_s +$$
$$+E_{66}\frac{\partial \eta_x}{\partial s} + \left(E_{66} + a_1 F_{66}\right)\frac{\partial \eta_s}{\partial x} + E_{66}\left(-\frac{\cos\varphi}{R_0}\right)\eta_s$$

$$N_{sx} = \left(A_{66} + b_1 B_{66} + b_2 D_{66} + b_3 E_{66}\right)\frac{\partial u_x}{\partial s} + A_{66}\frac{\partial u_s}{\partial x} - \left(\frac{\cos\varphi}{R_0}\right)\left(A_{66} + b_1 B_{66} + b_2 D_{66} + b_3 E_{66}\right)u_s +$$
$$+\left(B_{66} + b_1 D_{66} + b_2 E_{66} + b_3 F_{66}\right)\frac{\partial \beta_x}{\partial s} + B_{66}\frac{\partial \beta_s}{\partial x} - \left(\frac{\cos\varphi}{R_0}\right)\left(B_{66} + b_1 D_{66} + b_2 E_{66} + b_3 F_{66}\right)\beta_s + \tag{25}$$
$$+\left(E_{66} + b_1 F_{66} + b_2 L_{66} + b_3 H_{66}\right)\frac{\partial \eta_x}{\partial s} + E_{66}\frac{\partial \eta_s}{\partial x} - \left(\frac{\cos\varphi}{R_0}\right)\left(E_{66} + b_1 F_{66} + b_2 L_{66} + b_3 H_{66}\right)\eta_s$$

$$M_x = \left(B_{11} + a_1 D_{11}\right)\frac{\partial u_x}{\partial x} + B_{12}\left(\frac{\cos\varphi}{R_0}u_x + \frac{\partial u_s}{\partial s} + \frac{\sin\varphi}{R_0}w\right) +$$
$$+\left(D_{11} + a_1 E_{11}\right)\frac{\partial \beta_x}{\partial x} + D_{12}\left(\frac{\cos\varphi}{R_0}\beta_x + \frac{\partial \beta_s}{\partial s}\right) + \quad (26)$$
$$+\left(F_{11} + a_1 L_{11}\right)\frac{\partial \eta_x}{\partial x} + F_{12}\left(\frac{\cos\varphi}{R_0}\eta_x + \frac{\partial \eta_s}{\partial s}\right)$$

$$M_s = B_{12}\frac{\partial u_x}{\partial x} + \left(B_{11} + b_1 D_{11} + b_2 E_{11} + b_3 F_{11}\right)\left(\frac{\cos\varphi}{R_0}u_x + \frac{\partial u_s}{\partial s} + \frac{\sin\varphi}{R_0}w\right) +$$
$$+D_{12}\frac{\partial \beta_x}{\partial x} + \left(D_{11} + b_1 E_{11} + b_2 F_{11} + b_3 L_{11}\right)\left(\frac{\cos\varphi}{R_0}\beta_x + \frac{\partial \beta_s}{\partial s}\right) + \quad (27)$$
$$+F_{12}\frac{\partial \eta_x}{\partial x} + \left(F_{11} + b_1 L_{11} + b_2 H_{11} + b_3 M_{11}\right)\left(\frac{\cos\varphi}{R_0}\eta_x + \frac{\partial \eta_s}{\partial s}\right)$$

$$M_{xs} = B_{66}\frac{\partial u_x}{\partial s} + \left(B_{66} + a_1 D_{66}\right)\frac{\partial u_s}{\partial x} + B_{66}\left(-\frac{\cos\varphi}{R_0}\right)u_s +$$
$$+D_{66}\frac{\partial \beta_x}{\partial s} + \left(D_{66} + a_1 E_{66}\right)\frac{\partial \beta_s}{\partial x} + D_{66}\left(-\frac{\cos\varphi}{R_0}\right)\beta_s + \quad (28)$$
$$+F_{66}\frac{\partial \eta_x}{\partial s} + \left(F_{66} + a_1 L_{66}\right)\frac{\partial \eta_s}{\partial x} + F_{66}\left(-\frac{\cos\varphi}{R_0}\right)\eta_s$$

$$M_{sx} = \left(B_{66} + b_1 D_{66} + b_2 E_{66} + b_3 F_{66}\right)\frac{\partial u_x}{\partial s} + B_{66}\frac{\partial u_s}{\partial x} - \left(\frac{\cos\varphi}{R_0}\right)\left(B_{66} + b_1 D_{66} + b_2 E_{66} + b_3 F_{66}\right)u_s +$$
$$+\left(D_{66} + b_1 E_{66} + b_2 F_{66} + b_3 L_{66}\right)\frac{\partial \beta_x}{\partial s} + D_{66}\frac{\partial \beta_s}{\partial x} - \left(\frac{\cos\varphi}{R_0}\right)\left(D_{66} + b_1 E_{66} + b_2 F_{66} + b_3 L_{66}\right)\beta_s + \quad (29)$$
$$+\left(F_{66} + b_1 L_{66} + b_2 H_{66} + b_3 M_{66}\right)\frac{\partial \eta_x}{\partial s} + F_{66}\frac{\partial \eta_s}{\partial x} - \left(\frac{\cos\varphi}{R_0}\right)\left(F_{66} + b_1 L_{66} + b_2 H_{66} + b_3 M_{66}\right)\eta_s$$

3.2.3.2 Higher order moments

$$P_x = \left(E_{11} + a_1 F_{11}\right)\frac{\partial u_x}{\partial x} + E_{12}\frac{\cos\varphi}{R_0}u_x + E_{12}\left(\frac{\partial u_s}{\partial s} + \frac{\sin\varphi}{R_0}w\right)$$
$$+\left(F_{11} + a_1 L_{11}\right)\frac{\partial \beta_x}{\partial x} + F_{12}\left(\frac{\cos\varphi}{R_0}\beta_x + \frac{\partial \beta_s}{\partial s}\right) + \quad (30)$$
$$+\left(H_{11} + a_1 M_{11}\right)\frac{\partial \eta_x}{\partial x} + H_{12}\left(\frac{\cos\varphi}{R_0}\eta_x + \frac{\partial \eta_s}{\partial s}\right)$$

$$P_s = E_{12}\frac{\partial u_x}{\partial x} + \left(E_{11} + b_1F_{11} + b_2L_{11} + b_3H_{11}\right)\left(\frac{\cos\varphi}{R_0}u_x + \frac{\partial u_s}{\partial s} + \frac{\sin\varphi}{R_0}w\right) +$$
$$+F_{12}\frac{\partial \beta_x}{\partial x} + \left(F_{11} + b_1L_{11} + b_2H_{11} + b_3M_{11}\right)\left(\frac{\cos\varphi}{R_0}\beta_x + \frac{\partial \beta_s}{\partial s}\right) + \quad (31)$$
$$+H_{12}\frac{\partial \eta_x}{\partial x} + \left(H_{11} + b_1M_{11} + b_2N_{11} + b_3V_{11}\right)\left(\frac{\cos\varphi}{R_0}\eta_x + \frac{\partial \eta_s}{\partial s}\right)$$

$$P_{xs} = E_{66}\frac{\partial u_x}{\partial s} + \left(E_{66} + a_1F_{66}\right)\frac{\partial u_s}{\partial x} - E_{66}\left(\frac{\cos\varphi}{R_0}\right)u_s +$$
$$+F_{66}\frac{\partial \beta_x}{\partial s} + \left(F_{66} + a_1L_{66}\right)\frac{\partial \beta_s}{\partial x} - F_{66}\left(\frac{\cos\varphi}{R_0}\right)\beta_s + \quad (32)$$
$$+H_{66}\frac{\partial \eta_x}{\partial s} + \left(H_{66} + a_1M_{66}\right)\frac{\partial \eta_s}{\partial x} - H_{66}\left(\frac{\cos\varphi}{R_0}\right)\eta_s$$

$$P_{sx} = \left(E_{66} + b_1F_{66} + b_2L_{66} + b_3H_{66}\right)\frac{\partial u_x}{\partial s} + E_{66}\frac{\partial u_s}{\partial x} - \left(\frac{\cos\varphi}{R_0}\right)\left(E_{66} + b_1F_{66} + b_2L_{66} + b_3H_{66}\right)u_s +$$
$$+\left(F_{66} + b_1L_{66} + b_2H_{66} + b_3M_{66}\right)\frac{\partial \beta_x}{\partial s} + F_{66}\frac{\partial \beta_s}{\partial x} - \left(\frac{\cos\varphi}{R_0}\right)\left(F_{66} + b_1L_{66} + b_2H_{66} + b_3M_{66}\right)\beta_s + \quad (33)$$
$$+\left(H_{66} + b_1M_{66} + b_2N_{66} + b_3V_{66}\right)\frac{\partial \eta_x}{\partial s} + H_{66}\frac{\partial \eta_s}{\partial x} - \left(\frac{\cos\varphi}{R_0}\right)\left(H_{66} + b_1M_{66} + b_2N_{66} + b_3V_{66}\right)\eta_s$$

3.2.3.3 Shear forces

$$T_x = \left(A_{66} + a_1B_{66}\right)\left(\frac{\partial w}{\partial x} + \beta_x\right) + 3\left(D_{66} + a_1E_{66}\right)\eta_x \quad (34)$$

$$T_s = \left(A_{66} + b_1B_{66} + b_2D_{66} + b_3E_{66}\right)\left(-\frac{\sin\varphi}{R_0}u_s + \frac{\partial w}{\partial s} + \beta_s\right) +$$
$$+3\left(D_{66} + b_1E_{66} + b_2F_{66} + b_3L_{66}\right)\eta_s + \frac{2\sin\varphi}{R_0}\left(E_{66} + b_1F_{66} + b_2L_{66} + b_3H_{66}\right)\eta_s \quad (35)$$

3.2.3.4 Higher order shear resultants

$$Q_x = \left(D_{66} + a_1 E_{66}\right)\left(\frac{\partial w}{\partial x} + \beta_x\right) + 3\left(F_{66} + a_1 L_{66}\right)\eta_x \tag{36}$$

$$\begin{aligned} Q_s = {} & \left(D_{66} + b_1 E_{66} + b_2 F_{66} + b_3 L_{66}\right)\left(-\frac{\sin\varphi}{R_0}u_s + \frac{\partial w}{\partial s} + \beta_s\right) + \\ & + \left(F_{66} + b_1 L_{66} + b_2 H_{66} + b_3 M_{66}\right)\left(3 + \frac{2\sin\varphi}{R_0}\right)\eta_s \end{aligned} \tag{37}$$

$$S_x = \left(E_{66} + a_1 F_{66}\right)\left(\frac{\partial w}{\partial x} + \beta_x\right) + 3\left(L_{66} + a_1 H_{66}\right)\eta_x \tag{38}$$

$$\begin{aligned} S_s = {} & \left(E_{66} + b_1 F_{66} + b_2 L_{66} + b_3 H_{66}\right)\left(-\frac{\sin\varphi}{R_0}u_s + \frac{\partial w}{\partial s} + \beta_s\right) + \\ & + 3\left(L_{66} + b_1 H_{66} + b_2 M_{66} + b_3 N_{66}\right)\eta_s + \frac{2\sin\varphi}{R_0}\left(H_{66} + b_1 M_{66} + b_2 N_{66} + b_3 V_{66}\right)\eta_s \end{aligned} \tag{39}$$

3.2.4 Equilibrium equations

Here we use the principle of virtual displacements to derive the equilibrium equations consistent with the displacement field equations (2). The principle of virtual displacements can be stated in analytical form as:

$$\begin{aligned} & \int_{-\frac{h}{2}}^{+\frac{h}{2}} \int_{\Omega} \left(\sigma_x \delta\varepsilon_x + \sigma_s \delta\varepsilon_s + \tau_{xs}\delta\gamma_{xs} + \tau_{xn}\delta\gamma_{xn} + \tau_{sn}\delta\gamma_{sn}\right)\left(1 + \frac{\zeta}{R_\vartheta}\right) dx ds d\zeta - \int_{\Omega} p_x \delta u_x dx ds - \int_{\Omega} p_s \delta u_s dx ds + \\ & - \int_{\Omega} p_n \delta w dx ds - \int_{\Omega} m_x \delta\beta_x dx ds - \int_{\Omega} m_s \delta\beta_s dx ds - \int_{\Omega} r_x \delta\eta_x dx ds - \int_{\Omega} r_s \delta\eta_s dx ds = 0 \end{aligned} \tag{40}$$

where :

$$d\Omega = \left(1 + \frac{\zeta}{R_\vartheta}\right) R_0 \, d\vartheta dx$$

and $p_x, p_s, p_n, m_x, m_s, r_x, r_s$ are the external loads acting on the reference surface. Introducing Eqs. (3-7) into Eq. (40) and integrating the resulting expression by parts, and setting the coefficients of $\delta u_x, \delta u_s, \delta w, \delta\beta_x, \delta\beta_s, \delta\eta_x, \delta\eta_s$ to zero separately, the following equations of equilibrium are obtained:

$$
\begin{aligned}
&\delta u_x: \frac{\partial N_x}{\partial x}+\frac{\partial N_{sx}}{\partial s}+\frac{N_x-N_s}{R_0}\cos\varphi+p_x=0\\
&\delta u_s: \frac{\partial N_s}{\partial s}+\frac{\partial N_{xs}}{\partial x}+\frac{N_{xs}+N_{sx}}{R_0}\cos\varphi+\frac{\sin\varphi}{R_0}T_s+p_s=0\\
&\delta w: \frac{\partial T_x}{\partial x}+\frac{\partial T_s}{\partial s}+\frac{\cos\varphi}{R_0}T_x-\frac{\sin\varphi}{R_0}N_s+p_n=0\\
&\delta \beta_x: \frac{\partial M_x}{\partial x}+\frac{\partial M_{sx}}{\partial s}+\frac{M_x-M_s}{R_0}\cos\varphi-T_x+m_x=0\\
&\delta \beta_s: \frac{\partial M_{xs}}{\partial x}+\frac{\partial M_s}{\partial s}+\frac{M_{xs}+M_{sx}}{R_0}\cos\varphi-T_s+m_s=0\\
&\delta \eta_x: \frac{\partial P_x}{\partial x}+\frac{\partial P_{sx}}{\partial s}+\frac{P_x-P_s}{R_0}\cos\varphi-3Q_x+r_x=0\\
&\delta \eta_s: \frac{\partial P_{xs}}{\partial x}+\frac{\partial P_s}{\partial s}+\frac{P_{xs}+P_{sx}}{R_0}\cos\varphi-3Q_s-\frac{2\sin\varphi}{R_0}S_s+r_s=0
\end{aligned}
\tag{41}
$$

It is worth noting that Eqs. (41) are derived by taking into account the definitions (15-20) of forces and moment resultants. The first three equations of Eqs.(41) express the translational equilibrium along the meridional x, circumferential s, and normal ζ direction, respectively. The last four Eqs. (41) are rotational equilibrium equations about the s and x directions, respectively. In particular, the first two are the effective rotational equilibrium equations, whereas the second two represent fictitious equations, which derive by the computation of the additional terms of displacement.

Then, substituting the expressions (22-39) for the in-plane meridional, circumferential, and shearing force resultants $(N_x, N_s, N_{xs}, N_{sx})$, the analogous couples $(M_x, M_s, M_{xs}, M_{sx})$, and the transverse shear force resultants $(T_x, T_s, Q_x, Q_s, S_x, S_s)$, Eqs. (42) yield:

$$
\begin{bmatrix}
S_{11} & S_{12} & S_{13} & S_{14} & S_{15} & S_{16} & S_{17}\\
S_{21} & S_{22} & S_{23} & S_{24} & S_{25} & S_{26} & S_{27}\\
S_{31} & S_{32} & S_{33} & S_{34} & S_{35} & S_{36} & S_{37}\\
S_{41} & S_{42} & S_{43} & S_{44} & S_{45} & S_{46} & S_{47}\\
S_{51} & S_{52} & S_{53} & S_{54} & S_{55} & S_{56} & S_{57}\\
S_{61} & S_{62} & S_{63} & S_{64} & S_{65} & S_{66} & S_{67}\\
S_{71} & S_{72} & S_{73} & S_{74} & S_{75} & S_{76} & S_{77}
\end{bmatrix}
\begin{Bmatrix}
u_x\\ u_s\\ w\\ \beta_x\\ \beta_s\\ \eta_x\\ \eta_s
\end{Bmatrix}
=
\begin{Bmatrix}
p_x\\ p_s\\ p_n\\ m_x\\ m_s\\ r_x\\ r_s
\end{Bmatrix}
\tag{42}
$$

where the explicit forms of the equilibrium operators $S_{ij}, i, j = 1,...,7$ are listed in Appendix A.

It can be noticed that the analytical expressions of most of the equilibrium operators in (42) are characterized by the presence of the coefficients a_1, b_1, b_2, b_3 (21), which take into account the effect

of the initial curvature, as declared above. By putting $a_1 = b_1 = b_2 = b_3 = 0$, the effect of initial curvature can be neglected.

It should be noted that the loadings on the middle surface can be expressed in terms of the loadings on the upper and lower surfaces of the shell as follows.

$$
\begin{aligned}
p_x &= p_x^t\left(1+\frac{h\sin\varphi}{2R_0}\right)+p_x^b\left(1-\frac{h\sin\varphi}{2R_0}\right)\\
p_s &= p_s^t\left(1+\frac{h\sin\varphi}{2R_0}\right)+p_s^b\left(1-\frac{h\sin\varphi}{2R_0}\right)\\
p_n &= p_n^t\left(1+\frac{h\sin\varphi}{2R_0}\right)+p_n^b\left(1-\frac{h\sin\varphi}{2R_0}\right)\\
m_x &= p_x^t\frac{h}{2}\left(1+\frac{h\sin\varphi}{2R_0}\right)-p_x^b\frac{h}{2}\left(1-\frac{h\sin\varphi}{2R_0}\right)\\
m_s &= p_s^t\frac{h}{2}\left(1+\frac{h\sin\varphi}{2R_0}\right)-p_s^b\frac{h}{2}\left(1-\frac{h\sin\varphi}{2R_0}\right)\\
r_x &= p_x^t\frac{h^3}{8}\left(1+\frac{h\sin\varphi}{2R_0}\right)-p_x^b\frac{h^3}{8}\left(1-\frac{h\sin\varphi}{2R_0}\right)\\
r_s &= p_s^t\frac{h^3}{8}\left(1+\frac{h\sin\varphi}{2R_0}\right)-p_s^b\frac{h^3}{8}\left(1-\frac{h\sin\varphi}{2R_0}\right)
\end{aligned}
\qquad (43)
$$

where p_x^t, p_s^t, p_n^t are the meridional, circumferential and normal forces applied to the upper surface, and p_x^b, p_s^b, p_n^b are the meridional, circumferential and normal forces applied to the lower surface.

The boundary conditions considered in this study are the fully clamped edge boundary condition (C), the simply supported boundary condition (S) and the free edge boundary condition (F). They assume the following form:

Clamped edge boundary condition (C):

$$u_x = u_s = w = \beta_x = \beta_s = \eta_x = \eta_s = 0 \text{ at } x = 0 \text{ or } x = x_0, 0 \le s \le s_0, \qquad (44)$$

$$u_x = u_s = w = \beta_x = \beta_s = \eta_x = \eta_s = 0 \text{ at } s = 0 \text{ or } s = s_0, 0 \le x \le x_0, \qquad (45)$$

Supported edge boundary condition (S):

$$u_x = w = \beta_x = \eta_x = 0, N_x = M_x = P_x = 0 \text{ at } x = 0 \text{ or } x = x_0, 0 \le s \le s_0, \qquad (46)$$

$$u_s = w = \beta_s = \eta_s = 0, N_s = M_s = P_s = 0 \text{ at } s = 0 \text{ or } s = s_0, 0 \le x \le x_0, \qquad (47)$$

Free edge boundary condition (F):

$$N_x = N_{xs} = T_x = M_x = M_{xs} = P_x = P_{xs} = 0$$
$$\text{at } x = 0 \text{ or } x = x_{0,}\ 0 \le s \le s_0, \tag{48}$$
$$N_s = N_{sx} = T_s = M_s = M_{sx} = P_s = P_{sx} = 0$$
$$\text{at } s = 0 \text{ or } s = s_{0,}\ 0 \le x \le x_0, \tag{49}$$

In the above (44-49) boundary conditions, it has been assumed $s_0 = 2\pi R_0$. In order to analyze the whole shell of revolution, and not a panel, the kinematic and physical compatibility must be added to the previous external boundary conditions. Their analytical forms are proposed as follows:

Kinematic compatibility conditions along the closing meridian $(s = 0, 2\pi R_0)$:

$$\begin{aligned} &u_x(x,0) = u_x(x,s_0),\ u_s(x,0) = u_s(x,s_0),\\ &w(x,0) = w(x,s_0),\ \beta_x(x,0) = \beta_x(x,s_0),\\ &\beta_s(x,0) = \beta_s(x,s_0),\ \eta_x(x,0) = \eta_x(x,s_0),\\ &\eta_s(x,0) = \eta_s(x,s_0)\ 0 \le x \le x_0 \end{aligned} \tag{50}$$

Physical compatibility conditions along the closing meridian $(s = 0, 2\pi R_0)$:

$$\begin{aligned} &N_s(x,0) = N_s(x,s_0),\ N_{sx}(x,0) = N_{sx}(x,s_0),\\ &T_s(x,0) = T_s(x,s_0),\ M_s(x,0) = M_s(x,s_0),\\ &M_{sx}(x,0) = M_{sx}(x,s_0)\ , P_s(x,0) = P_s(x,s_0),\\ &P_{sx}(x,0) = P_{sx}(x,s_0),\ 0 \le x \le x_0 \end{aligned} \tag{51}$$

3.3 Discretized equations and stress recovery

The generalized differential quadrature method (GDQ) [66-90] is used to discretize the derivatives in the governing equations (42), as well as the external boundary conditions and the compatibility conditions. In this paper, the Chebyshev-Gauss-Lobatto grid distribution is adopted, where the coordinates of grid points along the reference surface are identified by the following relations:

$$x_i = \left(1-\cos\left(\frac{i-1}{N-1}\pi\right)\right)\frac{(x_1-x_0)}{2}+x_0 \qquad (52)$$
$$i=1,2,....,N,\quad for\ x\in[0,x_0]$$
$$s_j = \left(1-\cos\left(\frac{j-1}{M-1}\pi\right)\right)\frac{s_0}{2},$$
$$j=1,2,....,M,\quad for\ s\in[0,s_0]$$

where N, M are the total number of sampling points which discretize the domain in x and s directions, respectively. This particular choice of the C-G-L sampling points rule with respect to the others suggested in literature is justified by the tested efficiency of the GDQ technique.
By writing the fundamental equilibrium equations (42) by means of GDQ technique, the following matrix form is obtained:

$$\begin{bmatrix} \boldsymbol{K}_{bb} & \boldsymbol{K}_{bd} \\ \boldsymbol{K}_{db} & \boldsymbol{K}_{dd} \end{bmatrix}\begin{bmatrix} \boldsymbol{\delta}_b \\ \boldsymbol{\delta}_d \end{bmatrix} = \begin{bmatrix} \boldsymbol{p}_b \\ \boldsymbol{p}_d \end{bmatrix} \qquad (53)$$

In the present formulation the subscripts b and d stand for *boundary* and *domain*, respectively. The b-equations define the external boundary conditions and compatibility conditions written on the constrained edges of the conical shell, and the d-equations represent the scripture of the fundamental equations at the points which belong to the domain. The solution procedure by means of the GDQ technique is implemented with the support of a MATLAB code.
According to the Reddy's constrained theory, the transverse shear stresses satisfy a priori the zero shear condition on the upper and lower surfaces of the graded conical shell. As it is well known, and differently from the constrained theory by Reddy, the transverse shear stress determined from the 2D-Unconstrained Theory of first and third order does not satisfy the zero shear condition on the lateral surfaces of the open conical shell. A possible approach for solving this difficulty is to recovery the out of plane shear stress using 3D-equilibrium equations. Using the stationary principle of total potential energy, the 3D elastic equilibrium equations for a functionally graded conical shell are written as follows:

$$\frac{\partial \tau_{xn}^{'}}{\partial \zeta}+\tau_{xn}^{'}\left(\frac{\sin\varphi}{\zeta\sin\varphi+R_0}\right) = -\frac{\partial \sigma_x}{\partial x}-\frac{\cos\varphi}{\zeta\sin\varphi+R_0}(\sigma_x-\sigma_s)-\left(\frac{R_0}{\zeta\sin\varphi+R_0}\right)\frac{\partial \tau_{xs}}{\partial s} \qquad (54)$$

$$\frac{\partial \tau_{sn}^{'}}{\partial \zeta}+\tau_{sn}^{'}\left(\frac{2\sin\varphi}{\zeta\sin\varphi+R_0}\right) = -\frac{\partial \tau_{xs}}{\partial x}-\frac{2\cos\varphi}{\zeta\sin\varphi+R_0}\tau_{xs}-\frac{R_0}{\zeta\sin\varphi+R_0}\frac{\partial \sigma_s}{\partial s} \qquad (55)$$

$$\frac{\partial \sigma_n^{'}}{\partial \zeta}+\sigma_n^{'}\left(\frac{\sin\varphi}{\zeta\sin\varphi+R_0}\right)=-\frac{\partial \tau_{xn}^{'}}{\partial x}-\frac{\cos\varphi}{\zeta\sin\varphi+R_0}\tau_{xn}^{'}+\frac{\sin\varphi}{\zeta\sin\varphi+R_0}\sigma_s-\frac{R_0}{\zeta\sin\varphi+R_0}\frac{\partial \tau_{sn}^{'}}{\partial s} \tag{56}$$

By the knowledge of the membrane stresses ($\sigma_x,\sigma_s,\tau_{xs}$) and their derivatives in all the points of the 3D conical shell, the present equations (54-56) of the first order can be solved via the GDQ along the thickness direction. The C-G-L grid distribution is selected for the grid points ζ_m along the thickness direction:

$$\zeta_m=\left(1-\cos\left(\frac{m-1}{T-1}\pi\right)\right)\frac{h}{2}-\frac{h}{2},\ \ m=1,2..,T\ \ ,\ \ \zeta\in\left[-\frac{h}{2},-\frac{h}{2}\right] \tag{57}$$

By imposing the boundary conditions at the bottom surface of the shell, equations (54) and (55) are written via the GDQ method in the algebraic form and solved in terms of τ'_{xn},τ'_{sn}.

$$\begin{cases}\displaystyle\sum_{k=1}^{T}\zeta_{mk}^{\zeta(1)}\tau'_{xn(ijk)}+\tau'_{xn(ijm)}\frac{\sin\varphi_i}{R_{0i}+\zeta_m\sin\varphi_i}=-\left.\frac{\partial\sigma_x}{\partial x}\right|_{(ijm)}-\frac{\cos\varphi_i}{\zeta_m\sin\varphi_i+R_{0i}}\left(\sigma_{x(ijm)}-\sigma_{s(ijm)}\right)+\\ \displaystyle-\frac{R_{0i}}{\zeta_m\sin\varphi_i+R_{0i}}\left.\frac{\partial\tau_{xs}}{\partial s}\right|_{(ijm)}\quad m=2,3,...T\\ \tau'_{xn(ij1)}=p^{-}_{x(ij)}\end{cases} \tag{58}$$

$$\begin{cases}\displaystyle\sum_{k=1}^{T}\zeta_{mk}^{\zeta(1)}\tau'_{sn(ijk)}+\tau'_{sn(ijm)}\frac{2\sin\varphi_i}{\zeta_m\sin\varphi_i+R_{0i}}=-\left.\frac{\partial\tau_{xs}}{\partial x}\right|_{(ijm)}-\frac{2\cos\varphi_i}{R_{0i}+\zeta_m\sin\varphi_i}\tau_{xs(ijm)}+\\ \displaystyle-\frac{R_{0i}}{\zeta_m\sin\varphi_i+R_{0i}}\left.\frac{\partial\sigma_s}{\partial s}\right|_{(ijm)}\quad m=2,3...T\\ \tau'_{sn(ij1)}=p^{-}_{s(ij)}\end{cases}$$

(59)

The shear stress distributions τ'_{xn},τ'_{sn} carried out by the linear systems (58) and (59) do not satisfy the boundary condition at the top surface of shell structure. Consequently, the transverse shear stress representations are improved via the refinement suggested by Auricchio and Sacco [24] and Tornabene et al. [86], in the following manner:

$$\begin{aligned}\tau^{r}_{xn(ijm)}&=\tau'_{xn(ijm)}+\frac{p^{+}_{x(ij)}-\tau'_{xn(ijT)}}{h}\left(\zeta_m+\frac{h}{2}\right)\\ \tau^{r}_{sn(ijm)}&=\tau'_{sn(ijm)}+\frac{p^{+}_{s(ij)}-\tau'_{sn(ijT)}}{h}\left(\zeta_m+\frac{h}{2}\right)\quad m=1,2.....T\end{aligned} \tag{60}$$

Finally, the transverse normal stress σ_n' profiles are derived by solving the equation (56) via the GDQ method:

$$\begin{cases} \sum_{k=1}^{T} \zeta_{mk}^{\zeta(1)} \sigma'_{n(ijk)} + \sigma'_{n(ijm)} \dfrac{\sin\varphi_i}{R_{0i} + \zeta_m \sin\varphi_i} = -\left.\dfrac{\partial \tau_{xn}^r}{\partial x}\right|_{(ijm)} - \dfrac{\cos\varphi_i}{R_{0i} + \zeta_m \sin\varphi_i} \tau_{xn(ijm)}^r - \dfrac{R_{0i}}{R_{0i} + \zeta_m \sin\varphi_i} \left.\dfrac{\partial \tau_{sn}^r}{\partial s}\right|_{(ijm)} + \\ + \dfrac{\sin\varphi_i}{\zeta_m \sin\varphi_i + R_{0i}} \sigma_{s(ijm)} \quad m = 2,3,...T \\ \sigma'_{n(ij1)} = p_{n(ij)}^- \end{cases} \tag{61}$$

In order to satisfy the boundary condition at the top surface, the σ_n' distributions are also corrected as follows:

$$\sigma_{n(ijm)}^r = \sigma'_{n(ijm)} + \frac{p_{n(ij)}^+ - \sigma'_{n(ijT)}}{h} \left(\zeta_m + \frac{h}{2} \right) \quad m = 1,2....T \tag{62}$$

3.4 Stress profiles

In this numerical study, the static analysis of FGM open conical panels and shells is conducted and the through the thickness stress distributions are furnished. The theoretical formulations are based on two shear deformation models: the generalized unconstrained third (GUTSDT) and first order (GFSDT) shear deformation theories. They are labeled as generalized because they are enriched by the initial curvature effect. The stress recovery is also proposed in order to define the correct profile of the transverse shear and normal stress profiles, by the knowledge of the membrane stress components derived from the 2D shear deformation model. In this manner the shear effect is definitely improved. The numerical analysis is done by means of the GDQ numerical technique.

The basic constituents of FGM materials are taken to be Al_2O_3 (ceramic component) and aluminum (metal component). Young's modulus, Poisson's ratio for the Al_2O_3 are $E_c = 380GPa$, $\nu_c = 0.3$, and for the aluminum are $E_M = 70GPa$, $\nu_M = 0.3$. The ceramic volume fraction is varied by means of the four parameter power law distribution [64].

The main objectives of this numerical study are the followings:

1. to study the role of the four parameters of the power law function for various classes of graded materials;
2. to analyze the effect of geometric parameters (α, ϑ angles; R_0/h, $(L_0/\cos\alpha)/h$ aspect ratios) on the stress responces;
3. to compare the numerical results via the unconstrained third order model with those via the first order one;
4. to clarify the influence of the initial curvature effect in the numerical analysis, developed herein;
5. to compare the stress distributions of the open conical conical shell or panel with the ones for the cylindrical shell or panel;
6. to emphasize the key role of the stress recovery technique in determining the transverse normal and tangential stress components.

In order to characterize the effect of the volume fraction gradation as a function of the material coefficients, eight types of graded materials are investigated. In Fig.2*a* the distributions of the ceramic volume fraction V_C across the thickness for a wide range of p-values are presented for the $\mathrm{FGM1}_{(1,0,0,\mathrm{p})}$ class. It should be noticed that the lower surface $(\zeta/h = -0.5)$ of the composite structure is fully ceramic, and the top surface $(\zeta/h = 0.5)$ is purely metallic. For $0.1 \le \mathrm{p} \le 2$ (Fig.2*a*), the material composition is continuously graded throughout the thickness. Differently, for $\mathrm{p} = 5$ the ceramic volume fraction gradually changes only for $-0.5 \le \zeta/h \le 0.25$, and for the remaining

thickness it attains a null value. For $p = 8$, the ceramic volume fraction is continuously graded from the bottom surface to the middle layer, and for the rest it has a null value. For $p = 50,100$, the variation of the ceramic volume fraction is very restricted to the layers which are closer to the bottom one, and moving away the ceramic volume fraction becomes equal to zero. In Fig.2*b*, the distributions of the ceramic volume fraction are shown for the $FGM1_{(1,1,4,p)}$ class for several p-values [103]. All the $FGM1_{(1,1,4,p)}$ composite shells are fully ceramic at the top and bottom surfaces. For $p \le 1$ the ceramic volume fraction remains higher than 50%, whereas for $p = 2$ the ceramic volume fraction V_C has the analogous trend but it reaches values lower than 50%. For $0 \le \zeta / h \le 0.5$ and $p \le 1$, the ceramic volume fraction rapidly increases and it remains higher than 50%. For $p = 0.05$, the distribution of the ceramic volume fraction is quasi ceramic. For $p = 20,50$ the graded microstructure only belongs to the lower and upper layers of the $FGM1_{(1,1,4,p)}$ cylindrical shell, and reveals an homogeneous composition rich in the metal constituent inside the composite structure. In Fig.2*c*, the ceramic volume fraction of the $FGM1_{(1,0.5,2,p)}$ graded material is plotted versus the dimensionless shell thickness [103]. The bottom surface of the composite shell structure is fully ceramic for all the p- values. The top surface is made of a mixture of ceramic and metallic constituents for $p = 0.6,2,5$, with increasing metallic content with respect to the ceramic one, respectively. For $p = 10,20,50$ the ceramic volume fraction is continuously graded from the bottom surface till ζ / h variable, respectively, equal to 0.25, -0.25, -0.375. Consequently, the resulting composite material for $p = 50$ is prevalently metallic. In Fig.2*d*, the distributions of the ceramic volume fraction across thickness for several a-values are presented for the $FGM1_{(a,0.2,3,2)}$ class [103]. It appears that the bottom surface of the composite structure is purely ceramic, and the top surface changes its composition with the variation of the a-parameter. For $a = 0.2$ the top surface of the $FGM1_{(a,0.2,3,2)}$ cylindrical shell is also ceramic. By varying the a-parameter from 0.3 to 1, the top surface becomes a mixture of ceramic and metallic constituents. In particular, with the increase of a, the top surface becomes richer and richer of the metallic component. In Fig.3*a*, the distributions of the ceramic volume fraction across the thickness for several a-values are presented for the $FGM2_{(a,0.2,3,2)}$ class. In contrast with the previous case, it appears that the top surface of the composite structure is purely ceramic, and the bottom surface changes its composition with the variation of the a-parameter. For $a = 0.2$ the bottom surface of the $FGM2_{(a,0.2,3,2)}$ cylindrical shell is also ceramic. By varying the a-parameter from 0.3 to 1, the bottom surface is made from a mixture of ceramic and metallic constituents. In particular, with the increase of a, the bottom surface

becomes richer and richer of the metallic component. For all the a-values, the ceramic volume fraction is continuously graded throughout the shell thickness. In Fig.3*b*, the distributions of the ceramic volume fraction across the thickness for several a-values are presented for the $FGM2_{(0,b,2,1)}$ class [103]. It appears that the top surface of the composite structure is purely ceramic, and the bottom surface changes its composition with the variation of the b-parameter. By varying the b-parameter from -0.2 to -0.9, the bottom surface is made from a mixture of ceramic and metallic constituents. In particular, with the decrease of b, the bottom surface becomes richer and richer of the metallic component. For $b=-1$ the bottom surface is purely metallic. From Figs. 3a,b it appears that for all the a and b values, the ceramic volume fraction is continuously graded throughout the shell thickness. In Fig.3*c*, the ceramic volume fraction of the $FGM1_{(1,0.5,c,2)}$ curves versus the shell thickness is presented. It is noted that the top surface is compositionally made of the 25% in the ceramic constituent, and the 75% in the metallic one, for all the c-values. Differently, the bottom layer is fully ceramic. In Fig.3*d* the ceramic volume fraction profiles of the $FGM1_{(1,1,c,1)}$ are also proposed [103]. For all the c-values the ceramic volume fraction follows a parabolic pattern. The external surfaces are ceramic rich. With decreasing values of the c – parameter the ceramic volume fraction attains maximum values at layers nearer to the middle one.

3.4.1 The reference configuration

The sample configuration for the open conical panel and shell in terms of geometric parameters, boundary and loadings condition are assumed as follows. The thickness h is fixed at 0.1m, the parallel radius R_b and the conical length L_0 are both equal to 1m. The α-angle is equal to 11.25°, and the ϑ-angle for the panel is assumed equal to 120°. For the truncated conical panel, the boundary condition considers clamped all the edges (west, north, east, south). With reference to the conical shell the north and south edges are clamped, whereas the west and east edges shared the compatibility condition. Both the conical panel and shell are subjected to the uniform p_n pressure, fixed at -0.1MPa on the top surface of the graded panel or shell. The normal and shear stresses are calculated at the point $(0.25L_0; 0.25s_0)$ along the ζ- direction, being $s_0 = 2\pi R_0$. All the stress components are furnished by using the scaled form as follows:

$$\bar{g} = \alpha g\left(0.25L_0, 0.25s_0, \zeta\right)$$
$$g^* = \alpha g\left(0.25L_0, 0.25s_0, \zeta\right) \tag{63}$$

where $\bar{g}$ or g^* represent the scaled stress component, g is the stress component calculated at a fixed point and α the scale factor used for the representation and reported in caption.

3.4.1.1 The influence of the initial curvature effect with the semi vertex angle

The $FGM1_{(1,0,0,p)}$ conical panels and shells are firstly considered. The ceramic volume fraction is continuously graded from the top metallic layer to the bottom ceramic one. The reference configuration is considered. By varying the α-angle, the initial curvature is investigated on the tangential $\tau_{xn}^*, \tau_{sn}^*, \bar{\tau}_{xs}$ and normal $\bar{\sigma}_x, \bar{\sigma}_s, \sigma_n^*$ stress profiles of the $FGM1_{(1,0,0,0.5)}$ conical panel under top normal pressure $p_n = -0.1$ MPa, as shown in Figs.4a-f. The stress distributions $\tau_{xn}^*, \bar{\sigma}_x, \bar{\sigma}_s, \sigma_n^*$ are also proposed for the $FGM1_{(1,0,0,0.5)}$ conical shell under top normal and meridional constant loadings $p_n = p_x = -0.1$ MPa, as shown in Figs.5a-d. The GUTSDT and UTSDT are applied with the normal and shear stress recovery. It should be noticed that by fixing $\alpha = 0°$ the panel or shell under study becomes the cylindrical one.

Generally, by varying the α - semi vertex angle its own influence appears significant in all the stress distributions along the dimensionless thickness direction, except for the transverse normal ones which seem to be juxtaposed. The shear and circumferential stresses $\tau_{sn}^*, \bar{\sigma}_s$ in Figs.4b,e and the meridional and circumferential stresses $\bar{\sigma}_x, \bar{\sigma}_s$ in Figs.5b,c are influenced by the initial curvature effect, with particular reference to layers near to the middle one for the τ_{sn}^* - stress in Fig.4b, and layers near to the extreme surfaces for the $\bar{\sigma}_x$ - stress in Fig.5b and the $\bar{\sigma}_s$ -stress in Fig.4e,5c.

The $FGM2_{(0,b,2,1)}$ conical panels and shells are secondly considered. The ceramic volume fraction is continuously graded from the top ceramic layer to the bottom metallic one. The geometrical, boundary and loading conditions are unvaried with respect to the previous numerical examples for both the panel and the shell. The throughout the thickness tangential $\tau_{xn}^*, \tau_{sn}^*, \bar{\tau}_{xs}$ and normal $\bar{\sigma}_x, \bar{\sigma}_s, \sigma_n^*$ stress profiles of the $FGM2_{(0,-1,2,1)}$ conical panel and the stress distributions $\tau_{xn}^*, \bar{\sigma}_x, \bar{\sigma}_s, \sigma_n^*$ for the $FGM2_{(0,-1,2,1)}$ conical shell are shown, respectively in Figs.6a-f and Figs.7a-d. Analogous considerations could be done as in the previous case.

3.4.1.2 The influence of the initial curvature effect with the *p* - power exponent

The initial curvature effect is studied by considering the normal and shear stress response along the thickness direction of the $FGM1_{(1,0,0,p)}$ conical shells and panels for three values of the *p* - power exponent. The reference configuration is selected for the numerical analyses and the α - semi - vertex angle is fixed at 30°. The GUTSDT and UTSDT are applied with the normal and shear stress recovery. In Figs.8a-f the tangential $\tau_{xn}^{*}, \tau_{sn}^{*}, \bar{\tau}_{xs}$ and normal $\bar{\sigma}_x, \bar{\sigma}_s, \sigma_n^{*}$ stress profiles are proposed for the $FGM1_{(1,0,0,p)}$ conical panels, whereas in Figs.9a-d the tangential τ_{xn}^{*} and normal $\bar{\sigma}_x, \bar{\sigma}_s, \sigma_n^{*}$ stress distributions are suggested for the graded conical shells under investigation. It is noticed that by varying the *p*-power exponent the initial curvature effect could be appreciable on the τ_{sn}^{*} - shear stress profiles in Fig.8b and the $\bar{\sigma}_s$ - normal stress profiles in Fig.8e and in Fig.9c. Slight variations could be recognizable by examining the $\bar{\sigma}_x$ - normal stress response in Fig.8d for the panel and the $\bar{\sigma}_x$ normal ones in Fig.9b for the shell.

3.4.1.2.1 Comparisons between the first and third order stress responses with the initial curvature effect and the *p*-power exponent

The $FGM1_{(1,0,0,p)}$ conical panels are considered for $p = 0.5, 2$. The reference configuration is adopted and the shear constant load $p_s = -0.1$ MPa is applied on the top layer in addition to the normal one $p_n = -0.1$ MPa. The α - semi vertex angle is fixed at 30°. The first order and third order shear deformation theory are applied with the normal and shear stress recovery.

It appears that the shear $\tau_{xn}^{*}, \tau_{sn}^{*}, \bar{\tau}_{xs}$ - stress distributions in Figs.10a-c and the normal $\bar{\sigma}_x, \bar{\sigma}_s, \sigma_n^{*}$ stress ones in Figs.10d-f of the first and third order are strictly coincident.

3.4.1.3 The influence of the initial curvature effect with the *a* – material coefficient

The $FGM2_{(a,0.2,2,1)}$ conical panels and shells are investigated for $a = 0.2, 0.4, 0.6$. The top layer is completely ceramic. With the ceramic volume fraction variation throughout the thickness by increasing the *a* – material coefficient, the bottom layer passes from fully ceramic to partially ceramic and prevalently metallic microstructure. The reference configuration is chosen and the top $p_n = p_x = -0.1MPa$ uniform loadings are involved. The GUTSDT is applied with the normal and shear stress recovery. The tangential $\tau_{xn}^{*}, \tau_{sn}^{*}, \bar{\tau}_{xs}$ and normal $\bar{\sigma}_x, \bar{\sigma}_s, \sigma_n^{*}$ stress profiles of the graded panels are plotted along the thickness direction in Figs.11a-f,

whereas the shear τ_{xn}^{*} and normal $\overline{\sigma}_x, \overline{\sigma}_s, \sigma_n^{*}$ stress distributions of the graded shells are shown in Figs.12a-d. Both the effect of the a - material coefficient and the initial curvature are emphasized by the $\overline{\sigma}_s$ -stress distributions suggested in Fig.11e for the panel and in Fig.12c for the shell. In the other shear and normal stress responses furnished in the figures mentioned above, by varying the a - material coefficient the stress profiles appear less divergent and the influence of the initial curvature effect is more limited.

3.4.1.3.1 Comparisons between the first and third order stress responses with the initial curvature effect and the *a*-material coefficient

The $FGM2_{(a,0.2,2,1)}$ conical panels are investigated for $a = 0.8,1.$ The reference configuration is considered with the α -semi vertex angle fixed at 30° and the ϑ -angle at 180°. The top meridional and circumferential $p_x = p_s = -0.1MPa$ uniform loadings are applied. The GFSDT and the GUTSDT are used with the normal and shear stress recovery. The tangential $\tau_{xn}^{*}, \tau_{sn}^{*}, \overline{\tau}_{xs}$ and normal $\overline{\sigma}_x, \overline{\sigma}_s, \sigma_n^{*}$ stress profiles are shown in Figs.13a-f. It is noticed that the $\overline{\sigma}_x$ - stress curves in Fig.13d show relevant deviations between the GFSDT (or FSDT) and GUTSDT (or UTSDT) responses, in correspondence to layers near to the extreme surfaces. Whereas the $\overline{\sigma}_s, \sigma_n^{*}$ ones in Figs.13e,f exhibit the analogous divergence only nearer the top surface of the graded panels.

3.4.1.4 Comparisons between the first and third order stress responses with the initial curvature effect and the *b*-material coefficient

The $FGM2_{(0,b,2,1)}$ conical panels are analyzed for $b = -0.2, -1$. The ceramic volume fraction which are under examination create two different kind of composite structures , the former graded panel is characterized by a fully ceramic top layer and a prevalently ceramic and partially metallic bottom one. The latter graded panel is completely ceramic at the top and metallic at the bottom layer. The reference configuration is selected and the α -semi vertex angle is fixed at 22.5°. The top meridional and circumferential $p_x = p_s = -0.1MPa$ uniform loadings and the bottom normal $p_n = -0.1MPa$ constant pressure are applied. The GFSDT and the GUTSDT are used with the normal and shear stress recovery. The tangential $\tau_{xn}^{*}, \tau_{sn}^{*}, \overline{\tau}_{xs}$ and normal $\overline{\sigma}_x, \overline{\sigma}_s, \sigma_n^{*}$ stress distributions are plotted along the thickness direction in Figs.14a-f. The influence of the degree of the shear deformation theory remains limited in all the stress profiles. The initial curvature effect is

enhanced by considering the $\overline{\sigma}_s$ - stress curves in Fig.14e. In all the stress distributions, the effect of the *b*-material coefficient appears considerable with its own variation at the two levels under study.

3.4.1.5 The influence of the L/h aspect ratio with the α - angle

The $FGM1_{(1,0,0,p)}$ conical panels are investigated for $p=1.$ The ceramic volume fraction undergoes a linear pattern from the top metallic to the bottom ceramic layer. The geometrical parameters are chosen as follows: $\alpha=11.25°,22.5°$; $\vartheta=120°$; $R_b=1m$; $h=0.1m$. The L/h - aspect ratio is considered at three levels: 10,20,40. The tangential $\tau_{xn}^*,\tau_{sn}^*,\overline{\tau}_{xs}$ and normal $\overline{\sigma}_x,\overline{\sigma}_s,\sigma_n^*$ throughout the thickness stress distributions are shown in Figs.15a-f. The top normal constant pressure $p_n=-0.1$ MPa is applied. The GUTSDT is used with the normal and shear stress recovery. It is observed that the divergence between the stress curves in Fig.15a-e exists both when the α -angle is taken constant and the L/h - aspect ratio is varied and also in the opposite case. The σ_n^* - transverse stress profiles in Fig.15f show more limited deviations with the change of the α -angle or the L/h - aspect ratio.

3.4.1.5.1 The influence of the L/h aspect ratio with the ϑ - angle

The $FGM1_{(1,1,4,p)}$ conical panels are investigated for $p=2.$ Both the top and bottom layers are ceramic and the ceramic volume fraction undergoes a parabolic variation along the thickness direction. The geometrical parameters are fixed as follows: $R_b=1m$; $h=0.1m$; $\alpha=30°$; $\vartheta=90°,180°$. The L/h - aspect ratio is considered at three levels: 10,20,40. The tangential $\tau_{xn}^*,\tau_{sn}^*,\overline{\tau}_{xs}$ and normal $\overline{\sigma}_x,\overline{\sigma}_s,\sigma_n^*$ throughout the thickness stress distributions are shown in Figs.16a-f. The top normal constant pressure $p_n=-0.1$ MPa is applied. The GUTSDT is used with the normal and shear stress recovery. Analogous consideration could be formulated as in the previous case.

3.4.1.6 Comparisons between the first and third order recovered and un-recovered transverse stress distributions

The $FGM1_{(a,0.2,3,2)}$ conical panels are investigated for $a=0.5.$ The ceramic volume fraction passes from the 50%wt at the top layer to the full ceramic microstructure at the bottom one. The reference configuration is under consideration with the α - angle equal to 30°. The first and third order responses are compared as carried out from the 2D-shear deformation theory with the responses achieved by the shear stress recovery. Various loading conditions are taken under consideration. The un - recovered $\overline{\tau}_{xn},\overline{\tau}_{sn}$ and recovered τ_{xn}^*,τ_{sn}^* shear stress distributions are suggested for the

$FGM1_{(0.5,0.2,3,2)}$ conical panels under meridional and circumferential top uniform loadings $p_x = p_s = -0.1$MPa in Fig.17a,b,c,d and also under bottom normal pressure $p_n = -0.1$ MPa in Fig.17b,d. It is noticed that the recovered shear stress pattern satisfies the boundary condition by considering every shear or normal constant loadings at the extreme surfaces.

3.4.1.7 The influence of boundary conditions

3.4.1.7.1 The influence of the α -angle with the initial curvature effect

The $FGM1_{(1,1,c,1)}$ conical panels are investigated for $c = 5$. By following a parabolic pattern the ceramic volume fraction decreases away from the external layers which are entirely ceramic. The minimum value which it assumes is higher than 50%wt. The geometrical parameters are chosen as follows: $\alpha = 0°, 22.5°, 90°$; $\vartheta = 120°$; $R_b = 1m$; $h = 0.1m$. The normal uniform pressure $p_n = -0.1$ MPa is considered on the top external surface of the composite structure. The north-south-west-east edges of the graded structure are simply supported. The GUTSDT is used with the normal and shear stress recovery. The tangential $\tau^*_{xn}, \tau^*_{sn}, \bar{\tau}_{xs}$ and normal $\bar{\sigma}_x, \bar{\sigma}_s, \sigma^*_n$ throughout the thickness stress distributions are shown in Figs.18a-f. With the α - angle at 0° and 22.5° the deviation between the stress profiles by considering or not the initial curvature effect can be more appreciated in Fig.18e. The stress profiles for $\alpha = 90°$ are referred to a circular sector plate and exhibit strong differences with respect to the others.

3.4.1.7.2 Comparisons between the first and third order stress responses with the α -angle variation and the initial curvature effect

The $FGM1_{(1,0.5,2,p)}$ conical panels are investigated for $p = 2$. The ceramic volume fraction is varied with decreasing its value from the 100%wt at the lower surface to the 25% at the top one. The geometrical parameters are chosen as follows: $\alpha = 0°, 22.5°, 90°$; $\vartheta = 120°$; $R_b = 1m$; $h = 0.1m$. The meridional, circumferential and normal uniform loadings $p_x = p_s = p_n = -0.1$ MPa are applied on the top external surface of the composite structure. The north edge is clamped and all the others are free. The GUTSDT and GFSDT are used with the normal and shear stress recovery. The tangential $\tau^*_{xn}, \tau^*_{sn}, \bar{\tau}_{xs}$ and normal $\bar{\sigma}_x, \bar{\sigma}_s, \sigma^*_n$ throughout the thickness stress distributions are shown in Figs.19a-f. By fixing the α - angle, the third and first order stress responses show small deviation by considering both the stress curves derived from the generalized first and third order shear deformation theories and the un-generalized ones.

3.5 Comparison study

Aghdam et al. [37] conducted the static analysis of functionally graded conical panels under uniform distributed transverse pressure. They used the first order shear deformation theory and added the contribution of the initial curvature to the basic formulation of the first order. In the present paragraph, the results reported in the numerical work of Aghdam [37] are used for comparison. The graded material consists of the ceramic part ($E_{c_1} = 380GPa$ or $E_{c_2} = 151GPa$, $v = 0.3$) and the metallic one ($E_m = 70GPa$, $v = 0.3$). Various L/h ratios form moderately thick ($L/h = 10$) to thin ($L/h = 40$) $FGM2_{(1,0,0,2)}$ conical panels are considered. Panels are subjected to the uniform loading with geometric parameters: $L = R$, $\theta = 45°$. Tables 1 and 2 demonstrate variations of the normalized central deflection for conical panels with different semi vertex angle α. Numerical results show very good agreement.

3.6 Conclusion

The generalized third order shear deformation theory with the normal and shear stress recovery is extended to various types of functionally graded truncated conical panels and shells. By means of the GDQ method the shear $\tau_{xn}^*, \tau_{sn}^*, \bar{\tau}_{xs}$ and normal $\bar{\sigma}_x, \bar{\sigma}_s, \sigma_n^*$ stress distributions are accurately determined along the thickness direction. By considering the present formulation it is possible to apply uniform loading of various nature with the satisfaction of the boundary conditions in all the loading cases. It is shown how the mechanical response for graded open conical panels or shells changes with the variation of model (GUTSDT, UTSDT, GFSDT, FSDT), the α- angle, the ϑ-angle, the aspect ratios (L/h, R/h), the boundary conditions. It should be noticed that the procedure introduced in this paper can also be extended to other types of graded panels or shells.

References.

[1] Reissner E. **The effect of transverse shear deformation on the bending of elastic plates**. J. Appl Mech 1945; 12: A69-A77.

[2] Reissner E. **Small bending and stretching of sandwich type shells**. NACA-TN 1832, 1949.

[3] Mindlin RD. **Influence of rotary inertia and shear in flexural motion of isotropic elastic plates**. ASME J Appl Mech 1951; 18: 31-38.

[4] Whitney JM. **Shear correction factors for orthotropic laminates under static loads**. J Appl Mech 1973; 40: 302-304.

[5] Whitney JM. **The effect of transverse shear deformation in the bending of laminated plates**. J Compos Mater1969; 3:534-547.

[6] Whitney JM., Pagano NJ. **Shear deformation in heterogeneous anisotropic plates**. J Appl Mech 1970; 37: 1031-1036.

[7] Reissner E. **A consistent treatment of transverse shear deformations in laminated anisotropic plates**. AIAA J 1972; 10: 716-718.

[8] Schmidt R. **A refined nonlinear theory of plates with transverse shear deformation**. J Math Soc 1977; 27: 23-38.

[9] Lo KH., Christensen RM., Wu EM. **A higher order theory of plate deformation - part 1: homogeneous plates**. J Appl Mech, Trans ASME 1977; 44(4): 663-668.

[10] Lo KH., Christensen RM., Wu EM. **A High Order Theory of Plate Deformation - part 2: laminated plates**. J Appl Mech, Trans ASME 1977; 44(4): 669-676.

[11] Murthy MVV. **An improved transverse shear deformation theory for laminated anisotropic plates**. NASA Technical paper 1903 1981; 1-37.

[12] Levinson M. **An accurate simple theory for the static and dynamics of elastic plates**. J Appl Mech 1984; 51: 745-752.

[13] Kant T. **Numerical analysis of thick plates**. Comput Methods Appl Mech Eng. 1982; 31:1-18.

[14] Reddy JN. **A refined nonlinear theory of plates with transverse shear deformation**. Int J Solids Struct 1984; 20: 881-896.

[15] Reddy JN. **A simple higher order theory for laminated composite plates**. J Appl Mech 1984; 51: 745-752

[16] Reddy JN., Liew CF. **A higher order shear deformation theory of laminated elastic shells**. Int J Eng Sci 1985; 23: 319-330.

[17] Reddy JN. **A generalization of two dimensional theories of laminated composite plates**. Commun Appl Numer Methods 1987; 3: 173-180.

[18] Di Sciuva M. **An improved shear deformation theory for moderately thick multilayered anisotropic shells and plates**. J Appl Mech 1987; 54: 589-596.

[19] Di Sciuva M. **Bending, vibration and buckling of simply supported thick multilayered orthotropic plates: an evaluation of a new displacement field**. J Sound Vib 1986; 105: 425-442.

[20] Reddy JN., Kim J. **A nonlinear modified couple stress - based third - order theory of functionally graded plates**. Compos Struct 2012; 94: 1128-1143.

[21] Bisegna P., Sacco E. **A rational deduction of plate theories from the three dimensional linear elasticity**. Math Mech 1997; 77(5): 349-366.

[22] Bisegna P., Sacco E. **A layer wise laminate theory rationally deduced from the three dimensional elasticity.** Trans ASME 1997; 64: 538-544.

[23] Bischoff M., Ramm E. **On the physical significance of higher order kinematic and static variables in a three dimensional shell formulation**. Int J Solids Struct 2000; 37: 6933-6960.

[24] Auricchio F., Sacco E. **Refined First Order Shear Deformation Theory Models for Composites Laminates**. J Appl Mech 2003; 70: 381-390.

[25] Carrera E. **Developments, ideas and evaluations based upon Reissner's mixed variational theorem in the modelling of multilayered plates and shells**. Appl Mech Rev 2001; 54:301-329.

[26] Carrera E. **A study of transverse normal stress effect on vibration of multilayered plates and shells**. J Sound Vib 1999; 255(5): 803-829.

[27] Kulikov GM., Plotnikova SV. **Simple and effective elements based upon Timoshenko – Mindlin shell theory**. Comput Methods Appl Mech Eng 2002; 191: 1173-1187.

[28] Carrera E., Brischetto S. **Analysis of thickness locking in classical, refined and mixed theories for layered shells"**. Compos Struct 2008; 85:83-90.

[29] Matsunga H. **Free vibration and stability of functionally grade shallow shells according to a 2D higher order deformation theory**. Compos Struct 2008; 84: 132-146.

[30] Cinefra M., Belouettar S., Soave M., Carrera E. **Variable kinematic models applied to free-vibration analysis of functionally graded material shells**. European J Mech A/Solids 2010; 29: 1078-1087.

[31] Carrera E., Brischetto S., Cinefra M., Soave M. **Effects of thickness stretching in functionally graded plates and shells.** Compos B Eng 2011; 42: 123-133.

[32] Zenkour AM. **Generalized shear deformation theory for bending analysis of functionally graded plates**. Appl Math Modell 2006; 30: 67-84.

[33] Kashtalyan M., Menshykova M. **Three dimensional analysis of a functionally graded coating / substrate system of finite thickness**. Phil Trans R Soc A 2008; 366: 1821-1826.

[34] Koiter WT. **A consistent first approximation in the general theory of thin elastic shells**. In: Proceedings of first symposium on the theory of thin elastic shells, North-Holland, Amsterdam; 1959.

[35] Liew KM., Zhao X., Ferreira AJM. **A review of meshless methods for laminated and functionally graded plates and shells**. Compos Struct 2011; 93: 2031-2041.

[36] Asemi K., Salesi M., Akhlaghi M. **Elastic solution of a two dimensional functionally graded thick truncated cone with finite length under hydrostatic combined loads**. Acta Mech 2011; 217: 119-134.

[37] Aghdam MM., Shahmansouri N., Bigdeli K. **Bending analysis of moderately thick functionally graded conical panels**. Compos Struct 2011; 93: 1376-1384.

[38] Khatri KN., Asnani NT. **Vibration and damping analysis of multilayered conical shells**. Compos Struct 1995; 33(3): 143-157.

[39] Lam KY., LI H., Ng TY., Chua CF. **Generalized differential quadrature method for the free vibration of truncated conical panels**. J Sound Vib 2002; 251(2): 329-334.

[40] Liew KM., Ng TY., Zhao X. **Free vibration analysis of conical shells via the element-free k_p-Ritz method**. J Sound Vib 2005; 281:627-645.

[41] Li FM., Kishimoto K., Huang WH. **The calculations of natural frequencies and forced vibration responses of conical shell using the Rayleigh-Ritz method**. Mech Res Comm 2009; 36(5): 595-602

[42] Sofiyev AH. **The vibration and stability behaviour of freely supported FGM conical shells subjected to external pressure**. Compos Struct 2009; 89:356-366.

[43] Tornabene F., Viola E., Inman DJ., **2-D differential quadrature solution for vibration analysis of functionally graded conical, cylindrical shell and annular plate structures**. J Sound Vib 2009; 328: 259-290.

[44] Tornabene F., Viola E. **Free vibration analysis of functionally graded panels and shells of revolution**. Meccanica 2009; 44: 255-281.

[45] Cinefra M., Belouettar S., Soave M., Carrera E. **Variable kinematic models applied to free-vibration analysis of functionally graded material shells**. European J Mech A/Solids 2010; 29: 1078-1087.

[46] Zhao X., Liew KM. **Free vibration analysis of functionally graded conical shell panels by a meshless method**. Compos Struct 2011, 93: 649-664.

[47] Tornabene F., Liverani A., Caligiana G. **FGM and laminated doubly curved shells and panels of revoltion with a free-form meridian: A 2-D GDQ solution for free vibrations**. Int J Mech Sci 2011; 53: 446-470.

[48] Seide P. **Axisymmetric buckling of circular cones under axial compression**. J Appl Mech 1956; 23: 625-628.

[49] Mushtari KM., Sachenov AV. **Stability of cylindrical and conical shells of circular cross section with simultaneous action of axial compression and external normal pressure.** Nasa 1958; TM-1433.

[50] Singer J. **Bucking of circular conical shells under axisymmetrical external pressure**. J Mech Eng Sci 1961; 3:330-339.

[51] Seide P. **Calculations for the stability of thin conical frustums subjected to external uniform hydrostatic pressure and axial load**. J Aero Sci Tech 1962; 29(8): 951-955.

[52] Singer J. **Donnell – type equations for bending and buckling of orthotropic conical shells**. J Appl Mech 1963; 30: 303-305.

[53] Serpico JC., **Elastic stability of orthotropic conical and cylindrical shells subjected to axisymmetric loading conditions**. AIAA J 1963; 1: 128-137.

[54] Lu SY., Chang LK. **Non linear thermal buckling of conical shells**. Int J Mech Sci 1967; 34: 93-111.

[55] Baruch M., Harari O., Singer J. **Influence of in plane boundary conditions on the stability of conical shells under hydrostatic pressure**. Isr J Tech 1967; 5 (1-2):12-24.

[56] Bushnell D., Smith S. **Stress and buckling of non uniformly heated cylindrical and conical shells**. AIAA J 1971; 9: 2314-2321.

[57] Wu CP., Chiu SJ. **Thermally induced dynamic instability of laminated composite conical shells.** Int J Solids Struct 2002; 39: 3001-3021.

[58] Dulmir PC., Dube GP., Mullick A. **Axisymmetric static and dynamic buckling of laminated thick truncated conical cap**. Int J Non-Linear Mech 2003; 37: 903-910.

[59] Bhangale RK., Ganesan N., Padmanabhan C. **Linear thermoelastic buckling and free vibration behaviour of functionally graded truncated conical shells**. J Sound Vib 2006; 292(1-2): 341-371.

[60] Sofiyev AH., **Thermo-elastic stability of functionally graded truncated conical shells**. Compos Struct 2007; 77:56-65.

[61] Naj R., Sabzikar Boroujerdy M., Eslami MR. **Thermal and mechanical instability of functionally graded truncated conical shells**. Thin Wall Struct 2008; 46(1): 65-78.

[62] Sofiyev AH., **The buckling of FGM truncated conical shells subjected to combined axial tension and hydrostatic pressure**. Compos Struct 2010; 92(2): 488-498.

[63] Sofiyev AH., **Influence of the initial imperfection on the non linear buckling response of FGM truncated conical shells**. Compos Struct 2010; 92(2): 488-498.

[64] Viola E., Rossetti L., Fantuzzi N. **Numerical investigations of functionally graded cylindrical shells and panels using the generalized unconstrained third order theory coupled with the stress recovery**. Compos Struct 2012; 94: 3736-3758.

[65] Leung AYT. **An Unconstrained third order plate theory**. Comp Struct 1991; 40(4): 871-875.

[66] Bellman R., Casti J. **Differntial quadrature and long term integration**. J Math Analysis Applications. 1971; 34: 234-238.

[67] Bellman R., Kashef BG., Casti J. **Differential quadrature: a technique for the rapid solution of non linear partial differential equations**. J Comput Phys 1972; 10(1): 40-52.

[68] Civan F., Sliepcevich CM. **Differential quadrature for multi – dimensional problems**. J Math Analysis Applications 1984; 101(2): 423-443.

[69] Shu C. **Generalized differential – integral quadrature and application to the simulation of incompressible viscous flows including parallel computation**. University of Glasgow, Ph.D. Thesis, 1991.

[70] Shu C. **Differential and its application in engineering**. Berlin, Springer 2000.

[71] Bert CW., Malik M. **Differential quadrature method in computational mechanics: a review**. Appl Mech Rev 1996; 49(1):1-27.

[72] Artioli E. Gould PL., Viola E. **A differential quadrature method solution for shear - deformable shells of revolution**. Eng Struct 2005; 27: 1879-1892.

[73] Viola E., Tornabene F. **Vibration analysis of damaged circular arches with varying cross - section.** Structural Integrity & Durability (SID-SDHM) 2005; 1: 155-169.

[74] Viola E., Tornabene F. **Vibration analysis of conical shell structures using GDQ method**. Far East J Appl Math 2006; 25: 23-39.

[75] Tornabene F., Viola E. **Vibration analysis of spherical structural elements using the GDQ method**. Computers & Mathematics with Applications 2007; 53: 1538-1560.

[76] Viola E., Dilena M., Tornabene F. **Analytical and numerical results for vibration analysis of multi-stepped and multi-damaged circular arches**. J Sound Vib 2007; 299: 143-163.

[77] Marzani A., Tornabene F., Viola E. **Nonconservative stability problems via generalized differential quadrature method**. J Sound Vib 2008; 315: 176-196.

[78] Tornabene F., Viola E. **2-D solution for the vibration of parabolic shells using generalized differential quadrature method**. European J Mech - A/Solids 2008; 27:1001-1025.

[79] Tornabene F. **Vibration analysis of functionally graded conical, cylindrical and annular shell structures with a four-parameter power -law function**. Comput Methods Appl Mech Eng 2009; 198: 2911-2935.

[80] Tornabene F., Viola E. **Free vibrations of four-parameter functionally graded parabolic panels and shells of revolution**. European J Mech - A/Solids 2009; 28: 991-1013.

[81] Viola E., Tornabene F. **Free vibrations of three parameter functionally graded parabolic panels of revolution**. Mech Res Comm 2009; 36: 587-594.

[82] Tornabene F., Marzani A., Viola E., Elishakoff I. **Critical flow speeds of pipes conveying fluid by the generalized differential quadrature method**. Advances in Theoretical and Applied Mechanics 2010; 3: 121-138.

[83] Tornabene F. **2-D GDQ solution for free vibration of anisotropic doubly-curved shells and panels of revolution**. Compos Struct 2011; 93: 1854-1876.

[84] Tornabene F. **Free vibrations of anisotropic doubly-curved shells and panels of revolution with a free-form meridian resting on Winkler - Pasternak elastic foundations**. Compos Struct 2011; 94: 186-206.

[85] Tornabene F., Liverani A., Caligiana G. **General anisotropic doubly curved shell theory: a differential quadrature solution for free vibrations of shells and panels of revolution with a free-form meridian**. J Sound Vib 2012; 331: 4848-4869.

[86] Tornabene F., Liverani A., Caligiana G. **Laminated composite rectangular and annular plates: A GDQ solution for static analysis with a posteriori shear and normal stress recovery**. Compos Part B Eng 2012; 43(4): 1847-1872.

[87] Viola E., Tornabene F., Fantuzzi N. **General higher order shear deformation theories for the vibration analysis of completely double-curved laminated shells and panels**. Compos Struct 2013; 95(1): 639-666

[88] Tornabene F., Viola E. **Static analysis of functionally graded doubly-curved shells and panels of revolution**. Meccanica 2012; DOI:10.1007/s11012-012-9643-1

[89] Ferreira AJM., Roque C.M.C., Jorge R.M.N. **Analysis of composite plates by trigonometric shear deformation theory and multiquadrics**. Comput Struct 2005; 83: 2225-2237.

[90] Ferreira AJM., Roque C.M.C., Martins P.A.L.S. **Analysis of composite plates using higher order shear deformation theory and a finite point formulation based on the multiquadric radial basis function method**. Compos Part B 2003; 34: 627-636.

[91] Ferreira AJM., Castro L.M.S., Bertoluzza S. **A high order collocation method for the static and vibration analysis of composite plates using a first order theory**. Compos Struct 2009; 89: 424-432.

[92] Ferreira AJM., Carrera E., Cinefra M., Roque C.M.C., Polit O. **Analysis of laminated shells by a sinusoidal shear deformation theory and radial basis functions collocation, accounting for through-the-thickness deformations**. Compos Part B-Eng 2011; 42: 1276-1284.

[93] Daghia F., De Miranda S., Ubertini F., Viola E. **A hybrid stress approach for laminated composite plates within the first order shear deformation theory**. Int J Solids Struct 2008; 45: 1766-1787.

[94] De Miranda S., Patruno L., Ubertini F. **Transverse stress profiles reconstruction for finite element analysis of laminated plates**. Compos Struct 2012; 94: 2706-2715.

Figures.

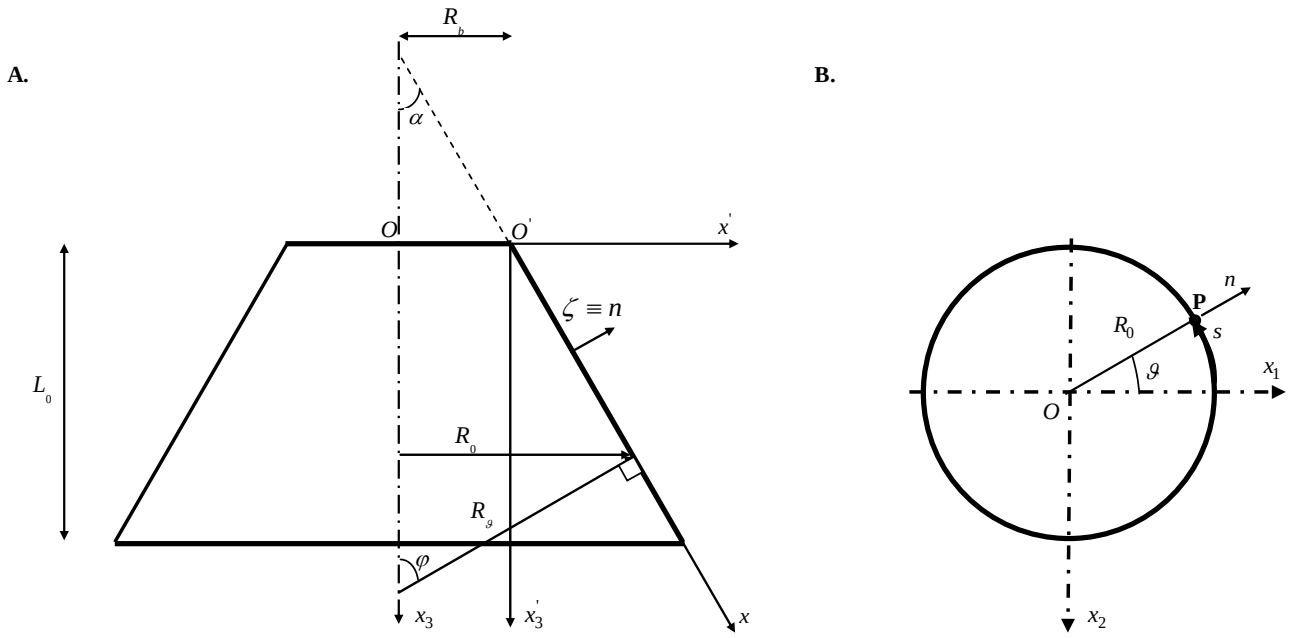

Fig.1: Open – conical shell geometry: Meridional Section (A.), Parallel Section (B.)

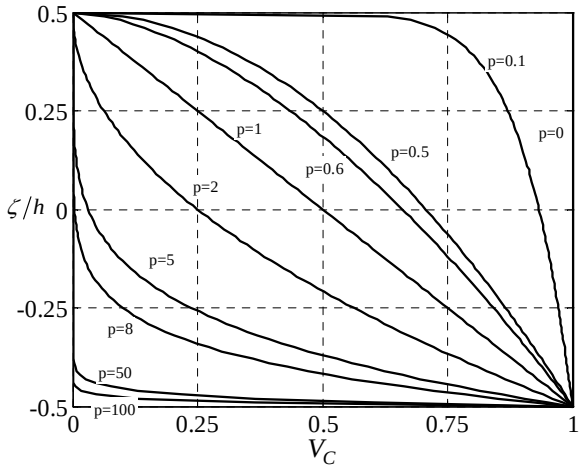

2*a*. FGM1$_{(1,0,0,p)}$

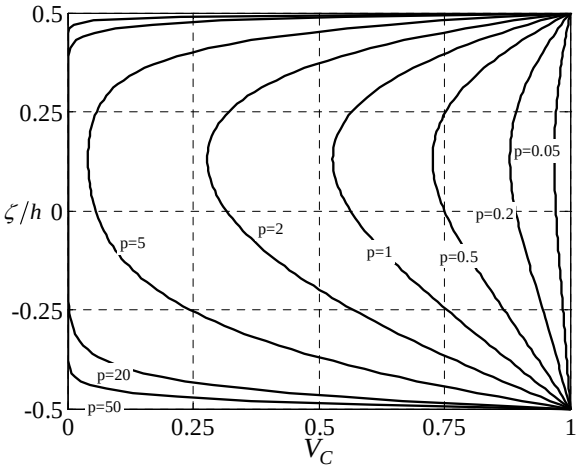

2*b*. FGM1$_{(1,1,4,p)}$

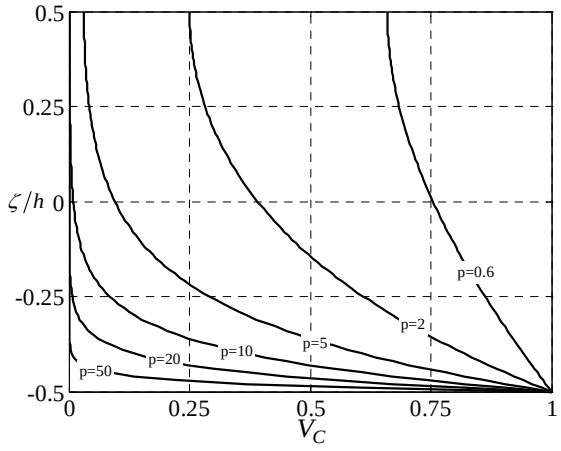

2*c*. FGM1$_{(1,0.5,2,p)}$

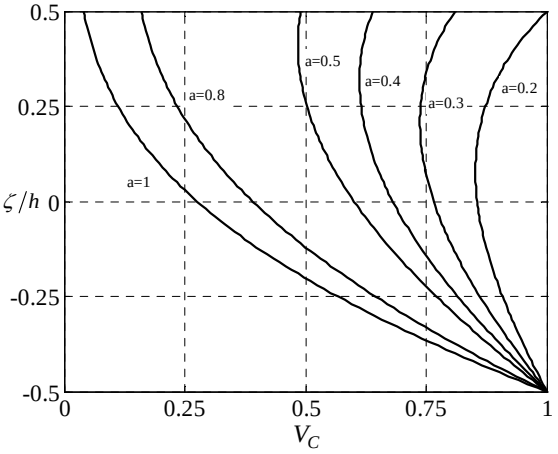

2*d*. FGM1$_{(a,0.2,3,2)}$

Figs.2*a*,*b*,*c*,*d*: Ceramic volume fraction V_c versus dimensionless thickness ζ/h for the FGM1 class.

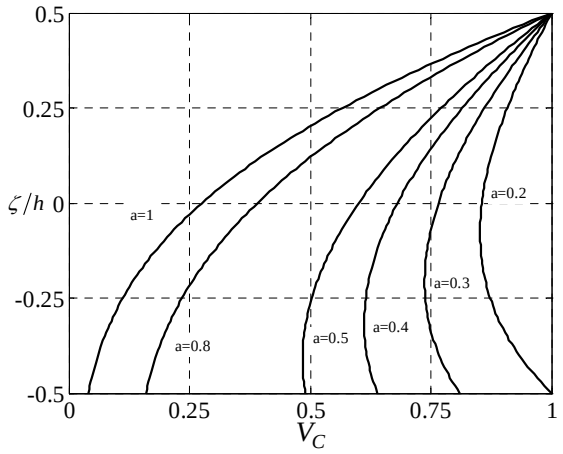

3*a*. FGM2$_{(a,0.2,3,2)}$

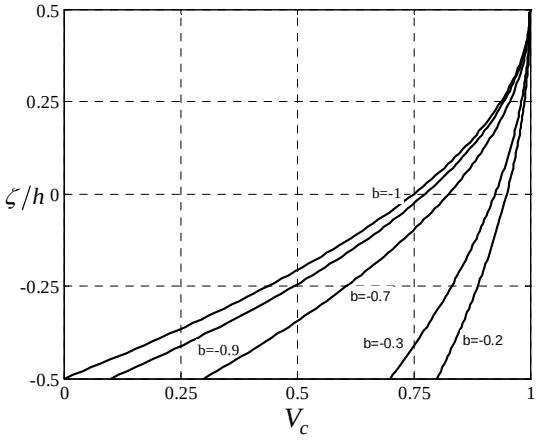

3*b*. FGM2$_{(0,b,2,1)}$

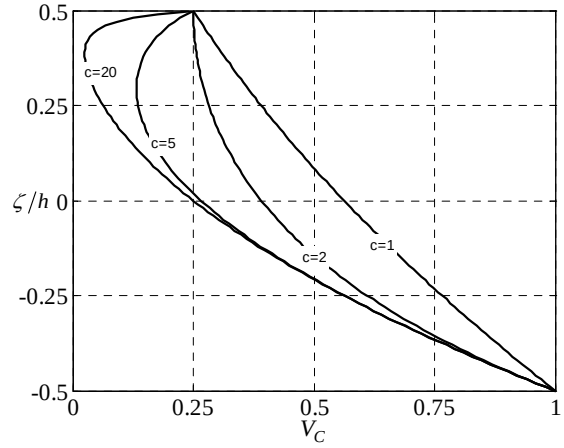

3*c*. FGM1$_{(1,0.5,c,2)}$

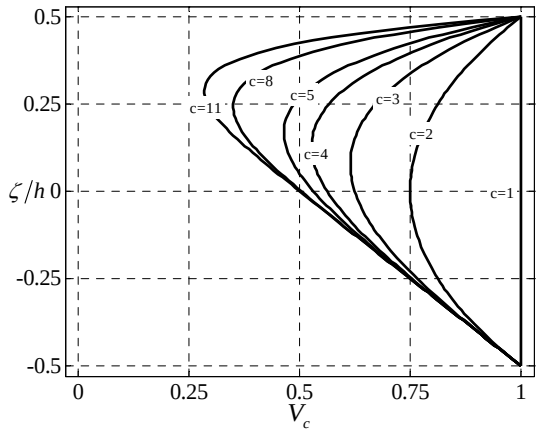

3*d*. FGM1$_{(1,1,c,1)}$

Figs.3*a*,*b*,*c*,*d*: Ceramic volume fraction V_c versus dimensionless thickness ζ/h for the FGM1 and FGM2 classes.

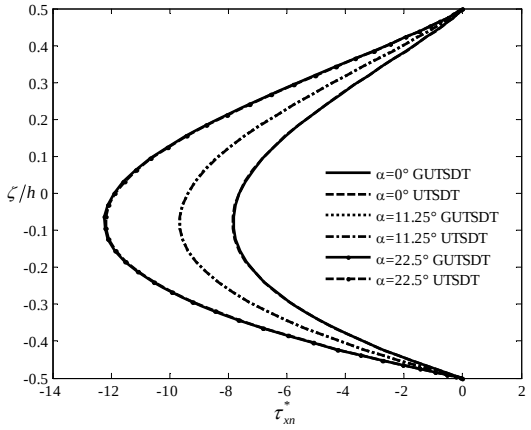

4*a*. transverse shear stress (τ^*_{xn})

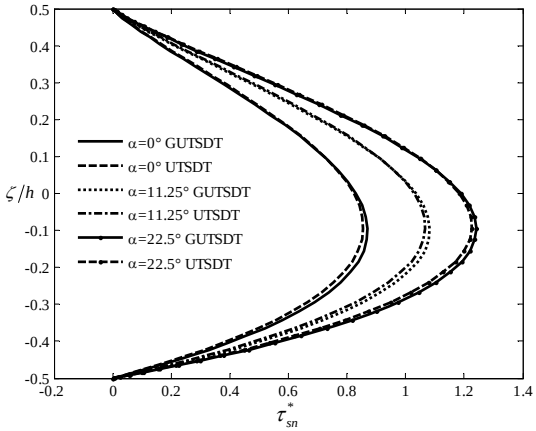

4*b*. transverse shear stress (τ^*_{sn})

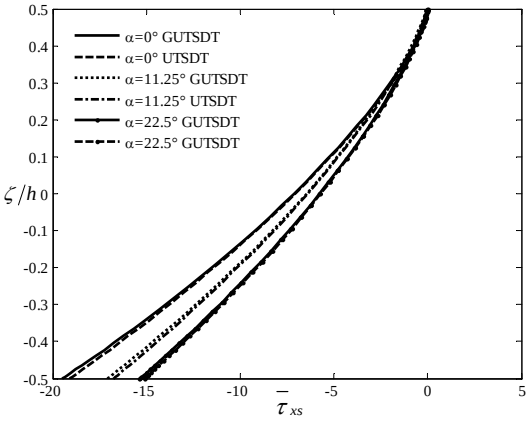

4*c*. membrane shear stress ($\bar{\tau}_{xs}$)

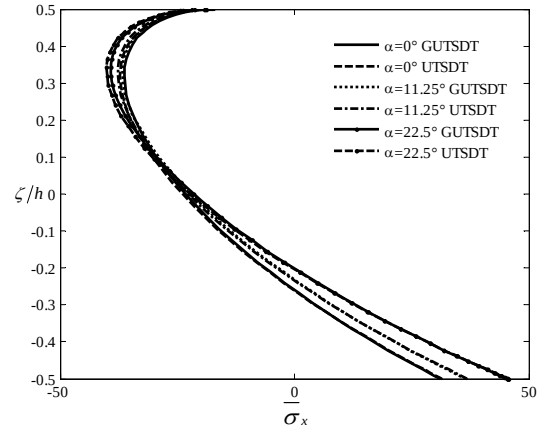

4*d*. meridional normal stress ($\bar{\sigma}_x$)

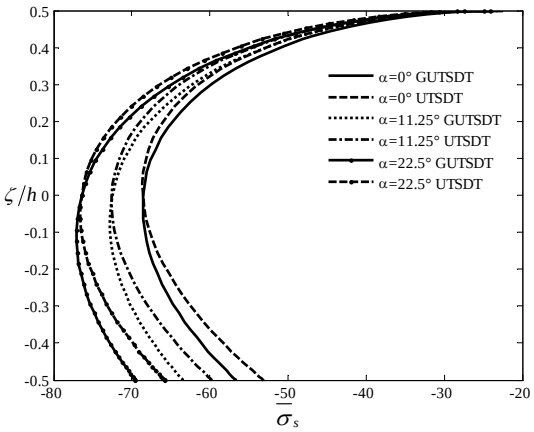

4*e*. circumferential normal stress ($\bar{\sigma}_s$)

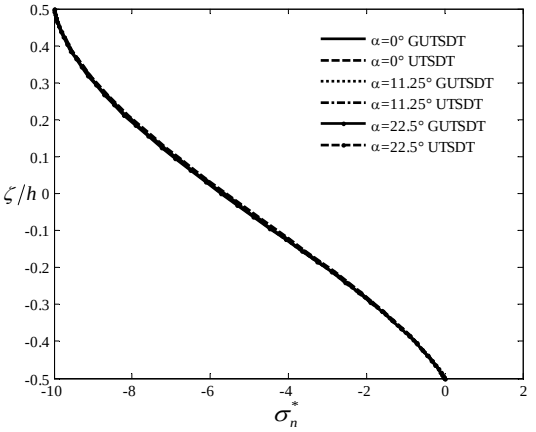

4f. transverse normal stress (σ^*_n)

Figs.4*a,b,c,d,e,f*. Stress profiles for $FGM1_{(1,0,0,p)}$ ($p = 0.5$) truncated conical panels via the GUTSDT under top normal pressure (scale factor: $\beta = 10^{-4}$)

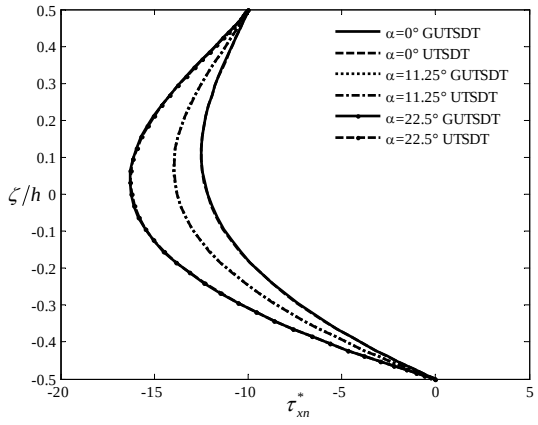

5a. transverse shear stress (τ^*_{xn})

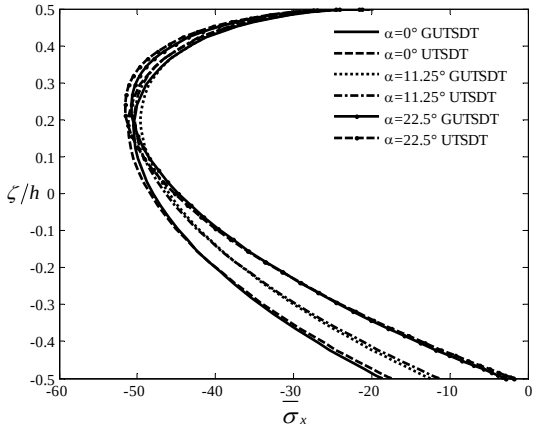

5b. membrane normal stress ($\overline{\sigma}_x$)

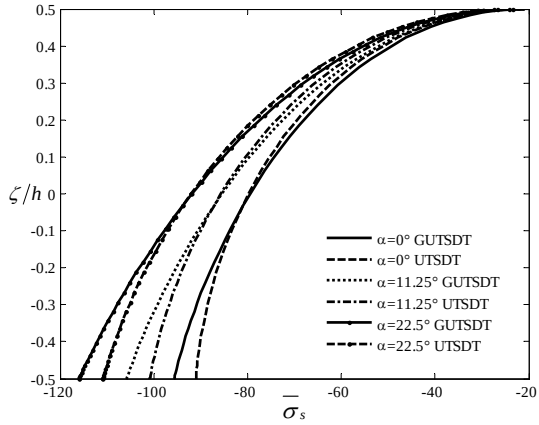

5c. membrane normal stress ($\overline{\sigma}_s$)

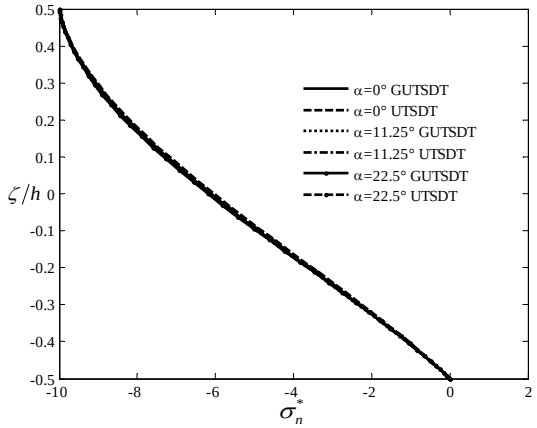

5d. transverse normal stress (σ^*_n)

Figs.5a,b,c,d: Stress profiles for $FGM1_{(1,0,0,p)}$ $(p = 0.5)$ truncated conical shells via the GUTSDT under top normal and meridional constant loadings (scale factor: $\beta = 10^{-4}$)

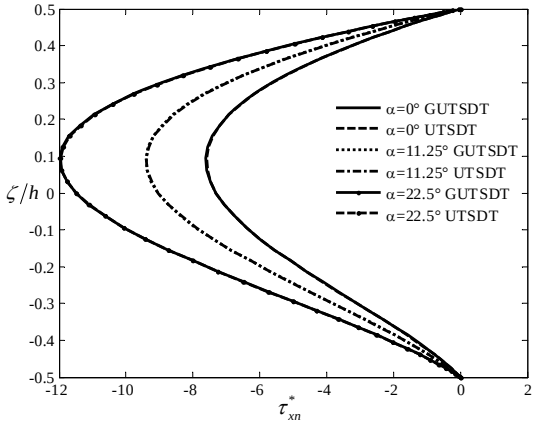

6*a*. transverse shear stress (τ^*_{xn})

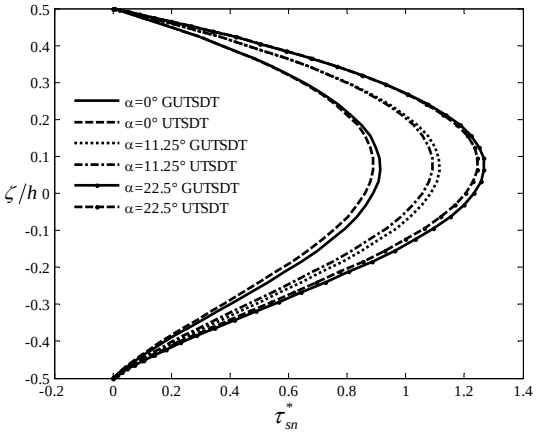

6*b*. transverse shear stress (τ^*_{sn})

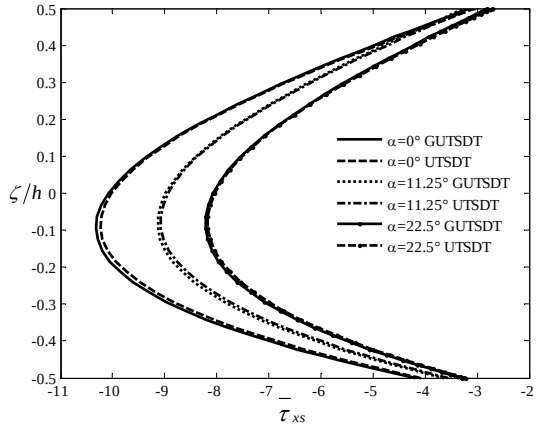

6*c*. membrane shear stress ($\bar{\tau}_{xs}$)

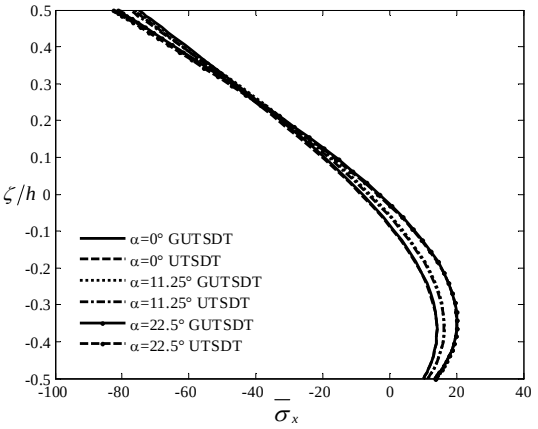

6*d*. meridional normal stress ($\bar{\sigma}_x$)

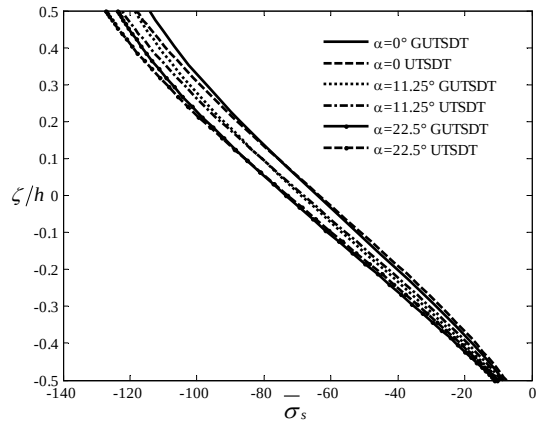

6*e*. circumferential normal stress ($\bar{\sigma}_s$)

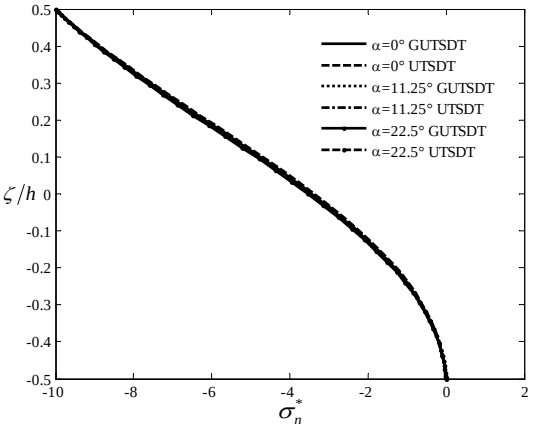

6f. transverse normal stress (σ^*_n)

Figs.6*a*,*b*,*c*,*d*,*e*,*f*: Stress profiles for $FGM2_{(0,b,2,1)}$ ($b=-1$) truncated conical panels via the GUTSDT under top normal uniform pressure (scale factor: $\beta=10^{-4}$).

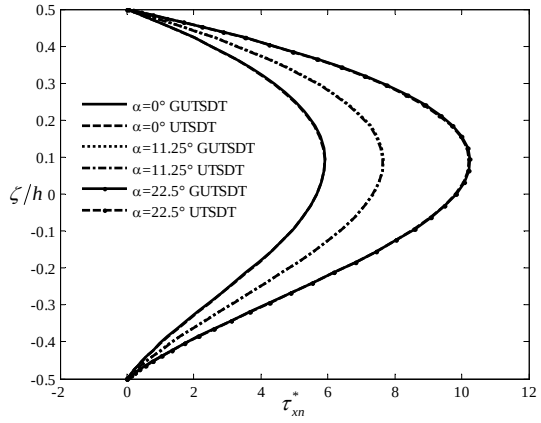

7a. transverse shear stress (τ^*_{xn})

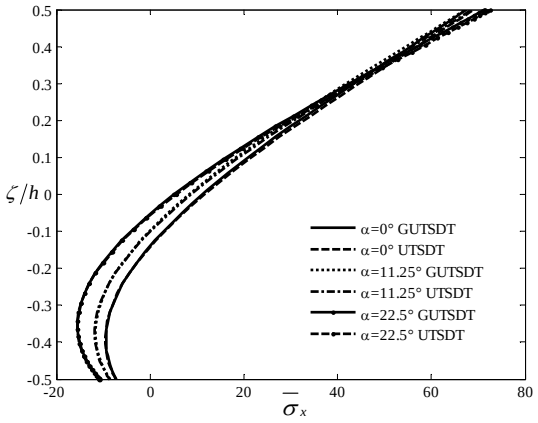

7b. membrane normal stress ($\overline{\sigma}_x$)

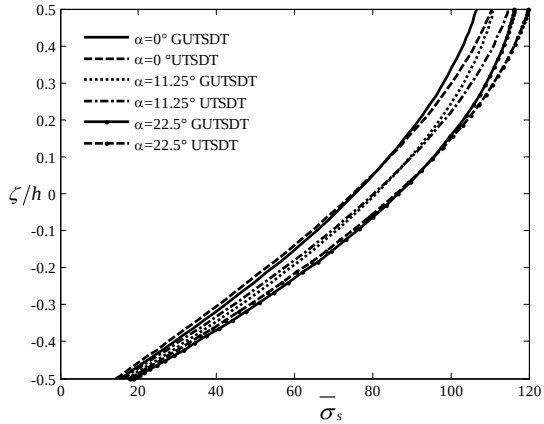

7c. membrane normal stress ($\overline{\sigma}_s$)

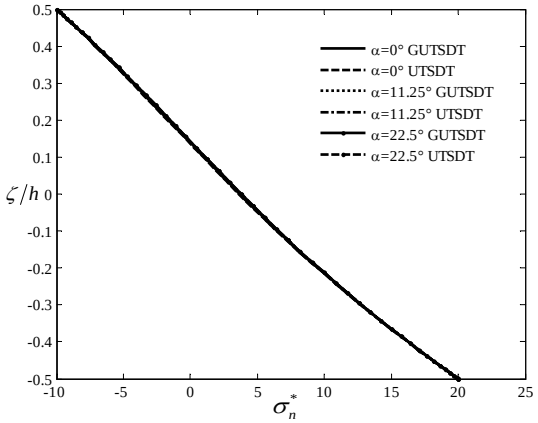

7d. transverse normal stress (σ^*_n)

Figs.7*a*,*b*,*c*,*d*: Stress profiles for $FGM2_{(0,b,2,1)}$ $(b=-1)$ truncated conical shells via the GUTSDT under top and bottom normal constant pressures (scale factor: $\beta = 10^{-4}$).

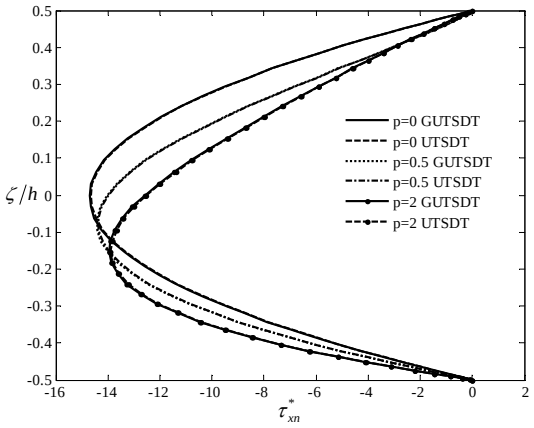

8*a*. transverse shear stress (τ^*_{xn})

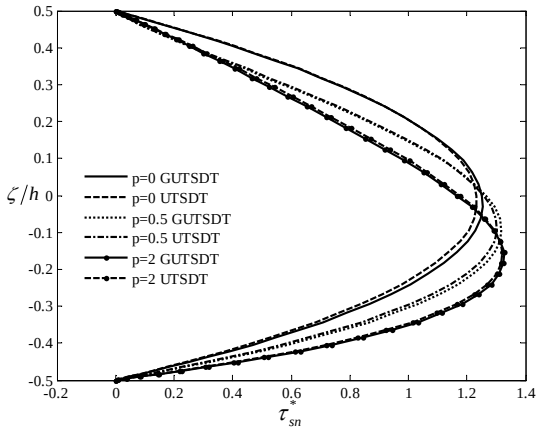

8*b*. transverse shear stress (τ^*_{sn})

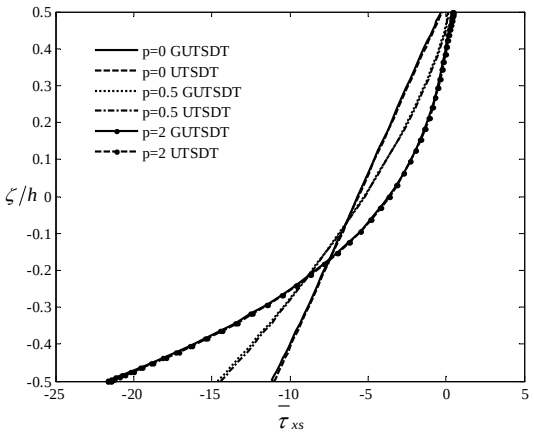

8*c*. membrane shear stress ($\bar{\tau}_{xs}$)

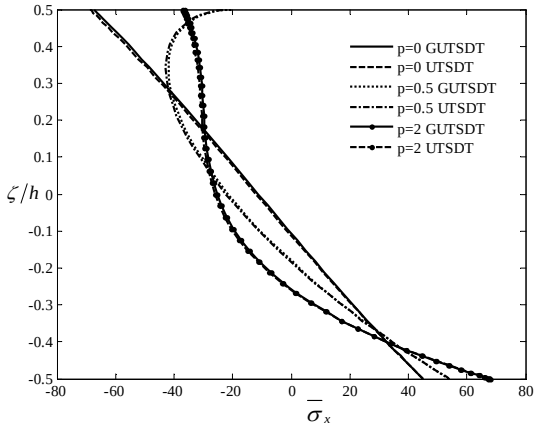

8*d*. meridional normal stress ($\bar{\sigma}_x$)

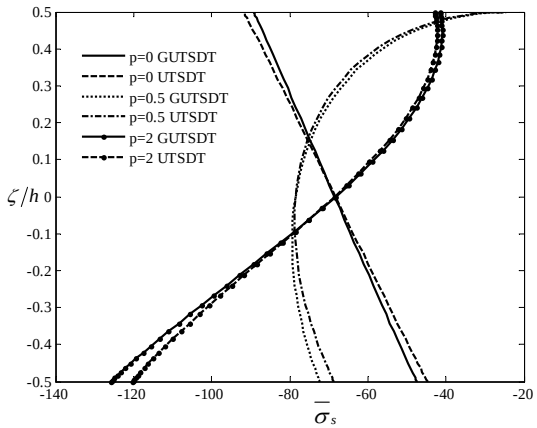

8*e*. circumferential normal stress ($\bar{\sigma}_s$)

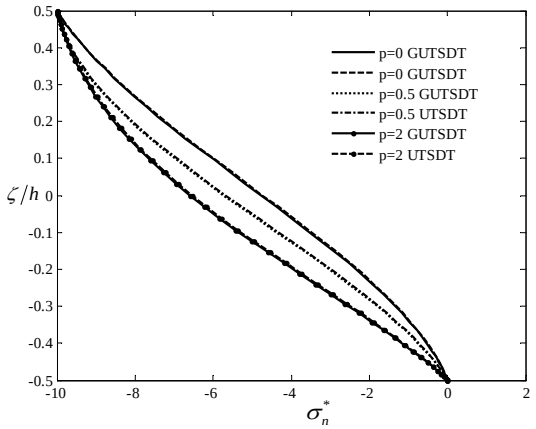

8f. transverse normal stress (σ^*_n)

Figs.8*a,b,c,d,e,f*: Stress profiles for $FGM1_{(1,0,0,p)}$ truncated conical panels via the GUTSDT and UTSDT under top normal constant pressure (scale factor: $\beta = 10^{-4}$).

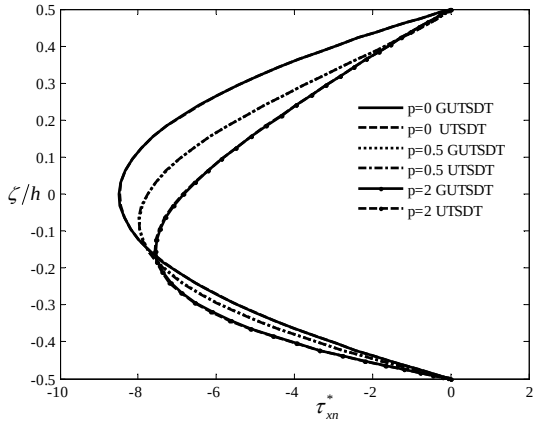

9a. transverse shear stress (τ^*_{xn})

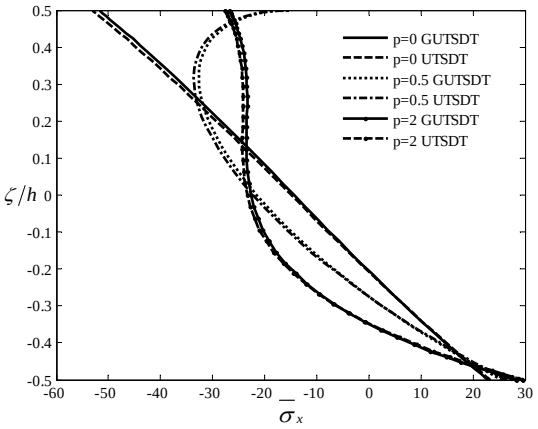

9b. membrane normal stress ($\bar{\sigma}_x$)

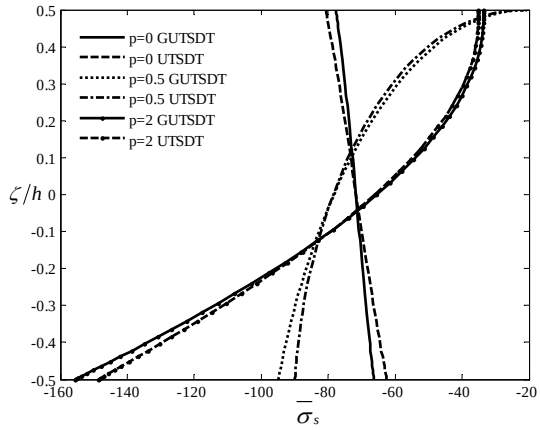

9c. membrane normal stress ($\bar{\sigma}_s$)

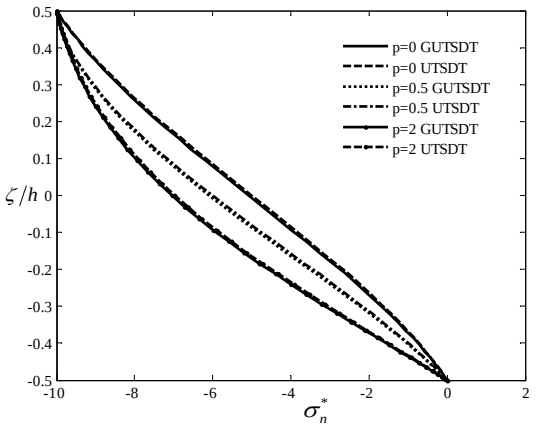

9d. transverse normal stress (σ^*_n)

Figs.9*a,b,c,d*: Stress profiles for $FGM1_{(1,0,0,p)}$ truncated conical panels via the GUTSDT and UTSDT under top normal constant pressure (scale factor: $\beta = 10^{-4}$).

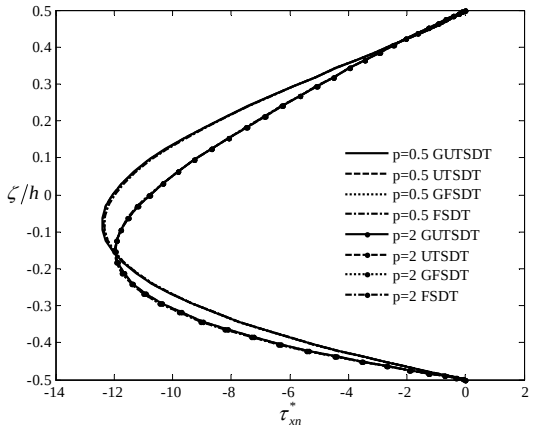

10*a*. transverse shear stress ($\bar{\tau}^*_{xn}$)

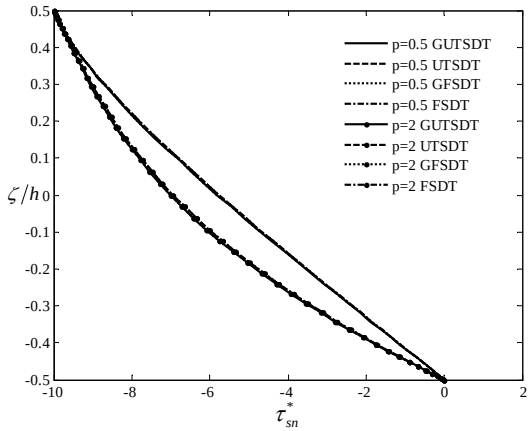

10*b*. transverse shear stress ($\bar{\tau}^*_{sn}$)

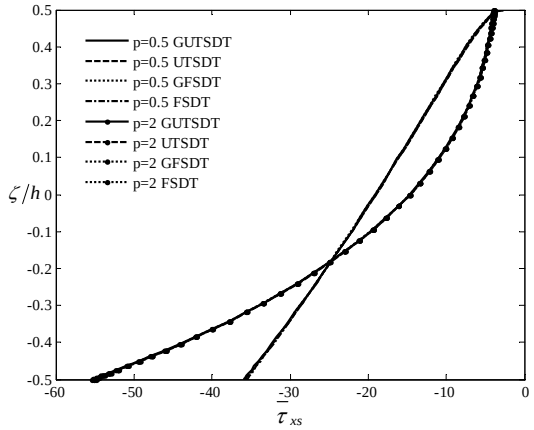

10*c*. membrane shear stress ($\bar{\tau}_{xs}$)

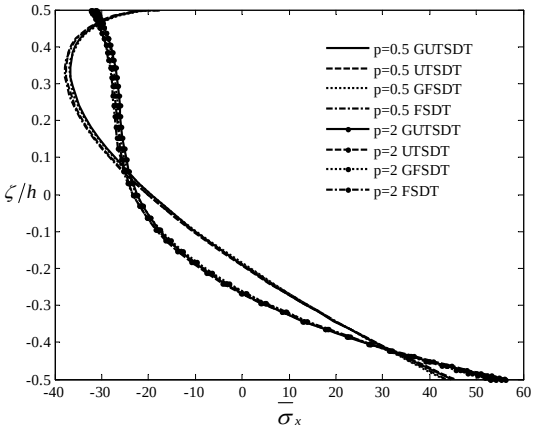

10*d*. meridional normal stress ($\bar{\sigma}_x$)

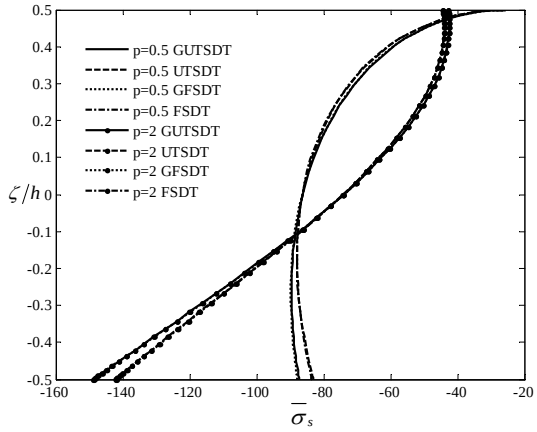

10*e*. circumferential normal stress ($\bar{\sigma}_s$)

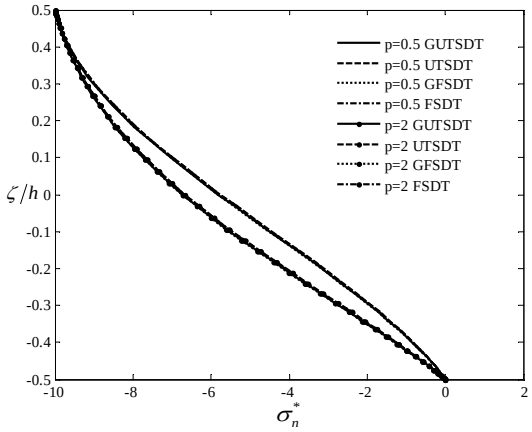

10f. transverse normal stress ($\bar{\sigma}^*_n$)

Figs.10*a,b,c,d,e,f*: Stress profiles for $FGM1_{(1,0,0,p)}$ truncated conical panels via the first and third order theories under top normal and circumferential uniform loadings (scale factor: $\beta = 10^{-4}$).

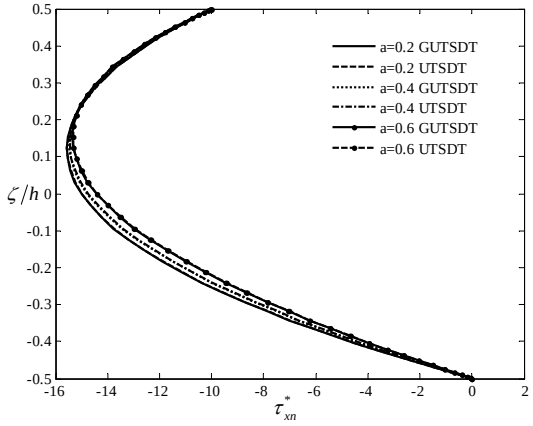

11*a*. transverse shear stress (τ^*_{xn})

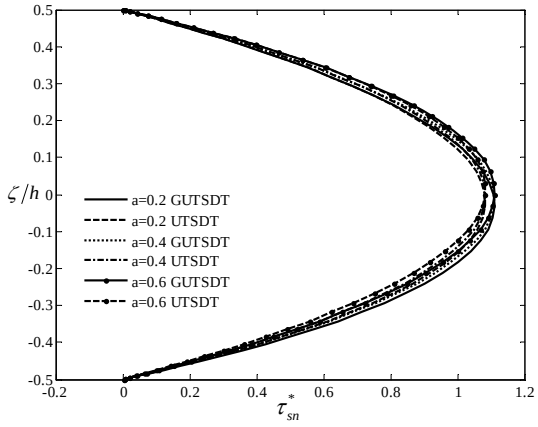

11*b*. transverse shear stress (τ^*_{sn})

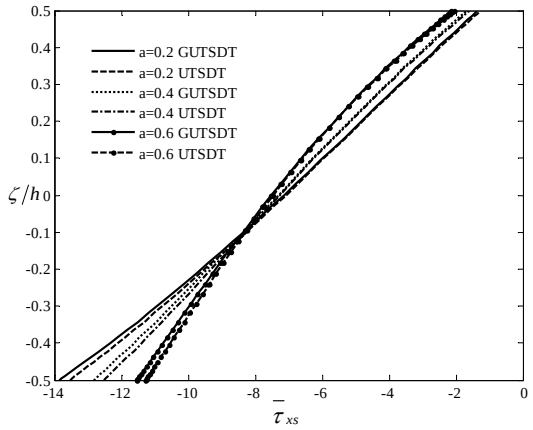

11*c*. membrane shear stress ($\bar{\tau}_{xs}$)

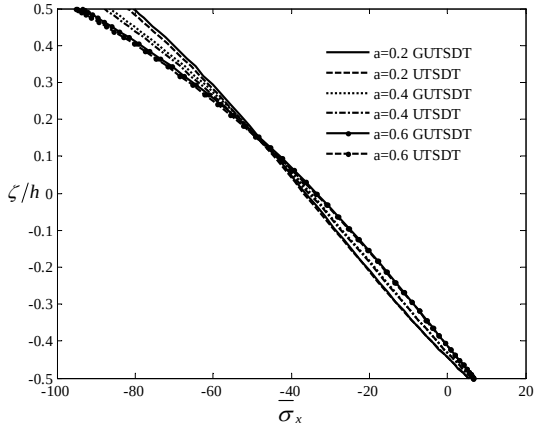

11*d*. meridional normal stress ($\bar{\sigma}_x$)

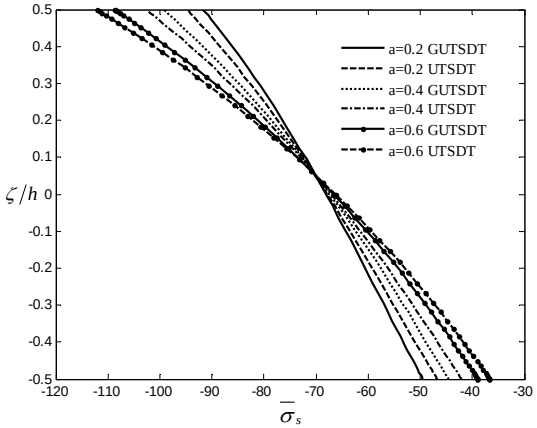

11*e*. circumferential normal stress (σ_s)

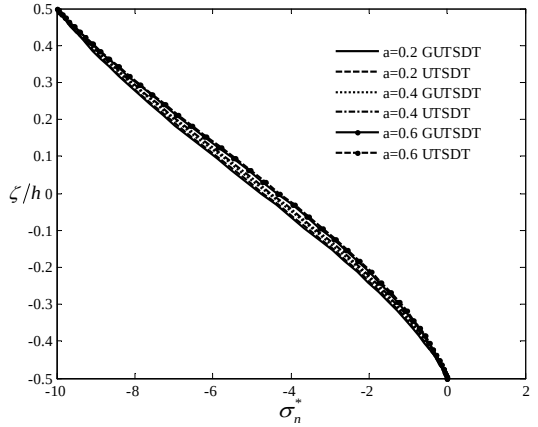

11*f*. transverse normal stress (σ_n)

Figs.11*a,b,c,d,e,f*: Stress profiles for $FGM2_{(a,0.2,2,1)}$ truncated conical panels via the GUTSDT under top normal and meriodional uniform loadings (scale factor: $\beta = 10^{-4}$).

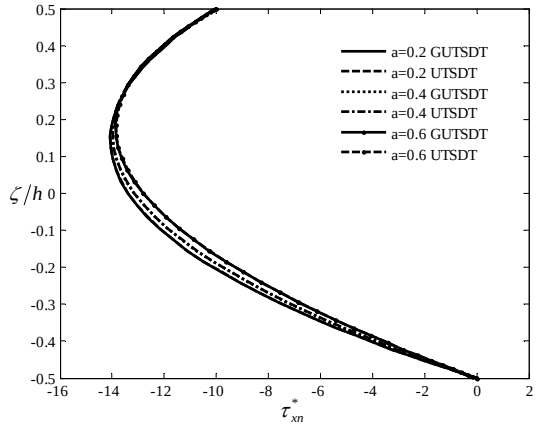

12a. transverse shear stress (τ^*_{xn})

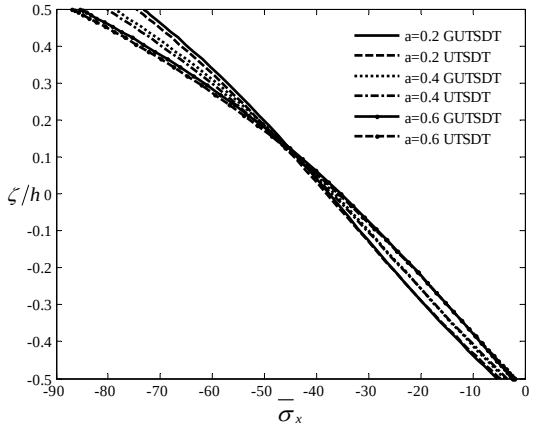

12b. membrane normal stress ($\overline{\sigma}_x$)

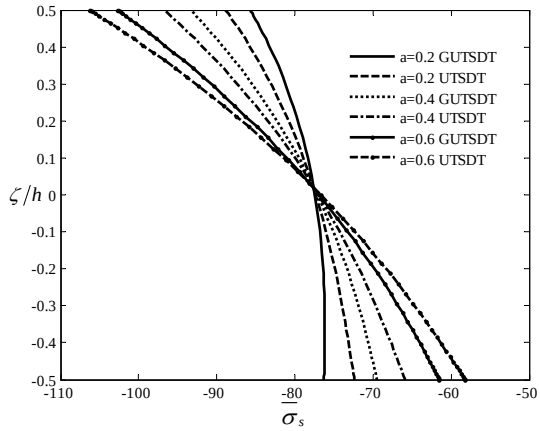

12c. membrane normal stress ($\overline{\sigma}_s$)

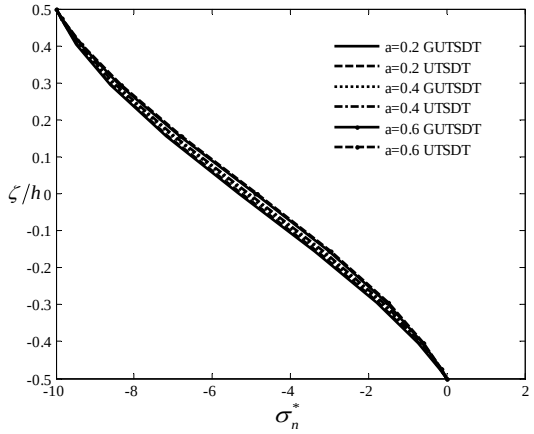

12d. transverse normal stress (σ^*_n)

Figs.12*a,b,c,d*: Stress profiles for $FGM2_{(a,0.2,2,1)}$ truncated conical shells via the GUTSDT under normal and meridional uniform loadings (scale factor: $\beta = 10^{-4}$).

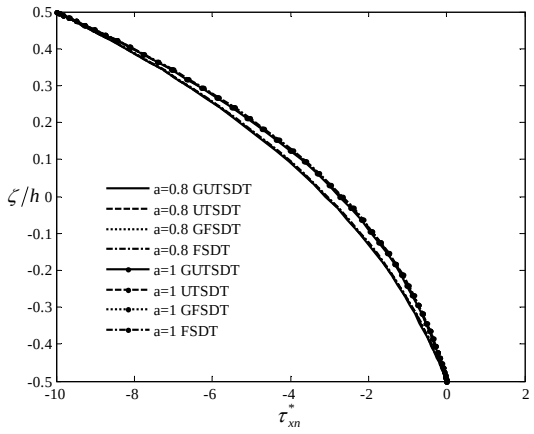

13*a*. transverse shear stress (τ^*_{xn})

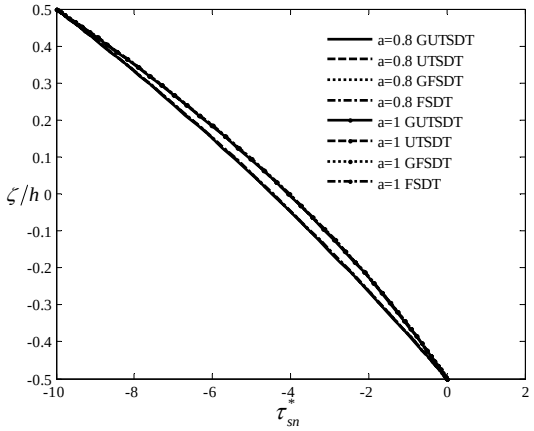

13*b*. transverse shear stress (τ^*_{sn})

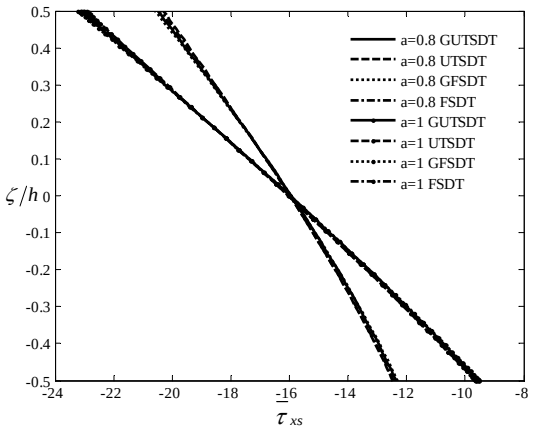

13*c*. membrane shear stress ($\bar{\tau}_{xs}$)

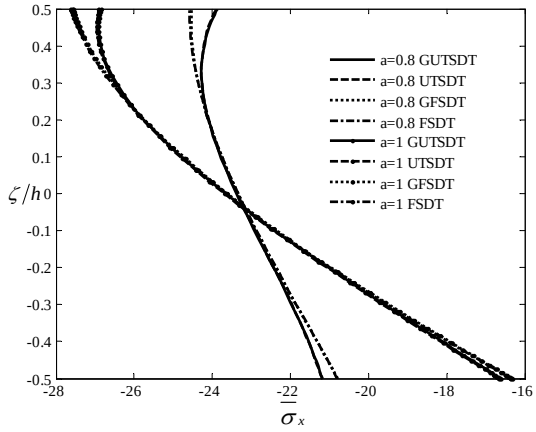

13*d*. meridional normal stress ($\bar{\sigma}_x$)

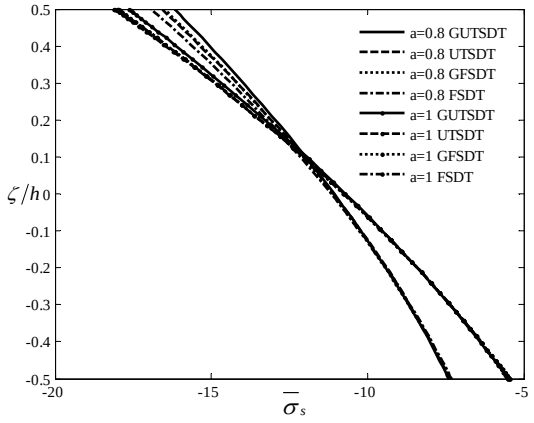

13*e*. circumferential normal stress ($\bar{\sigma}_s$)

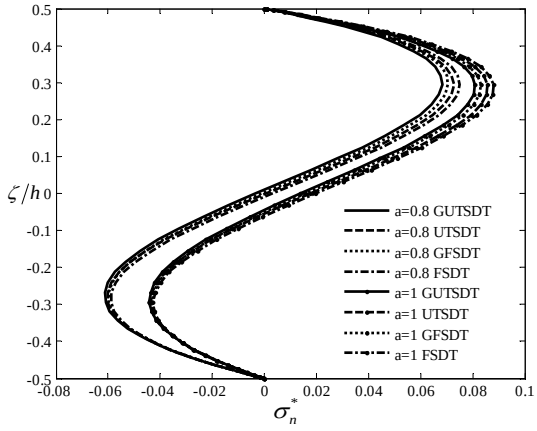

13*f*. transverse normal stress (σ^*_n)

Figs.13*a,b,c,d,e,f*: Stress profiles for $FGM2_{(a,0.2,2,1)}$ truncated conical panels via the GUTSDT under top meridional and circumferential uniform loadings (scale factor: $\beta = 10^{-4}$).

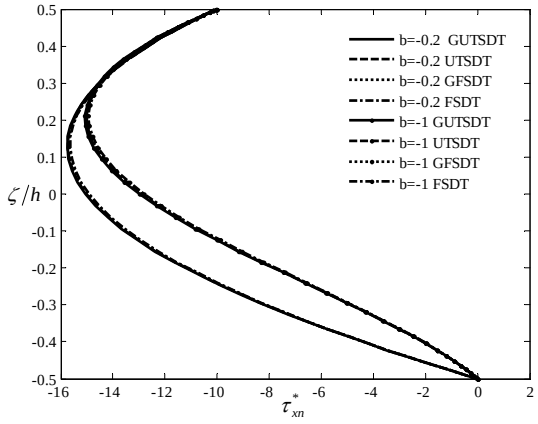

14*a*. transverse shear stress (τ^*_{xn})

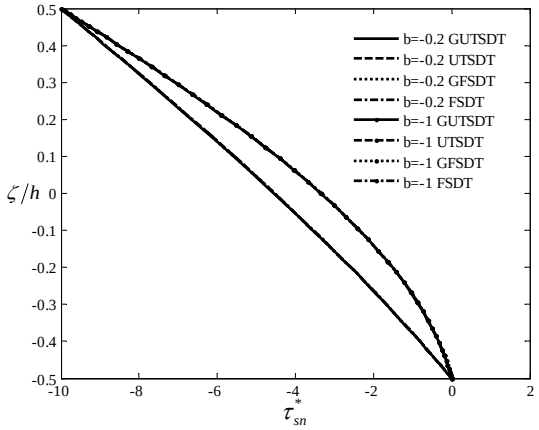

14*b*. transverse shear stress (τ^*_{sn})

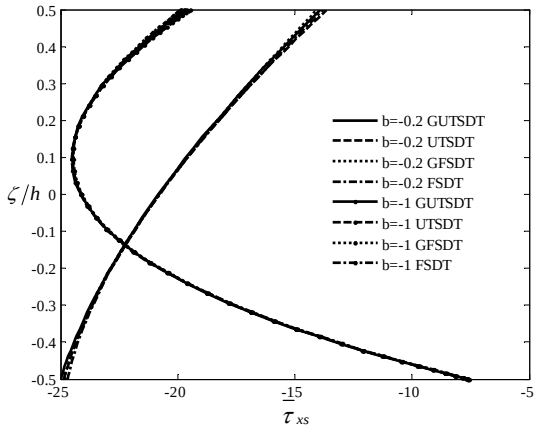

14*c*. membrane shear stress ($\bar{\tau}_{xs}$)

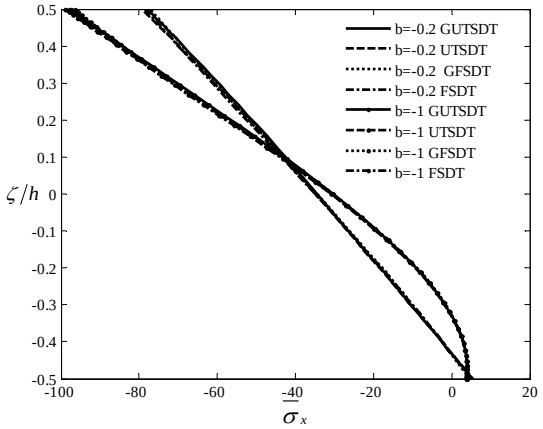

14*d*. meridional normal stress ($\bar{\sigma}_x$)

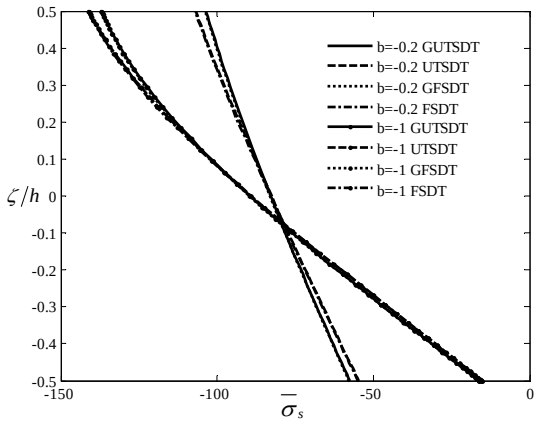

14*e*. circumferential normal stress ($\bar{\sigma}_s$)

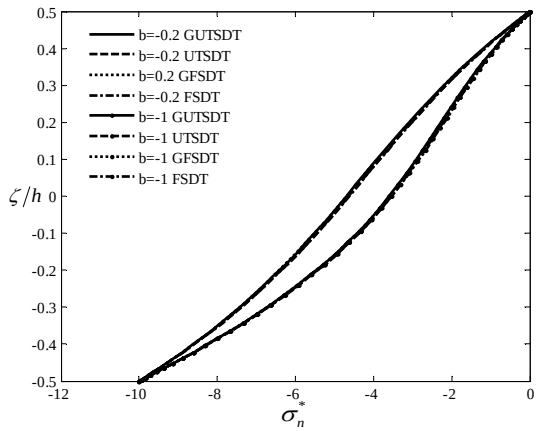

14*f*. transverse normal stress (σ^*_n)

Figs.14*a,b,c,d,e,f*: Stress profiles for $FGM2_{(0,b,2,1)}$ truncated conical panels via the first and third order theories under top meridional and circumferential uniform pressures and bottom normal uniform pressure (scale factor: $\beta = 10^{-4}$).

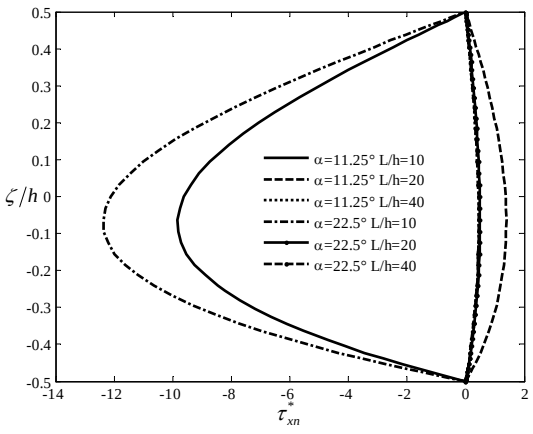

15*a*. transverse shear stress (τ^*_{xn})

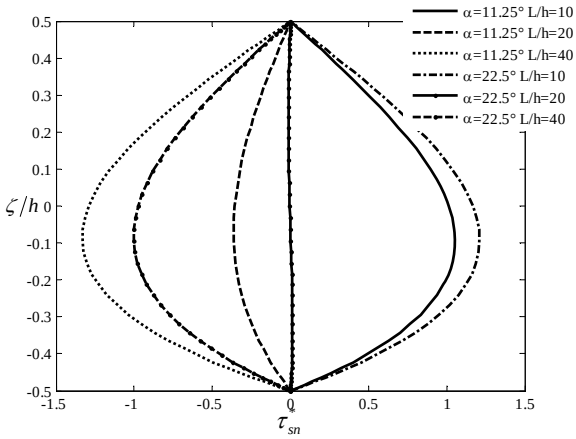

15*b*. transverse shear stress (τ^*_{sn})

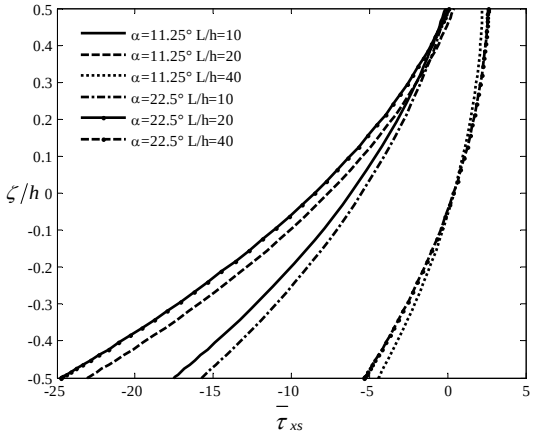

15*c*. membrane shear stress ($\bar{\tau}_{xs}$)

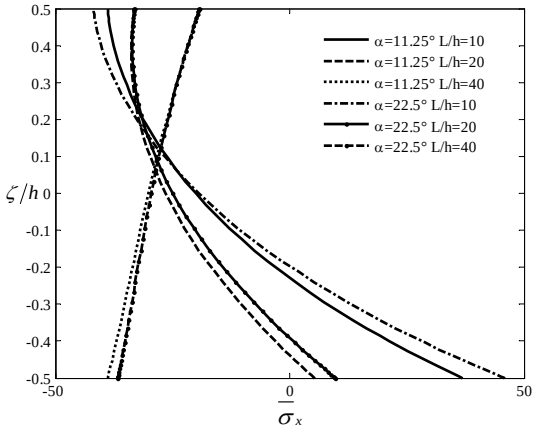

15*d*. meridional normal stress ($\bar{\sigma}_x$)

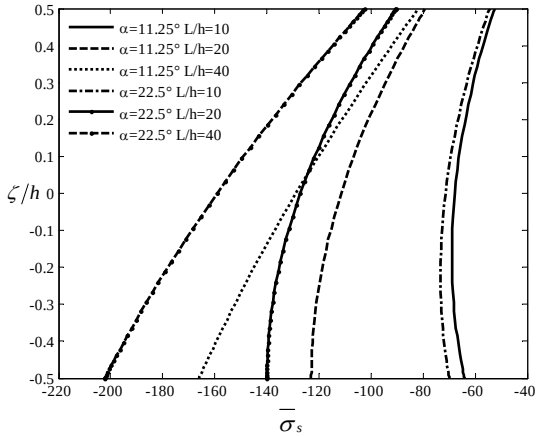

15*e*. circumferential normal stress ($\bar{\sigma}_s$)

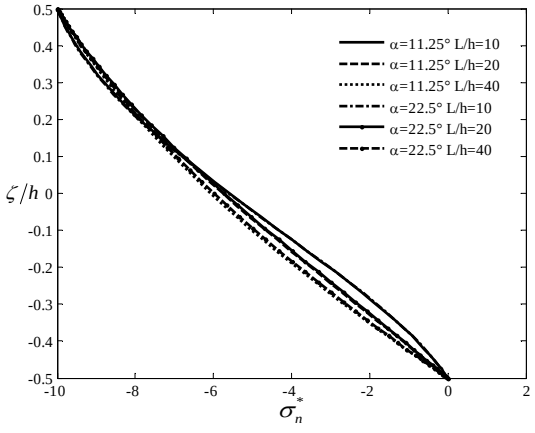

15*f*. transverse normal stress (σ^*_n)

Figs.15*a,b,c,d,e,f*: Stress profiles for $FGM1_{(1,0,0,p)}$ $(p=1)$ truncated conical panels via the GUTSDT under top normal uniform pressure (scale factor: $\beta = 10^{-4}$).

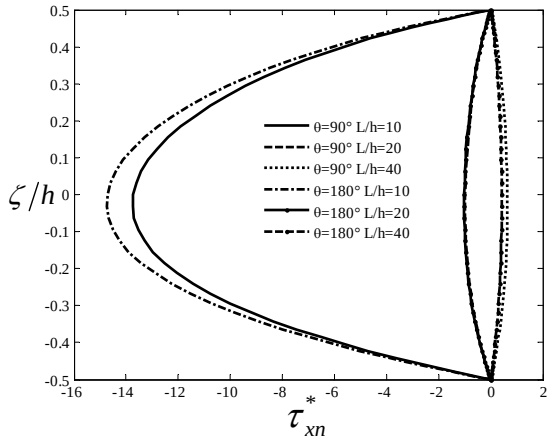

16*a*. transverse shear stress (τ_{xn}^{*})

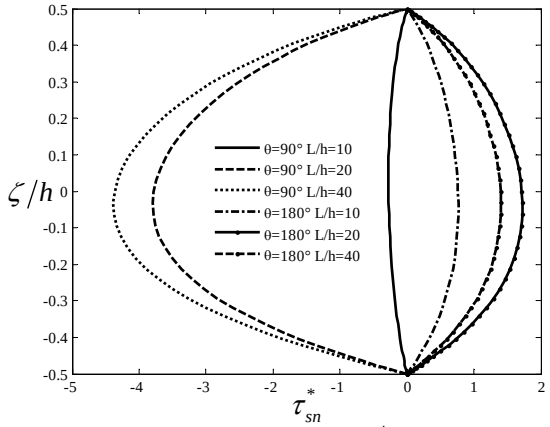

16*b*. transverse shear stress (τ_{sn}^{*})

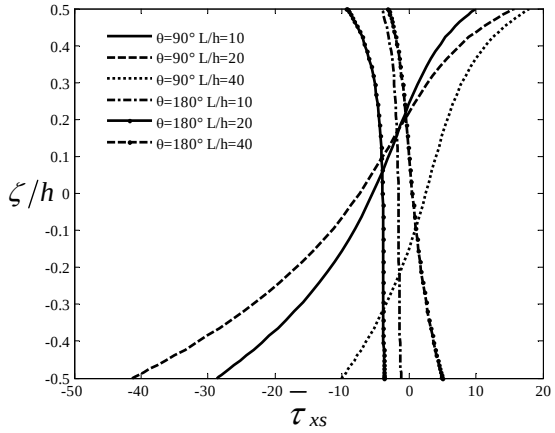

16*c*. membrane shear stress ($\bar{\tau}_{xs}$)

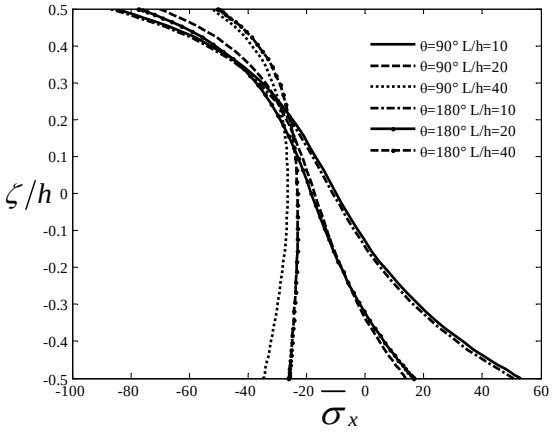

16*d*. meridional normal stress ($\bar{\sigma}_{x}$)

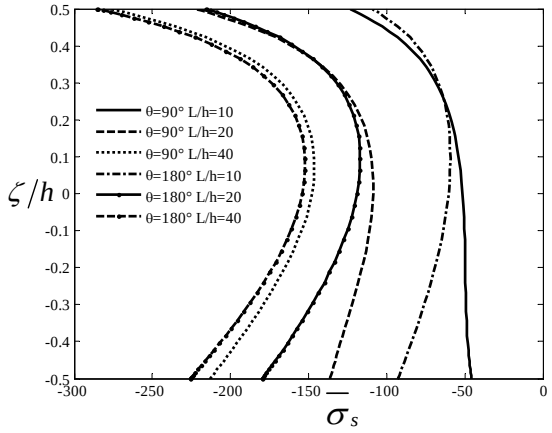

16*e*. circumferential normal stress ($\bar{\sigma}_{s}$)

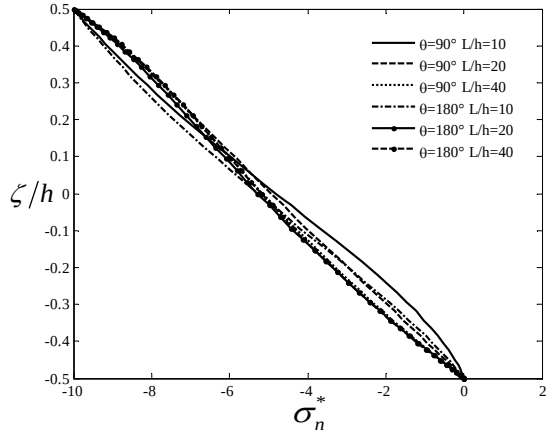

16*f*. transverse normal stress (σ_{n}^{*})

Figs.16*a,b,c,d,e,f*: Stress profiles for $FGM1_{(1,1,4,p)}$ ($p = 2$) truncated conical panels via the GUTSDT under top normal uniform pressure (scale factor: $\beta = 10^{-4}$).

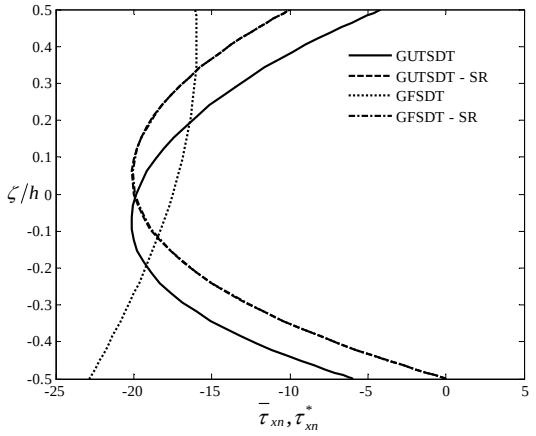

17*a*. unrecovered ($\bar{\tau}_{xn}$) and recovered (τ^*_{xn}) shear stress under $p_x - p_n$ top uniform loadings

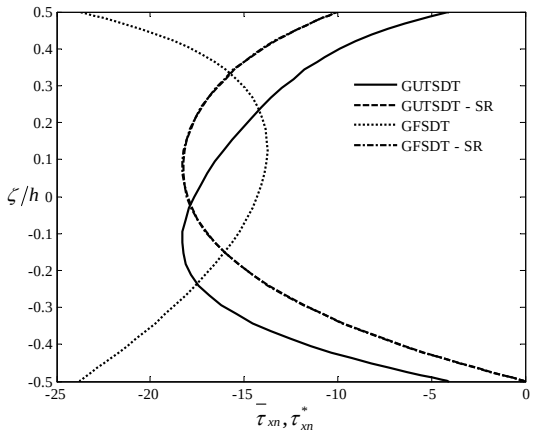

17*b*. unrecovered ($\bar{\tau}_{xn}$) and recovered (τ^*_{xn}) shear stress under $p_x - p_s$ top uniform loadings and p_n bottom uniform pressure

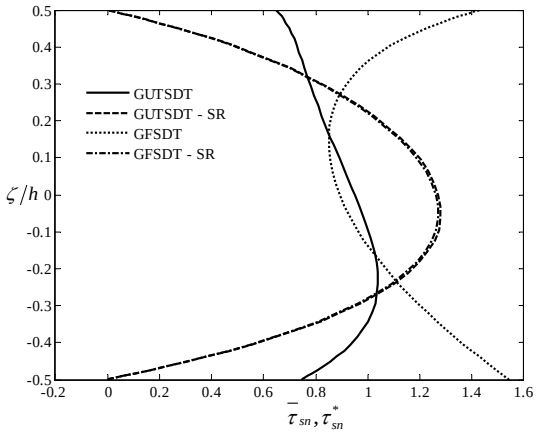

17*c*. unrecovered ($\bar{\tau}_{sn}$) and recovered (τ^*_{sn}) shear stress under $p_x - p_n$ top uniform loadings

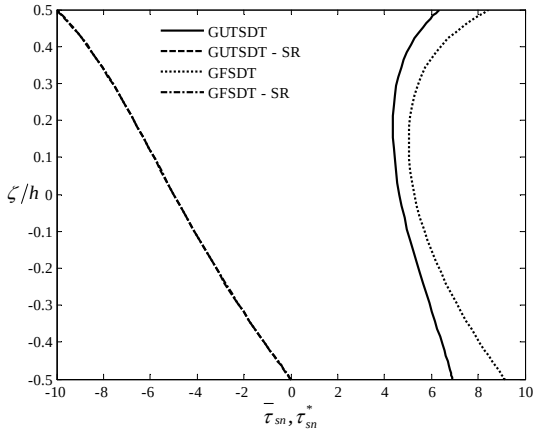

17*d*. unrecovered ($\bar{\tau}_{sn}$) and recovered (τ^*_{sn}) shear stress under $p_x - p_s$ top uniform loadings and p_n bottom uniform pressure

Figs.17*a,b,c,d* Stress profiles for $FGM1_{(a,0.2,3,2)}$ $(a = 0.5)$ truncated conical panels via the GUTSDT under various top and bottom uniform loadings (scale factor: $\beta = 10^{-4}$).

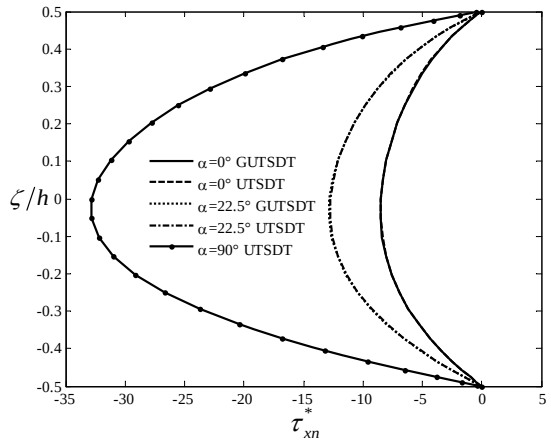

18*a*. transverse shear stress (τ^*_{xn})

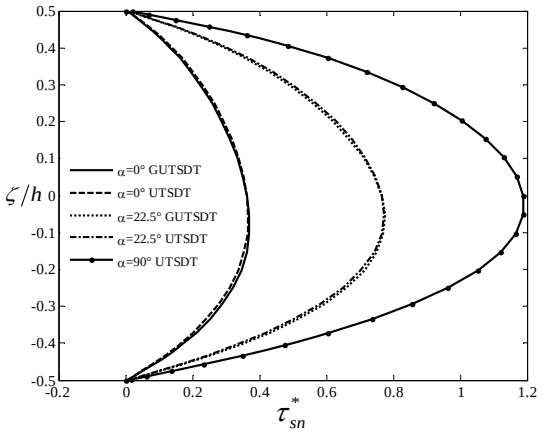

18*b*. transverse shear stress (τ^*_{sn})

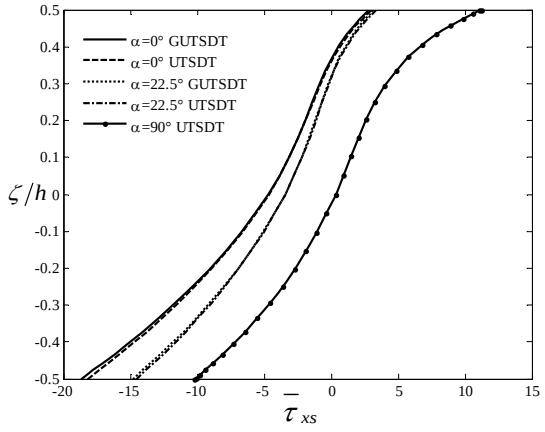

18*c*. membrane shear stress ($\bar{\tau}_{xs}$)

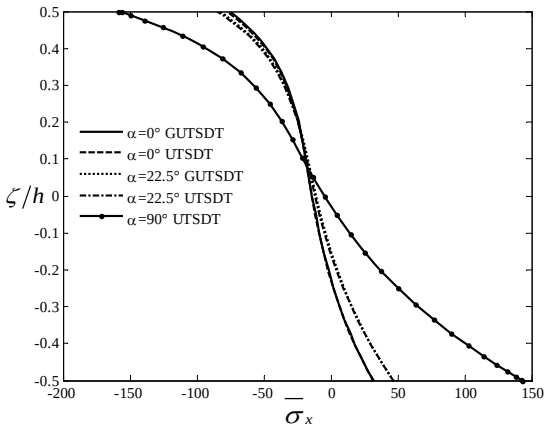

18*d*. meridional normal stress ($\bar{\sigma}_x$)

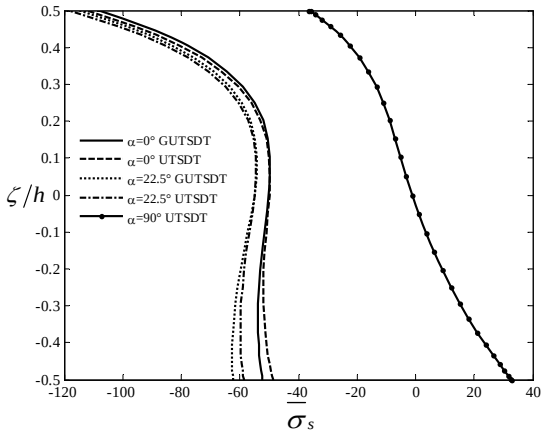

18*e*. circumferential normal stress ($\bar{\sigma}_s$)

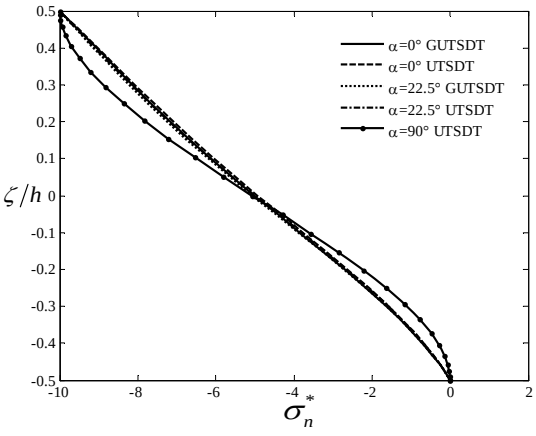

18*f*. transverse normal stress (σ^*_n)

Figs.18*a*,*b*,*c*,*d*,*e*,*f*: Stress profiles for $FGM1_{(1,1,c,1)}$ $(c=5)$ truncated conical panels via the GUTSDT or UTSDT under top normal uniform pressure (scale factor: $\beta=10^{-4}$).

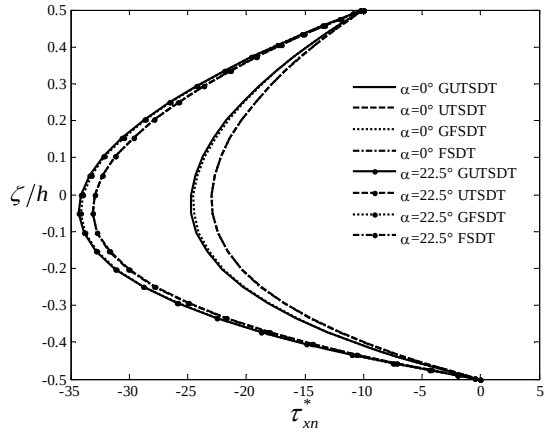

19*a*. transverse shear stress (τ^*_{xn})

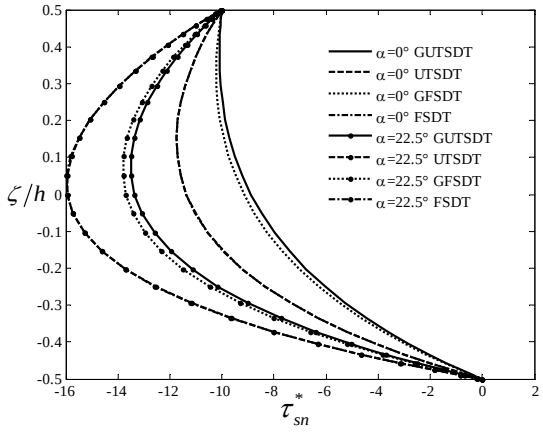

19*b*. transverse shear stress (τ^*_{sn})

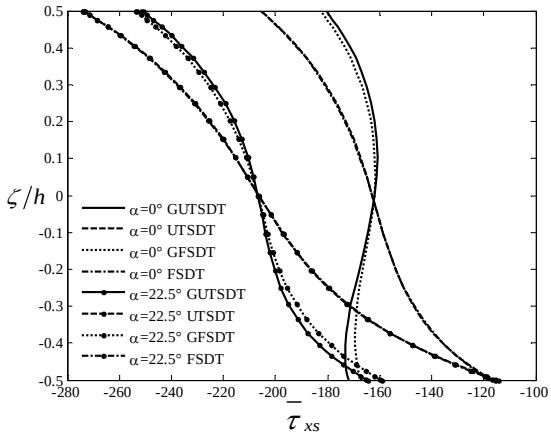

19*c*. membrane shear stress ($\bar{\tau}_{xs}$)

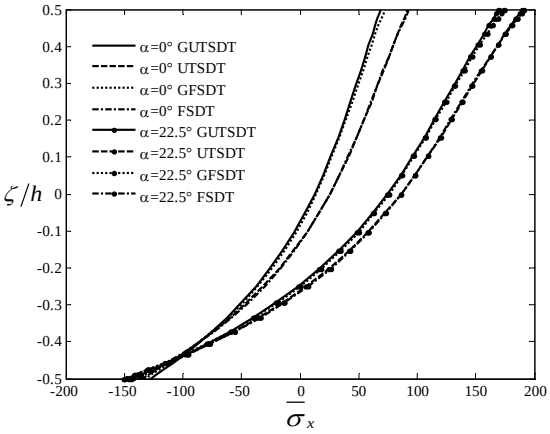

19*d*. meridional normal stress ($\bar{\sigma}_x$)

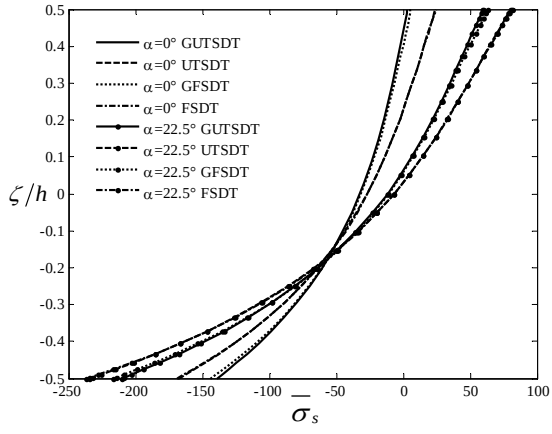

19*e*. circumferential normal stress ($\bar{\sigma}_s$)

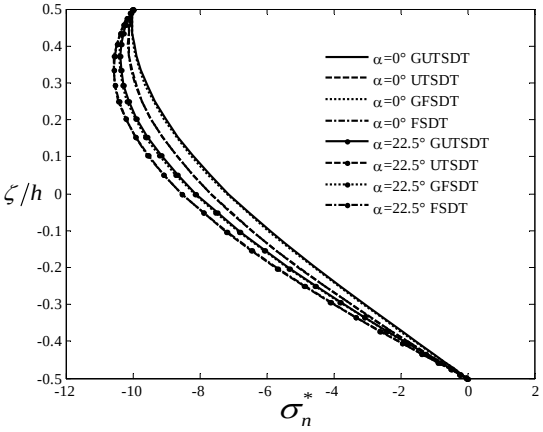

19*f*. transverse normal stress (σ^*_n)

Figs.19*a*,*b*,*c*,*d*,*e*,*f*: Stress profiles for $FGM1_{(1,0.5,2,p)}$ ($p = 2$) truncated conical panels via the GUTSDT or GFSDT under top normal, circumferential, meridional uniform loadings (scale factor: $\beta = 10^{-4}$).

Tables.

Table 1a. Normalized central deflection of graded conical panel ($E_{c_1} = 380GPa$) under uniform loading

p	α	L/h			$\overline{w}$
2	11.25°	10	Reference	ANSYS[37]	0.019500
				[37]	0.019600
			Present theories	FSDT	0.020057
				GFSDT	0.02003
				UTSDT	0.02003
				GUTSDT	0.019952
		20	Reference	ANSYS[37]	0.008850
				[37]	0.00884
			Present theories	FSDT	0.0090231
				GFSDT	0.0089951
				UTSDT	0.0090271
				GUTSDT	0.0089991
		40	Reference	ANSYS[37]	0.0027500
				[37]	0.00269
			Present theories	FSDT	0.0027931
				GFSDT	0.0027860
				UTSDT	0.0027934
				GUTSDT	0.0027871

Table 1b. Normalized central deflection of graded conical panel ($E_{c_1} = 380GPa$) under uniform loading

p	α	L/h			$\overline{w}$
	22.5°	10	Reference	ANSYS[37]	0.0241000
				[37]	0.024200
			Present theories	FSDT	0.024749
				GFSDT	0.024706
				UTSDT	0.024714
				GUTSDT	0.024671
		20	Reference	ANSYS[37]	0.011400
				[37]	0.0114
			Present theories	FSDT	0.01612
				GFSDT	0.01584
				UTSDT	0.01617
				GUTSDT	0.01589
		40	Reference	ANSYS[37]	0.0036300
				[37]	0.0035700
			Present theories	FSDT	0.0036890
				GFSDT	0.0036813
				UTSDT	0.0036890
				GUTSDT	0.0036821

Table 1c. Normalized central deflection of graded conical panel ($E_{c_1} = 380GPa$) under uniform loading

p	α	L/h			$\overline{w}$
	45°	10	Reference	ANSYS[37]	0.0354000
				[37]	0.0356000
			Present theories	FSDT	0.036121
				GFSDT	0.036108
				UTSDT	0.036108
				GUTSDT	0.036119
		20	Reference	ANSYS[37]	0.0200000
				[37]	0.0202000
			Present theories	FSDT	0.020351
				GFSDT	0.020330
				UTSDT	0.020362
				GUTSDT	0.020341
		40	Reference	ANSYS[37]	0.0075600
				[37]	0.0075400
			Present theories	FSDT	0.0076616
				GFSDT	0.0076534
				UTSDT	0.0076620
				GUTSDT	0.0076543

Table 1d. Normalized central deflection of graded conical panel ($E_{c_1} = 380GPa$) under uniform loading

p	α	L/h			$\overline{w}$
	60°	10	Reference	ANSYS[37]	0.043300
				[37]	0.043900
			Present theories	FSDT	0.044278
				GFSDT	0.044281
				UTSDT	0.044350
				GUTSDT	0.044354
		20	Reference	ANSYS[37]	0.0297000
				[37]	0.0300000
			Present theories	FSDT	0.030127
				GFSDT	0.030129
				UTSDT	0.030153
				GUTSDT	0.030144
		40	Reference	ANSYS[37]	0.0144000
				[37]	0.0145000
			Present theories	FSDT	0.014575
				GFSDT	0.014567
				UTSDT	0.014576
				GUTSDT	0.014568

Table 2a. Normalized central deflection of graded conical panel ($E_{c_2} = 151GPa$) under uniform loading

p	α	L/h			$\overline{w}$
2	11.25	10	Reference	ANSYS[37]	0.012700
				[37]	0.012700
			Present theories	FSDT	0.01313111
				GFSDT	0.013132017
				UTSDT	0.013064822
				GUTSDT	0.013066634
		20	Reference	ANSYS[37]	0.005980
				[37]	0.00596
			Present theories	FSDT	0.006106534375
				GFSDT	0.00610285375
				UTSDT	0.006107195
				GUTSDT	0.00610360875
		40	Reference	ANSYS[37]	0.0019400
				[37]	0.001900
			Present theories	FSDT	0.001965713281
				GFSDT	0.00196394375
				UTSDT	0.001966008203
				GUTSDT	0.00196428672

Table 2b. Normalized central deflection of graded conical panel ($E_{c_2} = 151GPa$) under uniform loading

p	α	L/h			$\overline{w}$
	22.5	10	Reference	ANSYS[37]	0.0156000
				[37]	0.015600
			Present theories	FSDT	0.01611321
				GFSDT	0.01611925
				UTSDT	0.01605432
				GUTSDT	0.01606036
		20	Reference	ANSYS[37]	0.007680
				[37]	0.00767
			Present theories	FSDT	0.00782321562
				GFSDT	0.007820761875
				UTSDT	0.0078244425
				GUTSDT	0.00782198875
		40	Reference	ANSYS[37]	0.0025600
				[37]	0.0025200
			Present theories	FSDT	0.002592894441
				GFSDT	0.002591124609
				UTSDT	0.002593189063
				GUTSDT	0.002591419531

Table 2c. Normalized central deflection of graded conical panel ($E_{c_2} = 151GPa$) under uniform loading

p	α	L/h			$\overline{w}$
	45°	10	Reference	ANSYS[37]	0.0226000
				[37]	0.0226000
			Present theories	FSDT	0.02310753
				GFSDT	0.02312112
				UTSDT	0.02306072
				GUTSDT	0.02307431
		20	Reference	ANSYS[37]	0.0132000
				[37]	0.0133000
			Present theories	FSDT	0.0134078562
				GFSDT	0.0134088
				UTSDT	0.0134106275
				GUTSDT	0.0134116312
		40	Reference	ANSYS[37]	0.0052600
				[37]	0.0052300
			Present theories	FSDT	0.005308357813
				GFSDT	0.005306942188
				UTSDT	0.005308652734
				GUTSDT	0.005307296094

Table 2d. Normalized central deflection of graded conical panel ($E_{c_2} = 151GPa$) under uniform loading

p	α	L/h			$\overline{w}$
	60°	10	Reference	ANSYS[37]	0.0274000
				[37]	0.0276000
			Present theories	FSDT	0.02792292
				GFSDT	0.027935
				UTSDT	0.02789423
				GUTSDT	0.0279048
		20	Reference	ANSYS[37]	0.0191000
				[37]	0.0192000
			Present theories	FSDT	0.0193232812
				GFSDT	0.0193270562
				UTSDT	0.0193289437
				GUTSDT	0.0193327187
		40	Reference	ANSYS[37]	0.0097500
				[37]	0.0097900
			Present theories	FSDT	0.009835644531
				GFSDT	0.009835644531
				UTSDT	0.009836824219
				GUTSDT	0.009836824219

Appendix.

The equilibrium operators $S_{ij}\ i=1,...,7;\ j=1,...,7$ for the functionally graded conical shell are reported in this section. It should be noticed that the ones $R_{ij}\ i=1,...,7;\ j=1,...,7$ for the functionally graded cylindrical shell are equal to S_{ij} by fixing $\varphi=\pi/2$.

Equilibrium operator of the 1st fundamental equation $S_{1j},\ j=1...7$

$$S_{11}=\left(A_{11}+a_1B_{11}\right)\frac{\partial^2}{\partial x^2}+\left(A_{66}+b_1B_{66}+b_2D_{66}+b_3E_{66}\right)\frac{\partial^2}{\partial s^2}+$$
$$+\frac{\cos\varphi}{R_0}\left(A_{11}+B_{11}\left(a_1-\frac{\sin\varphi}{R_0}\right)\right)\frac{\partial}{\partial x}-\left(\frac{\cos\varphi}{R_0}\right)^2\left(A_{11}+b_1B_{11}+b_2D_{11}+b_3E_{11}\right) \tag{A.1}$$

$$S_{12}=\left(A_{12}+A_{66}\right)\frac{\partial^2}{\partial x\partial s}-\frac{\cos\varphi}{R_0}\left(A_{66}+A_{11}+b_1\left(B_{66}+B_{11}\right)+b_2\left(D_{66}+D_{11}\right)\right)\frac{\partial}{\partial s} \tag{A.2}$$

$$S_{13}=\frac{A_{12}\sin\varphi}{R_0}\frac{\partial}{\partial x}-\frac{\cos\varphi\sin\varphi}{R_0^2}\left(A_{11}+b_1B_{11}+b_2D_{11}+b_3E_{11}\right) \tag{A.3}$$

$$S_{14}=\left(B_{11}+a_1D_{11}\right)\frac{\partial^2}{\partial x^2}+\left(B_{66}+b_1D_{66}+b_2E_{66}+b_3F_{66}\right)\frac{\partial^2}{\partial s^2}+\frac{\cos\varphi}{R_0}\left(B_{11}+D_{11}\left(a_1-\frac{\sin\varphi}{R_0}\right)\right)\frac{\partial}{\partial x}+$$
$$-\left(\frac{\cos\varphi}{R_0}\right)^2\left(B_{11}+b_1D_{11}+b_2E_{11}+b_3F_{11}\right) \tag{A.4}$$

$$S_{15}=\left(B_{12}+B_{66}\right)\frac{\partial^2}{\partial x\partial s}-\frac{\cos\varphi}{R_0}\left(\left(B_{11}+B_{66}\right)+b_1\left(D_{11}+D_{66}\right)+b_2\left(E_{11}+E_{66}\right)+b_3\left(F_{66}+F_{11}\right)\right)\frac{\partial}{\partial s} \tag{A.5}$$

$$S_{16}=\left(E_{11}+a_1F_{11}\right)\left(\frac{\partial^2}{\partial x^2}\right)+\left(E_{66}+b_1F_{66}+b_2L_{66}+b_3H_{66}\right)\frac{\partial^2}{\partial s^2}+\frac{\cos\varphi}{R_0}\left(E_{11}+F_{11}\left(a_1-\frac{\sin\varphi}{R_0}\right)\right)\frac{\partial}{\partial x}+$$
$$-\left(\frac{\cos\varphi}{R_0}\right)^2\left(E_{11}+b_1F_{11}+b_2L_{11}+b_3H_{11}\right) \tag{A.6}$$

$$S_{17}=\left(E_{12}+E_{66}\right)\frac{\partial^2}{\partial x\partial s}-\frac{\cos\varphi}{R_0}\left(E_{11}+E_{66}+b_1\left(F_{11}+F_{66}\right)+b_2\left(L_{11}+L_{66}\right)+b_3\left(H_{11}+H_{66}\right)\right)\frac{\partial}{\partial s} \tag{A.7}$$

Equilibrium operator of the 2nd fundamental equation S_{2j}, $j=1...7$

$$S_{21}=\left(A_{12}+A_{66}\right)\frac{\partial^2}{\partial s\partial x}+\frac{\cos\varphi}{R_0}\left(\left(A_{11}+A_{66}\right)+b_1\left(B_{11}+B_{66}\right)+b_2\left(D_{11}+D_{66}\right)+b_3\left(E_{11}+E_{66}\right)\right)\frac{\partial}{\partial s} \quad (A.8)$$

$$S_{22}=\left(A_{66}+a_1B_{66}\right)\frac{\partial^2}{\partial x^2}+\left(A_{11}+b_1B_{11}+b_2D_{11}+b_3E_{11}\right)\frac{\partial^2}{\partial s^2}+\frac{\cos\varphi}{R_0}\left(A_{66}+B_{66}\left(a_1-\frac{\sin\varphi}{R_0}\right)\right)\frac{\partial}{\partial x}+$$
$$-\left(\frac{\cos\varphi}{R_0}\right)^2\left(A_{66}+b_1B_{66}+b_2D_{66}+b_3E_{66}\right)-\left(\frac{\sin\varphi}{R_0}\right)^2\left(A_{66}+b_1B_{66}+b_2D_{66}+b_3E_{66}\right) \quad (A.9)$$

$$S_{23}=\frac{\sin\varphi}{R_0}\left(A_{11}+b_1B_{11}+b_2D_{11}+b_3E_{11}\right)\frac{\partial}{\partial s}+\frac{\sin\varphi}{R_0}\left(A_{66}+b_1B_{66}+b_2D_{66}+b_3E_{66}\right)\frac{\partial}{\partial s} \quad (A.10)$$

$$S_{24}=\left(B_{12}+B_{66}\right)\frac{\partial^2}{\partial s\partial x}+\frac{\cos\varphi}{R_0}\left(\left(B_{11}+B_{66}\right)+b_1\left(D_{11}+D_{66}\right)+b_2\left(E_{11}+E_{66}\right)+b_3(F_{11}+F_{66})\right)\frac{\partial}{\partial s} \quad (A.11)$$

$$S_{25}=\left(B_{66}+a_1D_{66}\right)\frac{\partial^2}{\partial x^2}+\left(B_{11}+b_1D_{11}+b_2E_{11}+b_3F_{11}\right)\frac{\partial^2}{\partial s^2}+\frac{\cos\varphi}{R_0}\left(B_{66}+D_{66}\left(a_1-\frac{\sin\varphi}{R_0}\right)\right)\frac{\partial}{\partial x}+$$
$$-\left(\frac{\cos\varphi}{R_0}\right)^2\left(B_{66}+b_1D_{66}+b_2E_{66}+b_3F_{66}\right)+\frac{\sin\varphi}{R_0}\left(A_{66}+b_1B_{66}+b_2D_{66}+b_3E_{66}\right) \quad (A.12)$$

$$S_{26}=\left(E_{12}+E_{66}\right)\frac{\partial^2}{\partial s\partial x}+\frac{\cos\varphi}{R_0}\left(\left(E_{11}+E_{66}\right)+b_1\left(F_{11}+F_{66}\right)+b_2\left(L_{11}+L_{66}\right)+b_3\left(H_{11}+H_{66}\right)\right)\frac{\partial}{\partial s} \quad (A.13)$$

$$S_{27}=\left(E_{66}+a_1F_{66}\right)\frac{\partial^2}{\partial x^2}+\left(E_{11}+b_1F_{11}+b_2L_{11}+b_3H_{11}\right)\frac{\partial^2}{\partial s^2}+\frac{\cos\varphi}{R_0}\left(E_{66}+F_{66}\left(a_1-\frac{\sin\varphi}{R_0}\right)\right)\frac{\partial}{\partial x}$$
$$-\left(\frac{\cos\varphi}{R_0}\right)^2\left(E_{66}+b_1F_{66}+b_2L_{66}+b_3H_{66}\right)+3\frac{\sin\varphi}{R_0}\left(D_{66}+b_1E_{66}+b_2F_{66}+b_3L_{66}\right)+ \quad (A.14)$$
$$+2\left(\frac{\sin\varphi}{R_0}\right)^2\left(E_{66}+b_1F_{66}+b_2L_{66}+b_3H_{66}\right)$$

Equilibrium operator of the 3rd fundamental equation S_{3j}, $j=1...7$

$$S_{31}=-\frac{\sin\varphi}{R_0}A_{12}\frac{\partial}{\partial x}-\frac{\sin\varphi\cos\varphi}{R_0^2}\left(A_{11}+b_1B_{11}+b_2D_{11}+b_3E_{11}\right) \tag{A.15}$$

$$S_{32}=-\frac{\sin\varphi}{R_0}\left(\left(A_{11}+A_{66}\right)+b_1\left(B_{11}+B_{66}\right)+b_2\left(D_{11}+D_{66}\right)+b_3(E_{11}+E_{66})\right)\frac{\partial}{\partial s} \tag{A.16}$$

$$S_{33}=\left(A_{66}+a_1B_{66}\right)\frac{\partial^2}{\partial x^2}+\left(A_{66}+b_1B_{66}+b_2D_{66}+b_3E_{66}\right)\frac{\partial^2}{\partial s^2}+\frac{\cos\varphi}{R_0}\left(A_{66}+B_{66}\left(a_1-\frac{\sin\varphi}{R_0}\right)\right)\frac{\partial}{\partial x}+$$
$$-\left(\frac{\sin\varphi}{R_0}\right)^2\left(A_{11}+b_1B_{11}+b_2D_{11}+b_3E_{11}\right) \tag{A.17}$$

$$S_{34}=\left(A_{66}+a_1B_{66}\right)\frac{\partial}{\partial x}-B_{12}\frac{\sin\varphi}{R_0}\frac{\partial}{\partial x}+\frac{\cos\varphi}{R_0}\left(A_{66}+a_1B_{66}\right)+$$
$$-\frac{\sin\varphi\cos\varphi}{R_0^2}\left(\left(B_{11}+B_{66}\right)+b_1D_{11}+b_2E_{11}+b_3F_{11}\right) \tag{A.18}$$

$$S_{35}=\left(A_{66}+b_1B_{66}+b_2D_{66}+b_3E_{66}\right)\frac{\partial}{\partial s}-\frac{\sin\varphi}{R_0}\left(B_{11}+b_1D_{11}+b_2E_{11}+b_3F_{11}\right)\frac{\partial}{\partial s} \tag{A.19}$$

$$S_{36}=3\left(D_{66}+a_1E_{66}\right)\frac{\partial}{\partial x}-\frac{\sin\varphi}{R_0}E_{12}\frac{\partial}{\partial x}+3\frac{\cos\varphi}{R_0}\left(D_{66}+a_1E_{66}\right)+$$
$$-\frac{\sin\varphi\cos\varphi}{R_0^2}\left(3E_{66}+E_{11}+b_1F_{11}+b_2L_{11}+b_3H_{11}\right) \tag{A.20}$$

$$S_{37}=\left(\begin{array}{l}3\left(D_{66}+b_1E_{66}+b_2F_{66}+b_3L_{66}\right)+\\+\frac{\sin\varphi}{R_0}\left(2E_{66}-E_{11}+b_1\left(2F_{66}-F_{11}\right)+b_2\left(2L_{66}-L_{11}\right)+b_3(2H_{66}-H_{22}\right)\end{array}\right)\frac{\partial}{\partial s} \tag{A.21}$$

Equilibrium operator of the 4th fundamental equation S_{4j}, $j=1...7$

$$S_{41}=\left(B_{11}+a_1D_{11}\right)\frac{\partial^2}{\partial x^2}+\left(B_{66}+b_1D_{66}+b_2E_{66}+b_3F_{66}\right)\frac{\partial^2}{\partial s^2}+\frac{\cos\varphi}{R_0}\left(B_{11}+D_{11}\left(a_1-\frac{\sin\varphi}{R_0}\right)\right)\frac{\partial}{\partial x}+$$
$$-\left(\frac{\cos\varphi}{R_0}\right)^2\left(B_{11}+b_1D_{11}+b_2E_{11}+b_3F_{11}\right) \tag{A.22}$$

$$S_{42}=\left(B_{12}+B_{66}\right)\frac{\partial^2}{\partial x\partial s}-\frac{\cos\varphi}{R_0}\left(\left(B_{11}+B_{66}\right)+b_1\left(D_{11}+D_{66}\right)+b_2\left(E_{11}+E_{66}\right)+b_3\left(F_{11}+F_{66}\right)\right)\frac{\partial}{\partial s} \tag{A.23}$$

$$S_{43}=\frac{\sin\varphi}{R_0}B_{12}\frac{\partial}{\partial x}-\left(A_{66}+a_1B_{66}\right)\frac{\partial}{\partial x}-\frac{\sin\varphi\cos\varphi}{R_0^2}\left(B_{11}+b_1D_{11}+b_2E_{11}+b_3F_{11}\right) \tag{A.24}$$

$$S_{44}=\left(D_{11}+a_1E_{11}\right)\frac{\partial^2}{\partial x^2}+\left(D_{66}+b_1E_{66}+b_2F_{66}+b_3L_{66}\right)\frac{\partial^2}{\partial s^2}+\frac{\cos\varphi}{R_0}\left(D_{11}+E_{11}\left(a_1-\frac{\sin\varphi}{R_0}\right)\right)\frac{\partial}{\partial x}+$$
$$-\left(\frac{\cos\varphi}{R_0}\right)^2\left(D_{11}+b_1E_{11}+b_2F_{11}+b_3L_{11}\right)-\left(A_{66}+a_1B_{66}\right) \quad \text{(A.25)}$$

$$S_{45}=\left(D_{12}+D_{66}\right)\frac{\partial^2}{\partial x\partial s}-\frac{\cos\varphi}{R_0}\left(D_{11}+D_{66}+b_1\left(E_{11}+E_{66}\right)+b_2\left(F_{11}+F_{66}\right)+b_3\left(L_{11}+L_{66}\right)\right)\frac{\partial}{\partial s} \quad \text{(A.26)}$$

$$S_{46}=\left(F_{11}+a_1L_{11}\right)\frac{\partial^2}{\partial x^2}+\left(F_{66}+b_1L_{66}+b_2H_{66}+b_3M_{66}\right)\frac{\partial^2}{\partial s^2}+\frac{\cos\varphi}{R_0}\left(F_{11}+L_{11}\left(a_1-\frac{\sin\varphi}{R_0}\right)\right)\frac{\partial}{\partial x}+$$
$$-\left(\frac{\cos\varphi}{R_0}\right)^2\left(F_{11}+b_1L_{11}+b_2H_{11}+b_3M_{11}\right)-3\left(D_{66}+a_1E_{66}\right) \quad \text{(A.27)}$$

$$S_{47}=\left(F_{12}+F_{66}\right)\frac{\partial^2}{\partial x\partial s}-\frac{\cos\varphi}{R_0}\left(\left(F_{11}+F_{66}\right)+b_1\left(L_{11}+L_{66}\right)+b_2\left(H_{11}+H_{66}\right)+b_3(M_{11}+M_{66})\right)\frac{\partial}{\partial s} \quad \text{(A.28)}$$

Equilibrium operator of the 5th fundamental equation S_{5j}, $j=1...7$

$$S_{51}=\left(B_{12}+B_{66}\right)\frac{\partial^2}{\partial x\partial s}+\frac{\cos\varphi}{R_0}\left(\left(B_{11}+B_{66}\right)+b_1\left(D_{11}+D_{66}\right)+b_2\left(E_{11}+E_{66}\right)+b_3(F_{11}+F_{66})\right)\frac{\partial}{\partial s} \quad \text{(A.29)}$$

$$S_{52}=\left(B_{66}+a_1D_{66}\right)\frac{\partial^2}{\partial x^2}+\left(B_{11}+b_1D_{11}+b_2E_{11}+b_3F_{11}\right)\frac{\partial^2}{\partial s^2}+\frac{\cos\varphi}{R_0}\left(B_{66}+D_{66}\left(a_1-\frac{\sin\varphi}{R_0}\right)\right)\frac{\partial}{\partial x}+$$
$$-\left(\frac{\cos\varphi}{R_0}\right)^2\left(B_{66}+b_1D_{66}+b_2E_{66}+b_3F_{66}\right)+\frac{\sin\varphi}{R_0}\left(A_{66}+b_1B_{66}+b_2D_{66}+b_3E_{66}\right) \quad \text{(A.30)}$$

$$S_{53}=\left(\frac{\sin\varphi}{R_0}\left(B_{11}+b_1D_{11}+b_2E_{11}+b_3F_{11}\right)-\left(A_{66}+b_1B_{66}+b_2D_{66}+b_3E_{66}\right)\right)\frac{\partial}{\partial s} \quad \text{(A.31)}$$

$$S_{54}=\left(D_{12}+D_{66}\right)\frac{\partial^2}{\partial x\partial s}+\frac{\cos\varphi}{R_0}\left(D_{11}+D_{66}+b_1\left(E_{11}+E_{66}\right)+b_2\left(F_{11}+F_{66}\right)+b_3(L_{11}+L_{66})\right)\frac{\partial}{\partial s} \quad \text{(A.32)}$$

$$S_{55}=\left(D_{66}+a_1E_{66}\right)\frac{\partial^2}{\partial x^2}+\left(D_{11}+b_1E_{11}+b_2F_{11}+b_3L_{11}\right)\frac{\partial^2}{\partial s^2}+\frac{\cos\varphi}{R_0}\left(D_{66}+E_{66}\left(a_1-\frac{\sin\varphi}{R_0}\right)\right)\frac{\partial}{\partial x}+$$
$$-\left(\frac{\cos\varphi}{R_0}\right)^2\left(D_{66}+b_1E_{66}+b_2F_{66}+b_3L_{66}\right)-\left(A_{66}+b_1B_{66}+b_2D_{66}+b_3E_{66}\right) \quad \text{(A.33)}$$

$$S_{56}=\left(F_{12}+F_{66}\right)\frac{\partial^2}{\partial x\partial s}+\frac{\cos\varphi}{R_0}\left(\left(F_{11}+F_{66}\right)+b_1\left(L_{11}+L_{66}\right)+b_2\left(H_{11}+H_{66}\right)+b_3\left(M_{11}+M_{66}\right)\right)\frac{\partial}{\partial s} \quad \text{(A.34)}$$

$$S_{57} = \left(F_{66} + a_1 L_{66}\right)\frac{\partial^2}{\partial x^2} + \left(F_{11} + b_1 L_{11} + b_2 H_{11} + b_3 M_{11}\right)\frac{\partial^2}{\partial s^2} + \frac{\cos\varphi}{R_0}\left(F_{66} + L_{66}\left(a_1 - \frac{\sin\varphi}{R_0}\right)\right)\frac{\partial}{\partial x}$$
$$-\left(\frac{\cos\varphi}{R_0}\right)^2\left(F_{66} + b_1 L_{66} + b_2 H_{66} + b_3 M_{66}\right) - 3\left(D_{66} + b_1 E_{66} + b_2 F_{66} + b_3 L_{66}\right) + \qquad \text{(A.35)}$$
$$-\frac{2\sin\varphi}{R_0}\left(E_{66} + b_1 F_{66} + b_2 L_{66} + b_3 H_{66}\right)$$

Equilibrium operator of the 6th fundamental equation S_{6j}, $j = 1...7$

$$S_{61} = \left(E_{11} + a_1 F_{11}\right)\frac{\partial^2}{\partial x^2} + \left(E_{66} + b_1 F_{66} + b_2 L_{66} + b_3 H_{66}\right)\frac{\partial^2}{\partial s^2} + \frac{\cos\varphi}{R_0}\left(E_{11} + F_{11}\left(a_1 - \frac{\sin\varphi}{R_0}\right)\right)\frac{\partial}{\partial x} +$$
$$-\left(\frac{\cos\varphi}{R_0}\right)^2\left(E_{11} + b_1 F_{11} + b_2 L_{11} + b_3 H_{11}\right) \qquad \text{(A.36)}$$

$$S_{62} = \left(E_{12} + E_{66}\right)\frac{\partial^2}{\partial x \partial s} - \frac{\cos\varphi}{R_0}\left(\left(E_{11} + E_{66}\right) + b_1\left(F_{11} + F_{66}\right) + b_2\left(L_{11} + L_{66}\right) + b_3(H_{11} + H_{66})\right)\frac{\partial}{\partial s} \qquad \text{(A.37)}$$

$$S_{63} = \left(\frac{\sin\varphi}{R_0}E_{12} - 3\left(D_{66} + a_1 E_{66}\right)\right)\frac{\partial}{\partial x} - \frac{\sin\varphi\cos\varphi}{R_0^2}\left(E_{11} + b_1 F_{11} + b_2 L_{11} + b_3 H_{11}\right) \qquad \text{(A.38)}$$

$$S_{64} = \left(F_{11} + a_1 L_{11}\right)\frac{\partial^2}{\partial x^2} + \left(F_{66} + b_1 L_{66} + b_2 H_{66} + b_3 M_{66}\right)\frac{\partial^2}{\partial s^2} + \frac{\cos\varphi}{R_0}\left(F_{11} + L_{11}\left(a_1 - \frac{\sin\varphi}{R_0}\right)\right)\frac{\partial}{\partial x} +$$
$$-\left(\frac{\cos\varphi}{R_0}\right)^2\left(F_{11} + b_1 L_{11} + b_2 H_{11} + b_3 M_{11}\right) - 3\left(D_{66} + a_1 E_{66}\right) \qquad \text{(A.39)}$$

$$S_{65} = \left(F_{12} + F_{66}\right)\frac{\partial^2}{\partial x \partial s} - \frac{\cos\varphi}{R_0}\left(F_{11} + F_{66} + b_1\left(L_{11} + L_{66}\right) + b_2\left(H_{11} + H_{66}\right) + b_3\left(M_{11} + H_{66}\right)\right)\frac{\partial}{\partial s} \qquad \text{(A.40)}$$

$$S_{66} = \left(H_{11} + a_1 M_{11}\right)\frac{\partial^2}{\partial x^2} + \left(H_{66} + b_1 M_{66} + b_2 N_{66} + b_3 V_{66}\right)\frac{\partial^2}{\partial s^2} + \frac{\cos\varphi}{R_0}\left(H_{11} + M_{11}\left(a_1 - \frac{\sin\varphi}{R_0}\right)\right)\frac{\partial}{\partial x} +$$
$$-\left(\frac{\cos\varphi}{R_0}\right)^2\left(H_{11} + b_1 M_{11} + b_2 N_{11} + b_3 V_{11}\right) - 9\left(F_{66} + a_1 L_{66}\right) \qquad \text{(A.41)}$$

$$S_{67} = \left(H_{12} + H_{66}\right)\frac{\partial^2}{\partial x \partial s} - \frac{\cos\varphi}{R_0}\left(\left(H_{11} + H_{66}\right) + b_1\left(M_{11} + M_{66}\right) + b_2\left(N_{11} + N_{66}\right) + b_3\left(V_{11} + V_{66}\right)\right)\frac{\partial}{\partial s} \tag{A.42}$$

Equilibrium operator of the 7th fundamental equation S_{7j}, $j = 1...7$

$$S_{71} = \left(E_{12} + E_{66}\right)\frac{\partial^2}{\partial x \partial s} + \frac{\cos\varphi}{R_0}\left(\left(E_{11} + E_{66}\right) + b_1\left(F_{11} + F_{66}\right) + b_2\left(L_{11} + L_{66}\right) + b_3(H_{11} + H_{66})\right)\frac{\partial}{\partial s} \tag{A.43}$$

$$S_{72} = \left(E_{66} + a_1 F_{66}\right)\frac{\partial^2}{\partial x^2} + \left(E_{11} + b_1 F_{11} + b_2 L_{11} + b_3 H_{11}\right)\frac{\partial^2}{\partial s^2} + \frac{\cos\varphi}{R_0}\left(E_{66} + F_{66}\left(a_1 - \frac{\sin\varphi}{R_0}\right)\right)\frac{\partial}{\partial x} +$$

$$-\left(\frac{\cos\varphi}{R_0}\right)^2\left(E_{66} + b_1 F_{66} + b_2 L_{66} + b_3 H_{66}\right) + 3\frac{\sin\varphi}{R_0}\left(D_{66} + b_1 E_{66} + b_2 F_{66} + b_3 L_{66}\right) + \tag{A.44}$$

$$+2\left(\frac{\sin\varphi}{R_0}\right)^2\left(E_{66} + b_1 F_{66} + b_2 L_{66} + b_3 H_{66}\right)$$

$$S_{73} = \left(\frac{\sin\varphi}{R_0}E_{11} - 3D_{66}\right)\frac{\partial}{\partial s} + \left(b_1\left(\frac{\sin\varphi}{R_0}F_{11} - 3E_{66}\right) + b_2\left(\frac{\sin\varphi}{R_0}L_{11} - 3F_{66}\right) + b_3\left(\frac{\sin\varphi}{R_0}H_{11} - 3L_{66}\right)\right)\frac{\partial}{\partial s} \tag{A.45}$$

$$S_{74} = \left(F_{12} + F_{66}\right)\frac{\partial^2}{\partial x \partial s} + \frac{\cos\varphi}{R_0}\left(\left(F_{11} + F_{66}\right) + b_1\left(L_{11} + L_{66}\right) + b_2\left(H_{11} + H_{66}\right) + b_3\left(M_{11} + M_{66}\right)\right)\frac{\partial}{\partial s} \tag{A.46}$$

$$S_{75} = \left(F_{66} + a_1 L_{66}\right)\frac{\partial^2}{\partial x^2} + \left(F_{11} + b_1 L_{11} + b_2 H_{11} + b_3 M_{11}\right)\frac{\partial^2}{\partial s^2} +$$

$$+\frac{\cos\varphi}{R_0}\left(F_{66} + L_{66}\left(a_1 - \frac{\sin\varphi}{R_0}\right)\right)\frac{\partial}{\partial x} - \left(\frac{\cos\varphi}{R_0}\right)^2\left(F_{66} + b_1 L_{66} + b_2 H_{66} + b_3 M_{66}\right) + \tag{A.47}$$

$$-3\left(D_{66} + b_1 L_{66} + b_2 H_{66} + b_3 L_{66}\right) - \frac{2\sin\varphi}{R_0}\left(E_{66} + b_1 F_{66} + b_2 L_{66} + b_3 H_{66}\right)$$

$$S_{76} = \left(H_{12} + H_{66}\right)\frac{\partial^2}{\partial x \partial s} + \frac{\cos\varphi}{R_0}\left(\left(H_{11} + H_{66}\right) + b_1\left(M_{11} + M_{66}\right) + b_2\left(N_{11} + N_{66}\right) + b_3\left(V_{11} + V_{66}\right)\right)\frac{\partial}{\partial s} \tag{A.48}$$

$$S_{77} = \left(H_{66} + a_1 M_{66}\right)\frac{\partial^2}{\partial x^2} + \left(H_{11} + b_1 M_{11} + b_2 N_{11} + b_3 V_{11}\right)\frac{\partial^2}{\partial s^2} + \frac{\cos\varphi}{R_0}\left(H_{66} + M_{66}\left(a_1 - \frac{\sin\varphi}{R_0}\right)\right)\frac{\partial}{\partial x} +$$
$$-\left(\frac{\cos\varphi}{R_0}\right)^2\left(H_{66} + b_1 M_{66} + b_2 N_{66} + b_3 V_{66}\right) - 9\left(F_{66} + b_1 L_{66} + b_2 H_{66} + b_3 M_{66}\right) +$$
$$-6\frac{\sin\varphi}{R_0}\left(F_{66} + b_1 L_{66} + b_2 H_{66} + b_3 M_{66}\right) - 6\frac{\sin\varphi}{R_0}\left(L_{66} + b_1 H_{66} + b_2 M_{66} + b_3 N_{66}\right) +$$
$$-4\left(\frac{\sin\varphi}{R_0}\right)^2\left(H_{66} + b_1 M_{66} + b_2 N_{66} + b_3 V_{66}\right) \qquad \text{(A.49)}$$